UNIVERSITEIT VAN PRETORIA
UNIVERSITY OF PRETORIA
YUNIBESITHI YA PRETORIA

Stability of gold and cerium oxide nanoparticles in aqueous environments, and their effects on *Pseudokirchneriella subcapitata* and *Salvinia minima*

Submitted in fulfilment of the requirements for the degree

Doctor of Philosophy in Microbiology

Department of Biochemistry, Genetics and Microbiology

in the

Faculty of Natural and Agricultural Sciences

at the

University of Pretoria

by

Ntombikayise Mahaye

Supervisor: Prof Don Cowan

Co-supervisor: Prof Ndeke Musee

2019

Declaration

I, Ntombikayise Mahaye, declare that this thesis, which I hereby submit for the degree of Doctor of Philosophy in the Department of Biochemistry, Genetics and Microbiology, University of Pretoria, is my own original work with guidance from the supervisors. In addition, I acknowledged and referenced all the sources used.

I have not used work previously produced by another student or any other person to hand in as my own.

I have not allowed, and will not allow, anyone to copy my work with the intention of passing it off as his or her own work.

SIGNATURE 

.....

Acknowledgements

Firstly, I would like to express my sincere gratitude to my supervisors Profs Don Cowan and Ndeke Musee for their guidance, support and reading through my thesis drafts. The accomplishment of this work and publication would not have been successful without their guidance and dedication.

I am grateful to Dr Melusi Thwala of the CSIR for the guidance and discussions relating to experimental work and background in toxicology.

I thank Miss Liesl Hill from CSIR for allowing me to use their facilities in the laboratory and for her guidance when algal experiments failed.

I thank the CSIR for providing me with an opportunity and funding to further my studies after an internship with them. Special thanks also go to all staff and students at the NRE and Source Directed and Scientific Measures Research Group for providing me with a good atmosphere to do my research.

I extend my gratitude to the DST-NRF Professional Development Programme for financial assistance. Without their support, I would not have been able to do this degree.

I thank the University of Pretoria; Emerging Contaminants Ecological Risk Assessment (ECERA) Research Group and Centre for Microbial Ecology and Genomics (CMEG) for their facilities and materials provided.

My deepest gratitude goes to a brother, friend and a mentor, Dr Ngogi Emmanuel Mahaye who had a huge trust in me and kept me motivated through difficulties.

Lastly, I am forever grateful dear Lord for blessing me with the opportunity to do this PhD degree.

Dedication

I dedicate this work to my late brother, Mr Sanele Mahaye who until his last day never got tired of encouraging me to study hard. He wanted me to have a PhD more than I wanted it myself. Ngiyabonga Nodange, ngaphandle kwakho nezifiso obunazo ngami bengingeke ngifike la engikhona.

List of publication(s) from this study

N. Mahaye, M. Thwala, D. Cowan, N. Musee. 2017. Genotoxicity of metal based engineered nanoparticles in aquatic organisms: A review. *Mutation Research Reviews*, 773: 134–160. THESIS CHAPTER 2

Conference outputs

Mahaye N, Thwala M, Cowan DA, Musee N. 2017. Do size and surface coating influence adsorption of gold nanoparticles to *Salvinia* aquatic plants*?* 8th International Young Water Professionals Conference, Cape Town International Conference Centre, Cape Town, South Africa, 10-13 December 2017.

Mahaye N, Thwala M, Cowan DA, Musee N. 2015. The effects of metal and metal oxide nanoparticles on DNA stability in aquatic organisms: a review. 5th CSIR Emerging Researchers Symposium, CSIR, Pretoria, South Africa, 8-9 October 2015.

TABLE OF CONTENTS

Page

LIST OF TABLES

Table Page

LIST OF FIGURES

LIST OF ACRONYMS

ζ potential	Zeta potential
ANOVA	Analysis of Variance
AP sites	apurinic/apyrimidinic sites
ARP	Aldehyde Reactive Probe
Au NPs	Gold nanoparticles
BER	Base excision repair
BET	Brunauer Emmett Teller method
BPEI	Branched polyethyleneimine coating
CeO_2 NPs	Cerium oxide nanoparticles
Chl *a*	Chlorophyll a
Cit	Citrate coating
DIW	De-ionised water
DTW	De-chlorinated tap water
DEEEP	Direct Estimation of Ecological Effect Potential guideline
DLS	Dynamic light scattering
EDX	Energy dispersive x-ray spectroscopy
ENMs	Engineered nanomaterials
ENPs	Engineered nanoparticles
GTS	Genomic template stability
HDD	Hydrodynamic diameter
HM	Hoagland's Medium
HR-SEM	High-resolution scanning electron microscope
HRTEM	High-resolution transmission electron microscope
ICP-MS	Inductively Coupled Plasma-Mass Spectroscopy
NOM	Natural organic matter
OD	Optical density

OECD	Organization for Economic Co-operation and Development
NTA	Nanoparticle Tracking Analysis
PCR	Polymerase chain reaction
PEG	Polyethylene glycol
PVP	Polyvinylpyrrolidone
RAPD	Random Amplified Polymorphism DNA
ROS	Reactive oxygen species

SUMMARY

Engineered nanoparticles (ENPs) are class of emerging environmental pollutants, generally found at low concentrations and are therefore likely to exert sub-lethal effects on aquatic organisms. Among different kinds of NPs, metal and metal oxides NPs are most widely used in consumer products, targeted drug delivery and optical bioimaging. Rapid increasing use and applications of ENPs and their consequent emission into the environments raised the need to understand their potential effects to ecological systems. Yet, currently, the environmental fate, behaviour and potential toxic effects of NPs in the environment are poorly understood. The aquatic environment is at risk of exposure to NPs, as it acts as a final recipient for most environmental contaminants. To address this knowledge gap, the current study seeks to generate data on the fate and behaviour of NPs in aquatic systems and investigates their potential toxic effects on aquatic organisms. Amongst the less studied, but widely produced NPs are gold and cerium oxide NPs, therefore, likely to be released into the environment in high quantities. Algae, *Pseudokirchneriella subcapitata* and aquatic higher plant, *Salvinia minima* were selected as models for this study owing to limited nano-ecotoxicity data available.

To investigate the influence of physicochemical properties of NPs and media constituents on the environmental fate and behaviour of NPs; the hydrodynamic diameters and zeta potentials for Au (5, 20 and 40 nm; citrate and branched polyethyleneimine coated) and CeO_2 (>25 nm, uncoated) NPs were characterized in de-ionised water (DIW), 10% Hoagland's medium, dechlorinated tap water and 10% BG-11 algal medium. Findings showed high agglomeration of NPs in biological media compared to DIW due to the low ionic strength of DIW. Instability of NPs in media was size and surface coating dependent, with smaller sized (5 nm) and citrate coated-Au NPs agglomerating rapidly. The much broader particle size distribution observed indicated (i) formation of agglomerates, (ii) instability of Au and CeO_2 NPs in ecotoxicological media and (iii) inaccuracy of light scattering techniques in size analysis for non-spherical NPs.

The interaction of Au and CeO_2 NPs with *S. minima* indicated that (i) NPs were not internalized by *S. minima* irrespective of NP size, coating variant, and type, (ii) NPs can be adsorbed on the roots of *S. minima* but without inducing morphological level effects such as growth retardation and necrosis and (iii) adsorption was established as mechanism of NPs accumulation in *S. minima*. Exposure of *P. subcapitata* to NPs showed that (i) citrate-Au and CeO_2 NPs neither inhibited *P. subcapitata* growth nor affected the cellular chlorophyll content; where slight

growth inhibition was observed at 72 h, algae recovered after 96 h, (ii) genotoxicity assays revealed potential toxicity of NPs to algae at molecular level although no effects observed at morphological level and (iii) algae show an increase in genomic stability under long-term exposure conditions. Overall, the study showed that the behaviour of NPs in aquatic systems and their interactions with aquatic organisms are influenced by their physicochemical characteristics, exposure medium composition and exposure period; also, genotoxicity assays are more sensitive than cytotoxicity assays.

CHAPTER 1: INTRODUCTION

1.1 Nanotechnology and engineered nanoparticles

Nanotechnology, in general, encompasses the manipulation and application of materials at the nanoscale (Garnett and Kallinteri 2006), which are collectively referred to as engineered nanomaterials (ENMs). The word "nano" means "dwarf" in the Greek language (Bergeron and Archambault 2005) and is used as a prefix for one-billionth (Scientific Committee on Emerging and Newly-Identified Health Risks (SCENIHR), 2007). Nanomaterials are any natural, incidental or manufactured material containing particles in a loose or aggregated state whereby 50 % or more of the particle sizes range from 1-100 nm (EU 2011). Included in this definition are engineered nanoparticles (ENPs), whose production is currently driving nanotechnology growth. Engineered NPs include metals, metal oxides and alloys, carbon-based materials (fullerenes, nanotubes and fibres, silicates and quantum dots) and polymer composites (Aitken *et al.* 2006; Chaudhry *et al.* 2008; Hansen *et al.* 2016). Among different kinds of NPs, metal-based NPs (term includes both metal and metal oxides NPs) are most widely used in consumer products (PEN 2014; Vance *et al.* 2015; Hansen *et al.* 2016). The small size of NPs with unique electrochemical properties makes them useful for industrial processes and consumer applications. However, the same useful properties have raised concerns about their toxicity in the environment.

The increased production and utilisation of NPs led to their release and accumulation in the environment (Klaine *et al.* 2008; Keller *et al.* 2013). This triggered concerns relating to their potential toxicity to humans and the environment a decade ago (Oberdörster *et al.* 2005; Nel *et al.* 2006). The aquatic environment is particularly at risk of exposure to NPs, as it acts as a final recipient for most environmental contaminants due to extensive use and disposal of NPs in everyday life (Scown *et al.* 2010; Keller *et al.* 2013). These concerns have been partly addressed through investigations on the potential effects of NPs at end-points such as genotoxicity, cytotoxicity, uptake, accumulation and transformation of NPs due to lack of knowledge regarding their environmental safety. Of these endpoints, bioaccumulation of NPs in plants was considered as a process affecting the environmental fate of NPs (Schwab *et al.* 2015). The presence of NPs at very low concentrations in the aquatic systems (Gottschalk *et al.* 2009; Baalousha *et al.* 2016; Bäuerlein *et al.* 2017) highlights the importance of acquiring genotoxicity data to support decision-making with the aim of protecting the health of aquatic

systems (as recognized by the Organization for Economic Co-operation and Development (OECD) (Warheit and Donner 2010; Kühnel and Nickel 2014).

Estimates for the global nanotechnology market were that it will reach $ 48.9 billion by 2017 (BCC Research 2012) and$ 64.2 billion by 2019 (BCC Research 2014). Even locally, from 2005 to 2012 there has been a rise in nanotechnology investment up to ZAR 2.622 billion to support research and development in order to stimulate growth in nanotechnology (DST 2012). This suggests that different countries including South Africa are aware of the potentially beneficial impacts of nanotechnology. Therefore, this study aims to contribute to this goal by generating data to be used for risk assessment of NPs in environmental systems.

1.2 Study motivation

While there has been a recent increase in research into the biological effects of NPs on aquatic organisms, little is known of the genotoxicity of NPs relative to endpoints such as mortality, growth inhibition and cell membrane damage. A recent review reported that of 4346 articles on NPs toxicity, only 112 focused on genotoxicity studies and 94 were *in vitro* studies (Magdolenova *et al*. 2014). In addition, genotoxicity studies on the effects of NPs have largely focused on mammalian systems (Karlsson, 2010; Rim *at al*. 2013; Magdolenova *et al*. 2014; Golbamaki *et al.* 2015) and terrestrial plants (Mehrian and De Lima 2016; Rizwan *et al.* 2017). The lack of genotoxicity data on the interactions between NPs and aquatic organisms has been recently highlighted (Mahaye *et al.* 2017). To date, bacteria, crustaceans and fish, and TiO_2 and Ag NPs, are the most studied organisms and NPs, respectively. There is limited genotoxicity data on algae and aquatic higher plants and other NPs. Therefore, this study aims to generate data to address this current gap.

The accumulation dynamics of NPs by aquatic plants are still poorly understood (Thwala *et al.* 2016). Most NP toxicity studies have focused on acute exposure conditions (Arndt *et al.* 2013; Klaper *et al.* 2014). The overall long-term impact of NPs on ecosystems has also been poorly studied (von Moos and Slaveykova 2014; Mahaye *et al*. 2017). Hence, this study aimed to generate data on *in vivo* genotoxicity and accumulation of NPs in aquatic organisms under acute and chronic exposure conditions at environmentally relevant NP concentrations. The choice of the study organisms was based on the limited and contradictory ecotoxicity data on organisms that play important roles in complex aquatic communities. Aquatic organisms from different trophic levels were selected. Algae are sensitive test species to environmental pollutants, are easy to culture and are known to play an important role as primary producers in

the structure and functioning of ecosystems (Saison *et al*. 2010; Ji *et al.* 2011). The aquatic higher plant, *Salvinia minima,* was used as a model plant species because it can readily be cultured under laboratory conditions, has a high growth rate, can rapidly accumulate metals and provides the necessary plant biomass for ecotoxicological assessments (Sune *et al.* 2007; Prado *et al*. 2010).

1.3 Aims and objectives

1.3.1 Aims

i. To investigate the stability of Au and CeO_2 NPs in different biological media.

ii. To investigate the accumulation of Au and CeO_2 NPs by the aquatic higher plant, *S. minima*.

iii. To investigate the genotoxicity potential of Au and CeO_2 NPs to microalgae, *Pseudokirchneriella subcapitata* (formerly *Selenastrum capricornutum*).

1.3.2 Objectives

i. Review the current state of knowledge on the genotoxicity of metal-based (metals and metal oxides) NPs to aquatic organisms.

ii. To investigate the influence of media composition on the agglomeration of Au and CeO_2 NPs in different biological media (BG-11 algal medium, filtered de-chlorinated tap water and 10% Hoagland's medium) used in ecotoxicity studies.

iii. To investigate the influence of particle size (5, 20 and 40 nm) and surface coatings (citrate, and branched polyethyleneimine) of Au NPs on accumulation, and the route of Au and CeO_2 NPs accumulation, by *S. minima*.

iv. To determine (1) the influence of NP size and surface coating on the genotoxicity (DNA damage) potential of Au NPs to *P. subcapitata* (2) compare short term (72 h) and long term (168 h) exposure conditions, (3) compare the effects of metal (Au NPs) and metal oxide (CeO_2 NPs) and (4) compare the effects of Au and CeO2 NPs to *P. subcapitata* at cellular and molecular levels.

1.4 Thesis layout

i. Chapter 1: Provides background information on nanotechnology, engineered nanoparticles, aims and objectives of the study and thesis layout.

ii. Chapter 2: Gives a review of the existing information relating to the effects of metal-based NPs on genotoxicity in aquatic organisms.

iii. Chapter 3: Characterization and stability of Au and CeO_2 NPs in different toxicological media.

iv. Chapter 4: Bioaccumulation of Au and CeO_2 NPs by an aquatic higher plant (*Salvinia minima)*

v. Chapter 5: Genotoxicity of Au and CeO_2 NPs to algae, *Pseudokirchneriella subcapitata*

vi. Chapter 6: Provides a summary of all the chapters of the study and concludes with future perspectives.

vii. Chapter 7: Provides a comprehensive list of references of all the chapters.

CHAPTER 2

Genotoxicity of metal based engineered nanoparticles in aquatic organisms: a review

2.1 Introduction

The dramatic growth in the commercialization of nano-enabled products is driven by recent advances in the precision tuning of the functionality of engineered nanoparticles (ENPs) to meet stringent specifications and performance expectations (Schmid and Riediker 2008; Peralta-Videa *et al*. 2011). For example, ENPs finds applications in cosmetics and sunscreens (Wiechers and Musee 2010), bioimaging probes (Nel *et al*. 2006; Perrault *et al*. 2010), photovoltaic cells (Robel *et al.* 2006), therapeutics (Czupryna and Tsourkas 2006), drug delivery (Jin and Ye 2007), and catalysis (Hutchings, 2005; Thompson, 2007), with the global nanotechnology market projected at a compound annual growth rate of about 17.5% from 2016 to 2022 (Global Nanotechnology Market Outlook 2022). Metal-based ENPs are most widely used in consumer products and applications (Bondarenko *et al*. 2013; Kahru and Ivask 2013; PEN 2014; Hansen *et al.* 2016), and these uses are summarised in Table 2.1. The increasing use of ENPs has led to their increasing release into the environment (Klaine *et al*. 2008; Scown *et al.* 2010; León-Silva *et al.* 2016) at different product lifecycle stages (Klaine *et al.* 2012), in wastewater treatment plants (Gottschalk *et al.* 2009; Sun *et al.* 2014; Bäuerlein *et al.* 2017) and river systems (Gottschalk *et al.* 2009; Musee, 2011; Gottschalk *et al.* 2013; Markus *et al*. 2016).

The increasing production and utilisation of ENPs has also triggered concerns relating to their potential environmental health implications (Oberdörster *et al*. 2005) with respect to aquatic organisms, including bacteria (Huang *et al.* 2008; Kaweeteerawat *et al.* 2015), invertebrates (Galloway *et al*. 2010; Park and Choi 2010; Buffet *et al.* 2013) and fish (Chen *et al.* 2011; Mohmood *et al*. 2015; Rocco *et al.* 2015; Kaya *et al.* 2016). To date, most nanotoxicity assessments have focused on phenotypic end point-based cytotoxicity (Lan *et al*. 2014). Studies have demonstrated that low concentrations of ENPs, as are typically found in environmental systems, may not cause gross cytotoxic effects but may have effects at a molecular level (Lee *et al.* 2009; Bayat *et al*. 2015). For example, Lee *et al*. (2009) found that the cytotoxic effects of titanium dioxide ($nTiO_2$), silicon dioxide or silica ($nSiO_2$) and cerium oxide ($nCeO_2$) nanoparticles on daphnids and chironomids were not apparent at the organism level for end-points such as mortality, growth, or reproduction, but adverse effects were observed at the genetic level. Also, $nTiO_2$ did not induce mortality in fish, *Piaractus mesopotamicus* under UV

and visible light conditions, but induced sub-lethal effects that were influenced by illumination conditions (Clemente *et al.* 2013).

To date, both field experimental (Schmid *et al.* 2010; Piccinno *et al*. 2012; Bäuerlein *et al.* 2017) and modelling (Musee, 2011; Gottschalk *et al.* 2013; Hendren *et al.* 2013; Sun *et al*. 2014; Markus *et al*. 2016) studies have reported very low concentrations of ENPs in various environments, including wastewater, freshwater systems and agricultural soils (Table 2.1). Such data, therefore, suggest that the most likely impacts of ENPs in environmental systems may be restricted to sub-lethal effects, at a molecular level rather than as organismal effects as previously observed for conventional chemical pollutants (Saha *et al.* 2006; Olsen *et al.* 2013). Review findings of Holden *et al.* (2014) indicated the measured or modelled ENPs environmental concentrations ranged from a low ≤ 0.001 ppm to a high > 1000 ppm. The lowest concentrations were ≤ 0.001 ppm in surface water, wastewater treatment plant (WWTP) effluent and solid media (soil, sediments, and biosolids). The highest concentrations were in WWTP effluent (0.11 to 1 ppm) and biosolids (>1000 ppm). In the European Union, genotoxicity is recognised as an important biomarker for the regulation of chemical usage and disposal, especially in undertaking risk assessments in the context of regulatory toxicology (Pratt and Barron 2003). The presence of ENPs at very low concentrations in the aquatic systems (Table 2.1) highlights the importance of acquiring genotoxicity data to support decision-making with the aim of protecting the health of aquatic systems (as recently recognized by the Organization for Economic Co-operation and Development (OECD) (Warheit and Donner 2010; Kühnel and Nickel 2014).

Genotoxicity biomarkers are regarded as useful tools for the assessment of chemical hazards in aquatic ecosystems (Bolognesi and Hayashi 2011). This is because chemicals, which damage DNA, even at very low concentrations, can significantly alter the functioning of ecological systems (Bolognesi and Cirillo 2014). The genotoxicity of a chemical entity can be assessed through a number of changes to the structure of DNA such as: strand breaks, point mutations, cytogenetic assays (induction of chromosomal aberrations and induction of micronucleus structures), changes in DNA repair processes, and via cell-cycle measurements (Ng *et al.* 2010). DNA damage can lead to various cellular responses including cell cycle arrest, apoptosis and interference with DNA repair mechanisms (Harris and Levine 2005). Where DNA damage is not repaired or is mis-repaired, there is a high likelihood of genomic mutations. Persistent mutations have a high potential to cause cell transformation or cell death (Sharma *et al.* 2012).

Genotoxicity studies of ENPs have, to date, largely focused on mammalian systems as evidenced by these reviews (Karlsson, 2010; Rim *at al*. 2013; Chen *et al.* 2014; Magdolenova *et al*. 2014; Golbamaki *et al.* 2015). Recent reviews reported on the genotoxicity of ENPs in terrestrial plants (Mehrian and De Lima 2016; Rizwan *et al.* 2017). The authors are unaware of any comprehensive review of the effects of ENPs in field of aquatic biology, but note that some relevant studies were included in the review of de Lima *et al*. (2012). Here, we review recent studies on the genotoxicity effects of ENPs in aquatic systems. To achieve our study objectives, peer-reviewed literature on aquatic geno-toxicology was collected from two databases, namely; Science direct and Google scholar. For both databases, the publication date of focus was 2007 to 2017. The search terms for both databases were nanoparticles, nanomaterials, genotoxicity, DNA damage, aquatic organisms, metals, metal oxides. A total of 936 studies were retrieved, but 860 papers were excluded from further analysis because they were abstracts, conference papers, reports, scientific proceedings, those reported genotoxicity of metal-based ENPs on humans and terrestrial organisms and genotoxicity of non-metal based ENPs (quantum dots and carbon nanotubes). After exclusion of such papers, only 76 peer-reviewed articles were found to be relevant to this review. Annual publication trends are shown in Figure 2.1. Our objective here is to: (i) highlight mechanisms of ENP-induced genotoxicity, (ii) identify key inherent nanoparticle and environmental factors that influence the observed genotoxic effects, and (iii) highlight the challenges and shortcomings of the reported data and provide recommendations on how these challenges might be addressed.

Table 2.1: Quantities, applications and likely concentrations of ENPs in different environmental systems

ENPs	Global production (tons/year)	Applications	Concentrations in environmental systems (modelled values)		
			WWTP effluent (µg/L)	WWTP sludge (µg/g)	Solid waste (µg/g)
TiO_2	3000[1] 88,000[2]	Paint [3], sunscreen [4]	16 [5]	170 [5]	12 [5]
Ag	55[1]; 452[2]	Personal care products, laundry additives, paints and textiles [6]	0.00017 [5]; 0.05−0.2 [7]	0.02 [5]	0.06 [5]
CeO_2	55[1]; 10,000[2]	Fuel catalyst [1]	0.00001[7]; <0.0001 [8]	<0.01 [8]	<0.01 [8]
SiO_2	5500[1]; 95,000[2]	UV-protection, ceramics, electronics, food, plastics, sunscreen [1]	0.0074 [8]	0.21 [8]	0.31 [8]
Fe_3O_4	55[1]	Biochemical assays, removal of contaminants, bio-manipulation [1]	-	-	-
ZnO	550[1]; 34,000[2]	Skin care products, sunscreens [9]	2.3 [5]; 0.5-1.5 [7]	24 [5]	0.89 [5]
Al_2O_3	55[1]; 35,000[2]	Batteries, grinding, fire protection, metal- and bio-sorption, paints [1]	0.0025 [8]	0.07 [8]	0.10 [8]
Au	No data	Drug delivery [10], and catalysis [11;12]	0.10 [8]	2.90 [8]	4.26 [8]

References: [1] Piccinno *et al.* 2012, [2] Keller *et al.* 2013, [3] Kaegi *et al.* 2008, [4] Gurr *et al.* 2005, [5] Sun *et al.* 2014, [6] Maynard 2006, [7] Gottschalk *et al.* 2013, [8] Boxall *et al.* 2007, [9] Christian *et al*. 2008, [10] Jin and Ye 2007, [11] Hutchings 2005, [12] Thompson 2007. Acronym: WWTP: wastewater treatment plant.

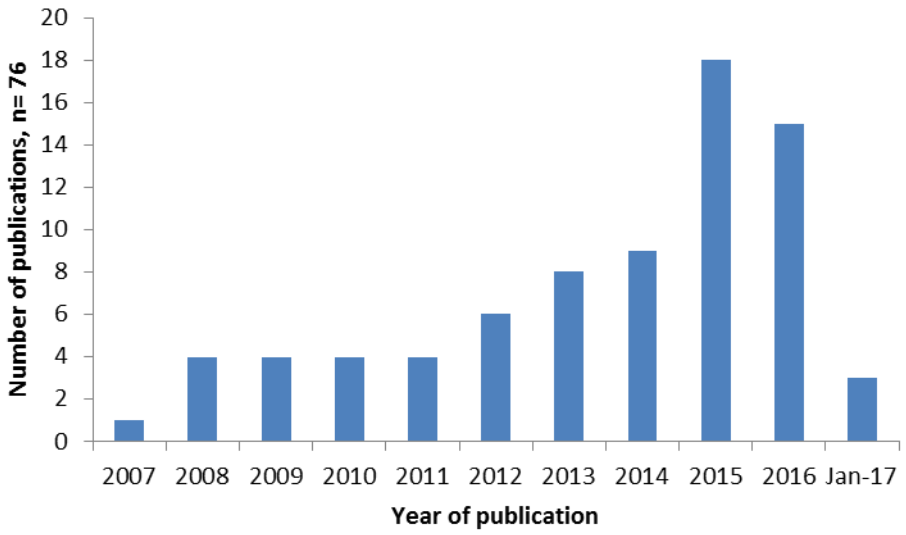

Figure 2.1: Number of publications per year

2.2 Mechanisms of ENP-induced genotoxicity

Detailed reviews of the biochemical and chemical processes that underpin ENPs genotoxicity have been presented elsewhere (Singh *et al.* 2009; Kwon *et al.* 2014; Magdolenova *et al.* 2014; Golbamaki *et al.* 2015; Carriere *et al.* 2017). However, for the purposes of laying a foundation for discussion in the following sections, we briefly highlight some basic concepts with respect to genotoxicity. Generally, genotoxicity is categorised into primary and secondary level effects. Primary genotoxicity can arise from the direct interaction of the genetic material with ENPs, and can be caused by the toxic action of particulates or released dissolved forms. In cases where ENPs do not cross into the nucleus but accumulate inside the cell, direct DNA contact is still possible during mitosis when the nuclear membrane breaks down. Primary genotoxicity can also occur in the absence of physical interactions between the DNA and ENPs, for instance as a result of ENPs interference with proteins essential for DNA replication, transcription, or repair (i.e. indirect DNA damage). Secondary ENPs genotoxicity mechanism occurs when ENPs induce a chronic *in vivo* inflammatory response that leads to excessive generation of ROS by macrophage and neutrophil cells, both as forms of defence response.

To date, only primary genotoxicity has been observed in aquatic biota (Table A2.1). It has been suggested that for aquatic biota the approach to investigate genotoxicity should involve initial *in vitro* screening for genotoxic potential using the Ames test followed by an *in vitro* cytogenetic assay. Non-genotoxicity should be assumed if both tests are negative; where one of the tests is positive, then an *in vivo test* should be considered (Handy *et al.* 2012). It must be emphasised that, for reliable results, dynamic *in vivo* tests are preferred over static *in vitro* tests.

2.3 Methods for testing genotoxicity of ENPs

DNA strand breaks and mutagenicity endpoints are commonly assessed using Comet, Ames, chromosome aberrations (CA) and micronucleus (MN) assays. Gene expression is assessed using the Random Amplified Polymorphism DNA Polymerase Chain Reaction (RAPD-PCR) technique, by DNA microarrays, and via Real Time PCR (RT-PCR) (Kim *et al.* 2013; Rajkishore *et al.* 2013). For the 76 studies assessed for this review, eight different genotoxicity assays were used. The Comet assay is most widely used (Table A2.1 and Figure 2.2), probably because of its ability to detect low levels of DNA damage (among other strengths; as listed in Table 2.2). The MN assay was favoured over the CA assay (Doak *et al.* 2012).

Results in Table A2.1 suggest the Ames test, which is commonly used in toxicity assessments of conventional chemicals, was the least favoured assay for ENPs. This was probably because the assay mutagenicity results showed insignificant differences irrespective of ENP type (e.g. nCuO, $nTiO_2$, nAg) (Warheit *et al.* 2007; Lopes *et al.* 2012; Ko and Kong 2014; Chen *et al.* 2015). In addition, there have been suggestions that the Ames test is insensitive to the genotoxic effects of ENPs compared to the comet or MN assays (Landsiedel *et al.* 2009; Oesch and Landsiedel 2012; George *et al.* 2017). The histone H2AX phosphorylation (H2AX) and 8-hydroxy-deoxyguanosine (8-OHdG) assays were reported in only one of the 76 studies (Table 2), and will not be considered in this review.

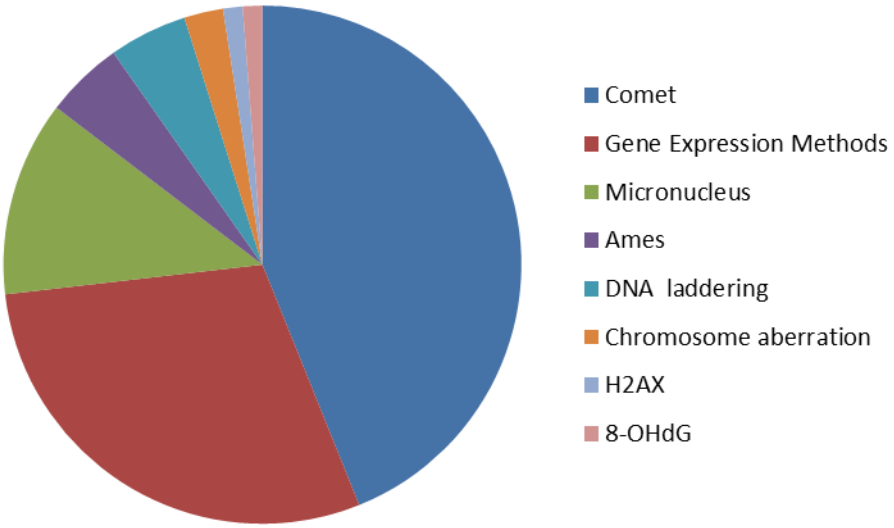

Figure 2.2: Number of studies each genotoxicity assay was used (n = 76). Gene expression methods included microarray, RT-PCR, DD-PCR and RAPD-PCR.

Table 2.2: Strengths and limitations of genotoxicity assays

Assay	Strengths	Limitations
Ames	Ease of use and inexpensive [1]	Poor at detecting genotoxins that induce large-scale DNA damage [1]
		Not suitable for genotoxicity of ENPs owing to poor uptake of particulates by cellular systems [2]
Comet	Simple and fast to undertake [3]	Limited sensitivity in mixed cell populations [4]
	Some indication of apoptosis [3]	Quality of experimental performance crucial during electrophoresis process [3]
	Detect DNA repair in cells [5]	DNA repair is problematic with ENPs as they may remain intracellular causing extra breaks (cannot be effectively removed through cleaning process) [5]
MN	Quick to perform, easy to analyse the results [3]	Cell division is needed [3]
	Measures both chromosome breakage and chromosome loss reliably [6]	Can only detect acentric fragments (for structural chromosome aberrations) [3]
	Ability to co-detect apoptosis and necrosis [3]	
	Not cell type dependent [3]	
MN with CB	Efficient in discrimination between cells with and without nuclear division [3]	Possible interference of cyto-B with test agent [3]
	Detects dicentric bridges as nucleoplasmic bridges [3]	Cytotoxicity of cyto-B varies between cell types [3]
CA	Identifies all chromosome mutation types [3]	Laborious, time consuming, and costly [3]
	Ability to co-detect mitotic indices [3]	Needs cell cultivation (mitosis) [3]

Agarose gel electrophoresis	Easily discriminates between apoptotic and necrotic modes of cell death [7]	Time consuming and prone to loss of low molecular weight fragments during centrifugation steps [7]
	Can detect plasmid DNA damage, DNA cleavage, and DNA fragmentation [7]	DNA isolation step requires relatively a large amount of starting material [7]
		Exhibits reduced sensitivity because of ethanol fixation as it removes smaller DNA [8]
RT-PCR	Requires small amounts of RNA [9]	Expensive to analyse thousands of different transcripts in many samples [10]
		Requires expensive equipment and reagents [10]
DNA microarrays	Simultaneously measure the expression level of thousands of genes within a particular mRNA sample [11]	False microarray data can be generated from degraded mRNA [11]
		There is a lack of rigorous standards for data collection, analysis and validation [11]
DD-PCR	Requires no prior knowledge about the gene or its sequence [12]	Low reproducibility [12]
		A significant incidence of false positives [12;13]
		Under-representation and redundancy of mRNA signals [14]
RAPD-PCR	Simple, sensitive and effective [15]	Concerns about reproducibility of RAPDs have limited their wider use in environmental biology [16]
	No preliminary work such as probe isolation,	
	filter preparation, or nucleotide sequencing is necessary [16]	

Table 2.2 References: [1] Doak *et al*. 2012, [2] Ko and Kong 2014, [3] SCENIHR, 2009, [4] David et al. 2011, [5] Karlsson, 2010, [6] Fenech, 2000, [7] Suman *et al*. 2012, [8] Telford *et al.* 1991, 1992, [9] Fryer *et al*. 2002, [10] Wong and Medrano 2005, [11] Russo *et al.* 2003,

[12] Tiao *et al.* 1996, [13] Yang *et al.* 1996, [14] Linskens *et al*. 1995, [15] Atienzar and Jha 2006, [16] Ali *et al*. 2004

2.3.1. The comet assay

The comet assay is used to detect single and double-stranded DNA breaks in individual cells, both *in vitro* and *in vivo* (Bajpayee *et al.* 2013; Kumar *et al.* 2013). In addition, it can quantify alkali-labile sites (ALSs), oxidative DNA damage, DNA–DNA or DNA–protein cross-links and abasic sites (Pavanello and Clonfero 2000; Collins *et al.* 2008; Kumar and Dhawan 2013). The comet assay can also be used to monitor DNA repair processes (Collins, 2004), although this application may be limited for ENPs as they may remain within the cell for prolonged periods and continue to generate DNA breaks (Karlsson, 2010).

The comet assay has been widely used in, for example, assessing genotoxicity of novel chemicals (Collins, 2004), monitoring environmental contaminants (Verschaeve and Gilles 1995; Dixon *et al.* 2002; de Lapuente *et al*. 2015; Oberholster *et al.* 2016), in DNA repair research (Tice *et al.* 2000; Collins, 2004) and measuring the genotoxicity of ENPs in human and other mammalian systems (Sharma *et al.* 2012; Golbamaki *et al.* 2015). Further details on the comet assay have been provided elsewhere (Collins, 2004; Karlsson 2010; Nandhakumar *et al.* 2011; Kumar and Dhawan 2013; Bolognesi and Cirillo 2014; Golbamaki *et al.* 2015). Recently, a number of studies have reported the use of the comet assay to estimate the genotoxicity of ENPs in aquatic biota (Table A2.1).

2.3.2 The micronucleus test

The micronucleus (MN) assay characterizes chromosome damage and loss (Fenech, 2000) and has been widely used in genotoxicity studies of conventional chemicals in environmental systems (Kirkland *et al*. 2011). Micronuclei may result from aneugenic (whole chromosome) or clastogenic (chromosome breakage) damage (Doherty, 2011). During *in vitro* genotoxicity testing using MN assay, cells are incubated with cytochalasin B (CB), an inhibitor of actin polymerization required for the formation of the microfilament ring that constricts the cytoplasm between the daughter nuclei during cytokinesis (Fenech, 2000). CB blocks cell division and MN are scored only in binucleate cells. Cytochalasin B is known to prevent endocytosis, and thus is likely to prevent uptake of ENPs. To overcome this challenge, Doak *et al.* (2012) incubated cells with ENPs prior to addition of CB and determination of MN

formation. OECD guidelines for the MN assay recommended removal of the test chemical(s) before addition of CB.

However, unlike conventional chemicals, ENPs cannot be completely removed from cells after exposure (Doak *et al.* 2009), hence limiting the application of the MN assay in nanoecotoxicological studies. The confounding factors affecting genotoxicity assessment, including use of CB and presence of fetal bovine serum in cell treatment medium have recently been highlighted (Li *et al.* 2017). Recommendations have been made when analysing the induction of micronuclei using the flow cytometry based method as ENPs spectral properties (fluorescence or optical properties) can lead to unexpected interactions with experimental detection systems (Li *et al.* 2017; Nelson *et al.* 2017). Micronucleus assay data have been reported for studies of the effects of different types of ENPs on several aquatic organisms (Table 2).

2.3.3 Chromosomal aberration assay

Chromosome aberrations (CA) result from failures in repair processes when breaks either do not re-join or re-join in abnormal configurations (OECD 475, 1997). The *in vitro* CA test was developed to identify agents that cause structural chromosome aberrations in cultured mammalian cells. However, genotoxicity data on aquatic biota using the CA assay are now available (Table 2). This assay is substantially slower to perform compared to the MN test and cannot detect some chromosomal abnormalities such as aneugens and clastogens (Doak *et al*. 2012).

2.3.4 The Ames test

The Ames test measures the frequency of mutagenesis in live cells by monitoring the production of the essential amino acid (histidine) in His^- bacterial clones (Ames *et al.* 1975; OECD 471, 1997; Mortelmans and Zeiger 2000). The ease and cost effectiveness of the test make it widely favoured in the safety analysis of chemical substances (Doak *et al.* 2012). However, this assay appears to be inappropriate for the assessment of mutagenicity caused by ENPs. For example, a number of ENPs genotoxicity studies, using the Ames test, failed to generate evidence of genotoxicity, irrespective of the ENP type (Warheit *et al*. 2007; Lopes *et a*l. 2012; Ko and Kong 2014; Chen *et al.* 2015). Results from this assay are also generally not consistent with those from other DNA damage assay methods. For example, Chen *et al.* (2015) showed that styrene-co-maleic anhydride (SMA) coated nAg did not generate a positive Ames

test result in S. *typhimurium,* while the same ENPs induced DNA damage in CHO-K1 (Chinese hamster ovary cell clone K1) cells as determined by the CA assay, attributed to inability of the Ames test to detect large scale DNA damage. This indicated that ENPs generated large deletions that are detectable in other assays, but not with the Ames assay maybe because of the deletion of the histidine gene, which blocks reversion of its defect and leads to cell death (Doak *et al.* 2012).

2.3.5 DNA laddering assay

The DNA laddering technique is used to visualize the endonuclease cleavage products of apoptosis (Wyllie, 1980). Induction of apoptosis is confirmed by an irregular reduction in the size of cells and by DNA fragmentation. DNA fragmentation is detected using techniques such as agarose gel electrophoresis, or by terminal deoxynucleotidyl transferase mediated dUTP-biotin nick end labelling (the TUNEL assay), and the comet assay (Otsuki, 2000; Chandna, 2004).

Agarose gel electrophoresis is the most widely used method to detect DNA fragmentation because it can easily discriminate between apoptotic and necrotic modes of cell death (Kerr *et al.* 1972; Pandey *et al*. 1994). In a DNA fragment ladder obtained during electrophoresis, genomic fragments of irregular sizes are typical of necrotic cells, while a ladder-like electrophoretic pattern indicates apoptotic inter-nucleosomal DNA fragmentation (Abdel-Khalek 2016). This method has drawbacks, such as a requirement for relatively large amounts of starting material, loss of smaller fragments during nucleic acid processing and a relatively long processing time. To address these limitations, Suman *et al.* (2012) modified the DNA isolation steps by inclusion of dimethyl sulphoxide (DMSO) in the lysis buffer. DMSO prevents the formation of folded DNA structures and helps reduce false DNA fragmentation (Kang *et al*. 2005).

The DNA ladder assay has been used for genotoxicity testing of different ENPs in aquatic organisms such as *Escherichia coli* (Huang *et al.* 2008; Kaweeteerawat *et al.* 2015), midge (Oberholster *et al.* 2011) and fish (Ramesh *et al.* 2013). Ramesh *et al*. (2013) showed that the DNA from zebrafish (*Danio rerio)* tissues treated with $nSiO_2$ was substantially fragmented whereas DNA from the control tissues remained intact.

2.4 Factors influencing genotoxicity of ENPs in aquatic systems

Following the release of ENPs into the aquatic systems, it is apparent that their biological effects, from molecular (Clemente *et al.* 2013; Garcia-Reyero *et al*. 2015; Mohmood *et al.* 2015) to subcellular (Huang *et al.*2008; Bondarenko *et al*. 2012; Kaweeteerawat *et al*. 2015) to higher trophic level organisms (Kim *et al.* 2013; Ramesh *et al*. 2013) and to population level effects (Oberholster *et al.* 2011) are influenced by numerous and complex factors.

These factors can be broadly categorized as: (i) the inherent or intrinsic physicochemical traits of ENPs (e.g. size, shape, chemical composition, surface coating, crystal structure, surface charge, etc.) (Kim and Choi 2008; Lee *et al.* 2009; Poynton *et al.* 2012; Garcia-Reyero *et al*. 2015), (ii) interactions with other co-pollutants present in the aquatic systems (Canesi *et al*. 2014; Fang *et al*. 2015; Falfushynska *et al.* 2015; Farkas *et al.* 2015), and (iii) extrinsic or functional properties such as ROS inducing capacity and dissolution (Bondarenko *et al*. 2012; Ali, 2014). The chemistry of the aqueous media (e.g. dissolved oxygen concentration, water hardness, pH, ionic strength and natural organic matter concentration (NOM)) has also been shown to influence the toxicity of ENPs (Cumberland and Lead 2009; El Badawy *et al*. 2010; von der Kammer *et al.* 2010; Ottofuelling *et al.* 2011; Li *et al*. 2010, 2012; Huynh and Chen 2011; Zhang *et al*. 2011, 2012; Piccapietra *et al*. 2012; Batley *et al.* 2013; Selck *et al.* 2016).

2.4.1 Physicochemical properties of ENPs

2.4.1.1 ENP size

Particle size may be an important factor in defining the influence of ENPs in biological systems (Podila and Brown 2013). As ENP size decreases, the surface area to mass or volume ratio increases, in turn affecting other physicochemical properties such as surface atom reactivity and electrical and optical properties (Grassian, 2008). A number of studies have demonstrated that the size of ENPs is inversely related to toxic potency (Chan 2006; Kim and Choi 2008; Lee *et al*. 2009).

For example, Kim and Choi (2008) and Lee *et al.* (2009) compared the DNA strand break effects in *Daphnia magna* cells exposed to 15 nm, 30 nm, and 45 nm $nCeO_2$ particles. The small- (15 nm) $nCeO_2$ caused a higher frequency of DNA strand breaks compared to larger particle sizes and neither $nSiO_2$ nor $nTiO_2$ induced DNA damage at the same concentration (1 mg/L) in M4 exposure media. No size-dependent DNA strand break effects have been reported for $nTiO_2$ and $nSiO_2$. This probably reflects the effect of the intrinsic chemical properties of

the ENPs, rather than particle size. Maltose-stabilized nAg showed size-dependent genotoxicity on mussel haemocytes and gill cells, with smaller (20 nm) ENPs being more toxic than larger (40 and 100 nm) ones (Katsumiti *et al*. 2015). Nano-sized Al_2O_3 (< 50 nm) has been reported to have induced genotoxicity to a greater extent than the same compounds in the macro form in bacteria (Bhuvaneshwari *et al.* 2016; Załęska-Radziwiłł and Doskocz 2016). Ruiz *et al.* (2015) reported a significant increase in micronuclei frequency in mussels exposed to nCuO compared to bulk CuO at the same Cu concentration (10 µg/L). Some apparently contradictory results have been reported; for example, Sharma *et al*. (2016) reported higher DNA damage by 29 nm nAg than by 18 nm particles at the same concentration (800 µg/L) in fish exposed for 7 days.

2.4.1.2. Crystal structure

Crystal structure influences the cytotoxicity (Buzea *et al.* 2007; Ji *et al.* 2011; Katsumiti *et al*. 2014) and genotoxicity (Gurr *et al.* 2005) of ENPs. The two widely used forms of $nTiO_2$ are anatase and rutile, and each has a crystalline structure with specific properties (Schlich *et al.* 2012). Anatase $nTiO_2$ is generally more toxic than rutile $nTiO_2$, as it has been shown to induce greater oxidative stress (Nel *et al.* 2006; Jin *et al*. 2011; Planchon *et al.* 2013). To date, few studies have reported the influence of ENPs crystal structure on genotoxicity (Clemente *et al.* 2015) and cytotoxicity (Ji *et al*. 2011; Katsumiti *et al*. 2015) in aquatic biota.

2.4.1.3 Surface charge

The surface charge of ENPs controls their agglomeration and affects their toxicity in aqueous environments (Jiang *et al.* 2009). Surface charge plays an important role in regulating cellular uptake of ENPs (Fröhlich, 2012), since both the plasma membrane and intracellular environment are negatively charged. For example, anionic ENPs may be endocytosed at lower rates than cationic ENPs. As DNA is negatively charged, cationic ENPs appear to interact more significantly with genetic material (Kwon *et al.* 2014). The higher toxicity of positively charged ENPs can be attributed to the negative charge on the phospholipid membrane of organisms, thus increasing their interaction (Bozich *et al.* 2014). Although many studies reported the ENPs surface charge property (Table 2), only a single study by Dominguez *et al.* (2015) investigated the link between surface charge and genotoxicity. However, studies have reported that surface charge influences the toxicity effects of ENPs (El Badawy *et al.* 2011; Bozich *et al.* 2014; Silva *et al.* 2014; Abbaszadegan *et al*. 2015; Nasser *et al*. 2016).

2.4.1.4 Morphology

The morphology of ENPs exerts a significant influence on their: (i) uptake (Pal *et al.* 2007; Shikha and Radhakrishna 2012), and (ii) fate (Khan *et al.* 2013). In studies where ENPs morphology was reported, no correlation to the observed genotoxicity was established. However, ecotoxicity studies have shown that morphology influences the toxicity effects of ENPs (Simon-Deckers *et al.* 2009; Shikha and Radhakrishna 2012; Nasser *et al*. 2016; Raman *et al.* 2016). For example, rod-shaped nZnO induced higher toxicity effects than nano-spheres to marine algae at similar concentrations (10 - 80 mg/L) (Peng *et al.* 2011). A shape-dependent interaction with *E. coli* has been reported, where truncated triangular nAg (1-100 µg/100 mL) displayed the highest biocidal action, compared with spherical and rod-shaped nAg particles (Pal *et al.* 2007). Silver nano-plates (0 – 25 µg/mL) were more toxic than wires and spheres in studies using a fish gill epithelial cell line (RT-W1) and zebrafish embryos (George *et al.* 2012). Raman *et al.* (2016) reported morphology-dependent toxicity of cobalt oxide ENPs (nCo_3O_4) at concentrations of 1 – 200 mg/L in the fish, *Danio rerio,* where block shaped nCo_3O_4 induced greater potent inhibition of liver GSH activity than spherical particles. Such effects probably result from the fact that changes in shape are accompanied by alterations in surface area, which is closely linked to toxicity (Lee *et al*. 2014).

2.4.1.5 Surface area

The size of ENPs is generally inversely proportional to surface area, solubility and chemical reactivity. Higher surface area and increased reactivity facilitates the uptake of ENPs by cells, potentially increasing cellular damage (Karakoti *et al.* 2006; Klaine *et al*. 2008; Johnston *et al.* 2010; Hsiao and Huang 2011; George *et al*. 2012). These general relationships may be useful guides in the design of 'environmentally friendly' ENPs and/or to predict their fate and transport in environmental systems (Mulvihill *et al.* 2010).

However, no clear relationship between ENPs surface area and genotoxicity has been established. Some studies have concluded that surface area is a less important parameter in dictating ENP toxicity than composition (Sayes *et al.* 2006; Gojova *et al.* 2007), but it is noted that the measurement of ENPs surface area in environmental systems is technically demanding (Fubini *et al.* 2010; Musee *et al.* 2010). The Brunauer, Emmett and Teller method (BET) commonly used for surface area determinations is effective for dry powder samples (Dhawan *et al.* 2009) and does not take into account the changes that occur during ENP exposure. The

ENP surface area is known to be associated with its agglomeration in the environmental media (Nel *et al.* 2009), which influences their bioavailability and toxicity (Warheit *et al.* 2009; Rabolli *et al.* 2011) and alters the available surface are for ENP-organism interaction (Djuris˘ic´ *et al.* 2015). Therefore, obtained surface area value using BET does not represent the actual surface area of the ENP agglomerates in the environmental media. Techniques and methodology for surface area measurements in the liquid and solid states are in an early stage of development (Bleeker *et al.* 2013). Currently, for ENPs in suspension, a relevant ENP parameter is the ENP agglomeration size than surface area.

2.4.1.6 Surface coating

Capping agents are used to stabilize highly reactive ENP surfaces in order to minimize aggregation and dissolution, and to retain certain properties (e.g. surface charge, size or shape) which are useful for targeted applications (Christian *et al*. 2008; Anantha *et al.* 2011). Surface coating has been shown to influence the chemical, physical and biological activities of ENPs in aqueous media (Baalousha *et al*. 2008; Li *et al.* 2013; Zhou *et al.* 2013; He *et al*. 2013; Zopes *et al.* 2013; Kim *et al.* 2016).

The chemistry of ENP coating can decrease or increase toxicity, depending on the nature of interactions with the target organism. For example, polyvinylpyrrolidone (PVP) - and citrate-coated nAg exhibited similar levels of toxicity to algae (IC_{50} values of 9.3 and 9.2 mg/L, respectively) whereas PEG-coated nAg was less toxic (IC_{50}, 49.3 mg/L) (Kalman *et al.* 2015). It should be noted that the concentrations used in these studies are much higher than those typically found in the environment. Garcia-Reyero *et al*. (2015) reported multiple uniquely expressed genes after exposure of the fish *Pimephales promelas* to $AgNO_3$ (3.81 µg/L), PVP-nAg (50.3 µg/L), and citrate-nAg (50.6 µg/L) at concentrations three orders of magnitude less than those used in the algal toxicity study (Kalman *et al.* 2015). Poynton *et al*. (2012) investigated the effects of PVP-nAg (1.05 µg/L), citrate-nAg (0.43 µg/L), and $AgNO_3$ (0.08 µg/L) on gene expression profiles of *D. magna*, and demonstrated that only PVP-nAg induced DNA damage-repair genes.

2.5 The influence of co-pollutants

Despite the growing concerns over the potential biological impacts of ENPs in aquatic environments, there is only limited information on their interactions with other chemicals (Canesi et al. 2014; Farkas *et al*. 2015). For example, Farkas *et al*. (2015) investigated the effects of $nTiO_2$ on the blue mussel (*Mytilus edulis*) and determined the influence of $nTiO_2$ on the toxicity of benzo (a) pyrene. Blue mussels were exposed to either $nTiO_2$ (0.2 and 2.0 mg/L) or benzo (a) pyrene (20 μg/ L) and to combinations of these two compounds. An increase in chromosomal damage in mussel haemocytes following exposure to either $nTiO_2$ or benzo (a) pyrene was observed, and co-exposure ($nTiO_2$ and benzo (a) pyrene) induced significantly higher levels of DNA damage. A significant increase in erythrocyte nuclear abnormalities (ENA) was observed in fish, *Anguilla anguilla* at short (2, 4, 8) h and long (16, 24, 48, 72) h exposure times to silica-coated iron oxide ENPs (nFe_3O_4). *In vitro* exposure to mercury (Hg) caused a significant increase in 8-OHdG levels at 8, 24, 48, and 72 h. However, co-exposure of nFe_3O_4 with Hg showed no ENA increase at 2 h. These results suggest that nFe_3O_4-Hg complex formation effectively eliminated the DNA damage induced by exposure to nFe_3O_4 or Hg at short time periods (Mohmood *et al.* 2015).

Canesi *et al.* (2014) investigated the effects of exposure of $nTiO_2$, and co-exposure of $nTiO_2$ and 2, 3, 7, 8-Tetrachlorodibenzo-p-Dioxin (TCDD), on mussel gill cells using the comet assay. They observed statistically significant DNA damage in mussel gill cells exposed *in vitro* to the mixture ($nTiO_2$ (100 μg/L) and TCDD (0.25 μg/L) ($p < 0.05$)), but not to $nTiO_2$ alone. Similar results were reported by Banni *et al*. (2016) in *M. galloprovincialis.* Furthermore, an increase in DNA damage was observed in mussel gill cells exposed *in vitro* to TCDD ($p < 0.05$). These results suggest that the genotoxicity of $nTiO_2$ was modulated by the organic additive. A study using the 8-OHdG assay in zebrafish (*D. rerio)* larvae indicated that $nTiO_2$ treatment alone induced neither DNA damage nor generation of ROS. However, when exposed to pentachlorophenol (3, 10, and 30 μg/L) alone or in combination with $nTiO_2$ (0.1 mg/L), both DNA damage and ROS generation were observed (Fang *et al.* 2015).

The effects of nZnO and the likely modulation by co-occurring environmental stressors were assessed in the mussel, *Unio tumidus*. *U. tumidus* was exposed to nZnO (0.3 mg/L), Zn^{2+} (0.3 mg/L), the Ca-channel blocker nifedipine (Nfd 0.1 mg/L) and combinations of nZnO and Nfd at 18 ^{0}C and 25 ^{0}C for 14 days. Exposure to nZnO alone induced a ~7-fold elevation of cathepsin D activity. Cellular responses to Zn^{2+} and nZnO were markedly different, an

indication that the response to nZnO was not exclusively due to Zn release. At 25 ^{0}C nZnO induced oxidative injury, DNA fragmentation, and caspase-3 mediated apoptosis. DNA fragmentation was also induced by exposure to organic toxins (alone and in combination with nZnO). Together, these data indicate that nZnO toxicity to mussels is significantly modulated by organic pollutants, and enhanced by elevated temperatures (Falfushynska *et al.* 2015).

An *in vivo* exposure of *M. galloprovincialis* to 0.1 mg/L $nTiO_2$ to did not affect *mt-20* gene transcription but a significant up-regulation of *mt-20* gene expression, compared to controls, was observed in mussel gills exposed to cadmium dichloride ($CdCl_2$) alone or a mixture of $CdCl_2$ and $nTiO_2$ (Torre *et al.* 2015). These results indicate that the presence of $CdCl_2$ enhances the toxicity of $nTiO_2$. The influence of $CdCl_2$ (0.1 mg/L) on the genotoxicity of $nTiO_2$ (1 mg/L) to the fish, *D. labrax,* was investigated at different genotoxicity end points (nuclear and micronuclei abnormalities, DNA damage, and genome template stability). The authors reported increased DNA damage in erythrocytes from fish exposed to $CdCl_2$ ($p < 0.05$), but not to $nTiO_2$. Exposure to $nTiO_2$ alone was responsible for chromosomal alteration but ineffective in DNA damage. Co-exposure prevented chromosomal damage and led to a partial recovery of the genome template stability (Nigro *et al.* 2015). The exposure of the polychaeta, *L. acuta,* to arsenic (As, 0.05 mg/L) and $nTiO_2$ (1 mg/L), separately and in combination showed that co-exposure increased ROS levels and enhanced both lipid and DNA damage, compared to individual exposures (Nunes *et al*. 2017).

2.6 Concentration and time dependent effects

Both the duration of exposure and ENP concentration have been reported to influence the genotoxicity of ENPs to aquatic organisms. For example, comet assay results indicated both concentration- and time-dependent DNA damage in freshwater snails, *Lymnaea luteola,* exposed to nZnO, nCuO and $nTiO_2$ (Ali *et al*. 2012; Ali *et al.* 2014; Ali *et al.* 2015) and *Radix luteola* (Ali *et al*. 2016). Similarly, significant concentration-dependent DNA damage was observed in the polychaete, *Arenicola marina,* after exposure to 1–3 g/kg $nTiO_2$ (Galloway *et al*. 2010). The RAPD-PCR technique was used to assess the genotoxicity potential of $nTiO_2$ (1 and 10 μg/L) to zebrafish (*D. rerio)* exposed for 14, 21 and 28 days. The highest genotoxic effect was observed at maximum concentrations of $nTiO_2$ (10 μg/L) after 21 days of exposure. Genome stability was reduced by 37% after 14 days of exposure, and increased with longer exposure times (Rocco *et al.* 2015).

Oberholster *et al*. (2011) investigated the genotoxicity of seven different ENPs (α-alumina, γ-alumina, precipitated silica, silica fume, calcined silica fume, colloidal antimony pentoxide (Sb_2O_5), and superfine amorphous ferric oxide (Fe_2O_3) at concentrations of 5–5000 mg/kg. The percentage survival of *Chironomus tentans* decreased with increasing ENPs concentrations. The highest growth inhibition and DNA damage was observed at 5000 mg/kg, however, such high concentrations are not representative of the ENPs concentrations expected (or measured) in natural aquatic systems. A number of other recent studies (Wise *et al*. 2010; Munari *et al*. 2014; Boran and Ulutas 2016; Schiavo *et al.* 2016; Sharma *et al.* 2016) have demonstrated both concentration- and time-dependent toxicity for a range of different ENPs and different test organisms (including the fish species *Oryzias latipes* and *D. rerio*, the mussel *Mytilus edulis*, and the alga *Dunaliella tertiolecta)*.

2.7 Illumination effects

Photoactive ENPs show photo-dissolution under exposure to visible and ultraviolet (UV) light (Han *et al.* 2010), and induce oxidative stress effects through the production of ROS (Cho *et al*. 2004). No increase in DNA damage was observed, for example, in fish cell line (RTG-2 cells) exposed to $nTiO_2$ (50 µg/mL) over 4 h (comet assay), 24 h (modified comet assay), or 48 h (MN assay) exposures in the absence of UVA irradiation, while a significant increase in DNA strand breaks was observed under UVA exposure. The observed DNA damage was linked to delayed cell proliferation, cell death and the induction of MN (Vevers and Jha 2008). The presence of $nTiO_2$ (0.01 mg/L) under UV radiation caused higher plasmid DNA and chromosome damage in *E. coli* compared to the effect of UV radiation alone (Huang *et al.* 2008). Both nZnO and $nTiO_2$ are well known as photoactive ENPs (Kim and An 2012).

Ultraviolet A irradiation of $nTiO_2$ treated cells showed an increase in DNA damage in a fish cell line (GFSk-S1) compared to $nTiO_2$ only, most likely due to hydroxyl radicals (Reeves *et al.* 2008). Fish (*Piaractus mesopotamicus*) were exposed to $nTiO_2$ (0, 1, 10, and 100 mg/L) under visible light, and visible light with UV light (22.47 J/cm^2/h) over 96 h (Clemente *et al.* 2013). Under both illumination conditions, exposure to 100 mg/L $nTiO_2$ inhibited intracellular acid phosphatase activity. However, this concentration is unlikely to be found in the environment. Under visible light, an increase in metallothionein levels in fish exposed to 1 mg/L $nTiO_2$ was observed. These findings demonstrate the importance of considering experimental conditions in nanoecotoxicological tests.

2.8 Particulate vs ionic species effects

Some ENPs undergo dissolution upon exposure to aqueous media. It is therefore important to understand if the toxicity observed is a product of the nanoparticulate or of the ionic form of the ENPs. A concentration dependent up-regulation of ROS related genes in *D. rerio* after exposure to nZnO (1-100 mg/L) was not duplicated after exposure to Zn^{2+}, an indication that the genotoxicity was due to the ENPs (Zhao *et al*. 2013). A study on the genotoxicity of nCu, nCuO, $nCu(OH)_2$ (CuPro and Kocide), micro Cu, micro CuO, and Cu^{2+} to *E. coli* and *Lactobacillus brevis* indicated that nCu and nCuO were more genotoxic than their microsized counterparts at the same Cu concentration. Although the toxicities of nCu and nCuO were comparable to those of the ionic Cu species, the latter form was more genotoxic. The degree of degradation of plasmid DNA in *E. coli* and *L. brevis* was also in the order of Cu^{2+} > nCu > microCu (Kaweeteerawat *et al*. 2015). The findings suggest a "Trojan-horse" mechanism for nCu toxicity, where ENPs are internalized within cells and then release high levels of toxic ions (Hsiao *et al*. 2015).

The expression of stress-related genes (metallothionein, HSP 70, GST, p53, CYP 1A and transferrin gene) in the fish, *O. latipes*, was investigated in the presence of nAg and ionic Ag. The results suggested that these two Ag forms have different mechanisms of toxicity: the nAg (1 and 25 µg/L) induced cellular and DNA damage, carcinogenic and oxidative stress, and induced genes related to metal detoxification, metabolic regulation and radical scavenging, whereas ionic Ag induced inflammatory responses and metallic detoxification processes and the ionic Ag caused a lower overall stress response than nAg (Chae *et al.* 2009).

A liver gene expression analysis in the organism *Oncorhynchus mykiss*, using a DNA microarray of 207 stress-related genes, showed statistical insignificant differences as about 12% of the target genes responded to nAg, while 10% of the target genes responded specifically to ionic Ag (Gagné *et al.* 2012). A comparison of the effects of Nickel (Ni) ENPs and ionic Ni on the ascidian, *Ciona intestinalis*, showed, that the particulate forms were generally more toxic than the ionic form of the metal (Gallo *et al.* 2016). A similar trend was observed in the exposure of the mussel *Mutilus trossulus* to nCuO (c.f. $CuCl_2$), using DNA damage as the determinant of genotoxicity (Chelomin *et al.* 2017).

2.9 Conclusions

The ENPs most commonly tested for genotoxicity are $nTiO_2$ and nAg. This is expected because both ENPs are among the most widely produced and are used in many consumer products and industrial applications (PEN, 2014; Hansen *et al.* 2016). A wider scope of genotoxicity studies, using other metal based ENPs, is therefore required.

The most commonly used test organisms for ENP genotoxicity studies are fish, invertebrates (daphnia, mussels, ascidian, snails, midge, clam and polychaetes) and bacteria. This is attributed to the availability of standardized test protocols and, to some extent, the position of the taxa in the food chain. No reports of genotoxicity studies using aquatic plants were found. We conclude that there is a clear need for further ENP genotoxicity research using a wider range of test organisms, particularly those that play important trophic roles in complex aquatic communities.

Gene expression analysis, the Ames test, the micronucleus test, the chromosome aberration assay, the comet assay and the DNA ladder assay have been widely used in genotoxicity studies. The comet assay is the mostly frequently used, presumably because of its technical simplicity and ability to detect low levels of DNA damage. Many of the ENPs assessed were found to cause genotoxic responses in the form of chromosomal fragmentation, DNA strand breaks and alterations in gene expression profiles. DNA and chromosome damage increased with increasing exposure times and ENP concentrations, but decreased as the size of ENPs increased. Different coatings on ENPs exhibited different toxicities. Genotoxicity was also found to be highly assay dependent. Where two assays were used in the same study, significant differences in the degree of toxicity were often noted. Our conclusion is that interpretations based on a single assay method may be misleading and *in vitro* tests need to be validated by *in vivo* tests, as suggested by the OECD.

Most published studies did not report the physical properties of the ENPs (e.g., surface coating, surface area, morphology, and surface charge). As a result, not all variables are considered in the analysis of the apparent effects of the ENPs and the interpretation of their mechanisms of action. Nevertheless, there is some evidence that the physicochemical properties of ENPs are an important factor in their toxicity potential. A more complete characterisation of ENPs before, during and after introduction into the exposure media is therefore necessary to

understand any changes in physicochemical properties and the impacts of those changes on ENPs genotoxicity.

We noted that in most studies where genotoxicity was reported, experiments were conducted at high ENPs concentrations unlikely to be found in the environment and under acute exposure conditions. ENPs exposure concentrations have been identified as one of the major concerns in hazard assessments (Holden *et al.* 2016), and it is recommended that high ENPs concentrations, that may alter media conditions, should be avoided. In practical terms, the highest ecological impacts from ENPs may result from chronic low dose exposures. We therefore strongly recommend that ENPs genotoxicity studies are conducted under chronic exposure conditions and at low ENP concentrations.

We also note that studies on the relative contributions of the particulate and ionic forms of ENPs to genotoxicity are often contradictory. We therefore recommend that such future studies should always include control experiments using the soluble form of the metal. The use of dynamic dissolution assays to measure dissolution rate in appropriate aqueous media would also be highly informative. We particularly note that studies that link the physical characteristics of ENPs (particle size, crystal structure, morphology, surface area, surface charge and surface coating) to the observed genotoxicity are limited in number and scope, and we stress that more work is required to address this knowledge gap.

CHAPTER 3

Behaviour of gold and cerium oxide nanoparticles in different ecotoxicological media: influence of nanoparticle size, surface coating and media composition

3.1 Introduction

The use of different types of nanoparticles (NPs) in consumer products such as medicinal products, food packaging and electronics (Zhao and Castranova 2011) is rapidly increasing, raising concerns on the behaviour and potential toxic effects of NPs in the environment (Farre´ *et al.* 2011; Sauve and Desrosiers 2014). Research on the behaviour and transformation processes of NPs in aquatic systems is necessary because of the known extent to which NPs currently enter aquatic systems (Gottschalk *et al.* 2013; Mahapatra *et al.* 2015; Bäuerlein *et al.* 2017; Peters *et al*. 2018). Understanding the stability of NPs is essential in order to evaluate their bioavailability and potential toxic effects toward living organisms (von Moos and Slaveykova 2014). Metal-based NPs (term includes both metal and metal oxide NPs) have been incorporated in many products with many different purposes (www.nanoproject.org). Among metal-based NPs, cerium oxide NPs are among the top ten NPs produced worldwide (Keller and Lazareva 2014). The use of CeO_2 NPs in diesel engines (O'Brien *et al.* 2011), as fuel additives (Cassee *et al*. 2011), and in paints and cosmetics (Quik *et al.* 2010) has greatly increased their production, which has been estimated from between 100 and 1000 tonnes/year (Piccinno *et al.* 2012) to 10 000 tonnes/year (Keller and Lazareva 2014). Currently, there has been an increased use of gold (Au) NPs in electronics and medicine (Mahapatra *et al.* 2015). Drug delivery applications using Au-NPs are forecasted to have a 21 % share of the USD 136 billion total markets of nano-drug delivery products by 2021 (Cientifica Ltd. 2012). The increased use of Au NPs could result in greater risk of environmental release and exposure at low concentrations (Tiede *et al.* 2009; Mahapatra *et al.* 2015).

When introduced into aquatic environments, metal-based NPs undergo numerous physicochemical transformations (Lee and Ranville 2012) and are subjected to environmental processes, such as dissolution, agglomeration, aggregation and sedimentation (Xiao *et al.* 2018). This, in turn, determines the fate, transport and toxicological properties of NPs (Lowry *et al.* 2012). Characterization of NP colloidal stability in the exposure medium is necessary for both scientific and regulatory viewpoints (Langevin *et al.* 2018). Nanoparticle exposure to such complex media alters the properties of NPs such as size, aggregation, agglomeration, surface chemistry and surface charge (Vijayakumar, 2014), attributed to the high ionic strength

of the exposure medium (Pamies *et al.* 2014), and adsorption of biomolecules from the medium on the NP surface (Cedervall *et al*. 2007; Monopoli *et al.* 2012). This leads to changes in the biological traits or toxicology of NPs (Canesi *et al.* 2012; Lee and Ranville 2012). Furthermore, the stability, reactivity and bioavailability of the NPs are influenced by the physicochemical characteristic of aquatic media such as media composition, pH, ionic strength and NOM (Batley *et al.* 2013; Clavier *et al.* 2015; Wang *et al.* 2016; Peng *et al.* 2017; Xiao *et al.* 2018). The high ionic strength of biological media and the presence of electrolytes can result in aggregation or agglomeration of NPs. Among transformations, agglomeration is an important factor affecting the behavior of NPs in the environment (von Moos and Slaveykova 2014; Röhder *et al.* 2014), as it transforms NPs into multi-micron clusters, which alters the NPs size distribution, transport characteristics and biological interactions (Peng *et al*. 2017).

Transformed NPs induce deleterious effects on organisms, such as reduced cell viability, enhanced oxidative stress and DNA damage (Goswami *et al.* 2017). The need for greater NP stability in high ionic strength media has driven researchers to explore different coating agents (Jokerst *et al.* 2011; Nghiem *et al.* 2012; Pyshnaya *et al.* 2014). To improve stability, NP surface chemistry has been modified with various capping agents. However, the coatings also change their bio-interactions (Medina-Velo *et al*. 2017).

Understanding the environmental fate and behaviour of NPs after release into aquatic systems is essential for the prediction of the environmental implications of nanotechnology (Ellis *et al.* 2018). To date, there are limited data on the stability of Au and CeO_2 NPs in toxicological media. The study of NP transformations is important as they affect exposure dose, the nature of the toxicant and have a direct impact on all (eco) toxicology data (Tejamaya *et al.* 2012). Therefore, the present study seeks to provide information on the fate and behaviour of Au and CeO_2 NPs in biological media. To achieve our aim, the behaviour of NPs was assessed in three ecotoxicological media representative of different compositions widely used for the toxicity assessment of NPs to aquatic biota: 10% Hoagland's medium (10% HM- used for duckweed and aquatic higher plants), BG-11 algal medium (10% BG-11-used for *algal sp*), dechlorinated tap water (DTW- used for *Daphnia* sp.) and de-ionised water (DIW - control) in the absence of organisms.

3.2 Materials and Methods

3.2.1 Characterization of Au and CeO_2 NPs

Commercial citrate and BPEI coated-gold nanosphere suspensions were purchased from Nanocomposix, San Diego, United States. The suspensions were of three average sizes: 5, 20 and 40 nm, according to the manufacturer's specifications. Suspension of uncoated CeO_2 NPs (nominal size <25 nm as reported by the supplier) were purchased from Sigma Aldrich (Johannesburg, South Africa). Before starting the exposure experiments, both the size and morphology of NPs were determined by high-resolution transmission electron microscope (HRTEM; JEOL JEM 2100, Japan operating at 200 kV). Nanoparticle samples were prepared for TEM characterization by placing 10 µL of aqueous NP suspension on a carbon-coated copper grid which was covered and allowed to air-dry at room temperature (ca. 25 °C) prior to TEM analysis. Ten images were taken for all NPs and the average of 100 particles was used for size estimations. The hydrodynamic diameter (HDD) and zeta (ζ) potential (a key indicator of the stability of colloidal dispersions) of NPs in DIW (15 MΩ/cm) and in testing media, 10% HM (Sigma Aldrich, catalog number-H2395), dechlorinated tap water (DTW) and 10% BG-11 algal medium were determined using dynamic light scattering (DLS; Malvern Zetasizer Nano ZS, Malvern Instruments, UK) and the nanoparticle tracking analysis (NTA, NanoSight NS500, NTA 3.0 software, Amesbury, UK).

The DLS was operated at an angle of 173° at a controlled temperature of 25 °C and measurements were taken at position 5.50 mm. Each sample had ten measurements of 60 s with three repetitions. For NTA, three runs of 60 s each were performed for each replicate at a fixed temperature of 25 °C. Both methods are based on the detection of the Brownian motion of particles in a liquid. Therefore, particles are illuminated by a laser and the scattered light is detected. The relationship between the size of a particle and its speed due to Brownian motion is defined in the Stokes-Einstein equation. All analyses for the mean sizes, size distributions, and ζ potentials were done in triplicate in all media types. The changes in the stability of CeO_2 and Au NPs in solution were examined by ultra-violet visible spectroscopy (UV-vis; DR3900 spectrophotometer, Germany) at a wavelength range of 320–800 nm at 0, 2, 6, 24 and 48 h. All samples were analyzed using a quartz cuvette with a 1 cm optical path length.

3.2.2 Exposure media

Three exposure media types: 10% Hoagland's medium (Hoagland and Arnon 1950), dechlorinated tap water (USEPA 2002) and 10% BG-11 algal medium (DEEEP, 2004) were used in this study. The composition of the media is shown in Table A3.1 – A3.3. The 10% HM was prepared by dissolving 0.16 g Hoagland-modified basal salts mixture purchased from Sigma Aldrich (Johannesburg, South Africa) in 1 L DIW. The solution was hand shaken for about 1 min to facilitate dissolution of the salts mixture and was stored in the dark for at least 24 h before use. The 10% BG-11 algal medium (referred to here as BG-11) was prepared as described in Direct Estimation of Ecological Effect Potential guideline (DEEEP, 2004). All chemicals were purchased from Sigma Aldrich and were dissolved in 1 L DIW. The BG-11 algal medium was autoclaved at 121 °C. For DTW, the tap water was filtered through a 0.45 µm filter and de-chlorinated by adding 12.5 mL of Tetra AquaSafe solution into 25 L of tap water. The pH of all the exposure media was adjusted to 7.0-7.5 with 0.1M HCl or NaOH.

3.2.3 Data Analysis

Three replicate tests were performed for each treatment, and the data are presented as means ± standard deviations (SD). The comparison between the treatments was performed by GraphPad Prism 7.04 software (GraphPad Prism software, La Jolla, CA, USA). A p-value < 0.05 was considered statistically significant.

3.3 Results and Discussion

3.3.1 Nanoparticle characterization

Characterisation with TEM revealed that both citrate and BPEI-coated Au NPs had mixed morphologies with spherical shapes being predominant whereas the rods and pentagons were few (Figure 3.1 (a-f)). Cerium oxide NPs showed a mixture of shapes including triangular, tetrahedral and hexagonal (Figure 3.1 (g)). The mean sizes (n=100) were observed to be in agreement with the supplier's specifications (Table 3.1). Although the majority of CeO_2 NPs was confirmed to be less than 25 nm, the formation of larger and more compact crystalline structures was observed. The reported measured size range by TEM (15-50 nm) referred to here is a diameter range regardless of particle shape. The presence of agglomerates larger than 25 nm suggested that, even after sonication, primary particle sizes could not be attained (Nur *et al.* 2015). Only a few independent crystals were found, most clustered together. The current findings agree with other studies (Singh *et al*. 2014; Leung *et al.* 2015; Alam *et al.* 2016;

Oriekhova and Stoll 2016; Yang *et al*. 2017), where CeO_2 NPs agglomerated and were of irregular or mixed shapes and non-homogeneous primary particle size variation.

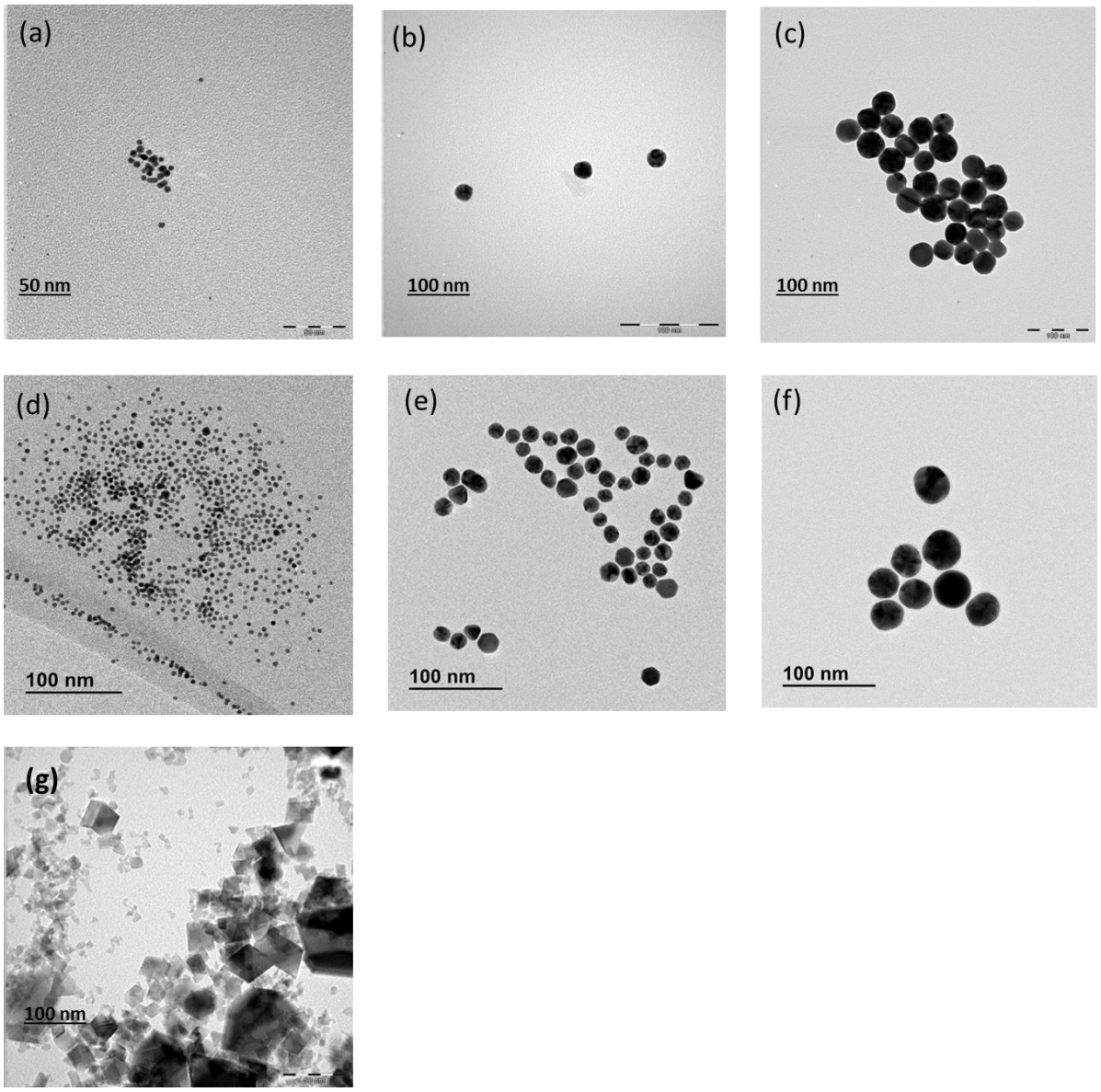

Figure 3.1: TEM images of Au NPs (a) 5 nm-Cit, (b) 20 nm-Cit, (c) 40 nm-Cit, (d) 5 nm-BPEI, (e) 20 nm-BPEI, (f) 40 nm-BPEI and (g) CeO_2 NPs.

Table 3.1: mean sizes of NPs as reported by TEM

	Manufactured size (nm)			
	5	20	40	<25
Cit-Au NPs	5.63 ± 1.38	20.71 ± 2.48	41.32 ± 4.02	
BPEI-Au NPs	5.03 ± 0.57	19.08 ± 2.65	41.33 ± 2.80	
CeO_2 NPs	-	-	-	15- 50

Results are reported as means (n =100) ± standard deviations.

3.3.2 Behaviour of NPs in different biological media

Figure 3.2 shows HDDs of Au and CeO_2 NPs analysed with DLS at different time intervals at pH 7. The 20 and 40 nm Au NPs of both coatings showed smaller sizes in DIW compared to biological media over 48 h, attributed to the high ionic strength of the medium (Peng *et al.* 2015). However, the same trend was not observed for both 5 nm Au NPs; these NPs were highly unstable in DIW compared to 20 and 40 nm Au NPs, reaching 657±195 nm (cit) and 1 021±409 nm (BPEI) in just 2 h. The agglomeration was size dependent; with 5 nm Au NPs agglomerating more rapidly and 40 nm Au NPs the least (agglomeration order: 5 nm > 20 nm> 40 nm). Similarly, high agglomeration from smaller sized NPs compared to larger counterparts has been observed elsewhere (Thwala *et al.* 2013; Iswarya *et al.* 2016). The effects are probably because of the increased surface area (Auffan *et al.* 2009). Agglomeration followed the order DTW > BG-11 > 10 HM > DIW for BPEI Au NPs; whereas, high agglomeration was observed in BG-11 for cit Au NPs and in DTW for CeO_2 NPs. The findings indicated that the surface coating of NPs and media constituents influence their agglomeration.

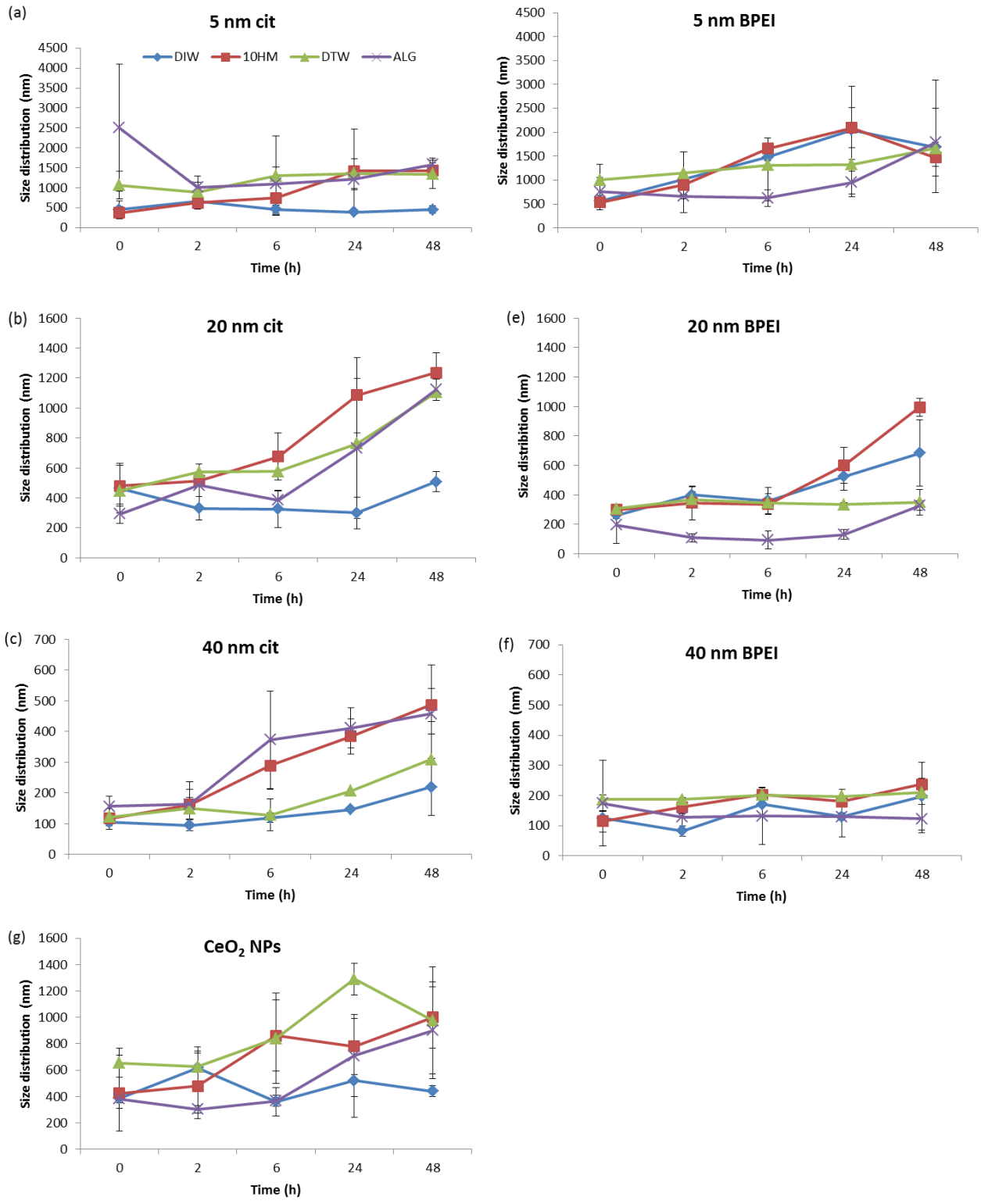

Figure 3.2: Influence of NP size and surface coating on the size distribution of Au and CeO_2 NPs in different media types over 48 h. Results are reported as means±standard deviations (*n* =3).

The fast agglomeration observed in all media types indicated rapid instability of CeO_2 NPs (Figure 3.2 (g)). The presence of non-spherical shaped NPs as observed by TEM may have introduced some uncertainties during size data evaluation due to the assumption of a spherical shape for all particles (Metreveli *et al*. 2016). Both NTA and DLS assume spherical NP shape, therefore the large particle sizes in DIW water could be because of heterogeneous light scattering due to particle shape. The NPs agglomerated immediately after introduction into DIW with HDD of 389±79 nm (0 h), 619±156 nm (2 h) reaching 441±43 nm after 48 h. Since CeO_2 NPs were not spherical, such baseline HDD can only represent agglomeration trend than the actual size distribution of the NPs. Similarly, uncoated CeO_2 NPs (28.4 nm) formed agglomerates between 200 -300 nm in ultrapure water (Oriekhova and Stoll 2016). After 48 h, the HDD in DIW decreased, but increased in 10HM and DTW suggesting agglomeration was induced by the high ionic strength of the testing media (Zhang *et al.* 2017). No further increase in size was observed after 24 h in DIW and DTW, suggesting that larger particles drop out of the solution and no longer contribute to size measurement.

Both Au and CeO_2 NPs exhibited net negative ζ potentials throughout the experiment duration (Figure 3.3). The ζ potentials were more negative in DIW than in the biological media for both NP types. The ζ potential shift towards zero indicated instability of NPs driven by the high ionic strength in different media types (Booth *et al*. 2015); and is consistent with the rapid agglomeration observed. Furthermore, the presence of phosphates in the medium has been reported to influence changes in ζ potentials and stability of CeO_2 NPs (Röhder *et al.* 2014). Contrary to the manufacturer's data of positively charged BPEI Au NPs, current findings showed that all BPEI Au NPs were negatively charged in all media types including DIW at pH 7. The pH of the media was then varied (pH 3, 5, 7, 9 and 11) in order to evaluate if the ζ potential values were pH dependent. The 5 and 20 nm BPEI Au NPs were only positively charged at pH 3 over 48 h in DIW, while 40 nm BPEI Au NPs were negatively charged at all tested pH ranges in all media types. The 5 BPEI Au NPs were positively charged at pH 3 and 5 from 0 to 24 h but became negatively charged at 48 h in 10 HM. Although Au NPs are known to be stable, current findings indicate that their stability changes during shipping (changes in temperature) and storage. Gold NPs have been reported to display alterations in ζ potentials after agglomeration (Pamies *et al.* 2014; Balog *et al*. 2015). Furthermore, Au NPs are known to have better stability at pH 10 compared to pH 6 and pH 7 (Tripathi *et al.* 2016).

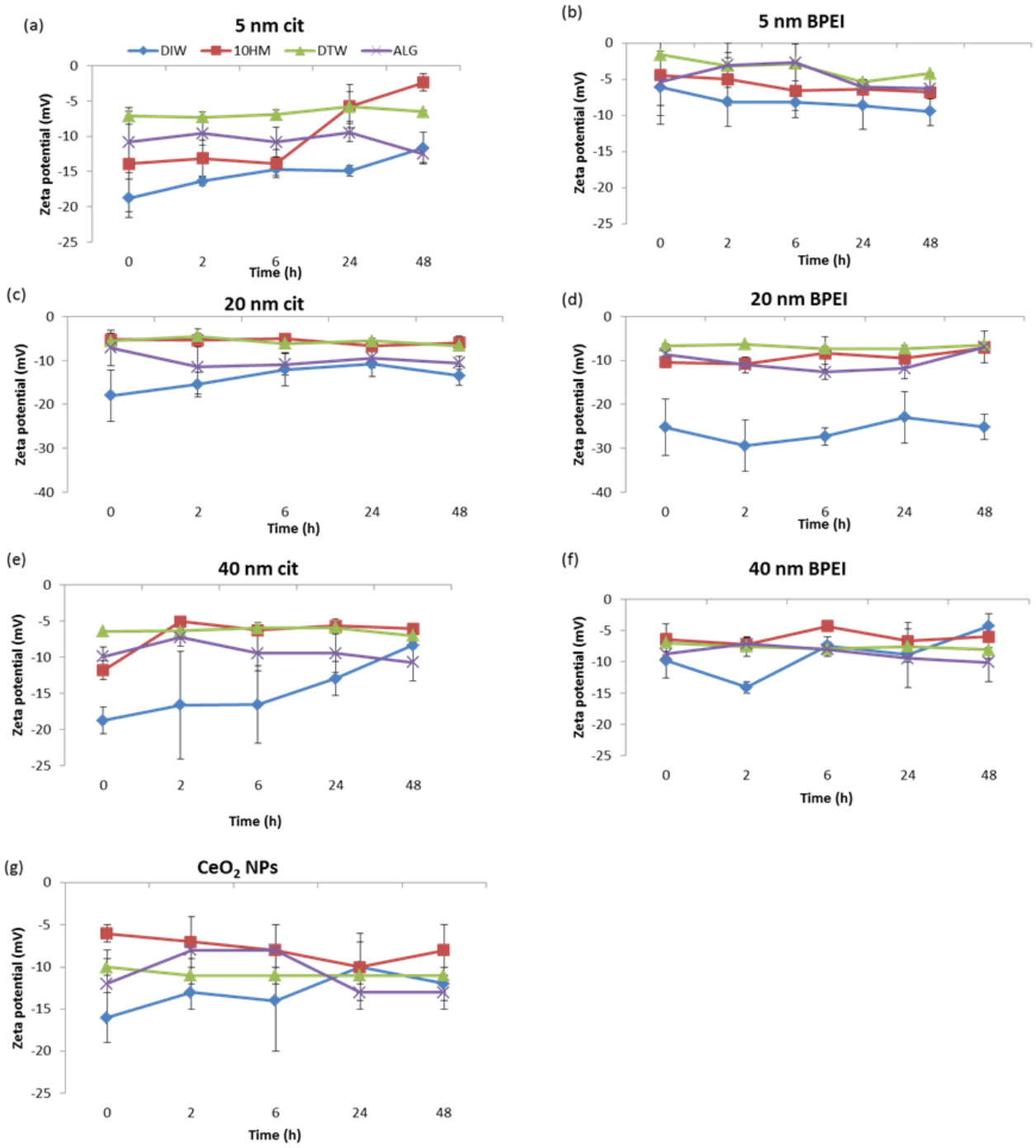

Figure 3.3: Influence of NP size and surface coating on the ζ potential of Au and CeO_2 NPs in different media types over 48 h. Results are reported as means±standard deviations (*n* =3).

The 5 nm Au NP samples were excluded from NTA analysis as the technique cannot measure sizes below 10 nm (NanoSight NS500 operating manual, Version P553S). Particle concentration in DIW was higher than in biological media attributed to the low ionic strength of DIW (Figures 3.4 and 3.5). The media contain mostly divalent cations ($Ca^{2+,}$ Mg^{2+} or Na^{2+}; Tables A3.1 and A3.2) that have been reported to induce higher agglomeration (Baalousha *et*

al. 2013; Xiao *et al.* 2018), thus causing sedimentation of NPs.The size distribution data obtained for all NPs using NTA (Figures 3.4 and 3.5) were smaller than that of DLS in all media types, in agreement with previous findings (Domingos *et al*. 2009; Kadar *et al.* 2010; Tantra *et al*. 2011; Oriekhova and Stoll 2016). This is because NTA measures NPs on a particle by particle basis as they move by Brownian motion in the solution (Hole *et al.* 2013). The different size measurement techniques can give complementary information on particle suspensions. In general, the polydispersity of NP suspensions poses a major challenge for accurate size determination. Furthermore, the difference in sizes obtained by DLS and TEM is due to size and shape polydispersity owing to the different measurement techniques (Zhang *et al.* 2012; Majedi *et al*. 2014; Miao *et al*. 2015).

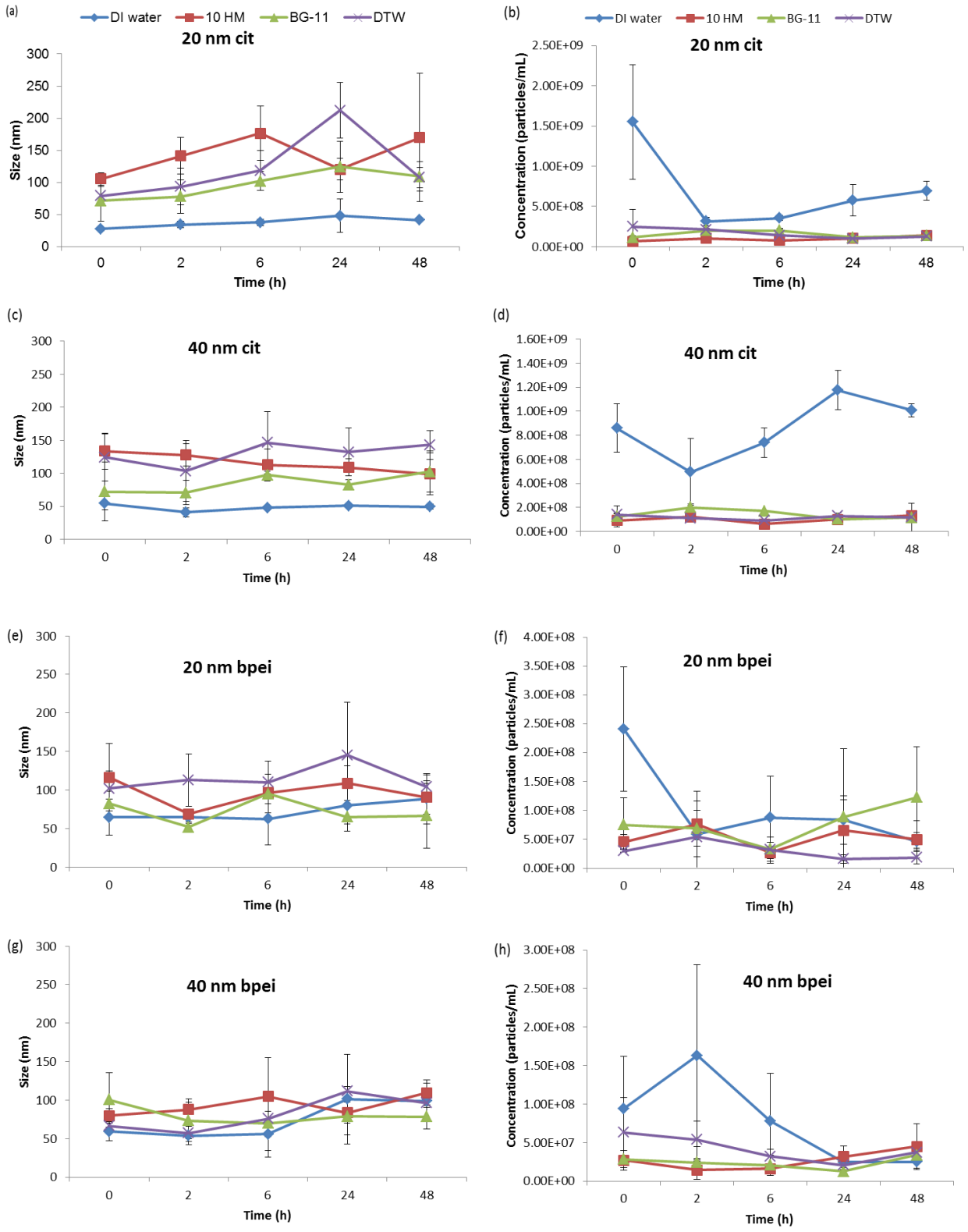

Figure 3.4: Au NPs size (a, c, e and g) and concentration (b, d, e, f and h) characterization data using NTA. Bars denote standard deviations (n = 3).

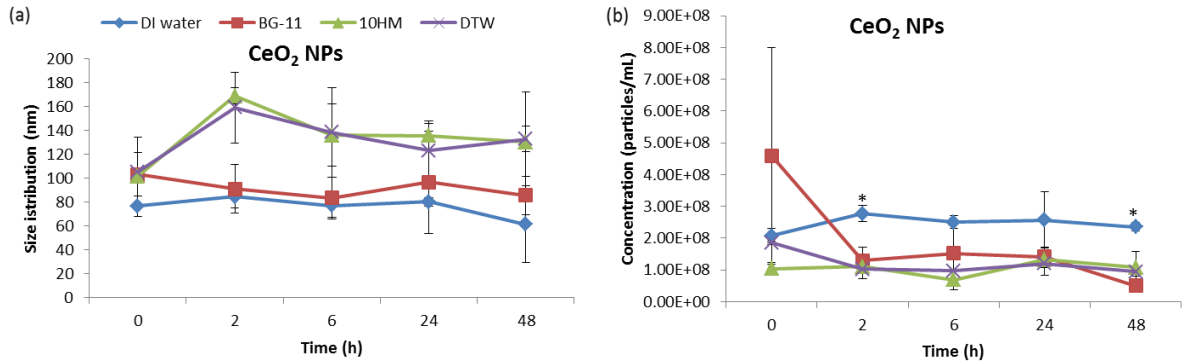

Figure 3.5: Characterization data of CeO_2 NPs using NTA (a) size and (b) concentration. Bars denote the standard deviations (n = 3). * denote statistical difference between DIW and biological media using one-way ANOVA, $p < 0.05$.

3.3.3 Ultraviolet visible absorption

UV–vis spectra provide information on the behaviour of NPs such as aggregation or agglomeration, dissolution and sedimentation (Afshinnia *et al*. 2018). The UV-visible absorbance spectra of CeO_2 NPs are shown in Figure 3.6. Studies have reported CeO_2 NPs to exhibit a strong absorption between 316 and 342 nm when dispersed in water (Dao *et al*. 2011; Girija *et al*. 2011; Tantra *et al*. 2011; Chelliah *et al.* 2012). The absorbance was higher at the maximum wavelength (λ_{max}) from 0 – 6 h for DTW followed by 10 HM, BG-11 then DIW (Figure 3.6 (a- c)). A decrease in absorbance at λ_{max} was observed after 24 and 48 h which either indicates NP agglomeration and/or dissolution (Baalousha *et al*. 2013; Baalousha *et al.* 2015). However, based on HDD results in this study, a decrease in absorbance was attributed to agglomeration. In 10 HM, CeO_2 NPs were highly unstable as indicated by a dramatic decrease in absorbance after 24 and 48h (Figures 3.6 (d), and (e)), suggesting loss of particle concentration (Tantra *et al.* 2011; Tejamaya *et al.* 2012) or sedimentation/aggregation (Römer *et al.* 2011; Hughes *et al.* 2017). In addition, the type of cations and anions present in the exposure medium is important for the agglomeration of NPs. For example, divalent cations have been reported to induce higher agglomeration than monovalent cations (Chen and Elimelech 2006; Huynh and Chen 2011; Baalousha *et al*. 2013; Topuz *et al*. 2014, 2015, Xiao *et al.* 2018).

The stability of the Au NPs was dependent on the size, surface coating of the NPs and the properties of the exposure medium, consistent with previous studies (Pinto *et al.* 2007; Pereira *et al.* 2014; Sharma *et al.* 2014). A size dependent absorption peak, for example, at 510, 520 and 525 nm was observed for 5, 20 and 40 cit-Au NPs, respectively in DIW (Figure 3.7 (a), (b) and (c)). The absorption peak for all BPEI –Au NPs was at 525 nm (Figure 3.7 (d), (e) and (f)). Earlier studies have reported that similarly sized Au NPs with different coatings exhibited different stabilities (Hitchman *et al.* 2013), with BPEI coated particles being more stable than citrate coated NPs (Diegoli *et al.* 2008). These findings suggest that the surface coating of NPs influences their stability. Furthermore, current findings are in good agreement with the results of Feichtmeier *et al.* (2015) where the maximum absorption of cit-Au NPs was observed at 523 nm.

A decrease in absorbance was observed after 2 h for BPEI-Au NPs in DIW followed by a peak broadening after 24 and 48 h for 40 BPEI-Au NPs (Figure 3.7 (f), suggesting particle agglomeration (Baalousha e*t al*. 2013; Baalousha *et al.* 2015). The 20 nm cit-Au NPs remained stable for the entire test duration and 40 nm cit-Au NPs became less stable after 48 h as indicated by a decrease in absorbance in DIW. A decrease and increase in absorbance in DTW on the same sample as time progresses indicated that both agglomeration and de-agglomeration processes took place. Gold NPs were unstable in the biological media (Figures 3.8-3.10.) compared to DIW as indicated by (i) an increase or decrease in absorbance at λ_{max} (ii) peak shift- appearance of a second peak at longer wavelengths (*ca.* 600 nm) and (iii) broadening of peaks. These observations suggested a loss of particle concentration from the solution as evident from the NTA results because of agglomeration (Römer *et al.* 2011) driven by the high ionic strength of the exposure medium (Clemente *et al.* 2013). The cit-Au NPs in media were stable for only 6 h, after which broadening of peak and a decrease in absorbance was observed. Wang *et al.* (2014) reported similar findings on cit and cetyl-trimethyl ammonium bromide (CTAB) coated Au NPs. For BPEI-Au NPs, the absorbance started to decrease after 2 h (indicative of stability changes), suggesting agglomeration as a second surface plasmon resonance (SPR) peak was observed at a longer wavelength (*ca*.600 nm). This shift indicated changes in the Au NPs surrounding layer due to a coating (Nghiem *et al.* 2010), suggesting the formation of BPEI-Au NPs complex as reported for other coatings such as, PVP-Au NPs, or polyethylene glycol (PEG)-Au NPs and bovine serum albumin (BSA)-Au NPs (Nghiem *et*

al. 2012; Barreto *et al.* 2015).

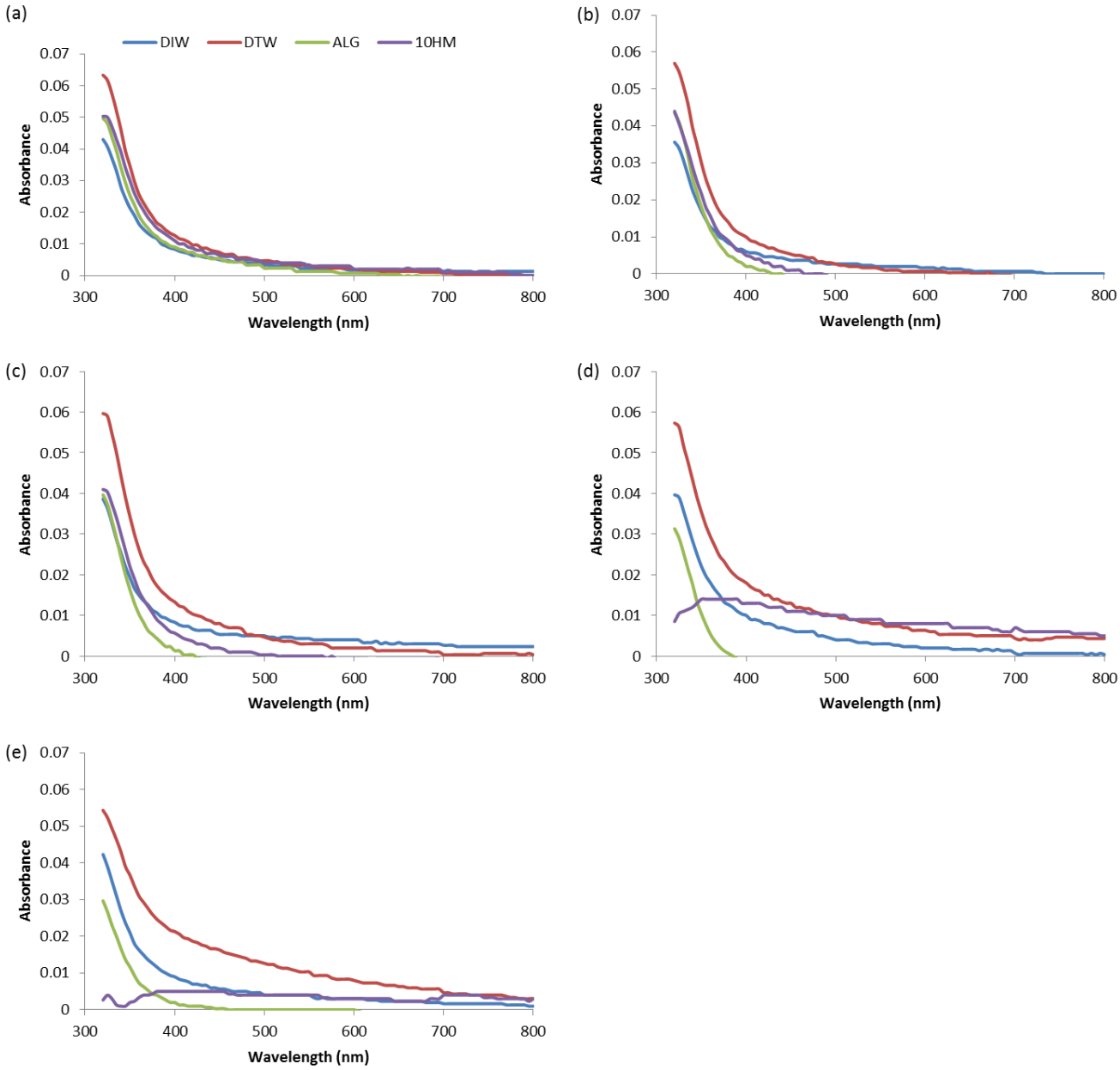

Figure 3.6: UV-visible absorption spectra of CeO_2 NPs in different media types at different time intervals, (a) 0 h, (b) 2 h (c) 6 h, (d) 24 h and, (e) 48 h. Data is presented as means ($n = 3$).

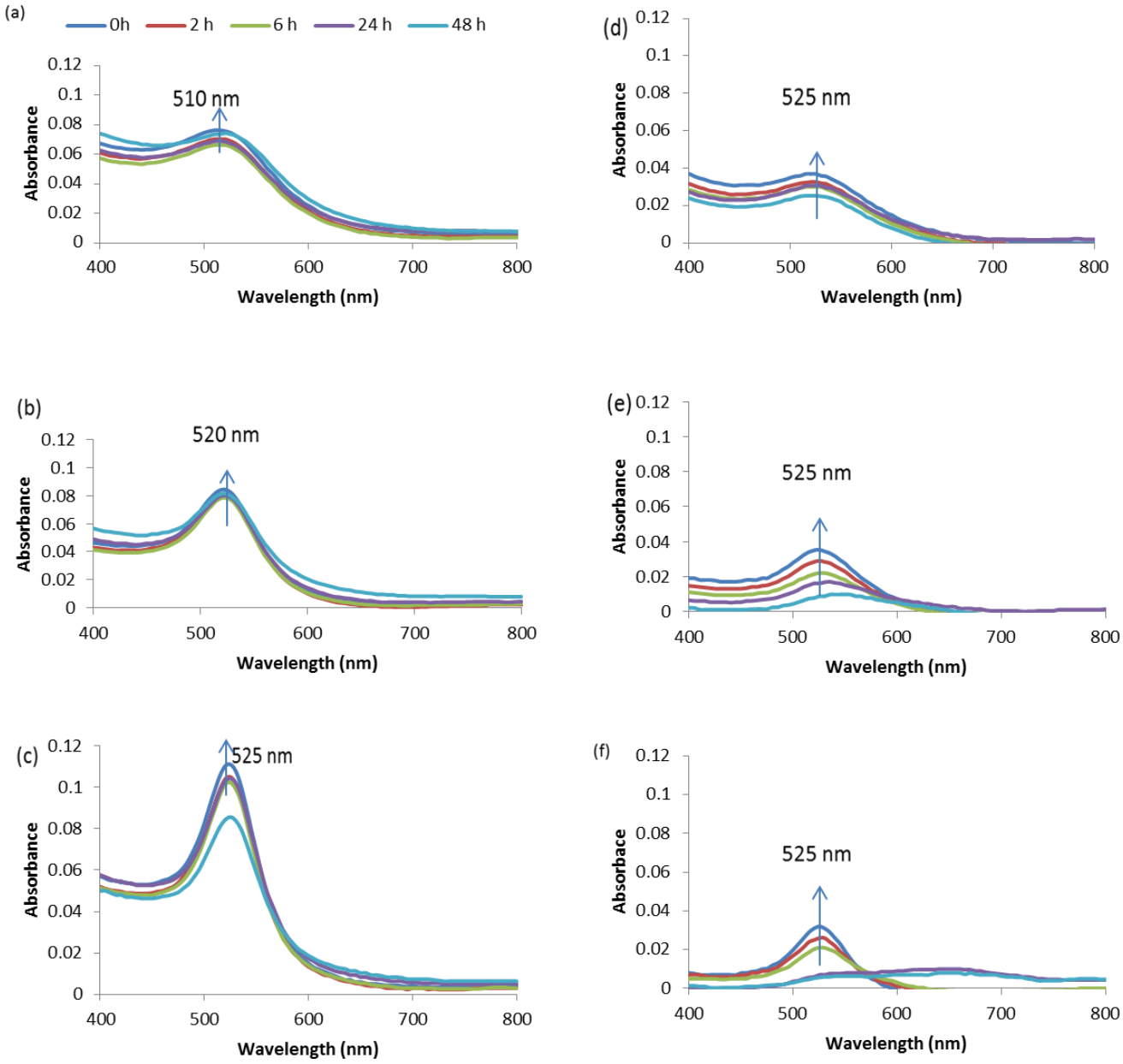

Figure 3.7: UV-vis of Au NPs in DIW (a) 5 nm Cit, (b) 20 nm Cit, (c) 40 nm cit, (d) 5 nm BPEI, (e) 20 nm BPEI and (f) 40 nm BPEI. Results are reported as means (*n* =3). Arrows show the position of the main peak.

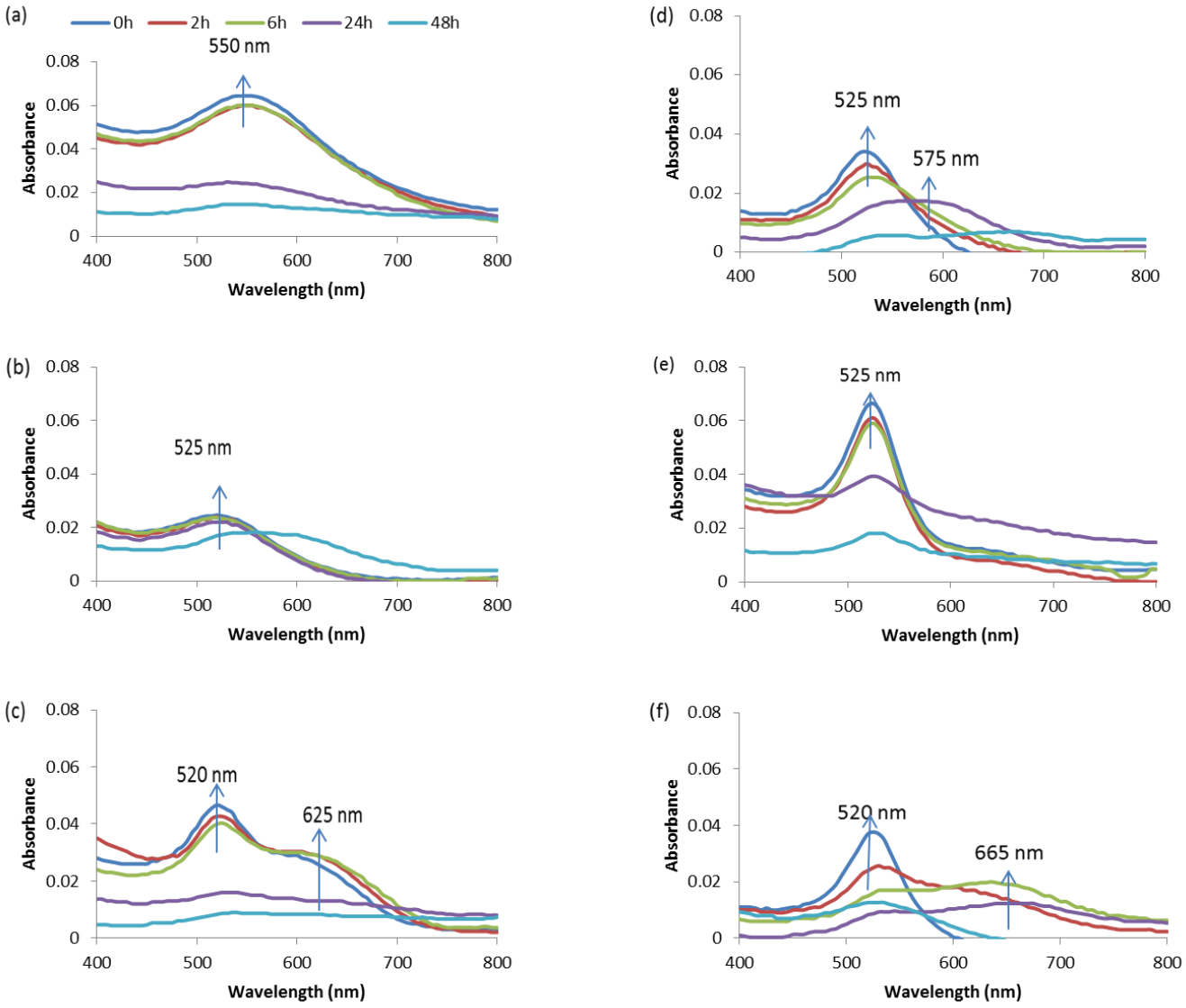

Figure 3.8: UV-vis of Au NPs in 10 HM (a) 5 nm Cit, (b) 20 nm Cit, (c) 40 nm cit, (d) 5 nm BPEI, (e) 20 nm BPEI and (f) 40 nm BPEI. Results are reported as means (*n* =3).

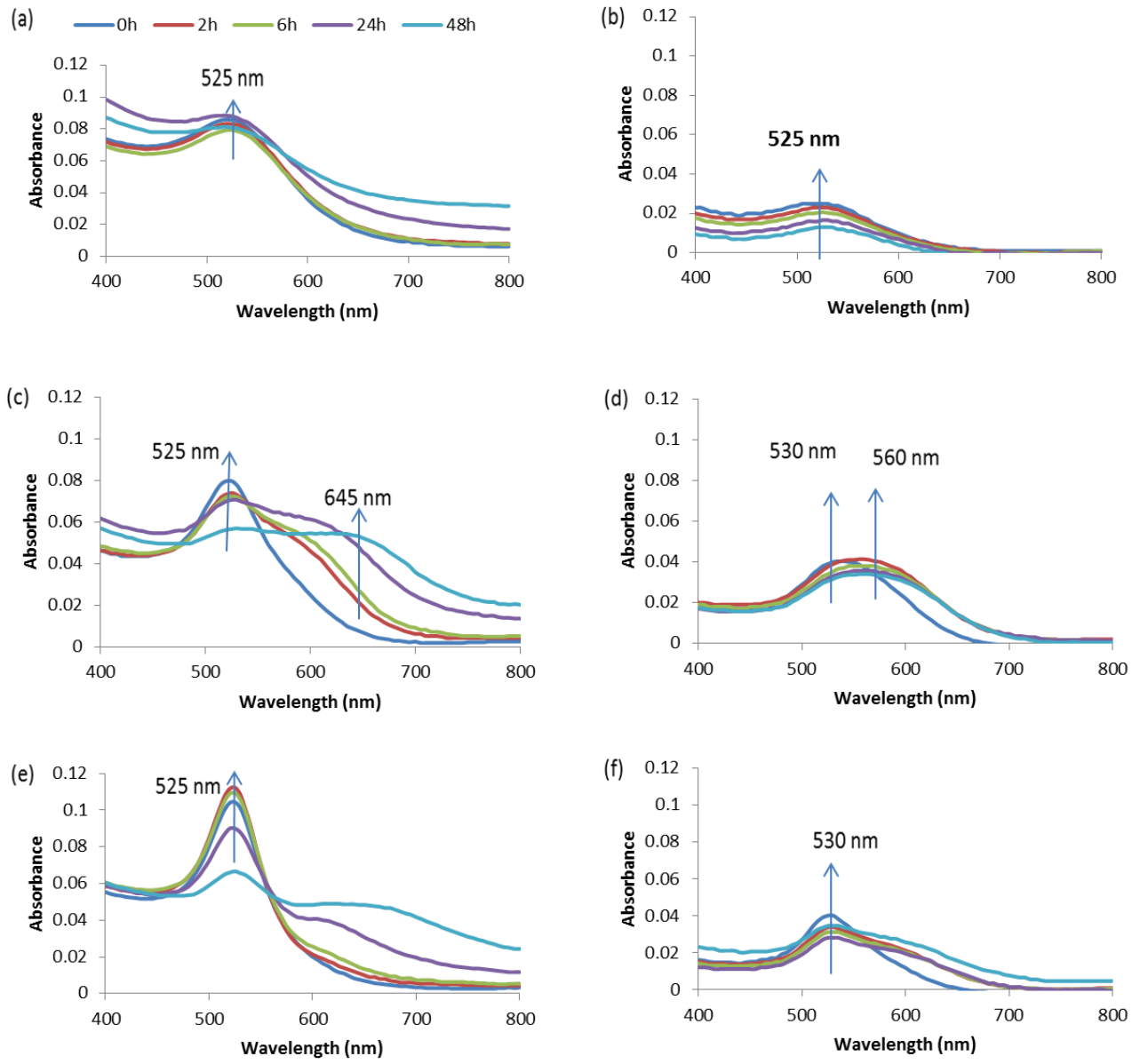

Figure 3.9: UV-vis of Au NPs in DTW (a) 5 nm-Cit, (b) 5 nm-BPEI, (c) 20 nm-Cit, (d) 20 nm-BPEI, (e) 40 nm-Cit, (f) 40 nm-BPEI. Results are reported as means (*n* =3).

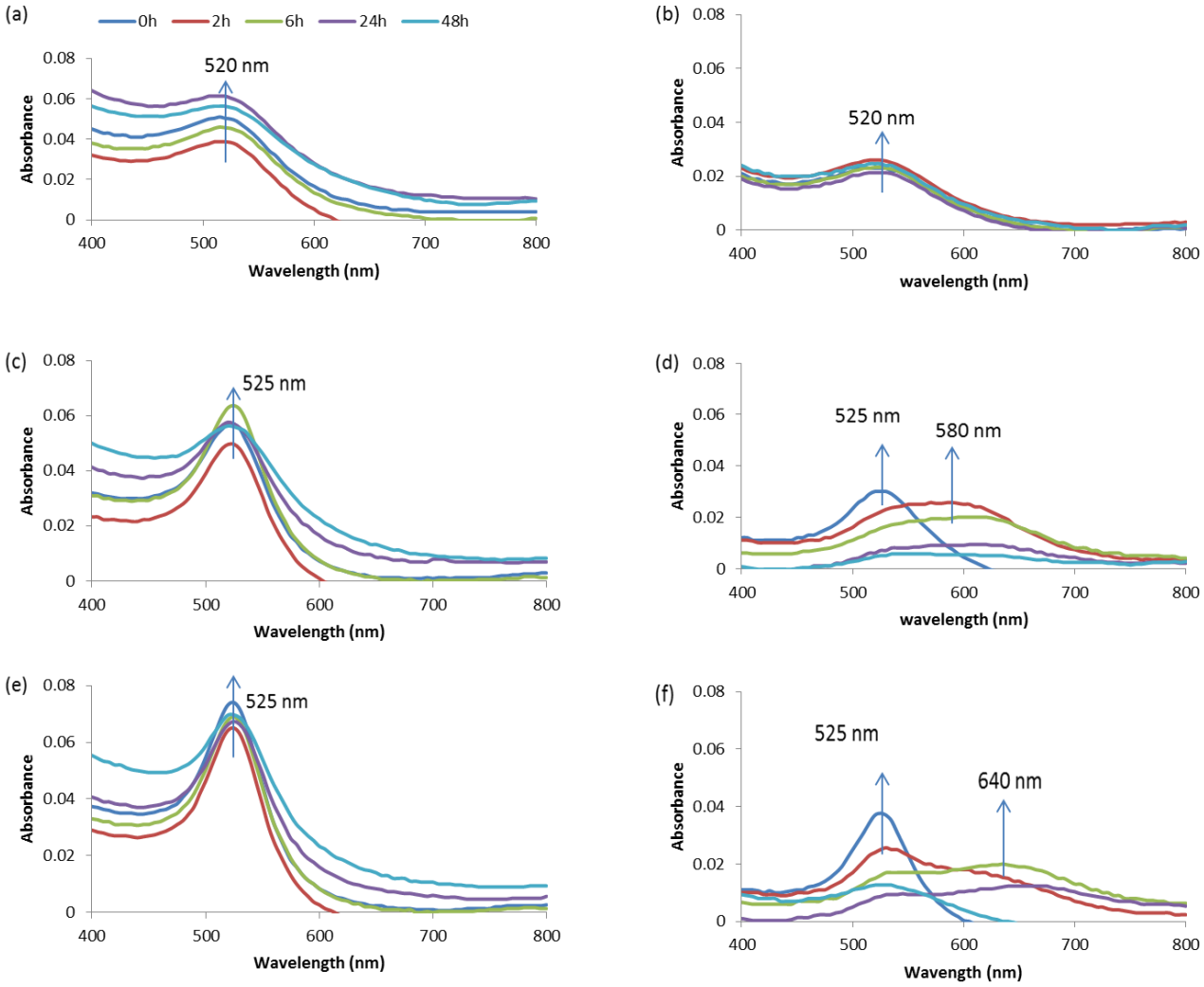

Figure 3.10: UV-vis of Au NPs in BG-11 algal medium (a) 5 nm-Cit, (b) 5 nm-BPEI, (c) 20 nm-Cit, (d) 20 nm-BPEI, (e) 40 nm-Cit, (f) 40 nm-BPEI. Results are reported as means (n =3).

3.4 Conclusions

The need to characterize the physicochemical properties of NPs before and during NP exposure is essential in understanding the environmental fate and behaviour of NPs. Stability (agglomeration and surface charge changes) of Au and CeO_2 NPs were investigated in different media types using NTA, DLS and UV-Vis spectrophotometry. Good agreement on the primary NP sizes was achieved by TEM. The use of multimethod approach for NP sizing increases the accuracy of data due to the complexity of NP samples and the limitations of each analytical technique. The use of light scattering techniques for size determination is limited for non-spherical particles. Therefore, for accurate determination of NP size, analytical techniques suitable for non-spherical shaped particles and standardised sample preparation methods are recommended.

The much broader particle size distribution observed indicated (i) formation of agglomerates, (ii) instability of Au and CeO_2 NPs in ecotoxicological media and (iii) inaccuracy of light scattering techniques in size analysis for non-spherical NPs. Instability of Au NPs was size and surface coating dependent and was confirmed by a decrease in absorbance, broadening of SPR peak over time and an increase in size distribution at pH 7, which is a biologically relevant pH. The agglomeration of NPs in biological media tends to limit their performance and has a strong influence on their final fate in the environment. An increased stabilization results in better transport in the environment. The zeta potential of NPs at the same pH is affected by differences in media composition. The ζ potentials were more negative in low ionic strength DIW compared to high ionic strength media. Agglomeration increased with a decrease in NP primary size. The knowledge of NP transformations in biological media with the known composition can be translated into understanding the fate and behaviour of NPs in natural environmental systems. Data can also help to correlate the properties of NPs with (eco) toxicological responses, thus enabling prediction of the behaviour of NPs in natural environments.

CHAPTER 4

Bioaccumulation of Au and CeO_2 NPs by an aquatic higher plant (*Salvinia minima)*

4.1 Introduction

The annual production of nanoparticles (NPs) is expected to reach 58,000 tonnes by 2020 (Royal Society and Royal Academy of Engineering Report on Nanotechnology, 2004). Due to their unique optical properties, low inherent toxicity and relatively simple surface functionalization (Bodelón *et al.* 2017), gold nanoparticles (Au NPs) are widely used in biomedicine (Abadeer and Murphy 2016; Dykman and Khlebtsov 2016; 2017), for photothermal therapy (Zong *et al.* 2017), drug delivery (Niikura *et al.* 2013; Zhang, 2015), and as catalysts (Priecel *et al.* 2016; Villa *et al.* 2016). Cerium oxide NPs (CeO_2 NPs) find wide applications like UV absorbent in sunscreens (Wu *et al.* 2010), fuel additive (Cassee *et al.* 2012), and in biomedicine (Xu and Qu 2014). Nanoparticles can persist in the aquatic systems due to their aggregation, sedimentation, and slow degradation rate. This, in turn, increases uptake, accumulation, and bio-magnification of NPs in the food chain (García 2011).

Accumulation of NPs in aquatic higher plants is driven by numerous factors, and the detailed account is found in recent reviews (Ma *et al.* 2010; Miralles *et al.* 2012; Schwab *et al*. 2016; Thwala *et al.* 2016). For instance, the accumulation of NPs has been reported to be dependent on the plant type, size of the cell wall pores, as well as size, concentration, morphology and surface properties of the NPs (Glenn et al. 2012; Taylor *et al*. 2014; Judy *et al.* 2011; 2012; Koelmel *et al.* 2013; Dan *et al.* 2016; Raliya *et al.* 2016; Song and Lee 2016; Khataee *et al.* 2017). Accumulation and transport of NPs also depend on the nature of the plant tissue and the presence of UV radiation (Regier *et al.* 2015). For example, exposure of aquatic macrophyte *Elodea nuttallii* to copper oxide (CuO) NPs at 10 mg/L or dissolved Cu (II) at 256 µg/L showed stronger Cu accumulation in plants exposed to CuO NPs relative to Cu (II). Accumulation increased for both copper types in the presence of UV radiation (Regier *et al.* 2015). A concentration dependent accumulation in *Spirodela polyrrhiza* roots was observed following exposure to CuO NPs (3 and 6 mg/L) where the presence of NPs in root tissues was apparent; whereas no evidence of Cu was observed from 1 mg/L exposure (Khataee *et al.* 2017).

In addition, findings of Glenn and Klaine (2013) indicated a size-dependent uptake of Au NPs in *Azolla caroliniana* where 4 nm NPs were readily taken up compared to larger sizes of 18 and 30 nm. A species dependent accumulation was reported in *Hydrilla verticillata* and

Phragmites australis exposed to ZnO (1000 mg/L). Results indicated higher Zn accumulation in *P. australis* than *H. verticillata*; indicating physiological differences among aquatic plants (Song and Lee 2016). Furthermore, the transformation of accumulated NPs was reported in *Landoltia punctate* exposed to different forms of Ag (Ag^0 or Ag_2S NPs, or $AgNO_3$). After 24 h, all three forms of Ag accumulated partially in the roots regardless of the form. Once associated with plant tissue, Ag^0 NPs transformed into silver sulfide and silver thiol species, suggesting plant defence mechanisms were active on the root surface (Stegemeier *et al.* 2017).

To date, there is limited but contradictory information on the accumulation of metal- and metal-oxide NPs in aquatic higher plants linked to factors associated with their inherent physicochemical properties, and water chemistry of the exposure media (Glenn *et al.* 2012; Glenn and Klein 2013; Li *et al.* 2013). Review of the literature data show Au NPs as least investigated, and as a result, the mechanisms of their uptake into plants are far from being determined. Au NPs uptake or translocation is poorly understood and the results are inconclusive (Zuverza-Mena *et al.* 2017). In addition, published data do not offer a clear relationship between the observed bioaccumulation and the influence of physical-chemical properties of NPs and plants characteristics, which limits the ability to compare the results nor draw firm conclusions on the key driving factors. For example, Nekrasova *et al.* (2011) reported Cu accumulation to decrease with increasing exposure concentration (0.025-5 mg/L) in *E. densa*, attributed to an increase in agglomeration. While accumulation of $CuSO_4$, bare (0.7-4.5 g/L) and styrene-co-butyl acrylate coated CuO NPs (0.3-1.2 g/L) increased with increasing NP exposure concentration in *Lemna gibba* for 48 h (Perreault *et al.* 2014). Zinc accumulation in *S. polyrhiza* was directly related to exposure concentration (1-50 mg/L) (Hu *et al.* 2013). The underpinning mechanisms of accumulation are also not well studied (Zhang *et al.* 2014, 2015; Movafeghi *et al.* 2017).

Since aquatic higher plants are at the base of aquatic food chains, they are likely to act both as reservoirs of NPs and as sources for subsequent trophic transfer (Thwala *et al.* 2013; Thwala *et al.* 2016). In addition, higher level toxicity effects such as growth inhibition and reduction in chlorophyll content have been reported in aquatic higher plants exposed to NPs (Song and Lee 2016; Blinova *et al*. 2018). Sub-cellular effects such as the induction of oxidative stress, reduction of cell viability, and effects at the genetic level can also occur in organisms exposed to NPs (Bacchetta *et al.* 2017; Goswami *et al.* 2017; Mahaye *et al.* 2017; Movafeghi *et al.* 2017).

Poor knowledge on the exact impact(s) of NPs accumulation in plants is exacerbated by the fact that published data were derived based on very high NPs exposure concentrations unlikely to be found in the aquatic systems (Gottschalk *et al.* 2009; Musee, 2011; Baalousha *et al.* 2016). For example, only at 300 mg/L Ag NPs were statistically significant changes in growth characteristics induced in *A. thaliana* plants under laboratory conditions (Sosan *et al.* 2016), which is much higher compared to the predicted environmental concentration of Ag NPs in different environmental compartments (Gottschalk *et al.* 2009; Holden *et al.* 2016; Choi *et al.* 2017). Therefore, to draw meaningful conclusions, studies should be conducted using environmentally relevant NP exposure concentrations, and for extended periods (chronic exposure conditions). The goal of the present study was to investigate the bioaccumulation of Au and CeO_2 NPs by the free-floating aquatic higher plant *Salvinia minima* under chronic exposure conditions (14 d) at environmentally relevant NP concentrations. Holden et al. (2014) showed that ENPs concentrations were lowest ($\leq$ 0.001 ppm) in surface water, wastewater treatment plant (WWTP) effluent and solid fractions (soil, sediments and biosolids). The highest concentrations were reported in WWTP effluent (0.11 to 1 ppm) and biosolids (>1000 ppm). *S. minima* was used as a model plant because it can readily be cultured under laboratory conditions, has a high growth rate, can rapidly accumulate metals and provides the necessary plant biomass for ecotoxicological assessments (Sune *et al.* 2007; Prado *et al*. 2010). Thus, the specific aims of the study were to: (i) determine the influence of particle size and surface coating on Au NP accumulation; and (ii) elucidate possible route(s) of Au and CeO_2 NPs accumulation in *S. minima*.

4.2 Materials and Methods

4.2.1 Nanoparticle characterization

Commercial citrate (cit) and branched polyethyleneimine (BPEI) coated-gold nanosphere suspensions were purchased from Nanocomposix, San Diego, United States. The suspensions were of three average sizes of 5, 20, and 40 nm according to the manufacturer's specifications. Suspensions of uncoated CeO_2 NPs (nominal size <25 nm as reported by the supplier) were purchased from Sigma Aldrich (Johannesburg, South Africa). Before starting the exposure experiments, both size and morphology of Au and CeO_2 NPs were determined by high-resolution transmission electron microscope (HRTEM; JEOL JEM 2100, Japan operating at 200 kV) as reported in Section 3.2.1.

4.2.2 Exposure medium

The 10% Hoagland's medium (10 HM) was prepared by dissolving 0.16 g Hoagland-modified basal salts mixture purchased from Sigma Aldrich (Johannesburg, South Africa) in 1 L DIW (15 MΩ.cm). The solution was stored under dark conditions for a minimum of 24 h before use. An exposure concentration of 1 mg/L for each NPs size-type was prepared in 10 HM in triplicate, and bath sonicated for 30 min before initiating the experiment. During the 14 d experiment, the particle size distribution and concentration of the NPs were recorded using NTA at 24 h intervals. The NTA was set to perform three runs of 60 s each for each replicate at a fixed temperature of 25 °C. The 5 nm Au NP samples were excluded from NTA analysis as the technique cannot measure sizes below 10 nm (NanoSight NS500 operating manual, Version P553S).

4.2.3 Test organism maintenance

Samples of *S. minima* plants were collected from Hartbeespoort Dam, North West Province, South Africa (25.7401° S, 27.8592° E), and transported to the Council for Scientific and Industrial Research (CSIR) laboratories in sampling site water. In the laboratory, the plants were rinsed in tap water to remove attached debris, and thereafter, were acclimatised in a glass tank containing 5 L of 10 HM under natural light conditions for 2 weeks. The culturing tanks were cleaned, and 10 HM solution was replaced after every 5 d.

4.2.4 Bioaccumulation

Plants from the culturing tank(s) were manually dried and 500 mg fresh weight biomass of healthy plants was used as the test sample. The plants were exposed to 50 mL of 10 HM containing 1 mg/L of Au or CeO_2 NPs in 250 mL acid pre-washed glass beakers covered with transparent perforated parafilm to minimize evaporation. The exposed plants were kept in a shaking incubator at 100 rpm for 14 d at 21 ± 2 °C under 16: 8 h light: dark conditions, and light intensity of 5000 lux. After 2, 7 and 14 d of exposure, plants were harvested and dried on absorbent paper for *ca* 1 min before weighing to determine the fresh biomass weight. The roots and fronds were separated, dried at 80 °C for 6 h in acid-washed and pre-weighed crucibles, and then their dry weight was obtained after cooling. Dried plant material within the crucible was dry-ashed at 530 °C for 12 h in a furnace (Delta DTA9696, England), and then digested using 250 µL HNO_3 until the ash was dissolved before dilution was done using DIW to achieve a 5% acid concentration. The resultant aqueous suspension was centrifuged at 3880 rpm for 10

min and total Au and Ce in the supernatant was measured using inductively coupled plasma mass spectrometry (ICP-MS) (Agilent ICP MS 7500cs, Agilent Technologies, Inc. 2006 Santa Clara, USA).

4.2.5 Internalization or adsorption of NPs by plant

After 14 d exposure, plant roots and fronds were separated. Each sample was fixed in 2.5% glutaraldehyde for 24 h and washed three times in 0.1M K-phosphate buffer pH 7.1 for 20 min, post-fixed with osmium tetroxide (OsO_4) for 2 h, and re-washed as above. Samples were then dehydrated using increasing ethanol concentrations (35, 50, 70, and 90% (aqueous, v/v) and then three times at 100%) where each cycle lasted for 20 min and left in 100% ethanol overnight. After dehydration, samples were embedded into a 50:50 mixture of 100% ethanol: quetol epoxy resin for 1 h, 100% quetol epoxy resin for 4 h, then into new 100% quetol epoxy resin. The samples were polymerized at 60 °C in a drying oven for 36 h before they were sectioned (90–100 nm thick) using an ultra-microtome and examined using TEM coupled with energy dispersive X-ray spectroscopy (EDX) to confirm the presence or absence of Au and Ce.

For the adsorption studies, the roots and fronds were separated after 14 d exposure, covered with aluminium foil and immediately frozen in liquid nitrogen. The samples were either immediately freeze-dried under vacuum using Advantage Pro Lyophilizer (SP Scientific, USA) for 28 h, or stored at - 80 °C until freeze-drying was undertaken. After freeze-drying, roots and fronds were mounted on scanning electron microscopy (SEM) stubs, carbon coated and viewed using SEM (SEM JOEL JSM 7500F; Japan using the secondary electron (SE) detector at an acceleration voltage of 2 kV); coupled with the EDX detector to map Au and Ce distribution at 15 kV.

4.2.6 Data analysis

Three replicates were performed for each treatment, and the data are presented as means ± standard deviation (SD). The significance of comparisons between the treatments was determined using GraphPad Prism 7.04 software (GraphPad Prism software, La Jolla, CA, USA), and $p < 0.05$ was considered significant.

4.3 Results and Discussion

4.3.1 Nanoparticle characterization

TEM results indicated that both cit- and BPEI-Au NPs had mixed morphologies with spheres as predominant compared to rods and pentagons shapes. CeO_2 NPs TEM results showed mixed morphologies, namely: triangular, tetrahedral and hexagonal (Figure 3.1, Section 3.3.1). The mean sizes obtained were in good agreement with the supplier's specifications (Table 3.1, Section 3.3.1). In 10 HM solution, 5 nm Au NPs were observed to agglomerate more rapidly compared to larger ones (20 and 40 nm) (Figure 4. 1). Agglomeration of metallic NPs has been reported to be size dependent (Zhang *et al.* 2011; Thwala *et al.* 2013; Iswarya *et al*. 2016) with higher agglomeration observed in smaller-sized NPs due to their high surface energy, and large surface area (Chen *et al.* 2007; Christian *et al.* 2008; Auffan *et al*. 2009; Ji *et al*. 2010). Herein, high agglomeration was observed in 10 HM than in DIW for both NP types. This is because Hoagland's medium has numerous cations and anions that, in turn, induced the higher agglomeration of NPs compared to low ionic strength DIW (Song *et al.* 2013b).

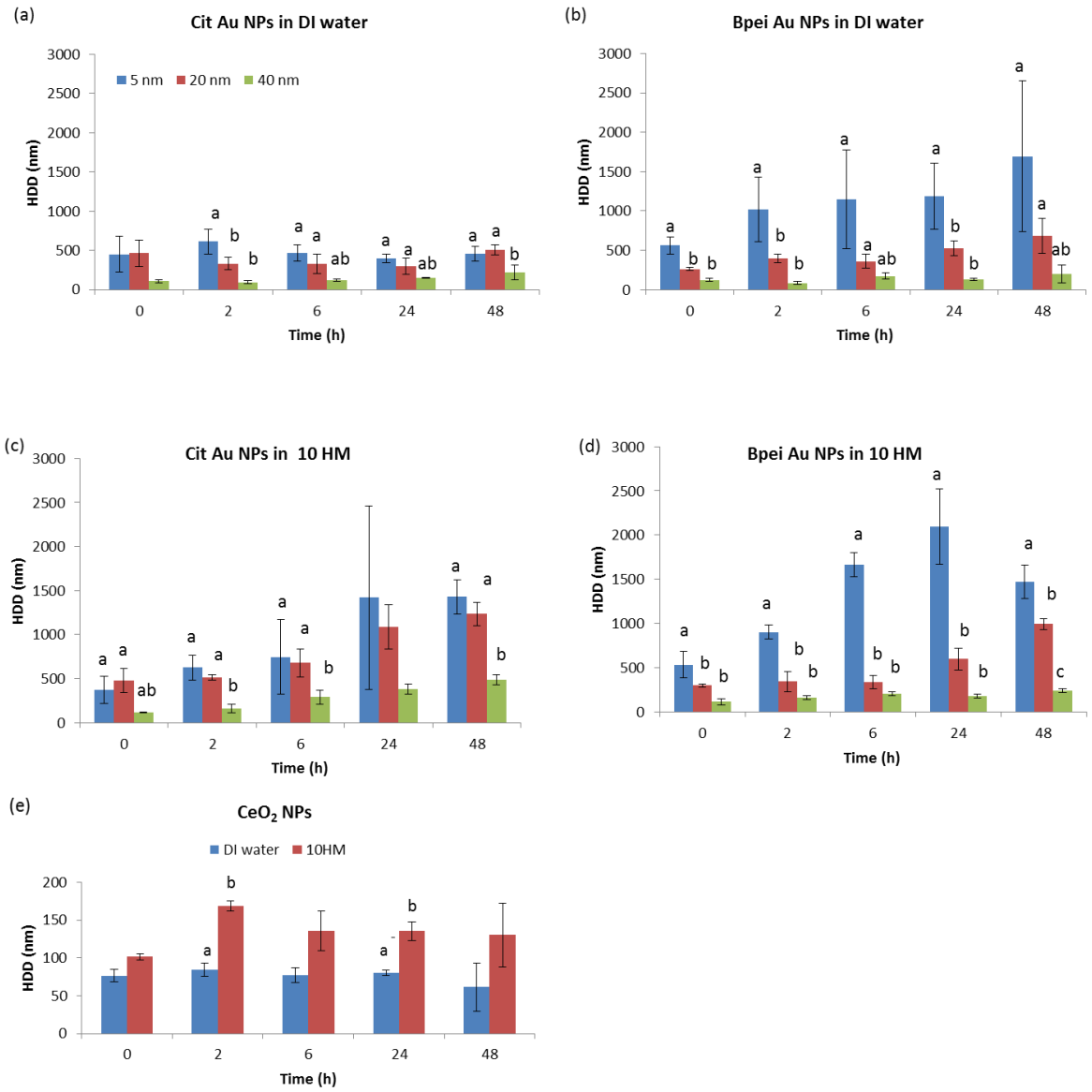

Figure 4.1: Hydrodynamic sizes of Au NPs measured using DLS in DIW (a and b), 10 HM (c and d), and (e) CeO_2 NPs over 48 h. Bars denote standard deviations (n = 3). Different letters indicate statistical difference between NP sizes using One-way ANOVA, $p < 0.05$.

4.3.2 *S. minima* growth rate

Exposure of *S. minima* to Au and CeO_2 NPs at concertation of 1 mg/L for 14 d did not cause significant loss of biomass ($p>0.05$), and no cellular necrosis (i.e. fronds remained green) was observed, irrespective of NPs sizes and coating type as well as NPs type (Figure 4.2). These findings indicate low toxicity of Au NPs and agree with earlier observations for *Ceratophyllum demersum*, where exposure of *C. demersum* to higher exposure concentrations of Au NPs

(1.18–3.64 mg/L) for17 d did not induce toxicity. However, over extended exposure periods (28 d) phytotoxicity was observed (Ostroumov *et al.* 2014). Exposure of *Hordeum vulgare* plants to cit-Au NPs (10 nm, 1–10 µg/mL) for 21 d showed growth promotion at low NP exposure concentrations (1 µg/mL) but inhibition at higher Au-NP concentrations (10 µg/mL). Seed germination was not affected (at 1 to 10 µg Au/mL); however, plant growth yielded insignificant lower biomass at exposure concentrations ≥ 3 µg Au/mL (Feichtmeier *et al.* 2015). Low concentrations of NPs have also been reported to activate the repair mechanism of plants and enhance their growth (hormesis effect) (Barrena *et al*. 2009). CeO_2 NPs have been shown to cause stimulatory (200–500 mg/L) and inhibitory (> 1000 mg/L) effects on *Arabidopsis thaliana* growth and the reduction in growth was linked to particulates forms of NPs and not Ce ionic species (Yang *et al.* 2017). However, the concentrations inducing plant growth inhibition are deemed too high and unlikely to be found in the environment. Furthermore, a study by Rico *et al.* (2015) reported an accumulation of CeO_2 NPs on *Hordeum vulgare* without effects on seed germination and root elongation. However, CeO_2 NPs may induce toxicity in plants at molecular levels (Rico *et al*. 2013a; Rico *et al.* 2013b). Therefore, to draw meaningful conclusions, genotoxicity data should support cytotoxicity studies on plants. In addition, long-term exposure may enhance the interaction of plants with NPs and facilitate the detection of toxicity effects at different growth stages of the plant.

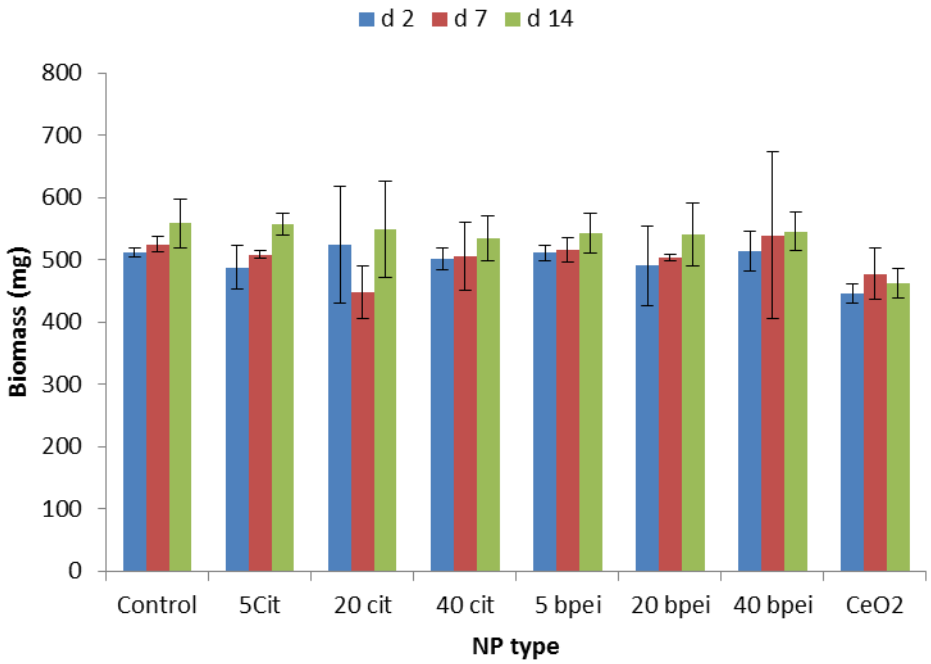

Figure 4.2: Plant biomass for treated plants and a control (plants exposed to 10 HM without NPs) over 14 d. Results are reported as mean values (*n*= 3) and bars denote standard deviations.

4.3.3 Adsorption of Au and Ce on plant tissues

Results indicated the interactions of the plants with Au and CeO_2 NPs occurred through root surface adsorption (Figure 4.3). Bright white materials were observed on the roots surface. These spots were analysed by EDX to confirm the presence of Au and Ce on the roots (Figure A4.1). To determine whether Au and Ce were retained on the root surface or could be transported up to the fronds, the concentrations of Au and Ce in plant roots and fronds were analysed using ICP-MS. Au and Ce concentrations in both roots and fronds of the control (plants exposed to 10 HM without NPs) were below detection levels (< 0.001 µg/mg). Findings for 20 and 40 nm Au NPs showed that plant roots generally accumulated higher NP concentrations compared to fronds (Figure 4.4 (c-f)), and hence in agreement with the literature (Shi *et al.* 2014; Conway *et al.* 2015). Nonetheless, roots may not be the only site of NPs absorption as aquatic plants can absorb nutrients via both roots and leaves (Denny, 1972).

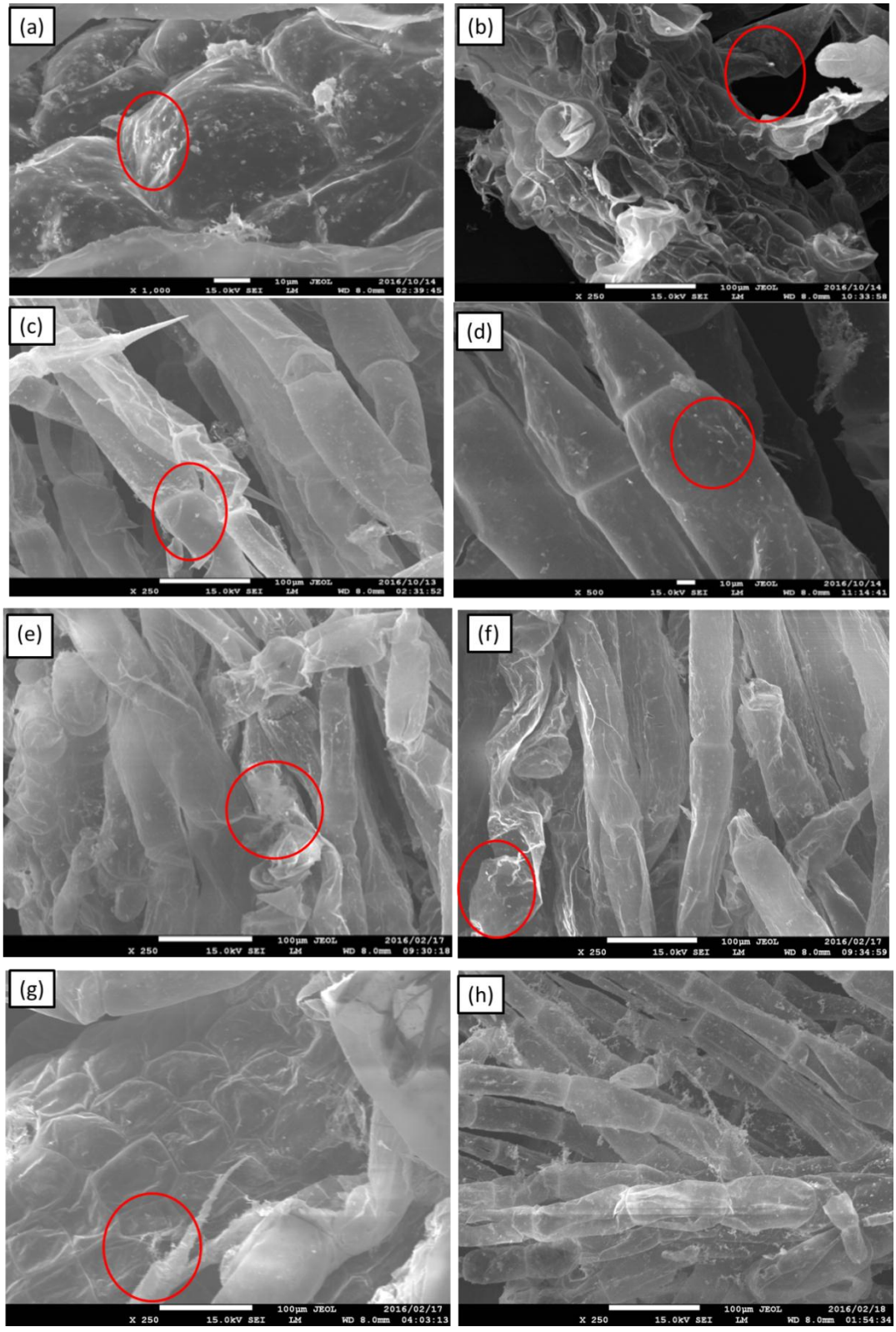

Figure 4.3: SEM images for NPs exposed plant roots (a) 5 nm-Cit, (b) 20 nm-Cit, (c) 40 nm-Cit, (d) 5 nm-BPEI, (e) 20 nm-BPEI, (f) 40 nm-BPEI, (g) CeO_2 NPs and (h) control. Red circles indicate spots where EDX scan was taken.

Similar to findings of Das and Goswami (2017) where Cu accumulation in *Salvinia cucullata* was observed on both roots and fronds, in this study, Au and Ce also exhibited a similar phenomenon. Accumulation on samples exposed to 5 nm-sized Au NPs (both coatings) and CeO_2 NPs was higher on the fronds than on roots (Figure 4.4 (a), (b), and (g)). The cause for a different trend to plants exposed to 5 nm Au NPs compared to larger forms is currently unclear. Although NPs can be translocated from roots to leaves (Zhu *et al.* 2008; Lin *et al.* 2009), no internalization was observed in this study, and therefore, translocation could not account for the high concentrations of Au and Ce found on the fronds. Therefore, the aspect requires further investigation. Whilst the absorption of nutrients in aquatic higher plants can also occur via leaves, currently, there is no credible justification why that process would only be selective for 5 nm Au NPs and CeO_2 NPs.

Au concentrations, except 40 nm cit Au NPs were highest on both roots and fronds at day 7 compared to day 2 but decreased to a minimum in day 14 (Figure 4.4), suggesting the release of NPs from the roots or fronds surface back into the solution. This is because Au NPs adsorbed to the plant roots surface can be released back to the solution (Feichtmeier *et al.* 2015). The findings did not differ based on coating type. For 40 nm Au NPs of both coatings, Au concentrations on the roots decreased with increasing exposure period (Figure 4.4 (e) and (f)). Cerium concentrations increased with exposure period (Figure 4.4 (g)). A decrease in Au accumulation over time was attributed to the loss of particle concentration from the 10 HM solution as NPs form larger agglomerates (Figure 3.4, Section 3.3.2). Agglomerates tend to sediment, and in turn, lead to lower solution Au concentrations available for plants accumulation. To date, studies on interactions of *S. minima* with metallic NPs are scarce; yet the plant is a hyperaccumulator of heavy metals such as manganese, lead and nickel (Lizieri *et al.* 2011; Fuentes *et al.* 2014; Leal-Alvarado *et al.* 2016). Therefore, findings of the current study contribute to the limited body of knowledge on the accumulation metallic NPs by *S. minima.*

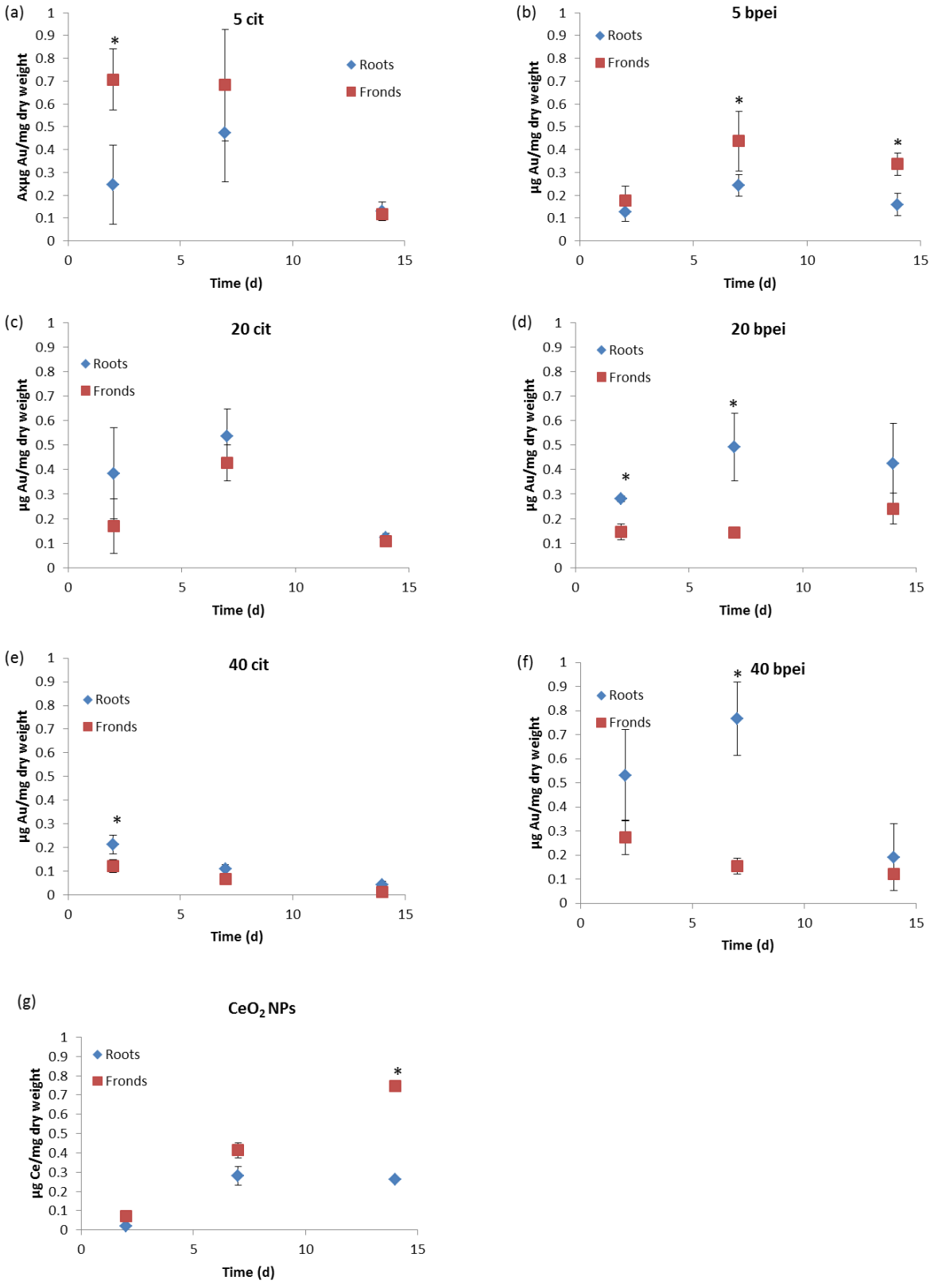

Figure 4.4: ICP-MS results of Au and Ce concentrations (µg/mg dry weight) on *S. minima* exposed to 10 HM at 1 mg /L. Each value is a mean of three replicates and bars denote standard deviations. * denotes statistically significant differences between data points. Student's t-test, $p < 0.05$.

4.3.4 Mechanism of Au and CeO_2 NPs accumulation

To date, numerous studies indicate that aquatic plants accumulate NPs through either internalization or adsorption processes due to a combination of influencing factors, namely: physicochemical properties of NPs, dose-exposure concentration and plant type as listed in Table 4.1. TEM coupled with EDX was used to qualitatively assess the internalization of Au and CeO_2 NPs in roots and fronds where after 14 d, no evidence of NPs internalization into *S. minima* roots or fronds was observed, irrespective of NP type, size and coating variants (Figure 4.5). Thus, in light of ICP-MS results in Figure 4.4, it was concluded that the adsorption mechanism accounted for the observed Au and CeO_2 NPs accumulation in *S. minima.* To date, only handful studies have reported internalization of NPs in aquatic higher plants (Table 4.1), and thus, dynamics of what underpins whether internalization or adsorption mechanism is predominant in a given case remain poorly understood. Amongst the challenges to establish the predominant mechanism is due to lack of analytical capability and standardisation of the generally adopted techniques. As a result, findings to date are not robust, and therefore, a conclusive analysis is not possible.

Although smaller particles are generally more rapidly internalized by plants (Stegemeier *et al.* 2017), other influencing factors such as NPs composition, size, surface properties, cell wall pore size, plant species type, and exposure conditions may drive plant internalization of NPs (Glenn *et al.* 2012; Glenn and Klaine 2013; Koelmel *et al.* 2013; Taylor *et al*. 2014; Judy *et al.* 2015; Stegemeier *et al.* 2015; Thwala et al. 2016). Therefore, in this study, the absence of internalization even for smaller-sized 5 nm Au NPs was attributed to high agglomeration observed in 10 HM (Figure 4.1 (c) and (d)). This is because agglomerates lead to NP sizes larger than cell wall pore size limit (where agglomerates of the size range of 114 to 2 095 nm were observed) of about 10 nm to 50 nm (Adani *et al.* 2011; Judy *et al.* 2012). For the same reason, among others, Taylor *et al.* (2014) observed no internalization of Au NPs (5 and 100 nm) in *Medicago sativa,* but only ionic Au.

Glenn *et al.* (2012) reported the adsorption of 18-nm Au NPs on *Myriophyllum simulans* and *Egeria densa* roots without internalization into the cells. In addition, Au NPs (5 and 20 nm; 10 and 50 µg/mL) did not enter *Hordeum vulgare* roots irrespective of size and dose-exposure concentration (Milewska-Hendel *et al.* 2017). In a study where Au NPs were applied directly into the cells of a root, Au NPs did not move into the neighbouring cells, suggesting that Au NPs do not translocate between the root cells (Milewska-Hendel *et al.* 2017). Other metallic

NPs (e.g. Pb NPs) were shown to adsorb on *S. minima* cell walls of roots and leaves irrespective of NPs' morphology (spherical or elongated) (Castro-Longoria *et al.* 2014). Furthermore, epidermal structures and exudate forms (e.g., amino acids, enzymes, or sugars) lining plant cell walls are known to present a layer that further transform NPs, and in turn, either facilitate or reject the uptake of NPs (Dietz and Herth 2011; Sabo-Attwood *et al.* 2012). Despite the absence of internalization, aquatic plants remain at risk as the aggregation of NPs on root surfaces can cause physical-linked damages to roots (Wang *et al.* 2015) by blocking cell wall pores and water transport capacity (Asli and Neumann 2009). This, in turn, reduces the concentrations of macronutrients (Ca, K, Mg and S) on the leaves, thus affecting the chlorophyll content (Martínez-Fernández *et al.* 2015). Therefore, further studies on the effects of NPs at different life cycle stages of plants are recommended.

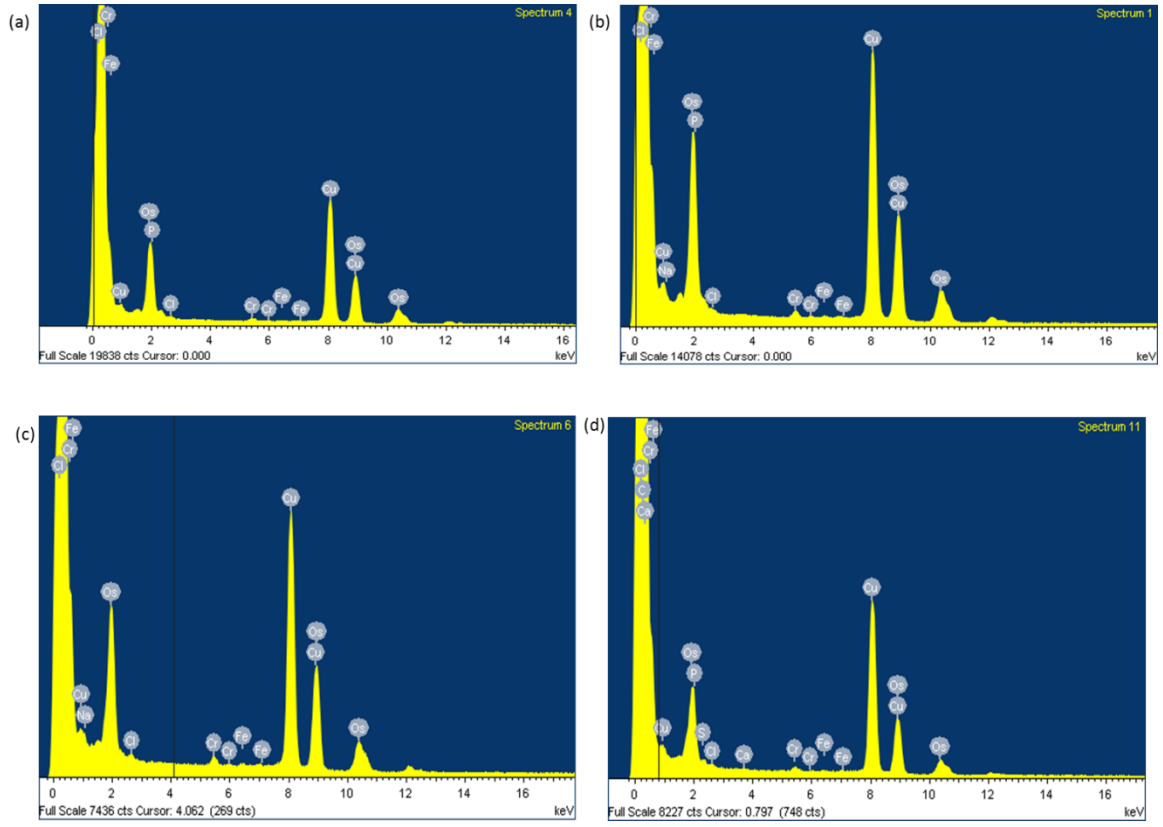

Figure 4.5: TEM EDX spectra confirming the absence of Au and Ce on plant: (a) 5 nm cit Au NPs, (b) 20 nm cit Au NPs, (c) 40 nm cit Au NPs, and (d) CeO_2 NPs.

4.4 Conclusions

This study contributes to the body of knowledge on the accumulation of Au and CeO_2 NPs by aquatic higher plants, and plausible mechanism of NPs interaction with plants. Results indicated that NPs were not internalized by *S. minima* irrespective of particle type, size, or surface coating variants. However, Au and CeO_2 NPs can be adsorbed on the roots of *S. minima;* without inducing morphological level effects such as growth retardation and necrosis at environmentally relevant NP concentrations. The lack of NP internalization and phytotoxicity was linked to high agglomeration of NPs in 10 HM. The study also demonstrated the importance of taking into account the physico-chemical properties of NPs in bioaccumulation investigation in aquatic systems. Nanoparticle size but not the surface coating influenced Accumulation of Au NPs by *S. minima*. High concentrations of 5 nm Au NPs and CeO_2 NPs accumulated in fronds compared to roots of 20 and 40 nm Au NPs. Currently, there is no credible justification why that process would only be selective for 5 nm Au NPs and CeO_2 NPs, and the aspect requires further investigation.

Although NPs can be translocated from roots to fronds, no internalization was observed in this study, and therefore, translocation could not account for the high concentrations of Au and Ce found on the fronds. This aspect merits further investigation. Adsorption of NPs on the roots surface was confirmed in all instances irrespective NP size, coating variant, and type. Thus, adsorption was established as the mechanism of Au and CeO_2 NPs accumulation in *S. minima.* Overall, results suggested that Au and CeO_2 NPs can be adsorbed on the plant roots without internalization and translocation into fronds in *S. minima.* Even though these NPs did not exert toxicity to plants at morphological level, the low concentrations of NPs as found in the environment are likely to exert sub-lethal effects. Therefore, further studies at different end-points at a molecular level (e.g., chromosomal abnormalities, DNA damage, and genome template stability) are recommended.

Table 4.1: Mechanisms of NPs accumulation by aquatic higher plants

Plant	Mechanism	Detection Method	ENP type	ENP Properties	Exposure media	Duration	Dosage	Controlling factor(s)	Ref
Myriophyllum simulans	Adsorption	TEM, STEM, SEM, EDX	Au	4 nm; spherical; ζ – 14.1 mV	Borehole water; pH 7.1; TOC;8.56 mg/L; CaCO3 107 mg/L; conductivity 210mS/cm	24 h	250 µg/L	Size: High accumulation from 4 nm Au NPs compared to 18 nm.	[1]
Azolla caroliniana	Internalization	TEM, STEM, SEM, EDX	Au	4 nm; 18 nm; spherical;z –14.1 mV; ζ –9.73 mV		24 h	250 µg/L	Species type: internalization due to the presence of root hairs used by the plant to acquire nutrients	[1]
Egeria densa	Adsorption	TEM, STEM, SEM, EDX	Au	4 nm; 18 nm; spherical; ζ –14.1 mV; ζ –9.73 mV		24 h	250 µg/L	Species type: *E. densa* did not absorb Au NPs of either size	[1]
Lemna minor	Adsorption (leaves)	SEM; TEM	TiO2	275–2398 nm; SSA 50 m2/g;	Steinburg growth medium; pH 5.5; CaCO3 166 mg/L	14 d	0.01–10 mg/L	Exposure concentration: Accumulation increased with exposure concentration	[2]
Salvinia natans	Adsorption	ICP-OES	ZnO	25 nm; uncoated; SSA; 90	OECD growth medium; pH 6.5	7 d	1-50 mg/L	Concentration: High agglomeration and settling of NPs at 20 and 50 mg/L	[3]

				m2/g; 1–10 mg/L					
Schoenoplectus tabernaemontani	Internalization (roots)	TEM	CuO; CdS QDs	38 nm; SSA 12.84 m2/g;z –2.8 Mv	Hoagland's	21 d	0.5-50 mg/L	NP type: Root uptake percentage for CuO NPs treatment ranged from 40.6 to 68.4%, while the values were 8.7 to 21.3% for CdS QDs	[4]
S. tabernaemontani	Internalization	SEM; TEM	ZnO	35 nm;SSA 43 m2/g;z -5.4 mV (start), -2.6 mV (end)	Nutrient solution, pH 6.4- 6.8	21d	10-1000 mg/L	Particulate vs ionic form: Uptake of Zn from ZnO NPs was greater than that for Zn^{2+}.	[5]
Spirodela polyrrhiza	Internalization	Epifluorescence microscopy	TiO2	8 nm, anatase	half-strength S. polyrrhiza specific culture medium	6 d	0.05-10 mg/L	Structural characteristics: Anatase and crystalline TiO_2 NPs allow their remarkable movement into the root cells	[6]
S. minima	Adsorption (leaves)	TEM, SEM, XPS	Pb	spherical, 17.2 ± 4.2 nm	Hoagland's	12 h	80 mM	Morphology: Spherical NPs were found within the cell wall while elongated ones were associated with the cell membrane.	[7]

S. minima	Adsorption (roots)	TEM, XPS	SEM,	Pb	Elongated, 53.7 ± 29.6 nm in length and 11.1 ± 2.4 nm wide	12 h	80 mM		[7]
S. minima	Adsorption (roots)	TEM, ICP-MS	SEM,	Au	5, 20, 40 nm; spherical; citrate and BPEI coated	10% Hoagland's medium, pH 7	14 d	1 mg/L	Size: high agglomeration observed for smaller NPs NP type: NP concentration (μg/mL) decreased as time increase for Au, and increased with duration for Ce.	[8]

[1] Glenn et al. 2012, [2] Li et al. 2013, [3] Hu et al. 2014, [4] Zhang et al. 2014, [5] Zhang et al. 2015, [6] Movafeghi et al. 2017, [7] Castro-Longoria et al. 2014, [8] current study.

CHAPTER 5

Genotoxicity of gold and cerium oxide nanoparticles to algae, *Pseudokirchneriella subcapitata*

5.1 Introduction

Rapid increasing use and applications of nanoparticles (NPs), and their consequent emission into the environments raise the need to understand their potential effects to ecological systems (Klaine *et al*. 2008; Scown *et al.* 2010; Châtel and Mouneyrac 2017). In aquatic ecosystems, microalgae play a crucial role as primary producers in the balance of aquatic ecosystems (Sadiq *et al.* 2011b). Algae are excellent aquatic model organisms for the toxicity examination of environmental pollutants due to their short generation time and high sensitivity to pollutants (Ji *et al*. 2011; Chen *et al.* 2012). The effects of nano-pollutants to algae could affect organisms at higher trophic levels (Mei *et al.* 2007; Rioboo *et al.* 2007). To date, the effects of NPs to algae have been examined at morphological level endpoints, such as growth rate, biomass and chlorophyll content (Ji *et al.* 2011; Chen *et al.* 2012; Angel *et al*. 2015; Aruoja *et al.* 2015; Gao *et al.* 2016; Sendra *et al.* 2017; Chen *et al.* 2018). However, to understand the mode of NP toxicity, cellular biological response data should be supported with genotoxicity data (Demir *et al.* 2014; Golbamaki *et al*. 2015; Koehlé-Divo *et al.* 2018). The investigation of the effects of the pollutants at the genetic level is recommended due to the sensitivity of genotoxicity assays over cytotoxicity assays (Amaeze *et al.* 2015). In addition, the OECD has recommended genotoxicity assessment of NPs for regulatory and risk assessment purposes (Nanogenotox, 2013; ANSES, 2014).

Numerous types of biomarkers have been used to measure the effects of environmental contaminants in different systems (Canesi *et al.* 2011; Mouneyrac *et al.* 2014) using different techniques. Among the techniques used range from ecophysiology to molecular tools; and the findings offer early warnings on physiological alterations in organisms exposed to environmental pollutants (Buffet *et al.* 2015) or molecular impact through DNA damage (Bolognesi and Hayashi 2011; Załęska-Radziwiłł and Doskocz 2016; Koehlé-Divo *et al.* 2018). To evaluate the DNA damage, many studies have employed the Comet assay as reviewed by Collins (2004) and Mahaye *et al.* (2017). Although the Comet assay is widely used, this assay measures DNA lesions that can easily be repaired and is frequently used for monitoring of DNA repair processes (Azqueta *et al.* 2014). Therefore, this assay may have limited value in the evaluation of long-term consequences of exposure to environmental genotoxicants (Srut *et al.* 2015). Using the Comet assay, DNA repair is challenging in the presence of NPs, as they

may remain intracellular for long periods causing extra DNA breaks (Karlsson, 2010). Therefore, the use of a wide range of robust methods to investigate NP-induced DNA damage is recommended.

Robust methods include random amplified polymorphic DNA (RAPD) markers, which screen for changes in DNA profiles and which have been previously used to evaluate genomic instability. The advantages of the RAPD assay are that it does not require prior knowledge of the genome and uses short primers (10 bp). The assay also permits the detection of genetic alterations, after contamination with pollutants in aquatic organisms, as well as detection of intrapopulational polymorphism (Salem *et al*. 2014). RAPD analysis has been used to determine the genotoxicity of various chemical and physical agents both *in vitro* and *in vivo* in various systems (Jin *et al.* 2009; Culcu *et al*. 2010; Orieux *et al.* 2011; Geffroy *et al*. 2012; Rocco *et al.* 2012; Lerebours *et al.* 2013; Srut *et al.* 2015). The RADP assay has also been used to investigate the genotoxicity of NPs to aquatic organisms. For example, Amjady *et al.* (2016) investigated genotoxicity of Ag and CuO NPs (<20 nm) in *E. coli.* The authors reported differences in the number of bands in the gel images of exposed samples showing alterations in the DNA sequence by NPs. Nigro *et al.* (2015) investigated the genotoxicity of the co-exposure of cadmium chloride ($CdCl_2$; 0.1 mg/L) and TiO_2 NPs (1 mg/L) to the fish, *D. labrax*. An increased chromosomal and DNA damage in fish exposed to $CdCl_2$ ($p < 0.05$) was observed, but not to TiO_2 NPs. Co-exposure prevented chromosomal damage and led to a partial recovery of the genome template stability (Nigro *et al.* 2015). The genotoxicity potential of TiO_2 NPs (1 and 10 µg/L) was also assessed in zebrafish (*D. rerio)* exposed for 14- 28 d. The highest genotoxic effect was observed at maximum concentrations of TiO_2 NPs after 21 d. Genome stability was reduced by 37% after 14 d, and increased with longer exposure times; attributed to activation of defence mechanisms against free oxygen radicals in fish exposed to TiO_2 NPs (Rocco *et al.* 2015). Furthermore, the RAPD assay can detect genotoxicity even in cases where the Comet assay failed (Orieux *et al*. 2011).

Another approach is the determination of abasic (apurinic/apyrimidinic, AP) sites which are ubiquitous DNA lesions generated by oxidative damage to DNA (Lindahl, 1993). AP sites are among the most frequent lesions in DNA, and occur as a result of one of the two processes: (i) hydrolysis of the *N*-glycosidic bond (depurination) (Lindahl, 1982; Loeb and Preston 1996), and, (ii) the removal of altered bases by DNA glycosylases (Weiss and Grossman 1987; Loeb

and Preston 1996) during the first stage of the base excision repair (BER) process (McCullough *et al.* 1999). Estimates are that 2 000–10 000 AP sites are generated spontaneously per cell per generation (Lindahl and Nyberg 1972; Lindahl, 1993), and if unrepaired, may lead to cell death and/or induce mutations (Loeb and Preston 1986). The assay has successfully been used, for example, to determine the formation of AP sites in Chinese Hamster Ovary cells (CHO) exposed to 0–300 μM of uranyl acetate (UA) over 48 h – where parent cell line did not show significant AP sites production when compared to control. These findings suggest that either UA did not induce AP site formation, or that BER mechanisms readily repaired the lesions. Using a repair-deficient cell line, UA induced AP sites after 24 h that were significantly reduced after 48 h (Yellowhair *et al.* 2018). Barbado *et al.* (2018) recently reported that an AP lyase-dependent pathway could repair AP sites generated by the spontaneous loss of N7-methylguanine in Arabidopsis. From a recent review by Mahaye *et al.* (2017) on genotoxicity testing of NPs based on various assays, no record of AP site assays applications was found for aquatic organisms. Yet the assay is essential in revealing whether repair mechanisms at DNA level occur following exposure of organisms to pollutants.

A recent review reported that of 4346 articles on the toxicity of NPs, only 112 focused on genotoxicity studies (Magdolenova *et al*. 2014). Furthermore, most genotoxicity studies on the effects of NPs largely focused on mammalian systems (Karlsson, 2010; Rim *at al*. 2013; Magdolenova *et al*. 2014; Golbamaki *et al.* 2015), and terrestrial plants (Mehrian and De Lima 2016; Rizwan *et al.* 2017). The lack of genotoxicity data on the interactions between NPs and aquatic organisms has been recently highlighted (Mahaye *et al.* 2017). To date, bacteria, crustaceans and fish, and TiO_2 and Ag NPs, are the most studied organisms and NPs, respectively. Gold (Au) and cerium oxide (CeO_2) NPs are among the priority NPs for immediate toxicity testing (OECD, 2010) – and are widely produced and used in consumer products and industrial applications (Piccinno *et al.* 2012; Hansen *et al.* 2016) – however, little is known on their potential genotoxic effects to algae and aquatic higher plants (Mahaye *et al.* 2017). Therefore, this study seeks to generate data in an endeavour to contribute to filling this knowledge gap. However, the current study only focuses on the genotoxicty of NPs to algae, as the growth of aquatic higher plants is seasonal and plants were unavailable during the study period. The aim of the current study was to investigate the genotoxicity potential of Au and CeO_2 NPs to the microalga, *Pseudokirchneriella subcapitata* (formerly *Selenastrum capricornutum*). Thus, the specific aims of the study were to (i) elucidate the influence of the physicochemical properties of NPs on the DNA integrity of algae, (ii) exposure duration (short-

(72 h) vs. long- term (168 h)), (iii) NPs type (metal (Au NPs) vs. metal oxide NPs (CeO_2 NPs)), and (iv) compare cellular effects of NPs and those at molecular levels.

5.2 Materials and Methods

5.2.1 Characterization of Au and CeO_2 NPs

Au NPs of different sizes (5, 20 and 40 nm) and surface coatings (cit and BPEI) were purchased from Nanocomposix (San Diego, United States). CeO_2 NPs (< 25 nm; uncoated) were purchased from Sigma Aldrich (Johannesburg, South Africa). Primary size and morphology of Au and CeO_2 NPs were examined using high-resolution transmission electron microscope (HRTEM; JEOL JEM 2100, Japan operating at 200kV). To determine the stability of NPs in 10% BG-11 algal medium their hydrodynamic diameter (HDD) was measured using dynamic light scattering (DLS; Malvern Zetasizer Nano ZS, Malvern Instruments, UK) over 72 h (0, 2, 6, 24, 48 and 72 h).

5.2.2 Test organism

The Algaltoxkit F^{TM} was purchased from ToxSolutions (Johannesburg, South Africa). The de-immobilization of *P. subcapitata* from the beads was performed according to the supplier's instructions. This is a 72 h assay based on the growth inhibition of the micro-algae *P. subcapitata*. This microbiotest strictly adheres to the protocols for regulatory testing with microalgae recommended by international organizations such as the Organization for Economic Co-operation and Development (OECD) (OECD 201, 2006) and the International Organization for Standardization (ISO) (ISO 8692, 2004).

5.2.3 Exposure conditions

To prepare an inoculant for experiments, algae was incubated under controlled conditions (temperature: 25 ± 1°C; light intensity: 6000 Lux; light: dark cycle: 12 h –12 h day and night, and shaken continuously at 100 rpm) for 3 –4 d. Exponentially growing algal cultures (3 – 4 d old) were collected by centrifugation (10 000 rpm, 10 min), washed twice with 0.1 mL phosphate-buffered saline (PBS), and then once with 0.1 mL OECD 201 algal medium. Algal biomass was determined by measuring optical density (OD_{684}) every 24 h for 72 h (Rodrigues *et al.* 2011) using a microplate reader (FLUOstar Omega BMG LABOTECH). All the

experiments were done using OECD algal medium (OECD 201, 1984). All chemicals ($NaHCO_3$, $NaNO_3$, NH_4Cl, $MgCl_2 \cdot 6(H_2O)$, $CaCl_2 \cdot 2(H_2O)$, $MgSO_4 \cdot 7(H_2O)$, K_2HPO_4, KH_2PO_4, $FeCl_3 \cdot 6(H_2O)$, $Na_2EDTA \cdot 2(H_2O)$, H_3BO_3, $MnCl_2 \cdot 4(H_2O)$, $ZnCl_2$, $CoCl_2 \cdot 6(H_2O)$, $Na_2MoO_4 \cdot 2(H_2O)$) for the OECD algal medium were purchased from Sigma Aldrich and were dissolved in 1 L DIW (15 MΩ.cm). The OECD algal medium was prepared in sterile autoclaved glassware and the pH was adjusted to 7-7.5.

5.2.4 Algal reference test with potassium dichromate

To assess the test reproducibility, microplate algal growth inhibition assay was first performed using potassium dichromate ($K_2Cr_2O_7$) as a reference toxicant. Algae were exposed to varied $K_2Cr_2O_7$ concentrations (0.32 -3.2 mg/L) over 72 h. The algal growth inhibition was measured as OD_{684} every 24 h.

5.2.5 Effects of Au and CeO_2 NPs to *P. subcapitata*

5.2.5.1 Effects of NPs on algal growth

Preliminary studies (Appendix B) showed that following the OECD test guideline (OECD 201, 2006), biomass increase in controls after 72 h was not high enough as should at least be 67x to meet the validity-criteria (ISO 8692). In addition, the biomass obtained after 72 h was insufficient for DNA extraction required in the genotoxicity studies. Therefore, Direct Estimation of Ecological Effect Potential guideline (DEEEP) test guideline (DEEEP, 2004) was followed and the culture was grown for 5-7 d before the test. Exponentially growing algal cultures (5 -7 d old) were collected as detailed in Section 5.2.3. All experiments were done in 10% BG-11 algal medium as described in the DEEEP guideline (DEEEP, 2004). The volume of algal stock culture and cell density (cells/ml (millions)) were calculated according to Equation 1 (USEPA 2002) and Equation 2 (Rodrigues *et al*. 2011), respectively:

$$Vol\ (mL) = \frac{flasks\ \ x\ vol\ /flask\ x\ 10\ 000\ cells/mL}{cells/mL} \qquad (1)$$

where vol is the volume of stock culture required, flasks is the number of test flasks used, vol/flask is the volume of test solution per flask, and cells/mL is the cell density in the stock culture given by the expression:

$$Cells/mL = e^{\frac{ln\lambda_{684}+16.439}{1.0219}} \quad (2)$$

where cells/mL is the algal cell density and λ_{684} is the OD at 684 nm

The algal cells were exposed to five concentrations of Au and CeO_2 NPs (0.0625, 0.125, 0.25, 0.5 and 1 mg/L) at cell densities of 200 000 cells/mL under controlled conditions for 72 h. The control had no NPs. Exposure period was extended to168 h to investigate long-term effects of NPs to algae. Experiments were done in triplicates per concentration in 10 mL 6-well microplates.

5.2.5.2 Effects of NPs on algal chlorophyll *a* content

After 72 and 168 h exposures, chlorophyll a (Chl *a*) was extracted and the content determined used the approach proposed by Harris (1989). Briefly, 1 mL from the control and exposed algal cells were centrifuged for 10 min at 13 000 rpm. The supernatant was discarded and the pellet was washed with DIW then 95% ethanol, vortexed for 2 min, and kept at 4 °C for 30 min. The suspension was centrifuged for 2 min and the OD of the supernatant was read at 665 and 649 nm. The content of Chl *a* was then calculated using the expression:

$$\text{Chl a} = 13.70A_{665} - 5.76A_{649} \quad (3)$$

where A_{665} and A_{649} are the OD values (n=3) at wavelengths of 665 nm and 649 nm, respectively.

5.2.6 Effects of Au and CeO_2 NPs to *P. subcapitata* at a molecular level

5.2.6.1 DNA isolation and visualization

Exposure conditions and durations were the same as for cytotoxicity studies (Section 5.2.3). Following the collection of NP-treated and untreated algal cells after 72 and 168 h post exposure, DNA was extracted using a commercial kit, MasterPure™ DNA purification kit (Epicentre, USA). The extraction was done in accordance with the supplier's instructions but– with three minor modifications. The modifications entailed samples incubated at 65 °C for 30 min instead of 15 min, 3 µL RNase cocktail was added and not 1 µL (to increase the efficiency of cell lysis), and an additional 1 h incubation step at -20 °C after addition of isopropanol to improve DNA precipitation. Protein precipitation and DNA purification were achieved

according to the manufacturer's protocol. DNA purity (OD_{260}/OD_{280}) and concentration (ng/µL) were determined using a Nanodrop 2000 Spectrophotometer (Thermo Scientific, US); with OD_{260}/OD_{280} ratio ≥1.7 denoting contaminant-free DNA, and < 1.7 DNA containing contaminants. The DNA (3 µL) from different exposures was separated on a 1.5% ethidium bromide-stained agarose gel dissolved in 1 X TAE buffer (Tris-acetate-EDTA buffer, pH 7.5) at 90 mV for 45 min, and visualised with a UV transilluminator.

5.2.6.2 RAPD assay

Random Amplified Polymorphic DNA (RAPD) was performed by two 10-base pair RAPD primers; OPB1 (5'-GTTTCGCTCC -3') and OPB14 (5'-TCCGCTCTGG-3') sourced form Inqaba Biotechnical Industries (Pty) Ltd (Pretoria, South Africa). Based on preliminary studies in Appendix B, reagents volumes were adjusted, for example, volumes of the primer and DNA were increased to enhance the DNA-primer binding and to obtain clearer bands. Amplification was performed in 25 µL reaction volumes containing 1 µL primers, 6 µL DIW, 2.5 µL BSA, 12.5 µL ready mix and 3 µL genomic DNA using a PCR thermocycler (T100™ Thermal Cycler). For the negative control, no genomic DNA was added but made up of 25 µL with DIW. The RAPD-PCR protocol entailed a warming step at 94 °C for 5 min, DNA denaturation at 94°C for 45 sec, annealing (46.8 °C for OPB1 and 44.3 °C for OPB14) for 30 sec, extension 68 °C for 1 min, and final extension at 68°C for 10 min for 40 cycles. The amplified product was kept at 4 °C until gel electrophoresis. Bands were separated on a 1.5% ethidium bromide-stained agarose gel at 80 mV for 2 h, then visualised using a UV transilluminator. A 10-kb universal DNA Ladder (Kapa Biosystems, Cape Town, South Africa) was used as the molecular weight standard. RAPD data analysis was performed by comparing the PCR product profiles for NP-treated samples with control samples. A genomic template stability (GTS) value was calculated as follows (Atienzar *et al.* 2002):

$$\mathrm{GTS\%} = \left(1 - \frac{a}{n}\right) * 100 \qquad (4)$$

where *a* is the average number of RAPD polymorphic bands detected in NP-treated samples and *n* is the number of total bands in the control. Polymorphisms in RAPD profiles include deletion of a normal band and induction of a new band in comparison to the control RAPD profiles. In this case, changes in RAPD profiles are expressed as a decrease in genomic stability of NP-treated samples in relation to profiles generated from the control.

5.2.6.3 AP site content

DNA lesions were investigated using the DNA Damage – AP site – Assay Kit (ab211154: Colorimetric, Biocom Africa, Pretoria, South Africa) in accordance with the supplier's instructions. The assay uses an Aldehyde Reactive Probe (ARP) designed specifically to react with an aldehyde group on the open ring form of AP sites. The kit used had a detection sensitivity range of 4-40 AP sites per 1 x 10^5 base pairs. The extracted DNA was diluted to a concentration of 100 µg/mL in TE buffer. Five µL of DNA (100 µg/mL) was mixed with 5 µL of ARP solution in micro-centrifuge tubes and incubated for 1 h at 37 °C. Ninety µL of TE buffer, 1 µL glycogen solution and 10 µL sodium acetate solution were added to each tube and then mixed by pipetting. Then 300 µL of 100 % ethanol was added to each tube before the mixture was incubated at -20 °C for 30 min. Then, mixtures were centrifuged at 14 000 x*g* for 20 min, the pellet was retained while the supernatant was discarded. The pellet was washed three times in 70 % ethanol, air dried for 10 min, and finally suspended in 50 µL TE buffer. After ARP reaction, the ARP-derived DNA was diluted to 1 µg/mL in TE buffer.

To determine AP sites in DNA, a 96 well DNA high binding plate was used. The standards were prepared as listed in Table 5.1. Fifty µL of DNA binding solution was added to 50 µL of ARP-derived DNA samples (1 µg/mL), and incubated at room temperature (*ca* 25 °C) for 2 h. The micro-well strips were washed three times in 250 µL 1X wash buffer and dried in an absorbent paper. Then, 100 µL of the diluted streptavidin-enzyme conjugate was added to each well, and the resultant solution was incubated at 37 °C for 1 h. Again, the micro-well strips were washed as above. One hundred µL of substrate solution was added to each well including blank wells and incubated in an orbital shaker for 20 min at room temperature. Then, 100µL of stop solution was added to each well including blank wells. Finally, the absorbance (OD_{450}) was recorded immediately after preparation on a microplate reader.

AP sites content was then determined by comparing the absorbance (OD_{450}) from treated and untreated samples with a standard curve generated by the DNA standards containing predetermined AP sites. An average of the duplicate measurements for each standard, treated and untreated algal DNA samples was performed. The mean absorbance values for the blank, standards and treated samples were calculated. Then the blank values were subtracted from

each standard and treated samples to obtain blank corrected absorbance. The trend-line equation was fitted on the standard curve data and was used to calculate the AP site content per 10^5 bp generated from treated and untreated algal DNA samples. The number of AP sites in treated samples was compared to the control to determine the level of genotoxicity (4-40 AP sites per 1 x 10^5 bp).

Table 5.1: Dilutions for the DNA standard containing predetermined AP sites (*n*=2)

Standard No.	ARP-DNA Standard (µL)	Reduced DNA Standard (µL)	TE Buffer (µL)	Final volume/ well (µL)	AP Sites per 10^5 bp
1	20	0	100	50	40
2	16	4	100	50	32
3	12	8	100	50	24
4	8	12	100	50	16
5	4	16	100	50	8
6	2	18	100	50	4
7	1	19	100	50	2
8 (blank)	0	20	100	50	0

5.3.6 Data Analysis

Three or two replicate tests were performed and the data are presented as means ± standard deviations. Data were analysed by analysis of variance (ANOVA) using GraphPad Prism V7.04 software (GraphPad Prism software, La Jolla, CA, USA). A *p*-value of < 0.05 (one-way ANOVA, two-way ANOVA or T-test) was considered statistically significant.

5.4 Results and Discussion

5.4.1 Nanoparticles characterization

The primary sizes and morphologies of the NPs used in this study are summarised in Chapter 3 (Figure 3.1 and Table 3.1). The hydrodynamic diameter (HDD) of Au and CeO_2 NPs in the BG-11 medium was studied over 72 h (Figure 5.1). CeO_2 NPs formed agglomerates of 382±32 nm at 0 h, which increased to 919±74 nm at 72 h. A non-significant ($p > 0.05$) increase in HDD was observed as exposure duration increased for CeO_2 NPs and all Au NPs except 40 nm-sized BPEI NPs. The 40 nm BPEI Au NPs showed a decrease in HDD with increasing exposure duration. Overall, the BPEI Au NPs were more stable (smaller HDD) than cit Au NPs (Figure 5.1). A size dependent increase in HDD of Au NPs for both coating types was observed, with 5 nm NPs exhibiting the highest HDD and 40 nm the least (Figure 5.1 (a) and (b)). This effect is thought to be due to the high surface reactivity of smaller NPs, which interact more readily with the components (cations and anions) present in the exposure media (Auffan *et al*. 2009; Park *et al.* 2011; Iswarya *et al.* 2016).

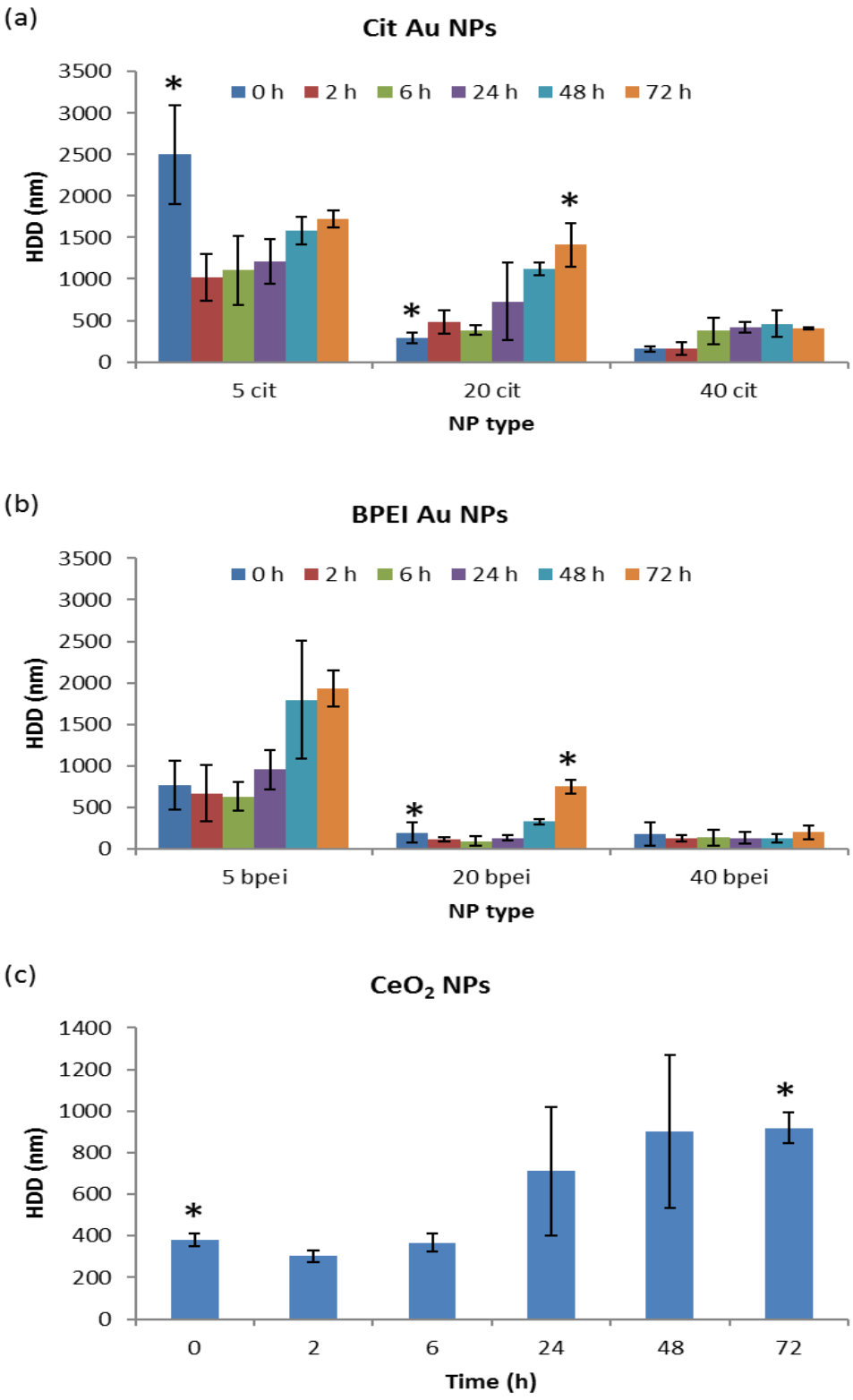

Figure 5.1: Hydrodynamic diameters (n=3) for Au and CeO_2 NPs in BG-11 algal medium. Bars indicate standard deviations. * denotes statistically significant differences between data points.

5.4.2 Cytotoxicity tests

5.4.2.1 Effects of NPs on algal growth

Growth inhibition curve of *P. subcapitata* following exposure to $K_2Cr_2O_7$ at concentrations of 0.32 -3.2 mg/L is shown in Figure 5.2 (a). Significant concentration dependent growth inhibition was observed following exposure to $K_2Cr_2O_7$ in comparison to the control. Algae exposed to CeO_2 NPs showed non-significant growth inhibition ($p > 0.05$) compared to the control up to 144 h, and at 168 h, exposure to NPs induced algal growth promotion (Figure 5.2 (b)). Similar growth patterns ($p > 0.05$) between exposed algal cells and the control were also observed for all cit-coated Au NPs (Figure 5.2 (c), (e), (g)); indicating non-toxicity of Au and CeO_2 NPs to algae at morphological level at concentrations tested in this study, or under high NP agglomeration regime. The presence of agglomerates larger than the pore sizes of the algal cell wall, which ranges between 5 and 20 nm (Zemke-White *et al.* 2000; Madigan *et al.* 2003) may contribute to non-toxicty as NPs were not taken up by algae. Furthermore, plants are known to export organic acids (Glenn *et al.* 2012), it is therefore plausible that citrate coating on the NPs hindered uptake (Glenn *et al.* 2012). Both citrate-coated Au and CeO_2 NPs were non-toxic to alga irrespective of NP sizes. Previous studies showed that uptake of uncoated and agglomerated CeO_2 NPs does not occur in algae (Röhder *et al.* 2014; Angel *et al*. 2015; Röhder *et al.* 2018).

A concentration dependent decrease in cell density was observed for 5 nm BPEI Au NPs at 48 and 72 h (Figure 5.2 (d)) compared to 5 cit Au NPs (Figure 5.2 (c)). After 96 h, cell recovery was observed for all concentrations of NPs except 1 mg/L (Figure 5.2 (d)). The highest exposure concentration (1 mg/L) showed a significant decrease in cell density compared to the control over 168 h. The findings indicate the influence of surface coating on the toxicity of NPs to algae. However, the precise mechanism by which NPs coating influences toxicity is still to be investigated (Becaro *et al.* 2015). The NPs coating has been reported to influence NPs interactions with algae. For example, exposure of *Chlorella vulgaris* to PVP- and citrate-coated Ag NPs had similar toxicity (IC_{50}: 9.3 and 9.2 mg/L, respectively) compared to PEG-Ag NPs (IC_{50}: 49.3 mg/L) (Kalman *et al.* 2015). Exposure of *Thalassiosira pseudonana* to 20 nm ZnO NPs with different coatings showed different toxicities. Uncoated and 3-aminopropyltrimethoxysilane -ZnO NPs were more toxic than dodecyltrichlorosilane-coated ZnO-NPs (Yung *et al.* 2017).

The lack of significant growth inhibition at tested NP concentrations hindered the calculation of the effective concentration that inhibits 50% growth of the population (EC_{50}). Nanoparticle concentrations > 1mg/L were not tested in this study, as they are unlikely to be found in natural waters. Previous reports showed that the EC_{50} concentrations for Au and CeO_2 NPs to *P. subcapitata* are above the concentrations used in this study (Table 5.2) or could not be calculated due to growth stimulation **(**Dědková *et al.* 2014).

5.4.2.2 Chlorophyll *a* content of *P. subcapitata*

The content of Chl *a* is an efficient indicator of the physiological health status in algal cells (Metzler *et al.* 2012; Li *et al*. 2015). The content of Chl *a* for *P. subcapitata* exposed to Au and CeO_2 NPs is shown in Figure 5.3. The Chl *a* content in 5 cit, 20 cit, 20 BPEI, and 40 BPEI, for example, irrespective of exposure concentration, was not significantly different from the control (algae exposed to BG-11 medium without NPs). Hence, exposure of algae to Au NPs did not influence the synthesis of Chl *a*. Exposure to 40 nm cit Au NPs, however, showed a significant promotion of Chl *a* at 0.5 and 1 mg/L compared to the control at 72 h (Figure 5.3(c)). After 168 h, significant Chl *a* reduction was observed at all tested concentrations (Figure 5.3 (c)), thus highlighting the importance of considering long-term exposure conditions. Similarly, short-term exposure of *P. subcapitata* to CeO_2 NPs (0-100 mg/L) showed non-significant effects on photosynthesis (Velzeboer *et al.* 2008). However, under long-term exposure, CeO_2 NPs inhibited photosynthesis and induce ROS (Rodea-Palomares *et al.* 2012). Furthermore, NPs bound onto algal membrane have been proposed to induce a reduction in light availability, and in turn, inhibit the photosynthesis process (Navarro *et al.* 2008; Schwabe *et al.* 2013). A decrease in Chl *a* content following exposure to 5 nm BPEI Au NPs at 1 mg/L (Figure 5.3 (d)) may account for the significant growth reduction of algae observed (Figure 5.2 (d)). However, smaller sized-NPs alone do not necessarily translate to higher toxicity. The findings also show the role of coating on the toxicity of NPs (Angel *et al.* 2015).

CeO_2 NPs enhanced Chl *a* content at 72 h ($p < 0.05$) and 168 h ($p > 0.05$) at all concentrations (Figure 5.3 (g)). Similarly, other metal oxide NPs, such as ZnO and TiO_2, were shown to enhance algal growth and to increase Chl *a* concentration in *Picochlorum* sp. (Hazeem *et al*. 2016) and *P. subcapitata* (Hong *et al*. 2005; Lei *et al.* 2007; Hartmann *et al.* 2010). Cerium nitrate was reported to promote chlorophyll content in *Vigna unguiculata* plants (Shyam and Aery 2012). The basis for the promotion of Chl *a* content in algal cells was suggested to be

caused by the conversion of other forms of pigments to Chl *a* as a response to reactive oxygen species (ROS) caused by exposure to NPs (Chen *et al.* 2012a). In this study, the observed biological effects on CeO_2 NP-exposed algae were associated to the particulates and not the Ce ionic species due to the low dissolution of CeO_2 NPs (Van Hoecke *et al.* 2009; Rogers *et al.* 2010; Angel *et* a*l.* 2015).

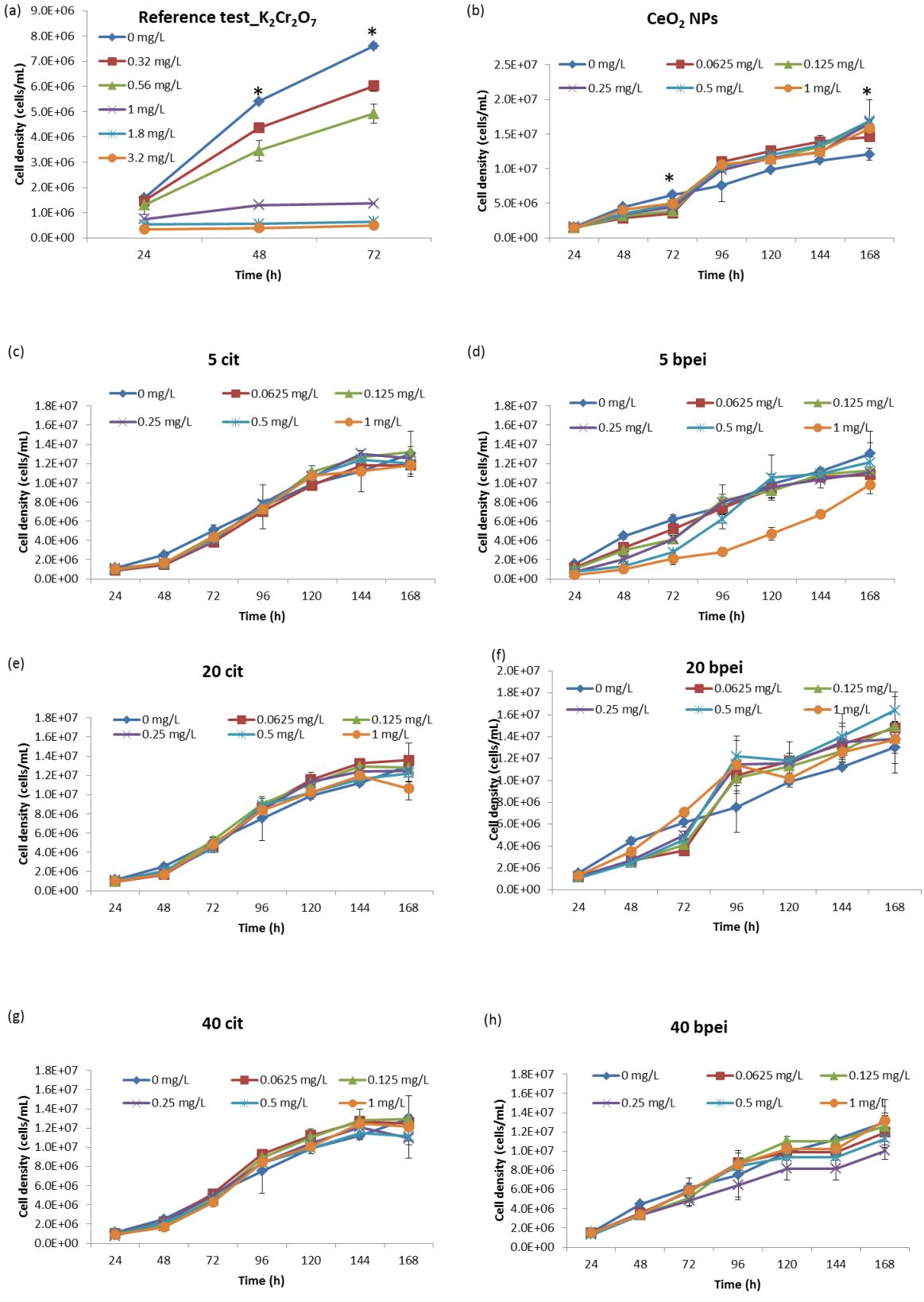

Figure 5.2: Algae growth curves of *P. subcapitata* at different concentrations of reference toxicant and NPs. * denotes significant differences between the control and treated samples.

Table 5.2: Summary of Au and CeO_2 NPs EC_x concentrations reported on *P. subcapitata*

NP type	NP properties	Duration	Exposure medium	Exposure concentration	ECx (mg/L)	Ref
CeO_2	10-20 nm; 5 µm, SA:80 m^2/g; uncoated	72 h	USEPA TG medium, pH 6.5	1-200 mg/L	10.3 ± 1.7 mg/L and 66 ± 22 mg/L (EC_{50})	Rogers *et al.* 2010
CeO_2	14, 20, 29 nm; SA:61, 42, 29 m^2/g,	72 h	OECD TG 201 (pH 7.4)	3.2, 5.6, 10, 18, and 32 mg/L	2.6 - 5.4 (EC_{10}); ≥ 0.052 and ≤ 0.108 mg/L (NOEC)	Van Hoecke *et al.* 2009
CeO_2	10-60 nm;30–60 m^2/g	72 h	OECD TG 201	0-1000 mg/L.	29.2 ± 3.0 mg/L for 50nm and 35.7 ± 2.3 mg/l for 25 nm (EC_{50})	Rodea-Palomares *et al.* 2011
CeO_2	10–34 nm, 1 µm	72 h	USEPA synthetic fresh water, pH 6.46–6.63	1-100 mg/L.	7.6–28 mg/L for 10–34 nm; 59 mg/L for 1 µm (EC_{50})	Angel *et al.* 2015
CeO_2	4 and 10 nm, PAA coated, spherical; ζ:−25 mV	72 h	OECD TG 201	0.015-0.2 mg/L	0.0058 mg/L (EC_{10}); 0.024 mg/L (EC_{50})	Booth *et al.* 2015
CeO_2	11-20 nm		OECD TG 201	0.2-25 mg/L	0.5 mg/L (EC_{10}); 1.1 mg/L (EC_{20}); 4.1 mg/L (EC_{50})	Manier *et al.* 2013
CeO_2	<25 nm, ζ:19 mV	72 h	OECD TG 201, pH 8.1, hardness: 25 mg/L conductivity: 165 µS/cm		2.8-7.5 mg/L (EC_{10}); 12-16.4 mg/L (EC_{50})	Manier *et al.* 2011
CeO_2	33-49 nm, 28 m^2/g		OECD TG 201		1.24 mg/L (EC_{50})	Cerrillo *et al.* 2016

	43.67 nm, in ascorbic acid	72 h	OECD TG 201	5.125 - 82 mg/L	14 mg/L (EC_{50}) 28 mg/L (EC_{50}) for non-coated Au NPs	Dědková *et al.* 2014
Au	43.67 nm, PVP coated	72 h	OECD TG 201	0.005125 - 0.08 mg/L	could not be calculated due to growth stimulation	Dědková *et al.* 2014
Au	5, 20, 40 nm, citrate and BPEI coated	72 -168 h	10% BG-11	0.0625- 1 mg/L	0.98 (EC_{50}), 0.26 mg/L (EC_{10}) for 5 nm BPEI. Could not be calculated for other Au NP types due to growth stimulation.	Current study
CeO_2	>25 nm, uncoated	72-168 h	10% BG-11	0.0625- 1 mg/L	Could not be calculated due to growth stimulation	Current study

Abbreviations: SA- NP surface area, ζ- zeta potential, PAA- poly-acrylic acid

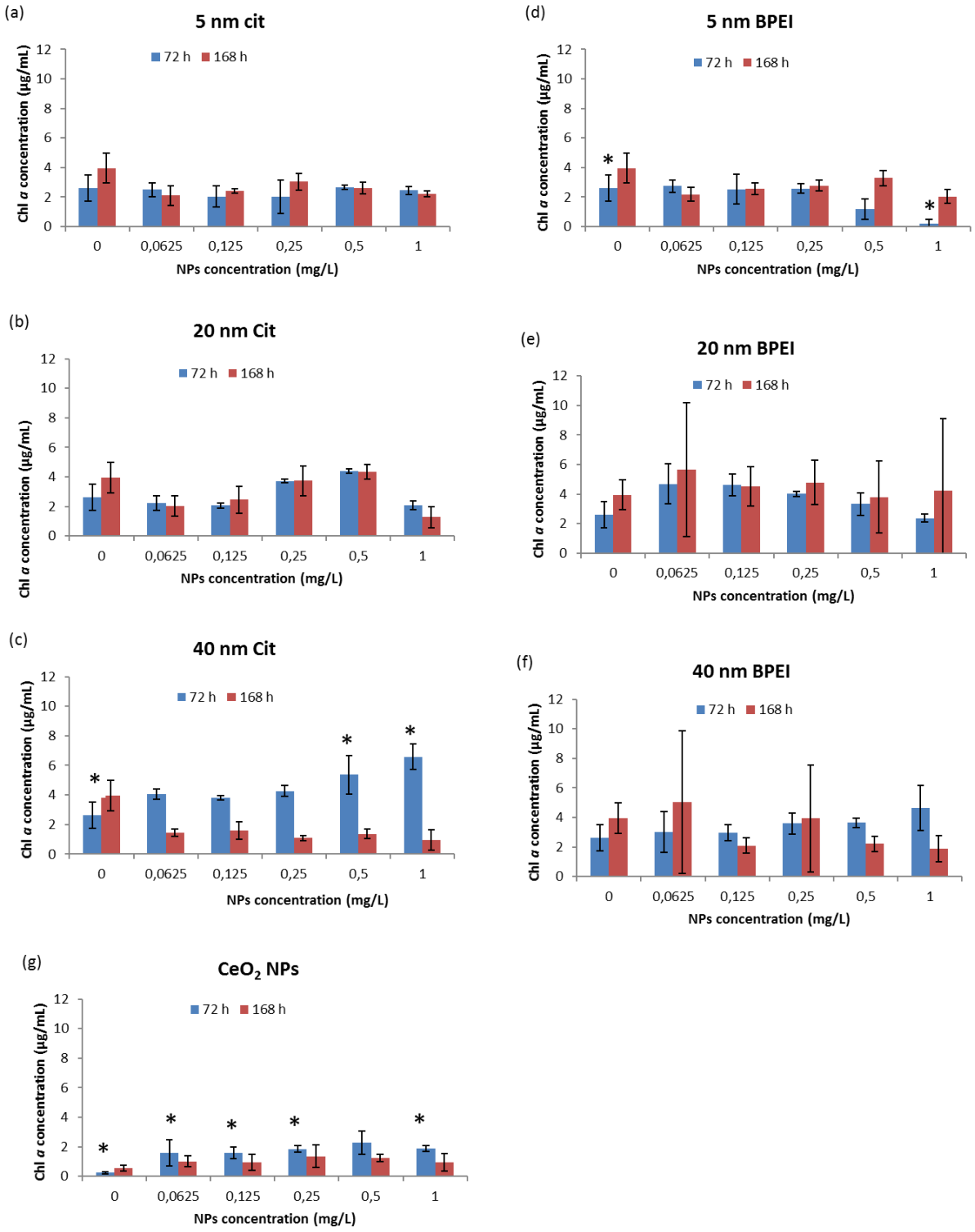

Figure 5.3: Effects of Au and CeO_2 NPs on chlorophyll *a* content of *P. subcapitata*. Results are reported as means ± standard deviations, *n*= 3. * denotes significant differences between the control and treated samples.

5.4.3 Genotoxicity studies

Changes in the genetic material induced by Au and CeO_2 NPs on DNA isolated from *P. subcapitata* were evaluated using the RAPD-PCR and AP-site techniques. The extracted DNA from all samples was pure enough for genotoxicity assays, with an absorbance ratio (OD_{280}/OD_{260}) ≥ 1.7 (Table A5.1). The DNA concentration was diluted to 40 and 100 ng/µL as initial concentrations for RAPD-PCR and AP site techniques, respectively. The results from preliminary studies (RAPD-PCR) revealed 46.8 °C and 44.3 °C to be optimum annealing temperatures for OPB1 and OPB14, respectively. As the cytotoxicity studies results did not differ based on the influence of concentration (Figure 5.2), three concentrations of NPs (0.0625, 0.25 and 1 mg/L) were selected for the genotoxicity studies.

5.4.3.1 RAPD PCR assay

Figure 5.4 shows the RAPD profiles of isolated genomic DNA from treated and untreated samples. These profiles were also used to analyse genomic stability using Equation 4. A negative control (no DNA) was included to ascertain whether any band observed was attributable to DNA amplification. The OPB1 primer demonstrated DNA alterations in exposed samples relative to the control. The alterations were in the form of appearance of new bands and/or disappearance of normal bands observed in the control. For example, normal bands observed in the control disappeared for 5 nm (0.065 mg/L) and 40 nm (0.25 mg/L) cit Au NPs at 72 h (Figure 5.4 (a)) with a genomic stability of 0%. The loss of normal bands and appearance of new bands compared to the control was observed for all NPs exposures using OPB 1 primer (Figure 5.4 (a)). The loss of normal bands is linked to DNA damage such as single- and double-strand breaks, modified bases, abasic sites or chromosomal rearrangements (Atienzar *et al.* 2002; Wolf *et al.* 2004). The appearance of new bands is likely due to DNA mutations (Atienzar and Jha 2006).

The OPB14 primer produced same RAPD profiles for untreated and treated algal DNA for all NPs at 72 and 168 h irrespective of NP size and coating type (Figure 5.4 (c), (d), and (h)), with a genomic template stability of 100%. Similarly, RAPD profile analysis after exposure of *Pseudomonas putida* to Al_2O_3 NPs showed no difference to the control, which suggests an induction of DNA repair mechanisms (Załęska-Radziwiłł and Doskocz 2016). Using the OPB14 primer for BPEI Au NPs at 72 h, showed the disappearance of a normal band and appearance of a new band compared to the control (Figure 5.4 (g)). The number of bands from

72 to 168 h either decreased, or remained unchanged for both coating types at all three tested concentrations. However, 5 nm (0.065 mg/L) and 40 nm (0.25 mg/L) cit Au NPs showed an increase from 0 to 2 and 3 bands, respectively. OPB14 results, however, were not included as no differences observed between the treated and untreated samples. RAPD profiles for CeO_2 NP treated algae using OPB1 were different from the control (Figure 5.5 (a)). However, the alterations were neither concentration nor time dependent, suggesting that NPs already induced the DNA damage at 72 h that persisted over 168 h. Using the OPB14 primer, CeO_2 NPs- treated algal DNA showed RAPD profiles similar to untreated DNA at 72 and 168 h (Figure 5.5 (b)) with a genomic stability of 100 %.

The genomic stability increased from 0-20% at 72 h to 40- 60% after168 h for cit-Au NPs. In agreement with the algal growth inhibition at 72 h and cell recovery at 96 h, results show an increase in genomic stability under long-term exposure conditions. This implies that under long-term exposure conditions, algae may acquire adaptive mechanisms to reverse the negative effects induced by NPs during early growth stages (Hazeem *et al.* 2015). Similarly, the genomic stability in zebrafish (*D. rerio)* exposed to TiO_2 NPs was reduced by 37% after 14 d, but increased after 21- 28 d; attributed to activation of defence mechanisms against free oxygen radicals in fish exposed to TiO_2 NPs (Rocco *et al.* 2015).

Results from the present study indicate RAPD PCR assay reveal potential toxicity of Au and CeO_2 NPs to algae at a molecular level although no effects were observed at a morphological level. Thus, the findings indicate the significant role of genotoxicity studies in assessing the potential environmental risks of NPs in aquatic biota. Similar to current findings, exposure of *Saccharomyces cerevisiae* to Au NPs showed DNA damage and ROS production without growth inhibition (de Alteriis *et al.* 2018). These findings support a recommendation made by Amaeze *et al.* (2015) that genotoxicity assays are more sensitive than cytotoxicity assays. The RAPD-PCR has been used successfully with NPs in different aquatic organisms such as bacteria (Amjady *et al.* 2016; Załęska-Radziwiłł and Doskocz 2016), and fish (Dedeh *et al*. 2015; Nigro *et al*. 2015; Rocco *et al.* 2015). Therefore, the current study contributes to limited data on the genotoxicity of NPs to different aquatic organisms especially algae, which play a crucial role as primary producers in the aquatic environment. Understanding the risk of NPs at lower trophic level could help predict the effects of NPs at higher trophic levels through the food chain.

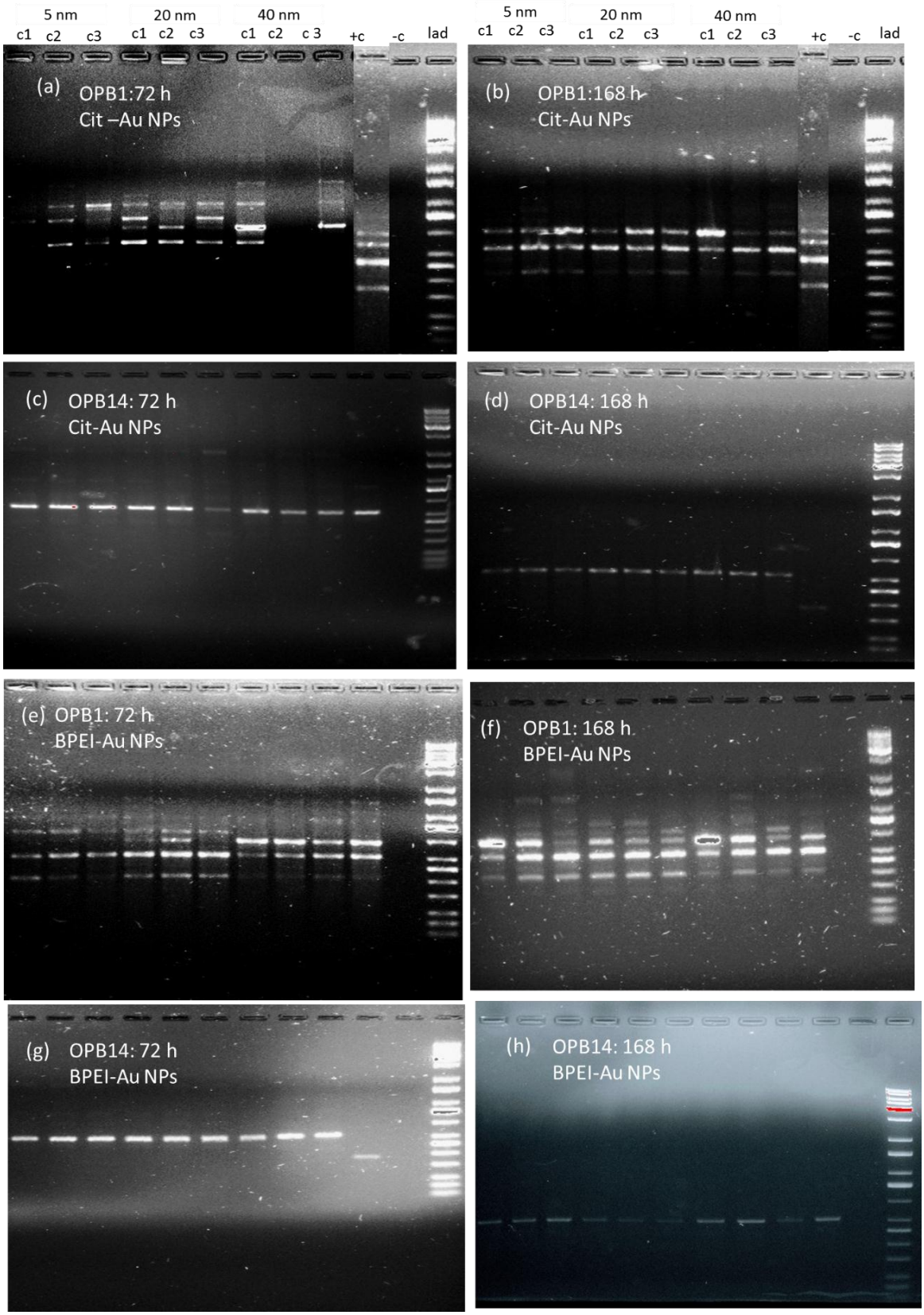

Figure 5.4: RAPD profiles generated using primers OPB1 and OPB14. Abbreviations: c1- 0.0625 mg/L, c2- 0.25 mg/L, c3- 1 mg/L, +c- untreated control, -c- negative control (no DNA) and lad- DNA ladder.

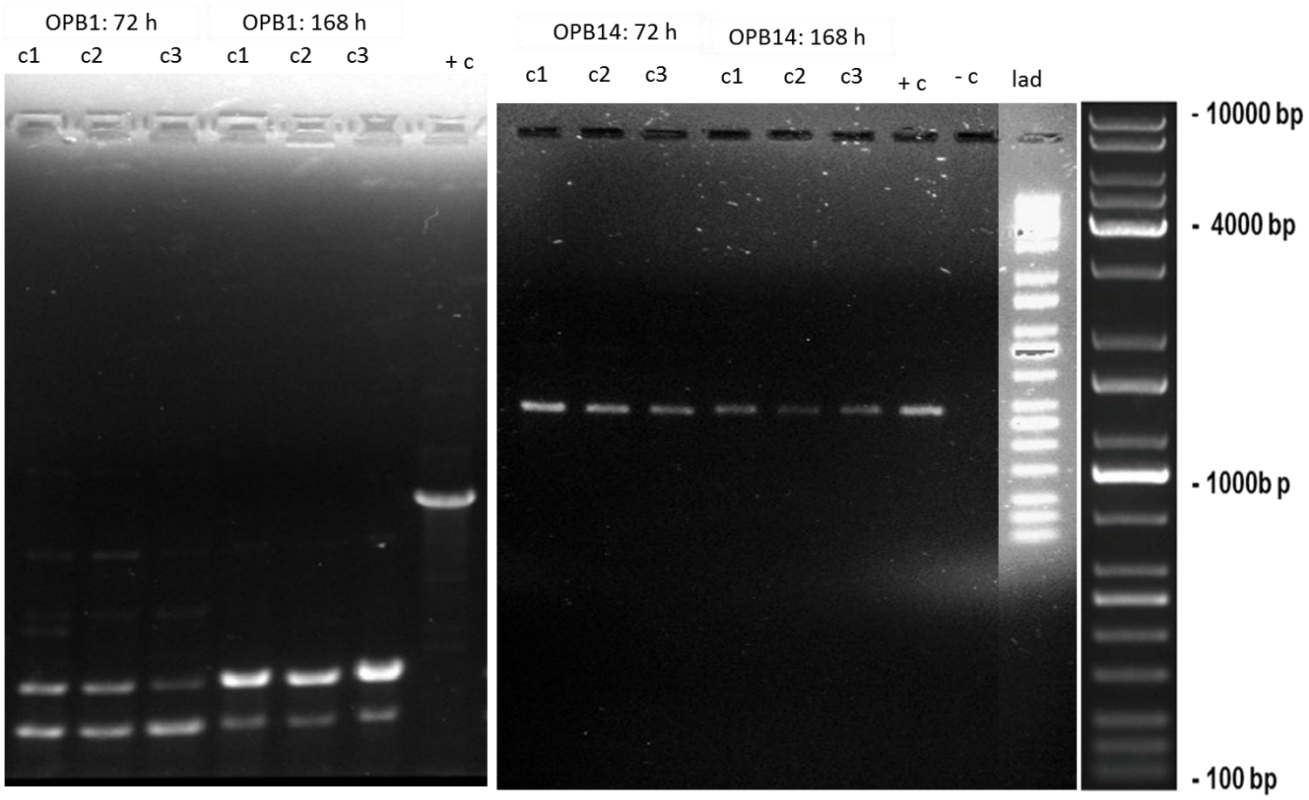

Figure 5.5: RAPD profiles of algae exposed to untreated control (+C), and 0.0625 (c1), 0.25 (c2) and 1 mg/L (c3) treatments of CeO_2 NPs with –C representing a negative control without DNA and lad is a DNA ladder.

5.4.3.2 AP site content assay

Boturyn *et al.* (1999) suggested that because of the relationship between the formation of AP sites and DNA damage, evaluation of AP site content could provide a measure of mutagen-induced DNA damage. Genotoxicity caused by CeO_2 NPs was not analysed using AP site assay as the initial DNA concentration was below the minimum required by the kit (100 ng/µL as shown in Table A5.1. The low DNA concentration was linked to significant growth inhibition in CeO_2 NP-treated samples after 72 h (Figure 5.2 (b)). Figure 5.6 depicts results of DNA standards (n = 2) containing predetermined AP sites. The trend-line equation ($y = 0.0711x + 0.088$; $R^2 = 0.9423$) was fitted on the standard curve data and was used to calculate AP sites generated from treated and untreated DNA samples, and results of AP sites formation are shown in Figure 5.7. To determine the level of genotoxicity, the number of AP sites in treated samples was compared to the control. Results indicated that the control samples had an AP site content of 15 ± 0.4 after 72 h (Figure 5.7 (a)) which increased to 18 ± 0.9 AP site per 10^5 bp at 168 h (Figure 5.7 (b)).

However, a significant increase in AP site content was observed for cit- and BPEI-Au NP-treated samples relative to the control at 72 and 168 h (Figure 5.7 (a), (b)) for all NPs except 40 nm-sized particles at 168 h (Figure 5.7 (b)) especially for BPEI coated ones. Thus, AP site content as a function of time (72 h and 168 h) exhibited significant differences with respect to size (no differences at lower sizes but apparent at the higher size of Au NPs); but none as a function of NP coating type and NP concentration. The 40 nm Au NPs for both coating types showed a significant reduction in AP site content after 168 h compared to 72 h at all three tested concentrations (Figure 5.7 (a) and (b)). It was noted that although statistically insignificant increase in AP site content (33 ± 0.4 to 42 ± 9 AP sites per 10^5 bp) at 168 h (Figure 5.7 (b)) was observed for the 5 nm BPEI Au NPs at 1 mg/L; results were consistent with significant growth inhibition (Figure 5.2 (d)) and Chl *a* content reduction observed (Figure 5.3 (d)). Therefore, for 5 nm BPEI Au NPs, genotoxicity findings closely correlate with cytotoxicity end-points (growth inhibition and reduction in chlorophyll a content). In addition, although 5 nm Au NPs showed high agglomeration compared to other sizes, the findings indicate that agglomeration does not reduce the reactivity of smaller sized NPs and their toxicity. Similarly, a study on the impact of agglomeration of Au NPs on the inflammatory response in rats showed that no major differences were observed between agglomerated (250 nm) and single (50 nm) Au NPs (Gosens *et al.* 2010).

The results for 40 nm Au NPs herein indicate that exposure duration play a significant role in genotoxicity response of algae to Au NPs. However, to date, most toxicity studies on algae have focused on the effects of NPs during the exponential growth phase of up to 72 h (Schiavo *et al*. 2016; Iswarya *et al*. 2017; Morelli *et al*. 2018); where plausible recovery is not considered as observed in this study. Findings from this study show that Au NPs can induce DNA damage to aquatic organisms such as algae at shorter exposure time, but repair can occur over extended exposure period due to DNA repair mechanisms active within algae. Repair of AP sites generated occur through the BER pathway by either AP endonucleases or AP lyase activities (Demple and Harrison 1994; Krokan and Bjørås 2013; Cunniffe *et al.* 2014; Barbado *et al.* 2018). Based on the current results it appears that the DNA repair mechanism is dependent on time and concentration. Thus, at higher NP concentration, no DNA repair was observed.

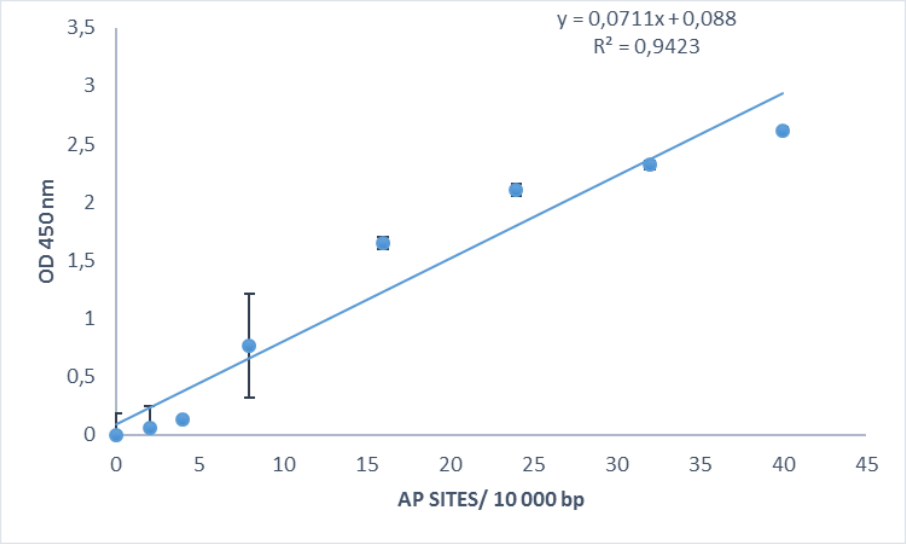

Figure 5.6: ARP-DNA standard curve with pre-determined AP sites

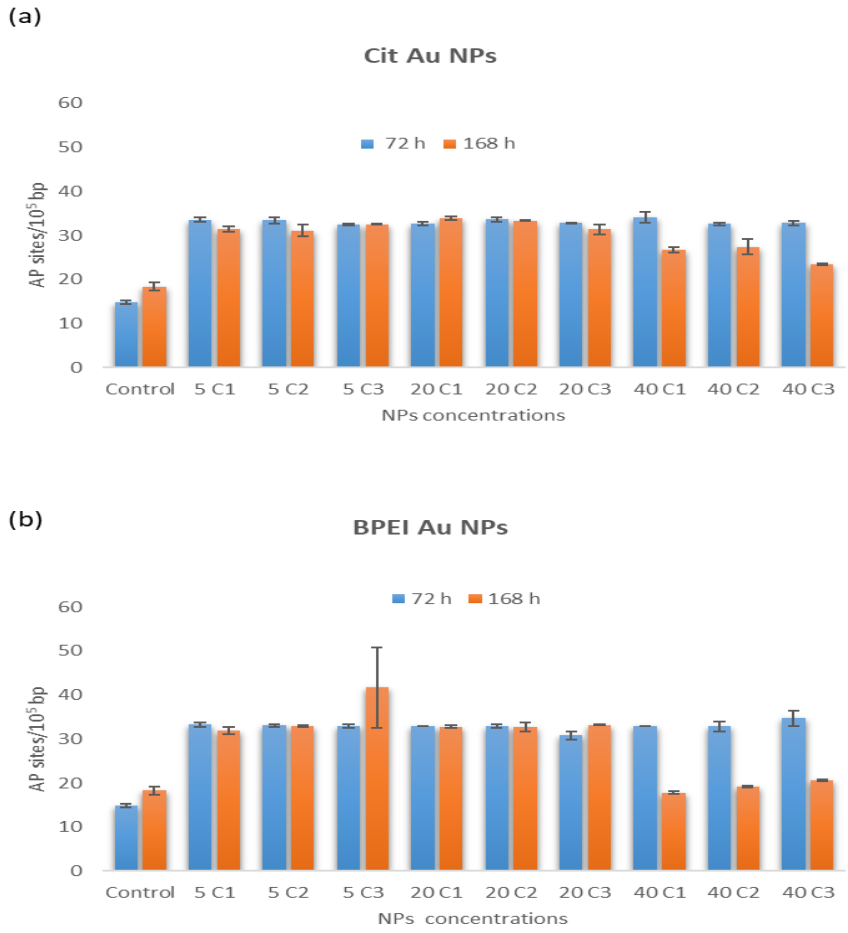

Figure 5.7: AP site content in algal DNA after exposure to NPs at 72 h and 168 h. Values are reported as means ± standard deviations, *n*=2. C1, C2 and C3 represent NP concentrations of 0.0625, 0.25 and 1 mg/L, respectively.

5.5 Conclusions

The study contributes to the understanding of the ecotoxicity of Au and CeO_2 NPs in the aquatic environment. It was observed that Au and CeO_2 NPs agglomerated immediately upon addition to BG-11 algal medium, indicating the importance of considering the interactions of NPs with media constituents. Citrate coated-Au and CeO_2 NPs, in the range of 0.0625–1 mg/L, neither inhibited *P. subcapitata* growth nor affected the cellular chlorophyll content. Where slight growth inhibition was observed at 72 h, the test organisms recovered after 96 h. Significant algal growth inhibition and Chl *a* content reduction was only observed with 5 nm BPEI Au NPs at 1 mg/L; suggesting the influence of physicochemical properties of NPs.

RAPD PCR and AP site content assays revealed potential toxicity of Au and CeO_2 NPs to algae at a molecular level although no effects were observed at a morphological level. Thus, the findings indicate the significant role of genotoxicity studies in assessing the potential environmental risks of NPs in aquatic biota; and that genotoxicity assays are more sensitive than cytotoxicity assays.

Exposure duration plays a significant role in genotoxicity response of algae to NPs. Results showed an increase in genomic stability under long-term exposure conditions (168 h), suggesting the presence of adaptive mechanisms to reverse the negative effects induced by NPs during early algal growth stages. Significant differences were observed with respect to NP size, but none as a function of NP coating type and NP concentration. Results also showed that for 5 nm BPEI Au NPs, genotoxicity closely correlated with cytotoxicity end-points, and agglomeration did not reduce reactivity of smaller sized NPs and their toxicity. Furthermore, results obtained using the OPB1 primer were more informative than for OPB14, from which it is concluded that the type of primer determines the reliability of the information obtained.

The current study contributes to the limited available data on the genotoxicity of metallic NPs to algae, which play a crucial role as primary producers in the aquatic environment. Understanding the risk of NPs at lower trophic level could help predict the effects of NPs at higher trophic levels through the food chain. Finally, Au and CeO_2 NPs could be considered as potential genotoxic nano-pollutants for algae.

CHAPTER 6: CONCLUDING REMARKS AND FUTURE PERSPECTIVES

6.1 Concluding remarks

Objective 1: Review on the genotoxicity of metal based engineered nanoparticles in aquatic organisms.

The literature survey undertaken showed that ENPs are generally found at low concentrations and are therefore likely to exert sub-lethal effects (genotoxicity) on aquatic organisms. Nanoparticles were reported to cause genotoxic responses such as DNA damage (single- or double strand breaks), apoptosis, chromosomal fragmentation or alterations in gene expression profiles on aquatic organisms. The effects of the NPs were dependent on their inherent physico-chemical properties (e.g. size, surface coating, surface area, morphology, surface charge, e.tc.), and the presence of co-pollutants. The fate and behaviour (dissolution, aggregation, agglomeration, and adsorption) of NPs in aquatic systems also influenced genotoxicity. However, less effort was put in correlating the observed effects of NPs to their inherent physico-chemical properties. A more complete characterisation of NPs before, during and after introduction into the exposure media is therefore necessary in order to understand any changes in physicochemical properties and the impacts of those changes on the genotoxicity of NPs.

Genotoxicity was also found to be assay dependent. For example, where more than one assay was used in the same study, significant differences in the degree of toxicity were often noted. Therefore, interpretations based on a single assay method may be misleading and *in vitro* tests need to be validated by *in vivo* tests, as recommended by the OECD. The comet assay was the most frequently used, presumably because of its technical simplicity and ability to detect low levels of DNA damage. The literature survey indicated TiO_2 and Ag as the most tested NPs for genotoxicity. This is expected as these NPs are among the most widely produced and are used in many consumer products and industrial applications (PEN, 2014; Hansen et al. 2016). To date, most genotoxicity studies have been conducted on fish, invertebrates (mostly daphnia) and bacteria, with limited information on algae and aquatic higher plants. Hence, there is a clear need for further genotoxicity research using a wider range of test organisms and NPs. Most studies where genotoxicity was reported, experiments were conducted at high NP concentrations unlikely to be found in the environment and under acute exposure conditions. Exposure NP concentrations have been reported as one of the major concerns in hazard assessments (Holden *et al.* 2016). High exposure concentrations of NPs that may alter media conditions, should be avoided.

Objective 2: Investigates the influence of NPs physico-chemical properties and media composition on the behaviour of Au and CeO_2 NPs in biological media.

Size and surface coating of the NPs and media constituents influenced the fate and behaviour of Au and CeO_2 NPs. All NPs agglomerated immediately upon introduction into media; with smallest 5 nm Au NPs for both coating types agglomerating more rapidly compared to larger counterparts (20 and 40 nm). BPEI-coated Au NPs were more stable (smaller HDD) compared to citrated-coated Au NPs. All NPs were stable (smaller HDD and lower ζ potentials) in DIW compared to biological media; attributed to the low ionic strength of DIW. Agglomeration followed the order DTW > BG-11 > 10 HM > DIW for BPEI-Au NPs. High agglomeration was observed in BG-11 for citrate-Au NPs and in DTW for uncoated-CeO_2 NPs. Instability of NPs in biological media was confirmed by a decrease in absorbance, broadening of SPR peak and an increase in size distribution over time at pH 7.

The use of multimethod approach for NP sizing (TEM, NTA and DLS) increases the accuracy of data due to the complexity of NP samples and the limitations of each analytical technique. However, the use of light scattering techniques for size determination is limited for non-spherical particles. Hence, the broader particle size distribution observed indicated (i) formation of agglomerates, (ii) instability of Au and CeO_2 NPs in ecotoxicological media or/and (iii) inaccuracy of light scattering techniques in size analysis for non-spherical NPs. Therefore, for accurate NPs size determination, analytical techniques suitable for non-spherical shaped particles and standardised sample preparation methods are recommended.

Objective 3: Investigates the influence of NPs physico-chemical properties and exposure period on bioaccumulation of Au and CeO_2 NPs by aquatic higher plant Salvinia minima.

Nanoparticles were not internalized by *S. minima* irrespective of particle type, size and coating type. Au and CeO_2 NPs can be adsorbed on the roots of *S. minima* but without inducing morphological level effects such as growth retardation and necrosis at environmentally relevant NP concentrations. The lack of NPs internalization and phytotoxicity was linked to high agglomeration of NPs in 10% Hoagland's medium. The findings demonstrated the importance of considering the influence of physico-chemical properties of NPs and medium composition on bioaccumulation by aquatic plants. NP size and type but not surface coating influenced accumulation. The high concentrations of 5 nm Au NPs and CeO_2 NPs accumulated in fronds

compared to roots of 20 and 40 nm Au NPs. NPs can be translocated from roots to fronds, however, in the absence of internalization in this study, translocation cannot be attributed to high concentrations of Au and Ce found on the fronds, thus the aspect requires further investigation.

Although NPs can be translocated from roots to fronds, no internalization was observed in this study, and therefore, translocation could not account for the high concentrations of Au and Ce found on the fronds. This aspect merits further investigation. Adsorption of NPs on the roots surface was confirmed in all instances irrespective NP size, coating variant, and type. Thus, adsorption was established as the mechanism of Au and CeO_2 NPs accumulation in *S. minima.* Overall, results suggested that Au and CeO_2 NPs can be adsorbed on the plant roots without internalization and translocation into fronds in *S. minima.* Even though these NPs did not exert toxicity to plants at morphological level; the low concentrations of NPs as found in the environment are likely to exert sub-lethal effects. Therefore, further studies at different end-points at a molecular level (e.g., chromosomal abnormalities, DNA damage, and genome template stability) are recommended.

Objective 4: Investigates the influence of physicochemical properties of NPs on the DNA integrity of algae under short- (72 h) and long- term (168 h) exposure durations at cellular and molecular levels.

Au and CeO_2 NPs agglomerated immediately upon addition to BG-11 algal medium, indicating the importance of considering the interactions of NPs with media constituents. Citrate coated-Au and CeO_2 NPs, in the range of 0.0625–1 mg/L, neither inhibited *P. subcapitata* growth nor affected the cellular chlorophyll content. Where slight growth inhibition was observed at 72 h, the test organisms recovered after 96 h. Significant algal growth inhibition and Chl *a* content reduction was only observed with 5 nm BPEI Au NPs at 1 mg/L; suggesting the influence of NP physicochemical properties.

RAPD PCR and AP site content assays revealed potential toxicity of Au and CeO2 NPs to algae at a molecular level although no effects observed at a morphological level. Thus, the findings indicate the significant role of genotoxicity studies in assessing the potential

environmental risks of NPs in aquatic biota; and that genotoxicity assays are more sensitive than cytotoxicity assays.

The exposure duration plays a significant role in genotoxicity response of algae to NPs. Results show an increase in genomic stability under long-term exposure conditions (168 h), suggesting the presence of adaptive mechanisms to reverse the negative effects induced by NPs during early algal growth stages. Significant differences were observed with respect to NP size, but none as a function of NP coating type and NP concentration. Results also showed that for 5 nm BPEI A u NPs, genotoxicity findings closely correlate with cytotoxicity end-points, and agglomeration does not reduce the reactivity of smaller sized NPs and their toxicity. Furthermore, results obtained using the OPB1 primer were more informative than for OPB14, therefore, the type of primer determines the reliability of information obtained.

The current study contributes to limited data on the genotoxicity of metallic NPs to algae, which plays a crucial role as primary producers in the aquatic environment. Understanding the risk of NPs at lower trophic level could help predict the effects of NPs at higher trophic levels through the food chain. Finally, Au and CeO_2 NPs could be considered as potential genotoxic nano-pollutants for algae.

6.2 Recommendations

- The transformation of NPs upon introduction to the exposure medium, indicate the importance of considering the interactions of NPs with media constituents. The knowledge of NPs transformations in biological media with the known composition can be translated to the fate and behaviour of NPs in natural environmental systems, thus enabling prediction of the behaviour of NPs in natural environments. A complete long-term characterisation of NPs before, during and after introduction into the exposure media is therefore necessary in order to understand any changes in physicochemical properties of NPs and the impacts of those changes on the biological effects of NPs.
- The use of multimethod approach for NP sizing increases the accuracy of data due to the complexity of NP samples and the limitations of each analytical technique. The light scattering techniques currently used for NP size determination are limited for non-spherical particles. Thus, for accurate NPs size determination, size analytical techniques suitable for non-spherical shaped particles and standardised sample preparation methods are recommended.
- Adsorption of NPs to roots of aquatic higher plants contribute to green phytoremediation and environmental safety as aquatic plants can be used to remove nano-pollutants from the aquatic systems. Therefore, more research in this area using a wide range of plant types is highly encouraged.
- The use of cytotoxicity and genotoxicity assays under short- and long-term exposure conditions revealed different biological effects. In addition to cytotoxicity studies, genotoxicity studies conducted under chronic exposure conditions at environmentally relevant NP concentrations are recommended to assess the environmental risks of NPs on aquatic biota. Based on insufficient research information available, further research is recommended to identify the exact mechanisms on the genotoxicity of NPs on aquatic biota.

CHAPTER 7: REFERENCES

Abadeer NS, Murphy CJ. 2016. Recent progress in cancer thermal therapy using gold nanoparticles. *Journal of Physical Chemistry* C, 120: 4691–716.

Abbaszadegan A, Ghahramani Y, Gholami A, Hemmateenejad B, Dorostkar S, Nabavizadeh M, Sharghi H. 2015. The effect of charge at the surface of silver nanoparticles on antimicrobial activity against Gram-Positive and Gram-Negative Bacteria: A Preliminary Study. *Journal of Nanomaterials*, 2015: 1-8.

Abdel-Khalek AA. 2016. Comparative evaluation of genotoxic effects induced by cuo bulk and nano-particles in Nile Tilapia, Oreochromis niloticus. *Water Air and Soil Pollution*, 227: 35.

Adani F, Papa G, Schievano A, Cardinale G, D'Imporzano G, Tambone F. 2011. Nanoscale structure of the cell wall protecting cellulose from enzyme attack. *Environmental Science and Technology*, 45:1107–1113.

Afshinnia K, Marrone B, Baalousha M. 2018. Potential impact of natural organic ligands on the colloidal stability of silver nanoparticles. *Science of the Total Environment*, 625: 1518–1526.

Aitken RJ, Chaudhry MQ, Boxall ABA, Hull M. 2006. Manufacture and use of nanomaterials: current status in the UK and global trends. *Occupational Medicine,* 56:300–306.

Alam B, Philippe A, Rosenfeldt RR, Seitz F, Dey S, Bundschuh M, Schaumann GE, Brenner SA. 2016. Synthesis, characterization, and ecotoxicity of CeO_2 nanoparticles with differing properties. *Journal of Nanoparticle Research*, 18:303.

Ale A, Bacchetta C, Rossi AS, Galdopórpora J, Desimone MF, de la Torre FR, Gervasio S, Cazenave J. 2018. Nanosilver toxicity in gills of a neotropical fish: Metal accumulation, oxidative stress, histopathology and other physiological effects. *Ecotoxicology and Environmental Safety*, 148: 976-984.

Ali BA, Huang T-H, Qin D, Wang X-M. 2004. A review of random amplified polymorphic DNA (RAPD) markers in fish research. *Reviews in Fish Biology and Fisheries*, 14: 443–453.

Ali D, 2014. Oxidative Stress-Mediated Apoptosis and Genotoxicity Induced by Silver Nanoparticles in Freshwater *Snail Lymnea luteola L. Biological Trace Element Research,* 162: 333–341.

Ali D, Alarifi S, Kumar S, Ahamed M, Siddiqui MA. 2012. Oxidative stress and genotoxic effect of zinc oxide nanoparticles in freshwater snail *Lymnaea luteola L. Aquatic Toxicology*, 124–125: 83–90.

Ali D, Ali H, Alarifi S, Kumar S, Serajuddin M, Mashih AP, Ahmed M, Khan M, Adil SF, Shaik MR , Ansari AA. 2015. Impairment of DNA in a freshwater gastropod (*Lymnea luteola*

L.) after exposure to titanium dioxide nanoparticles. *Archives of Environmental Contamination and Toxicology*, 68: 543–552.

Ali D, Ali H, Alarifi S, Masih AP, Manohardas S,Hussain SA. 2016. Eco-toxic efficacy of nano-sized magnesium oxide in freshwater snail *Radix leuteola L. Fresenius Environmental Bulletin*, 25(4/2016): 1234-1242.

Ali D, Ali H. 2015. Susceptibility of the freshwater pulmonate snail *Lymnea luteola L*. to copper oxide nanoparticle. *Toxicological and Environmental Chemistry*, 97(5): 576-587.

Ali D, Yadav PG, Kumar S, Ali H, Alarifi S, Harrath AH. 2014. Sensitivity of freshwater pulmonate snail *Lymnaea luteola L*., to silver nanoparticles. *Chemosphere*, 104: 134–140.

Ali D. 2015. Evaluation of environmental stress by comet assay on freshwater snail *Lymnea luteola L*. exposed to titanium dioxide nanoparticles. *Toxicological and Environmental Chemistry*, 96(8): 1185-1194.

Allen RT, Hunter WJ, Agrawal DK. 1997. Morphological and biochemical characterization and analysis of apoptosis, *Journal of Pharmacological and Toxicological Methods*, 37(4): 215–228.

Amaeze NH, Schnell S, Sozeri O, Otitoloju AA, Egonmwan RI, Arlt VM, Bury NR. 2015. Cytotoxic and genotoxic responses of the RTgill-W1 fish cells in combination with the yeast oestrogen screen to determine the sediment quality of Lagos lagoon. *Niger. Mutagen*, 30(1):117–127.

Ames BN, McCann J, Yamasaki E. 1975. Methods for detecting carcinogens and mutagens with the Salmonella/mammalian-microsome mutagenicity test. *Mutation Research*, 31: 347–364.

Amjady F, Golestani EB, Karimi F, Sevda T. 2016. An investigation of the effect of copper oxide and silver nanoparticles on E. coli genome by RAPD molecular markers. *Advances in Biotechnology and Microbiology***,** 1(2): 555-559.

Anantha AN, Daniel SCGK, Sironmani TA, Umapathia S. 2011. PVA and BSA stabilized silver nanoparticles based surface–enhanced plasmon resonance probes for protein detection. *Colloids and Surfaces B: Biointerfaces,* 85: 138–144.

Angel BM, Vallotton P, Apte SC. 2015. On the mechanism of nanoparticulate CeO_2 toxicity to freshwater algae. *Aquatic Toxicology,* 168: 90–97.

ANSES, 2014. Enjeux et mise à jour des connaissances.

Apoorva G, Lavanya K, Vidisha, Pavani, Kumar R, Hasan Q, Ramakrishna. 2013. Genotoxic effects of silver and titanium dioxide nanoparticles. proceedings of the "international conference on advanced nanomaterials & emerging engineering technologies" (ICANMEET-2013), organized by Sathyabama University, Chennai, India in association with DRDO, New Delhi, India, 24th -26th" July, 2013.

Arndt DA, Moua M, Chen J and Klaper RD. 2013. Core Structure and Surface Functionalization of Carbon Nanomaterials Alter Impacts to Daphnid Mortality, Reproduction, and Growth: Acute Assays Do Not Predict Chronic Exposure Impacts. *Environmental Science and Technology*, 47: 9444−9452.

Aruoja V, Pokhrel S, Sihtmäe M, Mortimer M, Mädler L, Kahru A. 2015. Toxicity of 12 metal-based nanoparticles to algae, bacteria and protozoa. *Environmental Science Nano*, 2: 630–644.

Asli S, Neumann PM. 2009. Colloidal suspensions of clay or titanium dioxide nanoparticles can inhibit leaf growth and transpiration via physical effects on root water transport. *Plant Cell and Environment*, 32:577– 584.

Atienzar FA and Jha AN. 2006. The random amplified polymorphic DNA (RAPD) assay and related techniques applied to genotoxicity and carcinogenesis studies: a critical review. *Mutation Research*, 613: 76–102.

Atienzar FA, Venier P, Jha AN, Depledge MH. 2002. Evaluation of the random amplified polymorphic DNA (RAPD) assay for the detection of DNA damage and mutations. *Mutation Research*, 521: 151–163.

Auffan M, Rose J, Wiesner MR and Bottero J. 2009. Chemical stability of metallic nanoparticles: A parameter controlling their potential cellular toxicity *in vitro*. *Environmental Pollution*, 157: 1127–1133.

Azqueta A, Slyskova J, Langie SA, O'Neill Gaiva˜o I, Collins A. 2014. Comet assay to measure DNA repair: approach and applications. *Frontiers in Genetics*, 5:1–8.

Baalousha M, Arkill KP, Romer I, Palmer RE, Lead JR. 2015. Transformations of citrate and Tween coated silver nanoparticles reacted with Na_2S. *Science of the Total Environment*, 502: 344–353.

Baalousha M, Manciulea A, Cumberland S, Kendall K, Lead J. 2008. Aggregation and surface properties of iron oxide nanoparticles: influence of pH and natural organic matter. *Environmental Toxicology and Chemistry*, 27(9): 1875-1882.

Baalousha M, Nur Y, Römer I, Tejamaya M, Lead JR. 2013. Effect of monovalent and divalent cations, anions and fulvic acid on aggregation of citrate-coated silver nanoparticles. *Science of the Total Environment*, 454–455:119–31.

Baalousha M, Yang Y, Vance ME, Colman BP, McNeal S, Xu J, Blaszczak J, Steele M, Bernhardt E, Hochella Jr. MF. 2016. Outdoor urban nanomaterials: the emergence of a new, integrated, and critical field of study. *Science of the Total Environment*, 557–558: 740–753.

Bacchetta C, Ale A, Simoniello MF, Gervasio S, Davico C, Rossi AS, Desimone MF, Poletta G, López G, Monserrath JM, Cazenave J. 2017. Genotoxicity and oxidative stress in fish after a short-term exposureto silver nanoparticles. *Ecological Indicators*, 76: 230–239.

Bajpayee M, Kumar A, Dhawan A. 2013. The comet assay: assessment of in vitro and in vivo DNA damage. *Methods in Molecular Biology*, 1044: 325-45.

Balog S, Rodriguez-Lorenzo L, Monnier CA, Obiols-Rabasa M, Rothen-Rutishauser B, Schurtenberger P, Petri-Fink A. 2015. Characterizing nanoparticles in complex biological media and physiological fluids with depolarized dynamic light scattering. *Nanoscale,* 7:5991–5997.

Banni M, Sforzini S, Balbi T, Corsi I, Viarengo A, Canesi L. 2016. Combined effectsofn-TiO2 and 2,3,7,8-TCDD in *Mytilus galloprovincialis* digestive gland: A transcriptomic and immunohistochemical study. *Environmental Research,* 145: 135–144.

Barbado C, Córdoba-Cañero D, Ariza RR, Roldán-Arjona T. 2018. Nonenzymatic release of N7-methylguanine channels repair of abasic sites into an AP endonuclease-independent pathway in *Arabidopsis*. *Proceedings of the National Academy of Sciences of the United States of America*, 115(5):916-924.

Barrena R, Casals E, Colón J, Font X, Sánchez A, Puntes V. 2009. Evaluation of the ecotoxicity of model nanoparticles. *Chemosphere*, 75(7): 850-857.

Barreto A, Luis LG, Soares AMVM, Oliveira M. 2015. Behavior of colloidal gold nanoparticles in different ionic strength media. *Journal of Nanoparticle Research*, 17:493.

Batley GE, Kirby JK, and Mclaughlin MJ. 2013. Fate and risks of nanomaterials in aquatic and terrestrial environments. *Accounts of Chemical Research*, 46(3): 854 – 862.

Bäuerlein PS, Emke E, Tromp P, Hofman JAMH, Carboni A, Schooneman F, de Voogt P, van Wezel AP. 2017. Is there evidence for man-made nanoparticles in the Dutch environment? *Science of the Total Environment,* 576: 273–283.

Bayat N, Lopes VR, Scholermann J, Jensen LD, Cristobal S. 2015. Vascular toxicity of ultra-small TiO_2 nanoparticles and single walled carbon nanotubes *in vitro* and *in vivo*. *Biomaterials,* 63: 1-13.

BCC Research, 2012. Nanotechnology: a realistic market research. NANO31E, Wellesley, USA.

BCC Research. 2014. Nanotechnology: a realistic market assessment. NAN031F, Wellesley, USA.

Becaro AA, Jonsson CM, Puti FC, Siqueira MC, Mattoso LHC, Correa DS, Ferreira MD. 2015. Toxicity of PVA-stabilized silver nanoparticles to algae and microcrustaceans. *Environmental Nanotechnology, Monitoring and Management,* 3: 22–29.

Bergeron S and Archambault E. 2005. Canadian stewardship practices for environmental nanotechnology. Science-Metrix Report prepared for Environment Canada, Montreal, Canada

Bhuvaneshwari M, Bairoliya S, Parashar A, Chandrasekaran N, Mukherjee A. 2016. Differential toxicity of Al_2O_3 particles on Gram-positive and Gram-negative sediment bacterial isolates from freshwater. *Environmental Science and Pollution Research*, 23: 12095–12106.

Bleeker EAJ, de Jong WH, Geertsma RE, Groenewold M, Heugens EHW, Koers-Jacquemijns M, van de Meent D, Popma JR, Rietveld AG, Wijnhoven SWP, Cassee FR, Oomen AG. 2013. Considerations on the EU definition of a nanomaterial: Science to support policy making. *Regulatory Toxicology and Pharmacology*, 65: 119–125.

Blinova I, Vija H, Lukjanova A, Muna M, Syvertsen-Wiig G, Kahru A. 2018. Assessment of the hazard of nine (doped) lanthanides-based ceramic oxides to four aquatic species. *Science of the Total Environment*, 612: 1171-1176.

Bodelón G, Costas C, Pérez-Juste J, Pastoriza-Santos I, Luis M. Liz-Marzán LM. 2017. Gold nanoparticles for regulation of cell function and behaviour. *Nano Today*, 13: 40–60.

Bolognesi C, Cirillo S. 2014. Genotoxicity biomarkers in aquatic bioindicators. *Current Zoology* 60(2): 273–284.

Bolognesi C, Hayashi M. 2011. Micronucleus assay in aquatic animals. *Mutagenesis*, 26 (1): 205–213.

Bondarenko O, Juganson K, Ivask A, Kasemets K, Mortimer M, Kahru A. 2013. Toxicity of Ag, CuO and ZnO nanoparticles to selected environmentally relevant test organisms and mammalian cells in vitro. *Archives of Toxicology*, 87: 1181–1200.

Booth A, Trond Størsetha, Altin D, Fornara A, Ahniyaz A, Jungnickel H, Laux P, Luch A, Sørensen L. 2015. Freshwater dispersion stability of PAA-stabilised cerium oxide nanoparticles and toxicity towards *Pseudokirchneriella subcapitata. Science of the Total Environment*, 505:596–605.

Boran H, Ulutas G. 2016. Genotoxic effects and gene expression changes in larval zebrafish after exposure to ZnCl2 and ZnO nanoparticles. *Diseases of Aquatic Organisms*, 117: 205–214.

Boturyn D, Constant J-F, Defrancq E, Lhomme J, Barbin A, Wild CP. 1999. A simple and sensitive method for in vitro quantitation of abasic sites in DNA. *Chemical Research in Toxicology*, 12: 476-482.

Boxall ABA, Chaudhry Q, Sinclair C, Jones A, Aitken R, Jefferson B, Watts C. 2007a. Current and future predicted environmental exposure to engineered nanoparticles. *Central Science Laboratory Publications*, York, UK, p. 89.

Bozich JS, Lohse SE, Torelli MD, Murphy CJ, Hamers RJ, Klaper RD. 2014. Surface chemistry, charge and ligand type impact the toxicity of gold nanoparticles to *Daphnia magna. Environmental Science: Nano,* 1(3): 260-270.

Bruneau A, Turcotte P, Pilote M, Gagné F, Gagnon C. 2016. Fate of silver nanoparticles in wastewater and immunotoxic effects on rainbow trout. *Aquatic Toxicology*, 174: 70–81.

Buffet P, Richard M, Caupos F, Vergnoux A, Perrein-Ettajani H, Luna-Acosta A, Akcha F, Amiard J, Amiard-Triquet C, Guibbolini M, Faverney CR, Thomas-Guyon H, Reip P, Dybowska A, Berhanu D, Valsami-Jones E, Mouneyrac C. 2013. A mesocosm study of fate and effects of Cuo nanoparticles on endobenthic species (*Scrobicularia plana, Hediste diversicolor*). *Environmental Science and Technology*, 47: 1620−47:1.

Buffet PE, Zalouk-Vergnoux A, Poirier L, Lopes C, Risso-de-Faverney C, Guibbolini M, Gilliland D, Perrein-Ettajani H, Valsami-Jones E, Mouneyrac C. 2015. Cadmium sulfide quantum dots induce oxidative stress and behavioral impairments in the marine clam Scrobicularia plana. *Environmental Toxicology and Chemistry*, 34: 1659‑1664.

Buzea C, Blandino IIP, Robbie K. 2007. Nanomaterials and nanoparticles: Sources and toxicity. *Biointerphases, 2 (4): MR17 - MR172.*

Canesi L, Ciacci C, Fabbri R, Marcomini A, Pojana G, Gallo G. 2012. Bivalve molluscs as a unique target group for nanoparticle toxicity. *Marine Environmental Research,* 76:16–21.

Canesi L, Frenzilli G,Balbi T, Bernardeschi M, Ciacci C, Corsolini S, Torre CD, Fabbri R, Faleri C, Focardi S, Guidi P, Kocan A, Marcomini A, Mariottini M, Nigro M, Pozo-Gallardo K,Rocco L, Scarcelli V, Smerilli A, Corsi I. 2014. Interactive effects of $nTiO_2$ and 2,3,7,8-TCDD on the marine bivalve *Mytilus galloprovincialis. Aquatic Toxicology*, 153: 53–65.

Canesi L, Negri A, Barmo C, Banni M, Gallo G, Viarengo A, Dondero F. 2011. The organophosphate Chlorpyrifos interferes with the responses to 17β-estradiol in the digestive gland of the marine mussel Mytilus galloprovincialis. *PLoS One,* 6: 19803.

Carp O, Huisman CL, Reller A. 2004. Photoinduced reactivity of titanium dioxide. *Progress in Solid State Chemistry*, 32: 33–177.

Carriere M, Sauvaigo S, Douki T, Ravanat J-L. 2017. Impact of nanoparticles on DNA repair processes: current knowledge and working hypotheses. *Mutagenesis*, 32(1): 203-213.

Cassee FR, Campbell A, Boere AJF, McLean SG, Duffin R, Krystek P, Gosens I, Miller MR. 2012. The biological effects of subacute inhalation of diesel exhaust following addition of cerium oxide nanoparticles in atherosclerosis-prone mice. *Environnmental Research,* 115:1–10.

Cassee FR, van Balen EC, Singh C, Green D, Muijser H, Weinstein K. Dreher K. 2011. Exposure, health and ecological effects review of engineered nanoscale cerium and cerium oxide associated with its use as a fuel additive. *Critical Reviews in Toxicology,* 41: 213–229.

Castro-Longoria E, Trejo-Guillén K, Vilchis-Nestor AR, Avalos-Borja M, Andrade-Canto SB, Leal-Alvarado DA, Santamarí JM. 2014. Biosynthesis of lead nanoparticles by the aquatic

water fern, Salvinia minima Baker, when exposed to high lead concentration. *Colloids and Surfaces B: Biointerfaces*, 114: 277– 283.

Cedervall T, Lynch I, Foy M, Berggard T, Donnelly SC, Cagney G, Linse S, Dawson KA. 2007. Detailed identification of plasma proteins adsorbed on copolymer nanoparticles. *Angewandte Chemie*, 119: 5856-5858.

Cerrillo C, Barandika G, Igartua A, Areitioaurtena O, Mendoza G. 2016. Towards the standardization of nanoecotoxicity testing: Natural organic matter 'camouflages' the adverse effects of TiO_2 and CeO_2 nanoparticles on green microalgae. *Science of the Total Environment*, 543: 95–104.

Chae YJ, Pham CH, Lee J, Bae E, Yi J, Gu MB. 2009. Evaluation of the toxic impact of silver nanoparticles on *Japanese* medaka (*Oryzias latipes*). *Aquatic Toxicology*, 94: 320–327.

Chan VS.2006. Nanomedicine: an unresolved regulatory issue. *Regulatory Toxicology and Pharmacology*, 46: 218–224.

Chandna S. 2004. Single-cell gel electrophoresis assay monitors precise kinetics of DNA fragmentation induced during programmed cell death. *Cytometry* Part A, 61A: 127–133.

Châtel A, Mouneyrac C. 2017. Signaling pathways involved in metal-based nanomaterial toxicity towards aquatic organisms. *Comparative Biochemistry and Physiology, Part C: Toxicology and Pharmacology*, 196: 61‑70.

Chaudhry Q, Scotter M, Blackburn J, Ross B, Boxall A, Castle L, Aitken R, Watkins R. 2008. Applications and implications of nanotechnologies for the food sector. *Food Additives and Contaminants*, 25(3):241-258.

Chelliah M, Rayappan JBB, Krishnan UM. 2012. Synthesis and characterization of cerium oxide nanoparticles by hydroxide mediated approach. *Journal of Applied Sciences*, 12(16): 1734-1737.

Chelomin VP, Slobodskova VV, Zakhartsev M, Kukla S. 2017. Genotoxic potential of copper oxide nanoparticles in the Bivalve Mollusk Mutilus trossulus. *Journal of Ocean University of China* (*Oceanic and Coastal Sea Research*), 16: 10-20.

Chen KL, Elimelech M. 2006. Aggregation and deposition kinetics of fullerene (C-60) nanoparticles. *Langmuir*, 22: 10994–11001.

Chen L, Zhou L, Liu Y, Deng S, Wu H, Wang G. 2012. Toxicological effects of nanometer titanium dioxide (nano-TiO_2) on *Chlamydomonas reinhardtii*. *Ecotoxicology and Environmental Safety*, 84: 155‑162.

Chen L, Zhou L, Liu Y, Deng S, Wu H, Wang G. 2012a. Toxicological effects of nanometer titanium dioxide (nano-TiO2) on *Chlamydomonas reinhardtii. Ecotoxicology and Environmental Safety*, 84: 155–162.

Chen LX, Rajh T, Wang Z, Thurnauer MC. 1997. XAFS studies of surface structures of TiO_2 nanoparticles and photocatalytic reduction of metal ions. *The Journal of Physical Chemistry B*, 101: 10688−10697

Chen P, Su C, Tseng C, Tan S, Cheng C. 2011. Toxicity assessments of nanoscale zerovalent iron and its oxidation products in medaka (*Oryzias latipes*) fish. *Marine Pollution Bulletin*, 63: 339–346.

Chen T, Yan J, Li Y. 2014. Genotoxicity of titanium dioxide nanoparticles. *Journal of Food and Drug Analysis*, 22(1): 95-104.

Chen X, Zhang C, Tan L, Wang J. 2018. Toxicity of Co nanoparticles on three species of marine microalgae. *Environmental Pollution,* 236: 454-461.

Chen YT, Wu JH, Tsai FJ, Chang YW, Hsu SH, Lin JJ, Sue HL, Liao JW. 2015. Genotoxicity tests of poly (styrene-co-maleic anhydride)-coated silver nanoparticles *in vivo* and *in vitro*. *Journal of Experimental Nanoscience*, 10:6: 449-457.

Cho M, Chung H, Choi W, Yoon J. 2004. Linear correlation between inactivation of *E. coli* and OH radical concentration in TiO_2 photocatalytic disinfection. *Water Research,* 38: 1096–1077.

Choi JE, Kim S, Ahn JH, Youn P, Kang JS, Park K, Yi J, Ryu D. 2010. Induction of oxidative stress and apoptosis by silver nanoparticles in the liver of adult zebrafish. *Aquatic Toxicology*, 100: 151–159.

Choi S, Johnston MV, Wang G.-S, Huang CP. 2017. Looking for engineered nanoparticles (ENPs) in wastewater treatment systems: qualification and quantification aspects. *Science of the Total Environment,* 59: 809–817.

Christian P, von der Krammer F, Baalousha M, Hofman T. 2008. Nanoparticles: structure, properties, preparation and behaviour in environmental media. *Ecotoxicology,* 17: 326-343

Chupani L, Niksirat H, Velíšek J, Stará A, Hradilová S, Kolařík J, Panáček A, Zusková E. 2018. Chronic dietary toxicity of zinc oxide nanoparticles in common carp (*Cyprinus carpio* L.): Tissue accumulation and physiological responses. *Ecotoxicology and Environmental Safety*, 147:110-116.

Cientifica Ltd. Market opportunities in nanotechnology drug delivery. Online, London, UK 2012.

Clavier A, Seijo M, Carnal F, Stoll S. 2015. Surface charging behavior of nanoparticles by considering site distribution and density, dielectric constant and pH changes – a Monte Carlo approach. *Physical Chemistry Chemical Physics*, 17: 4346—4353.

Clemente Z, Castro VL, Feitosa LO, Lima R, Jonsson CM, Maia AHN, Fraceto LF. 2015. Biomarker evaluation in fish after prolonged exposure to nano-TiO_2: Influence of illumination conditions and crystal phase. *Journal of Nanoscience and Nanotechnology*, 15: 5424–5433.

Clemente Z, Castro VL, Feitosa LO, Lima R, Jonsson CM, Maia AHN, Fraceto LF. 2013. Fish exposure to nano-TiO_2 under different experimental conditions: Methodological aspects for nanoecotoxicology investigations. *Science of the Total Environment*, 463–464: 647–656.

Collins AR, Oscoz AA, Brunborg G, Gaivao I, Giovannelli L, Kruszewski M, Smith CC, Stetina R. 2008. The comet assay: topical issues. *Mutagenesis*, 23: 143–51.

Collins AR. 2004. The Comet assay for DNA damage and repair. Principles, applications, and limitations. *Molecular Biotechnology*, 26*:* 249-261.

Conway JR, Beaulieu AL, Beaulieu NL, Mazer SJ, Keller AA. 2015. Environmental stresses increase photosynthetic disruption by metal oxide nanomaterials in a soil-grown plant. *American Chemical Society Nano*, 9(12):11737–11749.

Cui B, Ren L, Xu Q-H, Yin L-Y, Zhou X-Y, Liu J-X. 2016. Silver nanoparticles inhibited erythrogenesis during zebrafish embryogenesis. *Aquatic Toxicology*, 177: 295–305.

Culcu T, Sozen E, Tuylu BA. 2010. Determination of genotoxicants induced DNA damage by using RAPD-PCR in human peripheral blood lymphocytes. *Fresenius Environmental Bulletin*, 19:2205–2209

Cumberland SA, Lead JR. 2009. Particle size distributions of silver nanoparticles at environmentally relevant conditions. *Journal of Chromatography A*, 1216: 9099–9105.

Cunniffe S, O'Neill P, Greenberg MM, Lomax ME. 2014. Reduced repair capacity of a DNA clustered damage site comprised of 8-oxo-7,8-dihydro-2′-deoxyguanosine and deoxyribonolactone results in an increased mutagenic potential of these lesions. *Mutation Research/Fundamental and Molecular Mechanisms of Mutagenesis*, 762: 32-39.

Czupryna J, Tsourkas A. 2006. "Suicide gene delivery by calcium phosphate nanoparticles: a novel method of targeted therapy for gastric cancer," *Cancer Biology and Therapy*, 5(12): 1691–1692.

Dai L, Syberg K, Banta GT, Selck H, Forbes VE. 2013. Effects, uptake, and depuration kinetics of silver oxide and copper oxide nanoparticles in a marine deposit feeder, *Macoma balthica. ACS Sustainable Chemistry and Engineering*, 1: 760−767.

Dan Y, Ma X, Weilan Zhang W,Kun Liu K, Stephan C, Shi H. 2016. Single particle ICP-MS method development for the determination of plant uptake and accumulation of CeO_2 nanoparticles. *Analytical and Bioanalytical Chemistry*, 408:5157–5167.

Dao NN, Luu MD, Nguyen QK, Kim BS. 2011. UV absorption by cerium oxide nanoparticles/epoxy composite thin films. *Advances in Natural Sciences: Nanoscience and Nanotechnology*, 2: 1-4.

Das S, Goswami S. 2017. Copper phytoextraction by *Salvinia cucullata*: biochemical and morphological study. *Environmental Science and Pollution Research*, 24:1363–1371.

David RM, Dakic V, Williams TD, Winter MJ, Chipmana JK. 2011. Transcriptional responses in neonate and adult *Daphnia magna* in relation to relative susceptibility to genotoxicants. *Aquatic Toxicology*, 104: 192– 204.

de Alteriis E, Falanga A, Galdiero S ,Guida M , Maselli V , Galdiero E. 2018. Genotoxicity of gold nanoparticles functionalized with indolicidin towards Saccharomyces cerevisiae. *Journal of Environmental Sciences*, 66:138 – 145.

de Lapuente J, Lourenço J, Mendo SA, Borràs M, Martins MG, Costa PM, Pacheco M. 2015. The Comet Assay and its applications in the field of ecotoxicology a mature tool that continues to expand its perspectives, published in 04 June 2015 doi: 10.3389/fgene.2015.00180.

de Lima R, Seabra AB, Durán N. 2012. Silver nanoparticles: a brief review of cytotoxicity and genotoxicity of chemically and biogenically synthesized nanoparticles. *Journal of Applied Toxicology*, 32: 867–879.

Dedeh A, Ciutat A, Treguer-Delapierre M, Bourdineaud JP. 2014. Impact of gold nanoparticles on zebrafish exposed to a spiked sediment. *Nanotoxicology*, Early Online: 1–10.

Dědková K, Bures Z, Palarcík J, Vlcek M, Kukutschova J. 2014. Acute toxicity of gold nanoparticles to freshwater green algae. In: Conference NanoCon, Nov 5th -7th, Brno, Czech Republic.

Demir E, Kaya N, Kaya B. 2014. Genotoxic effects of zinc oxide and titanium dioxide nanoparticles on root meristem cells of *Allium cepa* by comet assay. *Turkish Journal of Biology*, 38: 31-39.

Demple B and Harrison L 1994. Repair of oxidative damage to DNA: Enzymology and biology. *Annual Review of Biochemistry*, 63:915–948.

Denny P. 1972. Sites of nutrient absorption in aquatic macrophytes. *Journal of Ecology*, 60: 819−829.

Department of Science and Technology (DST). 2012. South African National Survey of Research and Experimental Development. Statistical Report: 2011/12. Department of Science and Technology, Pretoria. South Africa.

Dhawan A, Sharma V, Parmar D. 2009. Nanomaterials: a challenge for toxicologists. Nanotoxicology, 3(1): 1-9.

Diebold U. 2003. The surface science of titanium dioxide. *Surface Science Reports*, 48: 53−229.

Diegoli S, Manciulea AL, Begum, S, Jones IP, Lead JR, Preece JA. 2008. Interaction between manufactured gold nanoparticles and naturally occurring organic macromolecules. *Science of the Total Environment*, 402: 51–61.

Dietz K, Herth S. 2011. Plant nanotoxicology. Trends in Plant Science, 16:582–589.

Dixon DR, Pruski AM, Dixon LR J, Jha AN. 2002. Marine invertebrate eco-genotoxicology: a methodological overview. *Mutagenesis* 17: 495–507.

Djuris˘ic´ AB, Leung YH, Ng AMC, Xu XY, Lee PKH, Degger N, Wu RSS. 2015. Toxicity of metal oxide nanoparticles: mechanisms, characterization, and avoiding experimental artefacts. *Small*, 11(1):26–44.

Doak SH, Griffiths SM, Manshian B, Singh N, Williams PM, Brown AP, Jenkins GJ. 2009. Confounding experimental considerations in nanogenotoxicology. *Mutagenesis*, 24: 285–293.

Doak SH, Manshian B, Jenkins GJS, Singh N. 2012. *In vitro* genotoxicity testing strategy for nanomaterials and the adaptation of current OECD guidelines. *Mutation Research,* 745: 104–111.

Doherty AT. 2011. The *in vitro* micronucleus assay. *Methods in Molecular Biology*, 817: 121-141.

Domingos RF, Tufenkji N, Wilkinson KJ. 2009. Aggregation of titanium dioxide nanoparticles: role of a fulvic acid. *Environmental Science and Technology*, 43: 1282–1286.

Dominguez GA, Lohse SE, Torelli MD, Murphy CJ, Hamers RJ, Orr G, Klaper RD. 2015. Effects of charge and surface ligand properties of nanoparticles on oxidative stress and gene expression within the gut of *Daphnia magna*. *Aquatic Toxicology*, 162: 1–9.

Dusinska M, Collins AR. 2008. The comet assay in human biomonitoring: gene–environment interactions. *Mutagenesis*, 23(3): 191–205.

Dykman LA, Khlebtsov NG. 2016. Biomedical applications of multifunctional gold-based nanocomposites. *Biochemistry*, 81**:** 1771–89.

Dykman LA, Khlebtsov NG. 2017. Immunological properties of gold nanoparticles. *Chemical Science*, 8: 1719−1735.

El Badawy AM, Silva RG, Morris B, Scheckel KG, Suidan MT, Tolaymat TM. 2011. Surface charge-dependent toxicity of silver nanoparticles. *Environmental Science and Technology, 45(1):* 283–287.

El Badawy AME, Luxton TP, Silva RG, Scheckel KG, Suidan MT, Tolaymat TM. 2010. Impact of environmental conditions (pH, ionic strength, and electrolyte type) on the surface charge and aggregation of silver nanoparticles suspensions. *Environmental Science and Technology*, 44:1260–6.

Ellis LA, Baalousha M, Valsami-Jones E, Lead JR. 2018. Seasonal variability of natural water chemistry affects the fate and behaviour of silver nanoparticles, *Chemosphere*, 191: 616-625.

European Union (EU). 2011. European Union Commission recommendation on the definition of nanomaterial. *Official Journal of the European Union*, 2011/696/EU.

Falfushynska H, Gnatyshyna L, Yurchak I, Sokolova I, Stoliar O. 2015.The effects of zinc nano oxide on cellular stress responses of the freshwater mussels *Unio tumidus* are modulated by elevated temperature and organic pollutants. *Aquatic Toxicology*, 162: 82–93.

Fang Q, Shi X, Zhang L, Wang Q, Wang X, Guo Y, Zhou B. 2015. Effect of titanium dioxide nanoparticles on the bioavailability, metabolism, and toxicity of pentachlorophenol in zebrafish larvae. *Journal of Hazardous Materials*, 283: 897–904.

Farkas J, Bergum S, Nilsen EW, Olsen AJ, Salaberria I, Ciesielski TM, Bączek T, Konieczna L, Salvenmoser W, Jenssen BM. 2015. The impact of TiO2 nanoparticles on uptake and toxicity of benzo(a)pyrene in the blue mussel (*Mytilus edulis*). *Science of the Total Environment*, 511: 469–476.

Farre´ M, Sanchı´s J, Barcelo´ D. 2011. Analysis and assessment of the occurrence, the fate and the behavior of nanomaterials in the environment. *TrAC Trends in Analytical Chemistry*, 30:517–527.

Feichtmeier NS, Walther P, Leopold K. 2015. Uptake, effects, and regeneration of barley plants exposed to gold nanoparticles. *Environmental Science and Pollution Research*, 22:8549–8558.

Fenech M. 2000. The *in vitro* micronucleus technique. *Mutation Research*, 455(1–2): 81–95.

Fjellsbø LM, Verstraelen S, Kazimirova A, Van Rompay AR , Magdolenova Z, Dusinska M. 2014. Genotoxic and mutagenic potential of nitramines. *Environmental Research*, 134: 39–45.

Fröhlich E. 2012. The role of surface charge in cellular uptake and cytotoxicity of medical nanoparticles. *International Journal of Nanomedicine*, 7: 5577–5559.

Fryer RM, Randall J, Yoshida T, Hsiao LL, Blumenstock J, Jensen KE, Dimofte T, Jensen RV, Gullans SR. 2002. Global analysis of gene expression: methods, interpretation, and pitfalls**.** *Experimental Nephrology*, 10(2): 64-74.

Fubini B, Ghiazza M, Fenoglo I. 2010. Physico-chemical features of engineered nanoparticles relevant to their toxicity. *Nanotoxicology*, 4(4): 347-363.

Fuentes II, Espadas-Gil F, Talavera-May C, Fuentes G, Santamaría JM. 2014. Capacity of the aquatic fern (*Salvinia minima* Baker) to accumulate high concentrations of nickel in its tissues, and its effect on plant physiological processes. *Aquatic Toxicology*, 155:142-50.

Gagné F, André C, Skirrow R, Gélinas M, Auclair J, van Aggelen G, Turcotte P, Gagnon C. 2012. Toxicity of silver nanoparticles to rainbow trout: A toxicogenomic approach. *Chemosphere*, 89: 615–622.

Gallo A, Boni R, Buttino I, Tosti E. 2016. Spermiotoxicity of nickel nanoparticles in the marine invertebrate *Ciona intestinalis* (ascidians). *Nanotoxicology*, 10(8): 1096-1104.

Galloway T, Lewis C, Dolciotti I, Johnston BD, Moger J, Regoli F. 2010. Sublethal toxicity of nanotitanium dioxide and carbon nanotubes in sediment dwelling marine polychaete. *Environmental Pollution*, 158: 1748–1755.

Ganesan S, Thirumurthi NA, Raghunath A, Vijayakumar S, Perumal E. 2016. Acute and sub-lethal exposure to copper oxide nanoparticles causes oxidative stress and teratogenicity in zebrafish embryos. *Journal of Applied Toxicology*, 36: 554–567

Gao C, De Schamphelaere KAC, Smolders E. 2016. Zinc toxicity to the alga *Pseudokirchneriella subcapitata* decreases under phosphate limiting growth conditions. *Aquatic Toxicology*, 173: 74–82.

Garcia-Reyero N, Thornton C, Hawkins AD, Escalon L, Kennedy AJ, Steevens JA, Willett KL. 2015. Assessing the exposure to nanosilver and silver nitrate on fathead minnow gill gene expression and mucus production. *Environmental Nanotechnology, Monitoring and Management*, 4: 58–66.

Garnett MC and Kallinteri P. 2006. Nanomedicines and nanotoxicology: some physiological principles. *Occupational Medicine*, 56(5):307-311.

George S, Lin S, Ji Z, Thomas CR, Li L, Mecklenburg M, Meng H, Wang X, Zhang H, Xia T, Hohman JN, Lin S, Zink JI, Weiss PS, Nel A. 2012. Surface defects on plate-shaped silver nanoparticles contribute to its hazard potential in a fish gill cell line and Zebrafish embryos. *American Chemical Society Nano*, 6 (5): 3745-3759.

Girardello F, Leite CC, Branco CS, Roesch-Ely M, Fernandes AN, Salvador M, Henriques JAP. 2016. Titanium dioxide nanoparticles induce genotoxicity but not mutagenicity in golden mussel *Limnoperna fortune*. *Aquatic Toxicology*, 170: 223–228.

Girija D, Naik HSB, Sudhamani CN, Kumar BV. 2011. Cerium oxide nanoparticles - a green, reusable, and highly efficient heterogeneous catalyst for the synthesis of Polyhydroquinolines under solvent-free conditions. *Archives of Applied Science Research*, 3 (3): 373-382.

Glenn JB, Klaine SJ. 2013. Abiotic and biotic factors that influence the bioavailability of gold nanoparticles to aquatic macrophytes. *Environmental Science and Technology*, 47:10223–10230.

Glenn JB, White SA, Klaine SJ. 2012. Interactions of gold nanoparticles with aquatic macrophytes are size and species dependent. *Environmental Toxicology and Chemistry*, 31(1): 194–201.

Global Nanotechnology Market Outlook 2022. December 2015, 175 pages. http://www.researchandmarkets.com/reports/3512791/global-nanotechnology-market-outlook-2022.

Gojova A, Guo B, Kota RS, Rutledge JC, Kennedy IM, Barakat AI. 2007. Induction of inflammation in vascular endothelial cells by metal oxide nanoparticles: effect of particle composition. *Environmental Health Perspectives*, 115: 403–409.

Golbamaki N, Rasulev B, Cassano A, Robinson RLM, Benfenati E, Leszczynski J, Cronin MTD. 2015. Genotoxicity of metal oxide nanomaterials: review of recent data and discussion of possible mechanisms. *Nanoscale*, 7: 2154-2198.

Gong X-Q, Selloni A, Batzill M, Diebold U. 2006. Steps on anatase TiO_2 (101). *Nature Materials*, 5: 665−670.

Gonzalez L, Sanderson BJ, Kirsch-Volders M. 2011. Adaptations of the in vitro MN assay for the genotoxicity assessment of nanomaterials. *Mutagenesis*, 26(1): 185-191.

Gosens I, Post JA, de la Fonteyne LJJ, Jansen EHJM, Geus JW, Cassee FR, de Jong WH. 2010. Impact of agglomeration state of nano- and submicron sized gold particles on pulmonary inflammation. *Particle and Fibre Toxicology*, 7:37.

Goswami L, Kim K-H, Deep A, Das P, Bhattacharya SS, Kumar S, Adelodun AA. 2017. Engineered nano particles: Nature, behavior, and effect on the environment. *Journal of Environmental Management*, 196: 297-315.

Gottschalk F, Sonderer T, Scholz RW, Nowack B. 2009. Modelled environmental concentrations of engineered nanomaterials (TiO_2, ZnO, Ag, CNT, fullerenes) for different regions. *Environmental Science and Technology*, 43: 9216–9222.

Gottschalk F, Sun TY, Nowack B. 2013. Environmental concentrations of engineered nanomaterials: review of modelling and analytical studies. *Environmental Pollution*, 181, 287-300.

Grassian VH. 2008. "When size really matters: size-dependent properties and surface chemistry of metal and metal oxide nanoparticles in gas and liquid phase environments" *Journal of Physical Chemistry C, 112*: 18303-18313.

Green ANM, Palomares E, Haque SA, Kroon JM, Durrant JR. 2005. Charge transport versus recombination in dye-sensitized solar cells employing nanocrystalline TiO2 and Sno2 films. *Journal of Physical Chemistry B*, 109: 12525−12533.

Griffitt RJ, Hyndman K, Denslow ND, Barber DS. 2009. Comparison of molecular and histological changes in zebrafish gills exposed to metallic nanoparticles. *Toxicological Sciences*, 107(2): 404–415.

Griffitt RJ, Lavelle CM, Kane AS, Denslow ND, Barber DS. 2013. Chronic nanoparticulate silver exposure results in tissue accumulation and transcriptomic changes in zebrafish. *Aquatic Toxicology*, 130–131: 192– 200.

Gurr J, Wang ASS, Chen C, Jan K. 2005. Ultrafine titanium dioxide particles in the absence of photo activation can induce oxidative damage to human bronchial epithelial cells, *Toxicology*, 213: 66–73.

Han J, Qiu W, Gao W. 2010. Potential dissolution and photo-dissolution of ZnO thin films. *Journal of Hazardous Materials*, 178: 115–122.

Handy RD, van den Brink N, Chappell M, Muhling M, Behra R, Dusinska´ M, Simpson P, Ahtiainen J, Jha AN, Seiter J, Bednar A, Kennedy A, Fernandes TF, Riediker M. 2012. Practical considerations for conducting ecotoxicity test methods with manufactured nanomaterials: what have we learnt so far? *Ecotoxicology*, 21: 933–972.

Hansen SF, Heggelund LR, Besora PR, Mackevica A, Boldrin A, Baun A. 2016. Nanoproducts: what is actually available to European consumers? *Environmental Science Nano*, 3: 169–180.

Harris E. 1989. The Chlamydomonas Sourcebook, pp. 607–608. Academic Press, San Diego.
Harris S and Levine AJ. 2005. The p53 pathway: positive and negative feedback loops. *Oncogene*, 24: 2899-2908.

Hartmann NB, Kammer FV, Hofmann T, Baalousha M, Ottofuelling S, Baun A. 2010. Algal testing of titanium dioxide nanoparticles—testing considerations, inhibitory effects and modifications of cadmium bioavailability. *Toxicology*, 269:190–197.

Hazeem LJ, Bououdina M, Rashdan S, Brunet L, Slomianny C, Boukherroub R. 2016. Cumulative effect of zinc oxide and titanium oxide nanoparticles on growth and chlorophyll a content of *Picochlorum sp. Environmental Science and Pollution Research,* 23:2821–2830.

Hazeem LJ, Waheed FA, Rashdan S, Bououdina M, Brunet L, Slomianny C, Boukherroub R, Elmeselmani WA. 2015. Effect of magnetic iron oxide (Fe_3O_4) nanoparticles on the growth and photosynthetic pigment content of Picochlorum sp. *Environmental Science and Pollution Research,* 22:11728‑11739.

He D, Bligh MW and Waite TD. 2013. Effects of aggregate structure on the dissolution kinetics of citrate- stabilized silver nanoparticles. *Environmental Science and Technology*, 47: 9148−9156.

Hendren CO, Badireddy AR, Casman E, Wiesner MR. 2013. Modeling nanomaterial fate in wastewater treatment: Monte Carlo simulation of silver nanoparticles (nano-Ag). *Science of the Total Environment*, 449: 418-425.

Hitchman A, Smith GHS, Ju-Nam Y, Sterling M, Lead JR. 2013. The effect of environmentally relevant conditions on PVP stabilised gold nanoparticles. *Chemosphere,* 90:410–416.

Hoagland DR and Arnon DI. 1950. The water-culture method for growing plants without soil. California agricultural experiment station circular, 347: 1-32.

Holden PA, Gardea-Torresdey JL Klaessig F, Turco RF, Mortimer M, Hund-Rinke K, Hubal EAC, Avery D, Barceló D, Behra R, Cohen Y, Deydier-Stephan L, Ferguson PL, Fernandes TF, Harthorn BH, Henderson WM, Hoke RA, Hristozov D, Johnston JM, Kane AB, Kapustka L, Keller AA, Lenihan HS, Lovell W, Murphy CJ, Nisbet RM, Petersen EJ, Salinas ER, Scheringer M, Sharma M, Speed DE, Sultan Y, Westerhoff P, White JC, Wiesner MR, Wong EM, Xing B, Horan MS, Godwin HA, Nel AE. 2016. Considerations of environmentally relevant test conditions for improved evaluation of ecological hazards of engineered nanomaterials. *Environmental Science and Technology,* 50: 6124−6145.

Holden PA, Klaessig F,Turco RF, Priester JH, Rico CM, Avila-Arias H, Mortimer M, Pacpaco K, Gardea-Torresdey JL. 2014. Evaluation of exposure concentrations used in assessing manufactured nanomaterial environmental hazards: Are they relevant? *Environmental Science and Technology,* 48: 10541−10551.

Hole P, Sillence K, Hannell C, Maguire MC, Roesslein M, Suarez G, Capracotta S, Magdolenova Z, Horev-Azaria L, Dybowska A, Cooke L, Haase A, Contal S, Manø S,Vennemann A, Sauvain J, Staunton KC, Anguissola S, Luch A, Dusinska M, Korenstein R, Gutleb AC, Wiemann M, Prina-Mello A. 2013. Interlaboratory comparison of size measurements on nanoparticles using nanoparticle tracking analysis (NTA). *Journal of Nanoparticle Research*, 15:2101.

Hong FH, Zhou J, Liu C, Yang F,Wu C, Zheng L, Yang P. 2005. Effects of nano-TiO_2 on photochemical reaction of chloroplasts of spinach. *Biological Trace Element Research*, 105:269–279.

Hsiao I and Huang Y. 2011. Effects of various physicochemical characteristics on the toxicities of ZnO and TiO2 nanoparticles toward human lung epithelial cells. *Science of the Total Environment*, 409: 1219–1228.

Hsiao I-L, Hsieh Y-K, Wang C-F, Chen I-C, Huang Y-J. 2015. Trojan-Horse mechanism in the cellular uptake of silver nanoparticles verified by direct intra- and extracellular silver speciation analysis. *Environmental Science and Technology,* 49: 3813−3821.

Hu C, Liu X, Li X, Zhao Y. 2014. Evaluation of growth and biochemical indicators of Salvinia natans exposed to zinc oxide nanoparticles and zinc accumulation in plants. Environ Sci Pollut Res 21:732–739.

Hu C, Liu Y, Li X, Li M. 2013. Biochemical responses of duckweed (*Spirodela polyrhiza*) to zinc oxide nanoparticles. *Archives of Environmental Contamination and Toxicology*, 64:643–651.

Huang J, Chan S, Hou S. 2008. Studies on the photokilling of *E. coli* with TiO_2 nanoparticles by using gel electrophoresis technology. *Tamkang Journal of Science and Engineering, 11(2): 139-144.*

Huang S, Chueh PJ, Lin YW, Shih TS, Chuang SM. 2009. Disturbed mitotic progression and genome segregation are involved in cell transformation mediated by nano-TiO_2 long-term exposure. *Toxicology and Applied Pharmacology,* 241: 182–194.

Hughes ZE, Nguyen MA, Li Y, Swihart MT, Walsh TR, Knecht MR. 2017. Elucidating the influence of materials-binding peptide sequence on Au surface interactions and colloidal stability of Au nanoparticles. *Nanoscale*,9: 421–432.

Hutchings GJ. 2005. Catalysis by gold. *Catalysis Today*, 100(1–2): 55–61.

Huynh KA and Chen KL. 2011. Aggregation kinetics of citrate and polyvinylpyrrolidone coated silver nanoparticles in monovalent and divalent electrolyte solutions. *Environmental Science and Technology*, 45(13): 5564–5571.

International Standard Organization (ISO) "Water quality– Fresh Water Algal Growth Inhibition Test with Unicellular Green Algae" (ISO standard 8692), 12 January 2004.

Isani G, Falcioni ML, Barucca G, Sekar D, Andreani G, Carpenè E, Falcioni G. 2013. Comparative toxicity of CuO nanoparticles and CuSO4 in rainbow trout. *Ecotoxicology and Environmental Safety*, 97: 40–46.

Iswarya V, Manivannan J, De A, Paul S, Roy R, Johnson JB, Kundu R, Chandrasekaran N, Mukherjee A, Mukherjee A. 2016. Surface capping and size-dependent toxicity of gold nanoparticles on different trophic levels. *Environmental Science and Pollution Research*, 23:4844–4858.

Iswarya V, Sharma V, Chandrasekaran N, Mukherjee. A 2017. Impact of tetracycline on the toxic effects of titanium dioxide (TiO2) nanoparticles towards the freshwater algal species, *Scenedesmus obliquus. Aquatic Toxicology*, 193: 168–177.

Ji Z, Jin X, George S, Xia T, Meng H, Wang X, et al. 2010. Dispersion and stability optimization of TiO2 nanoparticles in cell culture media. *Environmental Science and Technol ogy*, 44:7309–7314.

Ji J, Long Z and Lin D. 2011. Toxicity of oxide nanoparticles to the green algae *Chlorella sp. Chemical Engineering Journal*, 170: 525–530.

Jiang J, Oberdörster G, Biswas P. 2009. Characterisation of size, surface charge and agglomeration state of nanoparticle dispersions for toxicological studies. *Journal of Nanoparticle Research*, 11: 77–89.

Jiang J, Oberdorster G, Elder A, Gelein R, Mercer P, Biswas P. 2008. "Does nanoparticle activity depend upon size and crystal phase?" *Nanotoxicology*, 2(1): 33-42.

Jin C, Tang Y, Yang FG, Li XL, Xu S, Fan XY, Huang YY, Yang YJ. 2011. Cellular Toxicity of TiO_2 nanoparticles in anatase and rutile crystal phase. *Biological Trace Element Research*, 141: 3–15.

Jin S, Ye K. 2007. Nanoparticle-mediated drug delivery and gene therapy, *Biotechnology Progress*, 23(1): 32–41.

Johnston BD, Scown TM, Moger J, Cumberland SA, Baalousha M, Linge K, van Aerle R, Jarvis K, Lead JR, Tyler CR. 2010. *Environmental Science and Technology*, 449(3): 1144-1151.

Jokerst JV, Lobovkina T, Zare RN, Gambhir SS. 2011. Nanoparticle PEGylation for imaging and therapy. *Nanomedicine*, 6:715–728.

Judy JD, Unrine JM, Bertsch PM. 2011. Evidence for biomagnification of gold nanoparticles within a terrestrial food chain. *Environmental Science and Technology*, 45: 776–781.

Judy JD, Unrine JM, Rao W, Wirick S, Bertsch PM. 2012. Bioavailability of gold nanomaterials to plants: Importance of particle size and surface coating. *Environmental Science and Technology*, 46: 8467–8474.

Judy JD, McNear DH, Chen C, Lewis RW, Tsyusko OV, Bertsch PM, Rao W, Stegemeier J, Lowry GV, McGrath SP, Durenkamp M, Unrine JM. 2015. Nanomaterials in biosolids inhibit nodulation, shift microbial community composition, and result in increased metal uptake relative to bulk/dissolved metals. *Environmental Science and Technology*, 49(14): 8751−8758.

Kadar E, Simmance F, Martin O, Voulvoulis N, Widdicombe S, Mitov S, Lead JR, Readman JW. 2010. The influence of engineered Fe_2O_3 nanoparticles and soluble ($FeCl_3$) iron on the developmental toxicity caused by CO_2-induced seawater acidification. *Environmental Pollution*, 158: 3490-3497.

Kaegi R, Ulrich A, Sinnet B, Vonbank R, Wichser A, Zuleeg S, Simmler H, Brunner S, Vonmont H, Burkhardt M, Boller M. 2008. Synthetic TiO_2 nanoparticle emission from exterior facades into the aquatic environment. *Environmental Pollution*, 156: 233–239.

Kahru A, Ivask A. 2013. Mapping the dawn of nanoecotoxicological research. *Accounts of Chemical Research*, 46(3): 823–833.

Kalman J, Paul KB~~,Khan~~, Khan FR, Stone V, Fernandes TF. 2015. Characterisation of bioaccumulation dynamics of three differently coated silver nanoparticles and aqueous silver in a simple freshwater food chain. *Environmental Chemistry*, 12: 662-672.

Kang J, Lee MS, Gorenstein DG. 2005. The enhancement of PCR amplification of a random sequence DNA library by DMSO and betaine: application to in vitro combinatorial selection of aptamers. *Journal of Biochemical and Biophysical Methods*, 64: 147–151.

Karakoti AS, Hench LL, Seal S. 2006. The potential toxicity of nanomaterials—the role of surfaces. *The Journal of the Minerals*, 58: 77–82.

Karlsson HL. 2010. The comet assay in nanotoxicology research. *Analytical and Bioanalytical Chemistry*, 398: 651–666.

Katsumiti A, Berhanu D, Howard KT, Arostegui I, Oron M, Reip P, Valsami-Jones E, Cajaraville MP. 2014. Cytotoxicity of TiO2 nanoparticles to mussel haemocytes and gill cells in vitro: Influence of synthesis method, crystalline structure, size and additive. *Nanotoxicology*. Early online: 1–11.

Katsumiti A, Gilliland D, Arostegui I, Cajaraville MP. 2015. Mechanisms of toxicity of Ag nanoparticles in comparison to bulk and ionic Ag on mussel haemocytes and gill cells. PLoS ONE 10(6): e0129039.

Kaweeteerawat C, Chang CH, Roy KR, Liu R, Li R, Toso D, Fischer H,OAngela Ivask A, Ji Z, Zink JI, Zhou ZH, Chanfreau GF, Telesca D, Cohen Y, Holden PA, Nel AE, Godwin HA. 2015. Cu nanoparticles have different impacts in *Escherichia coli* and *Lactobacillus brevis* than their microsized and ionic analogues. *ACS Nano*, 9(7): 7215–7225.

Kaya H, Aydın F, Gürkan M, Yılmaz S, Ates M, Demir V, Arslan Z. 2016. A comparative toxicity study between small and large size zinc oxide nanoparticles in tilapia (*Oreochromis niloticus*): Organ pathologies, osmoregulatory responses and immunological parameters. *Chemosphere* 144: 571–582.

Keller AA and Lazareva A. 2014. Predicted releases of engineered nanomaterials: from global to regional to local. *Environmental Science and Technology Letters*, 1(1):65–70.
Keller AA, McFerran S, Lazareva A, Suh S. 2013. Global life cycle releases of engineered nanomaterials. *Journal of Nanoparticle Research, 15*(6): 1-17.

Kerr JF, Wyllie AH, Currie AR. 1972. Apoptosis: a basic biological phenomenon with wide-ranging implications in tissue kinetics. *British Journal of Cancer*, 26: 239–257.

Khan LA, Afrooz AR, Flora JR, Schierz PA,Ferguson PL, Sabo-Attwood T, Saleh NB. 2013. Chirality affects aggregation kinetics of single-walled carbon nonotubes. *Environmental Science and Technology*, 47: 1844-1852.

Khataee A, Movafeghi A, Mojaver N, Vafaei F, Tarrahi R, Dadpour MR. 2017. Toxicity of copper oxide nanoparticles on *Spirodela polyrrhiza:* assessing physiological parameters. *Research on Chemical Intermediates*, 43:927–941.

Kim I, Lee B, Kim H, Kim K, Kim SD, Hwang Y. 2016. Citrate coated silver nanoparticles change heavy metal toxicities and bioaccumulation of *Daphnia magna*. *Chemosphere*, 143: 99–105.

Kim K-T, Zaikova T, Hutchison JE and Tanguay RL. 2013. Gold nanoparticles disrupt zebrafish eye development and pigmentation. *Toxicological Sciences*, 133(2): 275–288.

Kim S, Choi J. 2008. Genotoxicity of CeO_2, SiO_2 and TiO_2 nanoparticles in the freshwater crustacean *Daphnia magna. Journal of Environmental Toxicology,* 23(2): 79-85.

Kim SW, An Y-J. 2012. Effect of ZnO and TiO_2 nanoparticles preilluminated with UVA and UVB light on *Escherichia coli* and *Bacillus subtilis*. *Applied Microbiology and Biotechnology*, 95: 243–253.

Kirkland D, Reeve L, Gatehouse D, Vanparys P. 2011. A core in vitro genotoxicity battery comprising the Ames test plus the in vitro micronucleus test is sufficient to detect rodent carcinogens and in vivo genotoxins. *Mutation Research,* 721(1):27-73.

Klaine SJ, Alvarez PJJ, Batley GE, Fernandes TF, Handy RD, Lyon DY, Mahendra S, McLaughlin MJ, Lead JR. 2008. Nanomaterials in the environment: behavior, fate, bioavailability, and effects. *Environmental Toxicology and Chemistry,* 27(9): 1825-1851.

Klaine SJ, Koelmans AA, Horne N, Carley S, Handy RD, Kapustka L, Nowack B, von der Kammer F. 2012. Paradigms to assess the environmental impact of manufactured nanomaterials. *Environmental Toxicology and Chemistry*, 31(1): 3-15.

Klaper R, Arndt D, Bozich J and Dominguez G. 2014. Molecular interactions of nanomaterials and organisms: defining biomarkers for toxicity and high-throughput screening using traditional and next-generation sequencing approaches. *Analyst*, 139:882–895.

Ko K, Kong IC. 2014. Toxic effects of nanoparticles on bioluminescence activity, seed germination, and gene mutation. *Applied Microbiology and Biotechnology*, 98: 3295–3303.

Koehlé-Divo V , Cossu-Leguille C, Pain-Devin S, Simonin C, Bertrand C, Sohm B, Mouneyrac C, Devin S, Giambérini L. 2018. Genotoxicity and physiological effects of CeO_2 NPs on a freshwater bivalve (*Corbicula fluminea*). *Aquatic Toxicology*, 198: 141-148.

Koelmel J, Leland T, Wang HH, Amarasiriwardena D, Xing BS. 2013. Investigation of gold nanoparticles uptake and their tissue level distribution in rice plants by laser ablation–inductively coupled–mass spectrometry. *Environmental Pollution*, 174: 222–228.

Krokan HE, Bjørås M. 2013. Base excision repair. *Cold Spring Harbor Perspectives in Biology*, 5: a012583.

Krysanov EY, Demidova TB, Pel'gunova LA, Badalyan SM, Rumyantseva MN, Gas'kov AM. 2009. Effect of hydrated Tin Dioxide ($SnO_2 \cdot xH_2O$) nanoparticles on Guppy (*Poecilia reticulate* Peters, 1860). *Doklady Biological Sciences,* 426: 288–289.

Kühnel D, Nickel C. 2014. The OECD expert meeting on ecotoxicology and environmental fate—towards the development of improved OECD guidelines for the testing of nanomaterials. *Science of the Total Environment,* 472: 347–353.

Kumar A, Dhawan A. 2013. Genotoxic and carcinogenic potential of engineered nanoparticles: an update. *Archives of Toxicology*, 87: 1883–1900.

Kumar A, Pandey AK, Singh SS, Shanker R, Dhawan A. 2011. Cellular uptake and mutagenic potential of metal oxide nanoparticles in bacterial cells. *Chemosphere,* 83: 1124–1132.

Kumar A, Sharma V, Dhawan A. 2013. Methods for detection of oxidative stress and genotoxicity of engineered nanoparticles. *Methods in Molecular Biology,* 1028: 231–246.

Kwon JY, Koedrith P, Seo YR. 2014. Current investigations into the genotoxicity of zinc oxide and silica nanoparticles in mammalian models in vitro and in vivo: carcinogenic/genotoxic potential, relevant mechanisms and biomarkers, artifacts, and limitations. *International Journal of Nanomedicine*, 9 (Suppl 2): 271–286.

Lan J, Gou N, Gao C, He M, Gu AZ. 2014. Comparative and mechanistic genotoxicity assessment of nanomaterials via a quantitative toxicogenomics approach across multiple species. *Environmental Science and Technology*, 48: 12937−12945.

Landsiedel R, Kapp MD, Schulz M, Wiench K, Oesch F. 2009. Genotoxicity investigations on nanomaterials: methods, preparation and characterization of test material, potential artifacts and limitations. Many questions, some answers. *Mutation Research*, 681(2-3): 241-258.

Langevin D, Lozano O, Salvati A, Kestens V, Monopoli M, Raspaud E, Mariot S, Salonen A, Thomas S, Driessen M, Haase A, Nelissen I, Smisdom N, Pompa PP, Maiorano G, Puntes V, Puchowicz D, Stępnik M, Suárez G, Riediker M, Benetti F, Mičetić I, Venturini M, Kreyling WG, van der Zande M, Bouwmeester H, Milani S, Rädler JO, Mülhopt S, Lynch I, Dawson K. 2018. Inter-laboratory comparison of nanoparticle size measurements using dynamic light scattering and differential centrifugal sedimentation. *NanoImpact*, 10: 97–107.

Leal-Alvarado DA, Espadas-Gil F, Sáenz-Carbonell L, Talavera-May C, Santamaría JM. 2016. Lead accumulation reduces photosynthesis in the lead hyper-accumulator *Salvinia minima* Baker by affecting the cell membrane and inducing stomatal closure. *Aquatic Toxicology*, 171:37–47.

Lee B and Ranville JF.2012. The effect of hardness on the stability of citrate-stabilized gold nanoparticles and their uptake by Daphnia magna. *Journal of Hazardous Materials*, 213– 214: 434– 439.

Lee JH, Ju JE, Kim BI, Pak PJ, Choi E-K, Lee H-S, Chung N. 2014. Rod-shaped iron oxide nanoparticles are more toxic than sphere-shaped nanoparticles to murine macrophage cells. *Environmental Toxicology and Chemistry*, 33(12): 2759–2766.

Lee SW, Kim SM, Choi J. 2009. Genotoxicity and ecotoxicity assays using the freshwater crustacean *Daphnia magna* and the larva of the aquatic midge *Chironomus riparius* to screen the ecological risks of nanoparticle exposure. *Environmental Toxicology and Pharmacology, 28*(1): 86-91.

Lei Z, SuMY, XiaoW, Chao L, Qu CX, Liang C, Hao H, Liu XQ, Hong FS. 2007. Effects of nano-anatase on spectral characteristics and distribution of LHCII on the thylakoid membranes of spinach. *Biological Trace Element Research*, 120:273–283.

Lerebours A, Cambier S, Hislop L, Adam-Guillermin C, Bourdineaud J-P. 2013. Genotoxic effects of exposure to waterborne uranium, dietary methylmercury and hyperoxia in zebrafish assessed by the quantitative RAPD-PCR method. *Mutation Research*, 755:55–60.

Leung YH, Yung MMN, Ng AMC, Ma APY, Wong SWY, Chan CMN, Ng YH, Djurišic´ AB, Guo M, Wong MT, Leung FCC, Chan WK, Leung KMY, Lee KH. 2015. Toxicity of CeO_2 nanoparticles – The effect of nanoparticle properties. *Journal of Photochemistry and Photobiology B: Biology*, 145: 48–59.

Li F, Liang Z, Zheng X, Zhao W, Wu M, Wang Z. 2015. Toxicity of nano-TiO2 on algae and the site of reactive oxygen species production. *Aquatic Toxicology*, 158: 1–13.
Li L, Sillanpaa M, Tuominen M, Lounatmaa K, Schultz E. 2013. Behavior of titanium dioxide nanoparticles in *Lemna minor* growth test conditions. *Ecotoxicology and Environmental Safety*, 88:89–94.

Li M, Lin D, Zhu L. 2013. Effects of water chemistry on the dissolution of ZnO nanoparticles and their toxicity to *Escherichia coli*. *Environmental Pollution*, 173: 97-102.

Li X, Lenhart JJ, Walker HW. 2010. Dissolution-accompanied aggregation kinetics of silver nanoparticles. *Langmuir*, 26: 16690–16698.

Li X, Lenhart JJ, Walker HW. 2012. Aggregation kinetics and dissolution of coated silver nanoparticles. *Langmuir*, 28: 1095–1104.

Li Y, Doak SH, Yan J, Chen DH, Zhou M, Mittelstaedt RA, Chen Y, Li C, Chen T. 2017. Factors affecting the in vitro micronucleus assay for evaluation of nanomaterials. *Mutagenesis*, 32(1): 151-159.

Lin S, Reppert J, Hu Q, Hudson JS, Reid ML, Ratnikova TA, Rao AM, Luo H, Ke PC. 2009. Uptake, translocation, and transmission of carbon nanomaterials in rice plants. *Small*, 5(10):1128−1132.

Lindahl T, Nyberg B. 1972. Rate of depurination of native deoxyribonucleic acid. *Biochemistry*, 11:3610–3618.

Lindahl T. 1982. DNA repair enzymes. *Annual Review of Biochemistry*, 51:61–87.

Lindahl T. 1993. Instability and decay of the primary structure of DNA. *Nature*, 362: 709–715.

Linskens MHK, Feng J, Andrews WH, Enlow BE, Saati SM, Tonkin LA, Funk WD, Villeponteau B. 1995. Cataloguing altered gene expression in young and senescent cells using enhanced differential display. *Nucleic Acids Research*, 23: 3244−3251.

Lizieri C, Aguiar R, Kuki KN. 2011. Manganese accumulation and its effects on three tropical aquatic macrophytes: *Azolla caroliniana, Salvinia minima* and *Spirodela polyrhiza. Rodriguésia*, 62(4): 909-917.

Loeb LA, Preston B. 1996. Mutagenesis by apurinic/apyrimidinic sites. *Annual Review of Genetics*, 20:201–230.

Loeb LA, Preston BD. 1986. Mutagenesis by apurinic/ apyrimidinic sites. *Annual Review of Genetics*, 20: 201-230.

Lopes I, Ribeiro R, Antunes FE, Rocha-Santos TAP, Rasteiro MG, Soares AMVM, Goncalves F, Pereira R. 2012. Toxicity and genotoxicity of organic and inorganic nanoparticles to the bacteria *Vibrio fischeri* and *Salmonella typhimurium*. *Ecotoxicology*, 21: 637–648.

Lowry GV, Gregory KB, Apte SC and Lead JR. 2012. Transformations of nanomaterials in the environment. *Environment Science and Technology*, 46: 6893−6899.

Ma X, Geiser-Lee J, Deng Y, Kolmakov A. 2010. Interactions between engineered nanoparticles (ENPs) and plants: Phytotoxicity, uptake and accumulation. *Science of the Total Environment*, 408: 3053–3061.

Madigan MT, Martinko JM, Parker J. 2003. Brock biology of microorganisms. Prentice Hall/Pearson Higher Education Group, Upper Saddle River, NJ

Magdolenova Z, Collins A, Kumar A, Dhawan A, Stone V, Dusinska M. 2014. Mechanisms of genotoxicity. A review of in vitro and in vivo studies with engineered nanoparticles. *Nanotoxicology*, 8(3): 233-278.

Magdolenova Z, Lorenzo Y, Collins A, Dusinska M. 2012b. Can standard genotoxicity tests be applied to nanoparticles? *Journal of Toxicology and Environmental Health, Part A: Current Issues*, 75: 1–7.

Mahapatra I, Sun TY, Clark JRA, Dobson PJ, Hungerbuehler K,Owen R, Nowack B, Lead J. 2015. Probabilistic modelling of prospective environmental concentrations of gold nanoparticles from medical applications as a basis for risk assessment. *Journal of Nanobiotechnology*, 13:93.

Mahaye N, Thwala M, Cowan DA, Musee N. 2017. Genotoxicity of metal based engineered nanoparticles in aquatic organisms: A review. *Mutation Research Reviews, Mutation Research,* 773: 134–160.

Majedi SM, Kelly BC, Lee HK. 2014. Role of combinatorial environmental factors in the behavior and fate of ZnO nanoparticles in aqueous systems: a multiparametric analysis. *Journal of Hazardous Materials*, 264: 370–379.

Manier N, Bado-Nilles A, Delalain P, Aguerre-Chariol O, Pandard P. 2013. Ecotoxicity of non-aged and aged CeO_2 nanomaterials towards freshwater microalgae. *Environmental Pollution*, 180: 63-70.

Manier N, Garaud M, Delalain P, Aguerre-Chariol O, Pandard P. 2011. Behaviour of ceria nanoparticles in standardized test media – influence on the results of ecotoxicological tests. *Journal of Physics: Conference Series*, 304:012058.

Martínez-Fernández D, Barroso D, Komárek M. 2015. Root water transport of Helianthus annuus L. under iron oxide nanoparticle exposure. *Environmental Science and Pollution Research, in press.* 10.1007/s11356-015-5423-5.

Massarsky A, Abraham R, Nguyen KC, Rippstein P, Tayabali AF, Trudeau VL, Moon TW. 2014. Nanosilver cytotoxicity in rainbow trout (*Oncorhynchus mykiss*) erythrocytes and hepatocytes. *Comparative Biochemistry and Physiology, Part C*, 159: 10–21.

Maynard AD. 2006. Nanotechnology: Managing the risks. *Nano Today*, 1: 22-33.

McCullough AK, Dodson ML, Lloyd RS.1999. Initiation of base excision repair: glycosylase mechanisms and structures. *Annual Review of Biochemistry*, 68:255–285.

Medina-Velo IA, Adisa I, Tamez C, Peralta-Videa JR, Gardea-Torresdey JL. 2017. Effects of surface coating on the bioactivity of metal-based engineered nanoparticles: lessons learned from higher plants. In: Yan B., Zhou H., Gardea-Torresdey J. (eds) Bioactivity of Engineered Nanoparticles. *Nanomedicine and Nanotoxicology*. *Springer*, *Singapore*.

Mehrian SK and De Lima R. 2016. Nanoparticles cyto and genotoxicity in plants: Mechanisms and abnormalities. *Environmental Nanotechnology, Monitoring and Management*, 6: 184–193.

Mei LI, Qin ZHU, Hu CW, Li CHEN, Liu ZL, Kong ZM. 2007. Cobalt and manganese stress in the microalga Pavlova viridis (Prymnesiophyceae): effects on lipid peroxidation and antioxidant enzymes. *Journal of Environmental Science*, 19: 1330-1335.

Methods for Direct Estimation of Ecological Effects Potential (DEEEP), 2004. Water Research Commission Report No. 1313/1/04.

Metreveli G, Frombold B, Seitz F, Grün A, Philippe A, Rosenfeldt RR, Bundschuh M, Schulz R, Manz W, Schaumann GE. 2016. Impact of chemical composition of ecotoxicological test media on the stability and aggregation status of silver nanoparticles. *Environmental Science Nano*, 3: 418–433.

Metzler DM, Erdem A, Tseng YH, Huang CP. 2012. Responses of algal cells to engineered nanoparticles measured as algal cell population, chlorophyll a, and lipid peroxidation: effect of particle size and type. *Journal of Nanotechnology*, 12: ID 237284.

Miao LZ, Wang C, Hou J, Wang PF, Ao YH, Li Y, Lv BW, Yang YY, You GX, Xu Y. 2015. Enhanced stability and dissolution of CuO nanoparticles by extracellular polymeric substances in aqueous environment. *Journal of Nanoparticle Research*, 17: 404.

Milewska-Hendel A, Zubko M, Karcz J, Stróż D, Kurczyńska E. 2017. Fate of neutral-charged gold nanoparticles in the roots of the *Hordeum vulgare L. cultivar Karat*. *Scientific Reports*, 7: 3014.

Miralles P, Church TL, Harris AT. 2012. Toxicity, uptake, and translocation of engineered nanomaterials in vascular plants. *Environmental Science and Technology*, 46: 9224−9239.

Mohmood I, Ahmad I, Asim M, Costa L, Lopes CB, Trindade T, Duarte AC, Pereira E. 2015. Interference of the co-exposure of mercury with silica-coated iron oxide nanoparticles can modulate genotoxicity induced by their individual exposures—a paradox depicted in fish under in vitro conditions. *Environmental Science and Pollution Research,* 22: 3687–3696.

Monopoli MP, Aberg C, Salvati A, Dawson KA. 2012. Biomolecular coronas provide the biological identity of nanosized materials, *Nature Nanotechnology*, 7: 779-786.

Morelli E, Gabellieri E, Bonomini A, Tognotti D, Grassi G, Corsi I. 2018. TiO2 nanoparticles in seawater: Aggregation and interactions with the green alga *Dunaliella tertiolecta. Ecotoxicology and Environmental Safety*, 148: 184–193.

Mortelmans K, Zeiger E. 2000. The Ames *Salmonella*/microsome mutagenicity assay. *Mutation Research,* 455: 29–60.

Mouneyrac C, Buffet PE, Poirier L, Zalouk-Vergnoux A, Guibbolini M, Risso-de Faverney C, Gilliland D, Berhanu D, Dybowska A, Châtel A, Perrein-Ettajni H, Pan JF, Thomas Guyon H, Reip P, Valsami-Jones E. 2014. Fate and effects of metal-based nanoparticles in two marine invertebrates, the bivalve mollusc *Scrobicularia plana* and the annelid polychaete *Hediste diversicolor*. *Environmental Science and Pollution Research*, 21: 7899‑7912.

Movafeghi A, Khataee A, Abedi M, Tarrahi R, Dadpour M, Vafaei F. 2017. Effects of TiO_2 nanoparticles on the aquatic plant *Spirodela polyrrhiza*: Evaluation of growth parameters, pigment contents and antioxidant enzyme activities. *Journal of Environmental Sciences,* 01049: 1-9.

Mulvihill MJ, Habas SE, Plante IJ, Wan J, Mokari T. 2010. Influence of size, shape, and surface coating on the stability of aqueous suspensions of CdSe nanoparticles. *Chemistry of Materials*, 22: 5251–5257.

Munari M, Sturve J, Frenzilli G, Sanders MB, Christiane P, Nigro M, Lyons BP. 2014. Genotoxic effects of Ag_2S and CdS nanoparticles in blue mussel (*Mytilus edulis*) haemocytes. *Chemistry and Ecology*, 30(8): 719–725.

Murugananthkumar R, Rajesh D, Senthilkumaran B. 2016. Copper nanoparticles differentially target testis of the Catfish, *Clarias batrachus: In vivo* and *In vitro* study. *Frontiers in Environmental Science*, 4: 67.

Musee N, Brent AC, Ashton PJ. 2010. A South African research agenda to investigate the potential environmental, health and safety risks of nanotechnology. *South African Journal of Science,* 106(3–4): 67–72.

Musee N. 2011. Simulated environmental risk estimation of engineered nanomaterials: A case of cosmetics in Johannesburg City**.** *Human and Experimental Toxicology*, 30(9): 1181-1195.

Musee, N, Oberholster, PJ, Sikhwivhilu, L, Botha AM. 2010. The effects of engineered nanoparticles on survival, reproduction, and behavior of freshwater snail, *Physa acuta* (Draparnaud 1805). *Chemosphere*, 81: 1196–1203.

Nandhakumar S, Parasuraman S, Shanmugam MM, Rao KR, Chand P, Bhat BV. 2011. Evaluation of DNA damage using single cell gel electrophoresis (Comet Assay). *Journal of Pharmacology and Pharmacotherapeutics*, 2: 107-111.

Nanogenotox, 2013. Facilitating the safety evaluation of manufactured nanomaterials by characterizing their potential genotoxic hazard. Online: www.nanogenotox.eu.

Nasser F, Davis A, Valsami-Jones E, Lynch I. 2016. Shape and charge of gold nanomaterials influence survivorship, oxidative stress and moulting of *Daphnia magna*. Nanomaterials, 6: 222.

Navarro E, Baun A, Behra R, Hartmann NB, Filser J, Miao AJ, Quigg A, Santschi PH, Sigg L. 2008. Environmental behavior and ecotoxicity ofengineered nanoparticles to algae, plants, and fungi. *Ecotoxicology*, 17:372–386.

Nekrasova GF, Ushakova OS, Ermakov AE, Uimin MA and Byzov IV. 2011. Effects of copper (II) ions and copper oxide nanoparticles on *Elodea densa* Planch. *Russian Journal of Ecology,* 42 (6): 458-463.

Nel A, Xia T, M¨adler L, Li N. 2006. Toxic potential of materials at the nanolevel. *Science,* 311: 622–627.

Nel AE, Mädler L, Velegol D, Xia T, Hoek EMV, Somasundaran P, Klaessig F, Castranova V, Thompson M. 2009. *Nature Materials*, 8: 543–557.

Nelson BC, Wright CW, Ibuki Y, Moreno-Villanueva M, Karlson HL, Hendriks G, Sims CM, Singh N, Doak SH. 2017. Emerging metrology for high-throughput nanomaterial genotoxicology. *Mutagenesis*, 32 (1): 215-232.

Ng C-T, Li JJ, Bay B-H, Yung L-Y L. 2010. Current studies into the genotoxic effects of nanomaterials. *Journal of Nucleic Acids*:

Nghiem THL, La TH, Vu XH, Chu VH, Nguyen TH, Le QH, Fort E, Do QH, Tran HN. 2010. Synthesis, capping and binding of colloidal gold nanoparticles to proteins. *Advances in Natural Sciences,* 1:025009.

Nghiem THL, Nguyen TT, Fort E, Nguyen TP, Hoang TMN, Nguyen TQ, Tran HN. 2012. Capping and in vivo toxicity studies of gold nanoparticles. *Advances in Natural Sciences: Nanoscience and Nanotechnology*, 3:015002.

Nigro M, Bernardeschi M, Costagliola D, Torre CD, Frenzilli G, Guidi P,Lucchesi P, Mottola F, Santonastaso M, Scarcelli V, Monaci F, Corsi I, Stingo V, Rocco L. 2015. n-TiO_2 and $CdCl_2$ co-exposure to titanium dioxide nanoparticles and cadmium: Genomic, DNA and

chromosomal damage evaluation in the marine fish European sea bass (*Dicentrarchus labrax*). *Aquatic Toxicology*, 168: 72–77.

Niikura K, Matsunaga T, Suzuki T, Kobayashi S, Yamaguchi H, Orba Y, Kawaguchi A, Hasegawa H, Kajino K, Ninomiya T, Ijiro K, Sawa H. 2013. Gold nanoparticles as a vaccine platform: influence of size and shape on immunological responses *in vitro* and *in vivo*. *ACS Nano*, 7: 3926−3938.

Nunes SM, Josende ME, Ruas CP, Gelesky MA, da Silva Júnior FMR, Fattorini D, Regoli F, Monserrat JM, Ventura-Lima J. 2017. Biochemical responses induced by co-exposition to arsenic and titanium dioxide nanoparticles in the estuarine polychaete *Laeonereis acuta. Toxicology*, 376: 51–58.

Nur Y, Lead JR, Baalousha M. 2015. Evaluation of charge and agglomeration behavior of TiO2 nanoparticles in ecotoxicological media. *Science of the Total Environment*, 535: 45–53.

O'Brien NJ, Cummins EJ. 2011. A risk assessment framework for assessing metallic nanomaterials of environmental concern: aquatic exposure and behaviour. *Risk Analysis*, 31: 706–726

Oberdörster G, Oberdörster E, Oberdörster J. 2005. Nanotoxicology: an emerging discipline evolving from studies of ultrafine particles. *Environmental Health Perspectives*, 113(7): 823–839.

Oberholster PJ, Hill L, Jappie S, Truter JC, Botha, A-M, 2016. Applying genotoxicology tools to identify environmental stressors in support of river management. *Chemosphere*, 144: 319-329.

Oberholster PJ, Musee N, Botha AM, Chelule PK ,Focke WW, Ashton PJ. 2011. Assessment of the effect of nanomaterials on sediment-dwelling invertebrate *Chironomus tentans* larvae. *Ecotoxicology and Environmental Safety*, 74*:* 416–423.

Organization for Economic Cooperation and Development (OECD) "Algal growth inhibition test". Guideline 201, 23 March 2006.

OECD guideline for the testing of chemicals draft proposal for a new guideline 487. 2004. *In Vitro* Micronucleus Test.

OECD, Guidelines 475 genetic toxicology: in vivo mammalian bone marrow cytogenetic test-chromosome analysis, OECD, Editor. 1997.

Oesch F, Landsiedel R. 2012. Genotoxicity investigations on nanomaterials. *Archives of Toxicology*, 86(7): 985-994.

Olsen GH, Klok C, Hendriks AJ, Geraudie P, De Hoop L, De Laender F, Farmen E, Grøsvik BE, Hansen BH, Hjorth M, Jansen CR, Nordtug T, Ravagnan E, Viaene K, Carroll J. 2013.Toxicity data for modeling impacts of oil components in an Arctic ecosystem. *Marine Environmental Research*, 90: 9-17.

Organization for Economic Co-operation and Development (OECD). 1997. In vitro mammalian chromosome aberration test. In: OECD guidelines for the testing of chemicals. Paris: OECD, p. 473.

Oriekhova O and Stoll S. 2016. Effects of pH and fulvic acids concentration on the stability of fulvic acids e cerium (IV) oxide nanoparticle complexes. *Chemosphere*, 144: 131-137.

Orieux N, Cambier S, Gonzalez P, Morin B, Adam C, Garnier-Laplace J, Bourdineaud J-P. 2011. Genotoxic damages in zebrafish submitted to a polymetallic gradient displayed by the Lot River (France). *Ecotoxicology and Environmental Safety*, 74:974–983.

Orts-Gil G, Natte K, Drescher D, Bresch H, Mantion A, Kneipp J, Österle W. 2011.Characterisation of silica nanoparticles prior to in vitro studies: From primary particles to agglomerates. *Journal of Nanoparticle Research*, *13*(4), 1593–1604.

Ostroumov SA, Poklonov VA, Kotelevtsev SV, Orlov SN. 2014. Toxicity of gold nanoparticles for plants in experimental aquatic system. *Moscow University Biological Sciences Bulletin,* 69(3): 108–112.

Otsuki Y. 2000. Various methods of apoptosis detection. *Acta Histochemica et Cytochemica,* 33: 235–241.

Ottofuelling S, Von der Kammer F, Hofmann T. 2011. Commercial titanium dioxide nanoparticles in both natural and synthetic water: comprehensive multidimensional testing and prediction of aggregation behavior. *Environmental Science and Technology*, 45: 10045–10052.

Pacheco A, Martins A, Guilhermino L. 2018. Toxicological interactions induced by chronic exposure to gold nanoparticles and microplastics mixtures in *Daphnia magna. Science of the Total Environment,* 628–629: 474-483.

Pal S, Tak, YK, Song, JM. 2007. Does the antibacterial activity of silver nanoparticles depend on the shape of the nanoparticle? A study of the gram-negative bacterium *Escherichia coli*. *Applied and Environmental Microbiology,* 73(6): 1712-1720.

Pamies R, Cifre J, Espı´n VF, Collado-Gonza´lez M, Ban˜os FGD and de la Torre GC. 2014. Aggregation behaviour of gold nanoparticles in saline aqueous media. *Journal of Nanoparticle Research,* 16:2376.

Pandey S, Walker PR, Sikorska M. 1994. Separate pools of endonuclease activity are responsible for inter-nucleosomal and high-molecular-mass DNA fragmentation during apoptosis. *Biochimie et Biologie Cellulaire*, 72: 625–629.

Park S, Choi J. 2010. Geno- and ecotoxicity evaluation of silver nanoparticles in freshwater crustacean *Daphnia magna*. *Environmental Engineering Research,* 15(1): 23-27.

Park J, Lim D, Lim H, Kwon T, Choi J, Jeong S, Choi I and Cheon J. 2011. Size dependent macrophage responses and toxicological effects of Ag nanoparticles. *Chemical Communications*, 47: 4382-4384.

Pavanello S, Clonfero E. 2000. Biological indicators of genotoxic risk and metabolic polymorphisms. *Mutation Research*, 463: 285–308.

PEN (Project on Emerging Nanotechnologies). 2014. Consumer Products Inventory. Retrieved [10 July 2014], http://www.nanotechproject.org/cpi/about/analysis.

Peng C, Zhang W, Gao H, Li Y, Tong X, Li K, Zhu X, Wang Y, Chen Y. 2017. Behavior and potential impacts of metal-based engineered nanoparticles in aquatic environments. *Nanomaterials*, 7: 21.

Peng X, Palma S, Fisher NS, Wong SS. 2011. Effect of morphology of ZnO nanostructures on their toxicity to marine algae. *Aquatic Toxicology*, 102: 186–196.

Peng Y-H, Tsai Y-C, Hsiung C-E, Lin Y-H, Shih Y-H. 2017. Influence of water chemistry on the environmental behaviors ofcommercial ZnO nanoparticles in various water and wastewater samples. *Journal of Hazardous Materials*, 322: 348–356.

Peng YH, Tso CP, Tsai YC, Zhuang CM, Shih YH. 2015. The effect of electrolytes on the aggregation kinetics of three different ZnO nanoparticles in water. *Science of the Total Environment*, 530-531: 183–190.

Peralta-Videa JR, Zhao L, Lopez-Moreno ML, de la Rosa G, Hong J, Gardea Torresdey JL. 2011. Nanomaterials and the environment: A review for the biennium 2008–2010. *Journal of Hazardous Materials*, 186: 1–15.

Pereira SO, Barros-Timmons A, Trindade T. 2014. Bio-functionalisation of colloidal gold nanoparticles via polyelectrolytes assemblies. *Colloid and Polymer Science*, 292:33–50.

Perrault SD, Chan WCW. 2010. In vivo assembly of nanoparticle components to improve targeted cancer imaging. *Proceedings of the National Academy of Sciences*, USA, 107(25): 11194-11199.

Peters RJB, van Bemmel G, Milani NBL, den Hertog GCT, Undas AK, van der Lee M, Bouwmeester H. 2018. Detection of nanoparticles in Dutch surface waters. *Science of the Total Environment*, 621: 210–218.

Pham CH, Yi J, Gu MB. 2012. Biomarker gene response in male Medaka (*Oryzias latipes*) chronically exposed to silver nanoparticle. *Ecotoxicology and Environmental Safety*, 78: 239–245.

Piccapietra F, Sigg L, Behra R. 2012. Colloidal stability of carbonate coated silver nanoparticles in synthetic and natural freshwater. *Environmental Science and Technology*, 46(2): 818–25.

Piccinno F, Gottschalk F, Seeger S, Nowack B. 2012. Industrial production quantities and uses of ten engineered nanomaterials for Europe and the world. *Journal of Nanoparticle Research*, 14: 1109–1120.

Pinto RJB, Marques PAAP, Martins MA, Neto CP, Trindade T. 2007. Electrostatic assembly and growth of gold nanoparticles in cellulosic fibres. *Journal of Colloid and Interface Science*, 312:506–512.

Planchon M, Ferrari R, Guyot F, Ge´labertb A, Menguy N, Chanéac C, Thill A, Benedetti MF, Spalla O.2013. Interaction between *Escherichia coli* and TiO_2 nanoparticles in natural and artificial waters. *Colloid Surface B*, 102: 158–164.

Podila R, Brown JM. 2013. Toxicity of engineered nanomaterials: A physicochemical perspective. *Journal of Biochemical and Molecular Toxicology*, 27(1): 50-55.

Poynton HC, Lazorchak JM, Impellitteri CA,Blalock BJ, Rogers K, Allen HJ, Loguinov A, Heckman JL, Govindasmawy S. 2012. Toxicogenomic responses of nanotoxicity in *daphnia* magna exposed to silver nitrate and coated silver nanoparticles. *Environmental Science and Technology*, 46: 6288−6296.

Prado C, Rodrıguez-Montelongo L, Gonzalez JA, Pagano EA, Hilal M, Prado FE. 2010. Uptake of chromium by *Salvinia minima*: Effect on plant growth, leaf respiration and carbohydrate metabolism. *Journal of Hazardous Materials*, 177:546–553.

Pratt IS, Barron T. 2003. Regulatory recognition of indirect genotoxicity mechanisms in the European Union. *Toxicology Letters*, 140-141: 53-62.

Priecel P, Salami HA, Padilla RH, Zhong ZYL, opez-Sanchez JA. 2016. Anisotropic gold nanoparticles: preparation and applications in catalysis. *Chinese Journal of Catalysis*, 37: 1619–50.

Pyshnaya IA, Razum KV, Poletaeva JE, Pyshnyi DV, Zenkova MA, Ryabchikova EI. 2014. Comparison of behaviour in different liquids and in cells of gold nanorods and spherical nanoparticles modified by linear polyethyleneimine and bovine serum albumin. *BioMedical Research International*, 2014:13.

Quik JTK, Lynch I, Hoecke KV, Miermans CJH, Schamphelaere KACD, Janssen CR, Dawson KA, Stuart MA, Van De Meent D. 2010. Effect of natural organic matter on cerium dioxide nanoparticles settling in model freshwater. *Chemosphere*, 81(6): 711–715.

Rabolli V, Thomassen LC, Uwambayinema F, Martens JA, Lison D. 2011. The cytotoxic activity of amorphous silica nanoparticles is mainly influenced by surface area and not by aggregation. *Toxicology Letters*, 206: 197–203.

Rajkishore SK, Subramanian KS, Natarajan N, Gunasekaran K. 2013. Nanotoxicity at various trophic levels: A review. *The Bioscan*, 8(3): 975-982.

Raliya R, Franke C, Chavalmane S, Nair R, Reed N, Biswas P. 2016. Quantitative understanding of nanoparticle uptake in watermelon plants. *Frontiers in Plant Science*, 7:1288.
Raman V, Suresh S, Savarimuthu PA, Raman T, Tsatsakis AM, Golokhvast KS,Vadivel VK. 2016. Synthesis of Co_3O_4 nanoparticles with block and sphere morphology, and investigation into the influence of morphology on biological toxicity. *Experimental and Therapeutic Medicine,* 11: 553-560.

Ramesh R, Kavitha P, Kanipandian N, Arun S, Thirumurugan R, Subramanian P. 2013. Alteration of antioxidant enzymes and impairment of DNA in the SiO2 nanoparticles exposed zebra fish (Danio rerio). Environmental Monitoring and Assessment, 185: 5873–5881.

Reeves JF, Davies SJ, Dodd NJF, Jha AN. 2008. Hydroxyl radicals (•OH) are associated with titanium dioxide (TiO_2) nanoparticle-induced cytotoxicity and oxidative DNA damage in fish cells. *Mutation Research,* 640: 113–122.

Regier N, Cosio C, von Moos N, Slaveykova VI. 2015. Effects of copper-oxide nanoparticles dissolved copper and ultraviolet radiation on copper bioaccumulation, photosynthesis and oxidative stress in the aquatic macrophyte Elodea nuttallii. Chemosphere, 128: 56–61.

Ribeiro F, Van Gestel CAM, Pavlaki MD, Azevedo S, Soares AMVM, Loureiro S. 2017. Bioaccumulation of silver in Daphnia magna: Waterborne and dietary exposure to nanoparticles and dissolved silver. *Science of the Total Environment,* 574:1633-1639.

Rico CM, Morales MI, McCreary R, Castillo-Michel H, Barrios AC, Hong J, Tafoya A, Lee WY, Varela-Ramirez A, Peralta-Videa JR, Gardea-Torresdey JL. 2013. Cerium oxide nanoparticles modify the antioxidative stress enzyme activities and macromolecule composition in rice seedlings. *Environmental Science and Technology*, 47:14110–14118.

Rico CM, Hong J, Morales MI, Zhao L, Barrios AC, Zhang JY, Peralta-Videa JR, Gardea-Torresdey JL. 2013. Effect of cerium oxide nanoparticles on rice: a study involving the antioxidant defense system and in vivo fluorescence imaging. *Environmental Science and Technology,* 47:5635–5642.

Rico CM, Barrios AC, Tan W, Rubenecia R, Lee SC, Varela-Ramirez A, PeraltaVidea JR, Gardea-Torresdey JL. 2015. Physiological and biochemical response of soil-grown barley (Hordeum vulgare L.) to cerium oxide nanoparticles. *Environmental Science and Pollution Research,* 22:10551–10558

Rim KT, Song SW, Kim HY. 2013. Oxidative DNA damage from nanoparticle exposure and its application to workers' health: a literature review. *Safety and Health at Work*, 4(4): 177-86.

Rioboo, C., Prado, R., Herrero, C., Cid, A., 2007. Population growth study of the rotifer

Brachionus sp. fed with triazine-exposed microalgae. *Aquatic Toxicology*, 83:247–253.

Rizwan M, Ali S, Qayyum MF, Ok YS, Adrees M, Ibrahim M, Zia-ur-Rehman M, Ibrahim M, Abbas F. 2017. Effect of metal and metal oxide nanoparticles on growth and physiology of globally important food crops: A critical review. *Journal of Hazardous Materials*, 322: 2–16.

Robel I, Subramanian V, Kuno M, Kamat PV. 2006. Quantum dot solar cells. Harvesting light energy with CdSe nanocrystals molecularly linked to mesoscopic TiO_2 films. *Journal of the American Chemical Society*, 128: 2385–2393.

Rocco L, Frenzilli G, Zito G, Archimandritis A, Peluso C, Stingo V. 2012. Genotoxic effects in fish induced by pharmacological agents present in the sewage of some Italian water-treatment plants. *Environmental Toxicology*, 27:18–25.

Rocco L, Santonastaso M, Mottola F, Costagliola D, Suero T, Pacifico S, Stingo V. 2015. Genotoxicity assessment of TiO_2 nanoparticles in the teleost *Danio rerio. Ecotoxicology and Environmental Safety,* 113: 223–230.

Rodea-Palomares I, Boltes K, Ferna´ndez-Pin˜as F, Legane´s F, Garcı´a-Calvo E, Santiago J, Rosal R. 2011. Physicochemical characterization and ecotoxicological assessment of CeO_2 nanoparticles using two aquatic microorganisms. *Toxicological Sciences,* 119(1): 135–145.

Rodea-Palomares I, Gonzalo S, Santiago-Morales J, Leganés F, García-Calvo E, Rosal R, Fernández-Piñas F. 2012.An insight into the mechanisms of nanoceria toxicity in aquatic photosynthetic organisms. *Aquatic Toxicology*, 122–123:133-143.

Rodrigues LHR, Arenzon A, Raya-Rodriguez MT, Fontoura NF. 2011. Algal density assessed by spectrophotometry: A calibration curve for the unicellular algae *Pseudokirchneriella subcapitata. Journal of Environmental Chemistry and Ecotoxicology*, 3(8):225-228.

Rogers NJ, Franklin NM, Apte SC, Batley GE, Angel BM, Lead JR, Baalousha M. 2010. Physico-chemical behaviour and algal toxicity of nanoparticulate CeO_2 in freshwater. *Environmental Chemistry*, 7: 50–60.

Röhder LA, Brandt T, Sigg L, Behra R. 2014. Influence of agglomeration of cerium oxide nanoparticles and speciation of cerium (III) on short term effects to the green algae *Chlamydomonas reinhardtii. Aquatic Toxicology,* 152: 121–130.

Röhder LA, Brandt T, Sigg L, Behra R. 2018. Uptake and eff ects of cerium (III) and cerium oxide nanoparticles *to Chlamydomonas reinhardtii*. *Aquatic Toxicology*, 197: 41-46.

Römer I, White TA, Baalousha M, Chipman K, Viant MR, Lead JR. 2011. Aggregation and dispersion of silver nanoparticles in exposure media for aquatic toxicity tests. *Journal of Chromatography A,* 1218(27): 4226-33.

Royal Society and Royal Academy of Engineering Report on Nanotechnology. Nanoscience and nanotechnologies: opportunities and uncertainties. The Royal Society and Royal Academy of Engineering; 2004.

Ruiz P, Katsumiti A, Nieto JA, Bori J, Jimeno-Romero A, Reip P, Arostegui I, Amaia Orbea, Cajaraville MP. 2015. Short-term effects on antioxidant enzymes and long-term genotoxic and carcinogenic potential of CuO nanoparticles compared to bulk CuO and ionic copper in mussels *Mytilus galloprovincialis*. *Marine Environmental Research xxx*: 1-14.

Russo G, Zegar C, Giordano A. 2003. Advantages and limitations of microarray technology in human cancer. *Oncogene*, 22: 6497–6507.

Sabo-Attwood T, Unrine JM, Stone JW, Murphy CJ, Ghoshroy S, Blom D, Bertsch PM, Newman LA. 2012. Uptake, distribution and toxicity of gold nanoparticles in tobacco (*Nicotiana xanthi*) seedlings. *Nanotoxicology,* 6:353–360.

Sadiq IM, Pakrashi S, Chandrasekaran N, Mukherjee A. 2011b. Studies on toxicity of aluminum oxide (Al_2O_3) nanoparticles to microalgae species: Scenedesmus sp. and Chlorella sp. *Journal of Nanoparticle Research,* 13 (8): 3287-3299.

Saha NC, Bhunia F, Kaviraj A. 2006. Comparative toxicity of three organic acids to freshwater organisms and their impact on aquatic ecosystems. *Human and ecological risk assessment*: *An International Journal*, 12:1, 192-202.

Saison C, Perreault F, Daigle J-C, Fortin C, Claverie J, Morin M, Popovic R. 2010. Effect of core‑shell copper oxide nanoparticles on cell culture morphology and photosynthesis (photosystem II energy distribution) in the green alga, Chlamydomonas reinhardtii. *Aquatic Toxicology*, 96: 109‑114.

Salem ZB, Capelli N, Grisey E, Baurand P-E, Ayadi H , Aleya L. 2014. First evidence of fish genotoxicity induced by heavy metals from landfill leachates: The advantage of using the RAPD-PCR technique. *Ecotoxicology and Environmental Safety*, 101:90–96.

Sauve S, M Desrosiers. 2014. A review of what is an emerging contaminant. *Chemistry Central Journal*, 8: 15.

Sayes MC, Wahi R, Kurian PA, Liu Y, West JL, Ausman KD, Warheit DB, Colvin VL. 2006a. Correlating nanoscale titania structure with toxicity: a cytotoxicity and inflammatory response study with human dermal fibroblasts and human lung epithelial cells. *Toxicological Sciences*, 92: 174–85.

Scientific Committee on Emerging and Newly-Identified Health Risks (SCENIHR), The appropriateness of the risk assessment methodology in accordance with the Technical Guidance Documents for new and existing substances for assessing the risks of nanomaterials, 21-22 June 2007.

Scientific Committee on Emerging and Newly-Identified Health Risks (SCENIHR) (2007). The scientific aspects of the existing and proposed definitions relating to products of Nanoscience and Nanotechnologies. Brussels, European Commission Health & Consumer Protection.

Schiavo S, Oliviero M, Miglietta M, Rametta G, Manzo S. 2016. Genotoxic and cytotoxic effects of ZnO nanoparticles for *Dunaliella tertiolecta* and comparison with SiO_2 and TiO_2 effects at population growth inhibition levels. *Science of the Total Environment*, 550: 619–627.
Schlich K, Terytze K, Hund-Rinke K. 2012. Effect of TiO_2 nanoparticles in the earthworm reproduction test. *Environmental Sciences Europe*, 24: 5.

Schmid K, Danuser B, Riediker M. 2010. Nanoparticle usage and protection measures in the manufacturing Industry e a representative survey. *Journal of Occupational and Environmental Hygiene*, 7 (4): 224-232.

Schmid K, Riediker M. 2008. Use of nanoparticles in Swiss industry: A targeted survey. *Environmental Science and Technology*, 42: 2253–2260.

Schwab F, Zhai G, Kern M, Turner A, Schnoor JL, Wiesner MR. 2016. Barriers, pathways and processes for uptake, translocation, and accumulation of nanomaterials in plants. Critical review. *Nanotoxicology*, 10 (3), 257−278.

Schwabe F, Schulin R, Limbach LK, Stark W, Burge D, Nowack B. 2013.Influence of two types of organic matter on interaction of CeO_2 nanoparticles with plants in hydroponic culture. *Chemosphere*, 91:512–520.

Scown TM, van Aerle R, Tyler CR. 2010. Review: Do engineered nanoparticles pose a significant threat to the aquatic environment? *Critical Reviews in Toxicology*, 40(7): 653–670.

Sekar D, Falcioni ML, Barucca G, Falcioni G. 2014. DNA damage and repair following *in vitro* exposure to two different forms of titanium dioxide nanoparticles on trout erythrocyte. *Environmental Toxicology*, 29(1): 117-27.

Selck H, Handy RD, Fernandes TF. Klaine SJ, Petersen EJ. 2016. Nanomaterials in the aquatic environment: A European Union–United States Perspective on the status of ecotoxicity testing, research priorities, and challenges ahead. *Environmental Toxicology and Chemistry*, 35(5): 1055–1067.

Sendra M, Sánchez-Quiles D, Blasco J, Moreno-Garrido I, Lubiána LM, Pérez-García S, Tovar-Sánchez A. 2017. Effects of TiO_2 nanoparticles and sunscreens on coastal marine microalgae: Ultraviolet radiation is key variable for toxicity assessment. *Environment International*, 98: 62–68.

Sharma N, Rather MA, Ajima MNO, Gireesh-Babu P, Kumar K, Sharma R. 2016. Assessment of DNA damage and molecular responses in *Labeo rohita* (Hamilton, 1822) following short-term exposure to silver nanoparticles. *Food and Chemical Toxicology*, 96: 122-132.

Sharma V, Anderson D, Dhawan A. 2012. Zinc oxide nanoparticles induce oxidative DNA damage and ROS-triggered mitochondria mediated apoptosis in human liver cells (HepG2). *Apoptosis*, 17: 852–870.

Sharma VK, Siskova KM, Zboril R, Gardea-Torresdey JL. 2014. Organic-coated silver nanoparticles in biological and environmental conditions: Fate, stability and toxicity. *Advances in Colloid and Interface Science,* 204: 15–34.

Shi J, Peng C, Yang Y, Yang J, Zhang H, Yuan X, Chen Y, Hu T. 2014. Phytotoxicity and accumulation of copper oxide nanoparticles to the Cu-tolerant plant *Elsholtzia splendens*. *Nanotoxicology*, 8(2):179–188.

Shikha N and Radhakrishna S. 2012. Effects of nanoparticle charge and shape anisotropy on translocation through cell membranes. *Langmuir*, 28: 17666−17671.

Shyam R, Aery NC. 2012. Effect of cerium on growth, dry matter production, biochemical constituents and enzymatic activities of cowpea plants [(*Vigna unguiculata (L.) Walp.]*. *Journal of Soil Science and Plant Nutrition,* 12: 1-14.

Sigg L. 1994. The regulation of trace elements in lakes: the role of sedimentation. In: Buffle, J., de Vitre, R.R. (Eds.). The Chemical and Biological Regulation of Aquatic Systems 2nd ed. Lewis, Boca Raton, FL, USA, pp. 633–651.

Silva T, Pokhrel LR, Dubey B, Tolaymat TM, Maier KJ, Liu X. 2014. Particle size, surface charge and concentration dependent ecotoxicity of three organo-coated silver nanoparticles: Comparison between general linear model-predicted and observed toxicity. *Science of the Total Environment*, 468–469: 968–976.

Simon-Deckers A, Loo S, Mayne-L'Hermite M, Herlin-Boime N, Menguy N, Reynaud C, Gouget B, Carriere M. 2009. Size, composition and shape dependent toxicological impact of metal oxide nanoparticles and carbon nanotubes toward bacteria. *Environmental Science and Technology*, 43: 8423-8429.

Singh C, Friedrichs S, Ceccone G, Gibson N, Jensen KA, Levin M, Infante HG, Carlander D, Rasmussen K. 2014. Cerium dioxide, NM-211, NM-212, NM-213. Characterisation and test item preparation. European Commission, Joint Research Centre, European Union. http://dx.doi.org/10.2788/80203.

Singh N, Manshian B, Jenkins GJS, Griffiths SM, Williams PM, Maffeis TGG, Wright CJ, Doak SH. 2009. NanoGenotoxicology: The DNA damaging potential of engineered nanomaterials *Biomaterials*, 30: 3891–3914.

Song U and Lee S. 2016. Phytotoxicity and accumulation of zinc oxide nanoparticles on the aquatic plants *Hydrilla verticillata* and *Phragmites Australis*: leaf-type-dependent responses. *Environmental Science and Pollution Research*, 23:8539–8545.

Song U, ShinM, Lee G, Roh J, KimY, Lee E. 2013b. Functional analysis of TiO_2 nanoparticle toxicity in three plant species. *Biological Trace Element Research,* 155:93–103.

Sosan A, Svistunenko D, Straltsova D, Tsiurkina K, Smolich I, Lawson T, Subramaniam S, Golovko V, Anderson D, Sokolik A, Colbeck I, Demidchik V. 2016. Engineered silver nanoparticles are sensed at the plasma membrane and dramatically modify the physiology of *Arabidopsis thaliana* plants. *Plant Journal*, 85: 245–257.

Srut M, Stambuk A, Bourdineaud J-P, Klobucar GIV. 2015. Zebrafish genome instability after exposure to model genotoxicants. *Ecotoxicology*, 24:887–902.

Stegemeier JP, Colman BP, Schwab F, Wiesner MR, Lowry GV. 2017. Uptake and distribution of silver in the aquatic plant *Landoltia punctate* (Duckweed) exposed to silver and silver sulfide nanoparticles. *Environmental Science and Technology*, 51: 4936−4943.

Stegemeier JP, Schwab F, Colman BP, Webb SM, Newville M, Lanzirotti A, Winkler C, Wiesner MR, Lowry GV. 2015. Speciation Matters: Bioavailability of silver and silver sulfide nanoparticles to Alfalfa (*Medicago sativa*). *Environmental Science and Technology*, 49 (14): 8451−8460.

Suman S, Pandey A, Chandna S. 2012. An improved non-enzymatic ‘‘DNA ladder assay’’ for more sensitive and early detection of apoptosis. *Cytotechnology*, 64: 9–14.

Sun TY, Gottschalk F, Hungerbühler K, Nowack B. 2014. Comprehensive probabilistic modelling of environmental emissions of engineered nanomaterials. *Environmental Pollution*, 185: 69-76.

Sune N, Sa´nchez G, Caffaratti S, Maine MA. 2007. Cadmium and chromium removal kinetics from solution by two aquatic macrophytes. *Environmental Pollution,* 145: 467-473.

Tantra R, Jing S, Pichaimuthu SK., Walker N, Noble J and Hackley VA. 2011. Dispersion stability of nanoparticles in ecotoxicological investigations: the need for adequate measurement tools. *Journal of Nanoparticle Research*, 13(9): 3765–3780.

Taylor AF, Rylott EL, Anderson CWN, Bruce NC. 2014. Investigating the toxicity, uptake, nanoparticle formation and genetic response of plants to gold. PLOS one 9(4): e93793.

Tejamaya M, Isabella Römer I, Merrifield RC, Lead JR. 2012. Stability of citrate, PVP, and PEG coated silver nanoparticles in ecotoxicology media. *Environmental Science and Technology*, 46: 7011−7017.

Telford WG, King LE, Fraker PJ. 1991. Evaluation of glucocorticoid- induced DNA fragmentation in mouse thymocytes by flow-cytometry. *Cell Proliferation,* 24: 447–459.

Telford WG, King LE, Fraker PJ. 1992. Comparative evaluation of several DNA binding dyes in the detection of apoptosis-associated chromatin degradation by flow cytometry. *Cytometry* 13: 137–143.

Thompson DT. 2007. Using gold nanoparticles for catalysis. *Nanotoday*, 2(4): 40-43.

Thwala M, Klaine SJ, Musee N. 2016. Interactions of metal-based engineered nanoparticles with aquatic higher plants: a review of the state of current knowledge. *Environmental Toxicology and Chemistry*, 35(7): 1677–1694.

Thwala M, Musee N, Sikhwivhilu LM, Wepener V. 2013. The oxidative toxicity of Ag and ZnO nanoparticles towards the aquatic plant *Spirodela punctuta* and the role of testing media parameters. *Environmental Science Processes and Impacts*, 15:1830–1843.

Tiao GM, Hudson K, Lieberman MA Fischer JE, Hasselgren PO. 1996. Identification of altered gene expression in skeletal muscle during sepsis using differential display. *Journal of Surgical Research,* 64: 63−67.

Tice RR, Agurell E, Anderson D, Burlinson B, Hartmann A, Kobayashi H, Miyamae Y, Rojas E, Ryu JC, Sasaki YF. 2000. Single cell gel/comet assay: Guidelines for in vitro and in vivo genetic toxicology testing. *Environmental and Molecular Mutagenesis,* 35(3): 206–221.

Tiede K, Hasselloev M, Breitbarth E, Chaudhry Q, Boxall ABA. 2009. Considerations for environmental fate and ecotoxicity testing to support environmental risk assessments for engineered nanoparticles. *Journal of Chromatography A,* 1216:503–509.

Topuz E, Traber J, Sigg L, Talinli I. 2015. Agglomeration of Ag and TiO_2 nanoparticles in surface and wastewater: Role of calcium ions and of organic carbon fractions, *Environmental Pollution,* 204: 313–323.

Topuz E, Sigg L, Talinli I. 2014. A systematic evaluation of agglomeration of Ag and TiO_2 nanoparticles under freshwater relevant conditions. *Environmental Pollution*, 193: 37–44.

Torre CD, Balbi T, Grassi G, Frenzilli G, Bernardeschi M, Smerilli A, Guidi P, Canesi L, Nigro M, Monaci F, Scarcelli V, Rocco L, Focardi S, Monopoli M, Corsi I. 2015. Titanium dioxide nanoparticles modulate the toxicological response to cadmium in the gills of *Mytilus galloprovincialis. Journal of Hazardous Materials*, 297: 92–100.

Tripathi A, Kumari S, Kumar A. 2016. Toxicity evaluation of pH dependent stable Achyranthes aspera herbal gold nanoparticles. *Applied Nanoscience*, 6(1):61-69.

Tweats D, Trunz BB, Torreele E. 2012. Genotoxicity profile of fexinidazole—a drug candidate in clinical development for human African trypanomiasis (sleeping sickness). *Mutagenesis,* 27(5): 523–532.

Van Hoecke K, Quik JTK, Mankiewicz-Boczek J, De Schamphelaere KAC, Elsaesser A, Van der Meeren P, Barnes C, McKerr G, Howard CV, Van DeMeent D, Rydzynski K, Dawson KA, Salvati A, Lesniak A, Lynch I, Silversmit G, De Samber B, Vincze L, Janssen CR. 2009. Fate and effects of CeO_2 nanoparticles in aquatic ecotoxicity tests. *Environnmental Science and Technology,* 43:4537–4546.

Vance ME, Kuiken T, Vejerano EP, McGinnis SP, Hochella Jr. MF, Rejeski D, Hull MS. 2015. Nanotechnology in the real world: Redeveloping the nanomaterial consumer products inventory. *Beilstein Journal of Nanotechnology,* 6: 1769–1780.

Vannuccini ML, Grassi G, Leaver MJ, Corsi I. 2015. Combination effects of nano-TiO2 and 2, 3, 7, 8-tetrachlorodibenzo-p-dioxin (TCDD) on biotransformation gene expression in the liver of European sea bass *Dicentrarchus labrax*. *Comparative Biochemistry and Physiology, Part C,* 176–177: 71–78.

Velzeboer I, Hendriks AJ, A.M.J. Ragas, D. van de Meent. 2008. Aquatic ecotoxicity tests of some nanomaterials. *Toxicological and Environmental Chemistry*, 27:1942-1947.

Verschaeve L, Gilles J. 1995. Single-cell gel electrophoresis assay in the earthworm for the detection of genotoxic compounds in soils. *Bulletin of Environmental Contamination and Toxicology*, 54: 112–119.

Vevers WF and Jha AN. 2008. Genotoxic and cytotoxic potential of titanium dioxide (TiO2) nanoparticles on fish cells *in vitro*. *Ecotoxicology*, 17: 410–420.

Vignardi CP, Hasue FM, Sartório PV, Cardoso CM, Machado ASD, Passos MJACR, Santos TCA, Nucci JM, Hewer TLR, Watanabe I, Gomes V, Ngan V. Phan NN. 2015. Genotoxicity, potential cytotoxicity and cell uptake of titanium dioxide nanoparticles in the marine fish *Trachinotus carolinus* (Linnaeus, 1766). *Aquatic Toxicology*, 158: 218–229.

Vijayakumar S. 2014. In vitro stability studies on gold nanoparticles with different stabilizing agents. International Journal of Current Science, 11: 84-93.

Villa A, Dimitratos N, Chan-Thaw C E, Hammond C, Veith G M, Wang D, Manzoli M, Prati L and Hutchings G J. 2016. Characterisation of gold catalysts. *Chemical Society Reviews*, 45: 4953–94.

von der Kammer F, Ottofuelling S, Hofmann T. 2010. Assessment of the physico-chemical behavior of titanium dioxide nanoparticles in aquatic environments using multidimensional parameter testing. *Environmental Pollution*, 158: 3472–3481.

von Moos N and Slaveykova VI. 2014. Oxidative stress induced by inorganic nanoparticles in bacteria and aquatic microalgae – state of the art and knowledge gaps. *Nanotoxicology*, 8(6):605-630.

Wang A, Ng HP, Xu Y, Li Y, Zheng Y, Yu J, Han F, Peng F, Fu L. 2014. Gold nanoparticles: synthesis, stability test, and application for the rice growth. *Journal of Nanomaterials*, 2014: 1-6.

Wang S, Liu H, Zhang Y, Xin H. 2015. The effect of CuO NPs on reactive oxygen species and cell cycle gene expression in roots of rice. *Environmental Toxicology and Chemistry*, 34(3):554-61.

Wang Z, Zhang L, Zhao J, Xing B. 2016. Environmental processes and toxicity of metallic nanoparticles in aquatic systems as affected by natural organic matter. Environmental Science Nano, 3:240–255.

Warheit DB and Donner EM. 2010. Rationale of genotoxicity testing of nanomaterials: regulatory requirements and appropriateness of available OECD test guidelines. *Nanotoxicology*, 4: 409-413.

Warheit DB, Hoke RA, Finlay C, Donner EM, Reed KL, Sayes CM. 2007. Development of a base set of toxicity tests using ultrafine TiO2 particles as a component of nanoparticle risk management. *Toxicology Letters*, 171(3): 99-110.

Warheit DB, Reed KL, Sayes CM. 2009. A role for nanoparticle surface reactivity in facilitating pulmonary toxicity and development of a base set of hazard assays as a component of nanoparticle risk management. *Inhalation Toxicology,* 21: 61–67.

Weiss B, Grossman L. 1987. Phosphodiesterases involved in DNA repair. *Advances in Enzymology and Related Areas of Molecular Biology*, 60:1–34.

Wiechers JW, Musee N. 2010. Engineered inorganic nanoparticles and cosmetics: facts, issues, knowledge gaps and challenges. *Journal of biomedical nanotechnology,* 6(5), 408-431.

Wise Sr. JP, Goodale BC, Sandra S. Wise SS, Craig GA, Pongan AF, Walter RB, Thompson WD, Ng A-K, Aboueissa A-M, Mitani H, Spalding MJ, Mason MD. 2010. Silver nanospheres are cytotoxic and genotoxic to fish cells. *Aquatic Toxicology*, 97: 34–41.

Wolf HD, Blust R, Backeljau T. 2004. The use of RAPD in ecotoxicology. *Mutation Research,* 566: 249–262.

Wong ML and Medrano JF. 2005. Real-time PCR for mRNA quantitation. *BioTechniques,* 39: 75-85.

Wu W, Li S, Liao S, Xiang F, Wu X. 2010. Preparation of new sunscreen materials Ce1−x Zn x O2−x via solid-state reaction at room temperature and study on their properties. Rare Metals, 29: 149–153.

Wu H, Jiang M, Zhu Z-G,Zhao Y, Qu R, Liu j-j. 2013. Toxic response of *Daphnia magna* to *Microcystis aeruginosa*. *Asian Journal of Chemistry*, 25(6):2965-2969.

Wyllie AH. 1980. "Glucocorticoid-induced thymocyte apoptosis is associated with endogenous endonuclease activation," *Nature*, 284(5756): 555–556.

Xiao Y, Vijver MG, Peijnenburg WJGM. 2018. Impact of water chemistry on the behavior and fate of copper nanoparticles. *Environmental Pollution*, 234: 684-691.

Xu C, Qu, X.2014. Cerium oxide nanoparticle: a remarkably versatile rare earth nanomaterial for biological applications, NPG Asia Materials, 6: 90

Yang X, Nakao Y, Pater MM, Pater A. 1996. Identification of two novel cellular genes associated with multistage carcinogenesis of human endocervical cells by mRNA differential display. *Carcinogenesis*, 17: 563−567.

Yang X, Pan H, Wang P, Zhao F-J. 2017. Particle-specific toxicity and bioavailability of cerium oxide (CeO_2) nanoparticles to *Arabidopsis thaliana. Journal of Hazardous Materials*, 322: 292–300.

Yellowhair M, Romanotto MR, Stearns DM, Lantz RC. 2018. Uranyl acetate induced DNA single strand breaks and AP sites in Chinese hamster ovary cells. *Toxicology and Applied Pharmacology*, 349: 29–38.

Yu R, Wu J, Liu M, Zhu G, Chen L, Chang Y, Lu H . 2016. Toxicity of binary mixtures of metal oxide nanoparticles to *Nitrosomonas europaea. Chemosphere*, 153: 187-197.

Yung MMN, Fougères P-A, Leung YH, Liu F, Djurišić AB, Giesy JP, Leung KMY. 2017. Physicochemical characteristics and toxicity of surface-modifed zinc oxide nanoparticles to freshwater and marine microalgae. *Scientific Reports*, 7: 15909.

Załęska-Radziwiłł M, Doskocz N. 2016. DNA changes in *Pseudomonas putida* induced by aluminium oxide nanoparticles using RAPD analysis. *Desalination and Water Treatment*, 57(3): 1573-1581.

Zemke-White WL, Clements KD, Harris PJ. 2000. Acid lysis of macroalgae by marine herbivorous fishes: effects of acid pH on cell wall porosity. *Journal of Experimental Marine Biology and Ecology*, 245:57–68.

Zhang D, Hua T, Xiao F, Chen C, Gersberg RM, Liu Y, Ng WJ, Tan SK. 2014. Uptake and accumulation of CuO nanoparticles and CdS/ ZnS quantum dot nanoparticles by *Schoenoplectus tabernaemontani* in hydroponic mesocosms. *Ecological Engineering*, 70:114–123.

Zhang D, Hua T, Xiao F, Chen C, Gersberg RM, Liu Y, Stuckey D, Ng WJ, Tan SK. 2015. Phytotoxicity and bioaccumulation of ZnO nanoparticles in *Schoenoplectus tabernaemontani*. *Chemosphere*, 120 (2015) 211–219.

Zhang H, Smith JA, Oyanedel-Craver V. 2012. The effect of natural water conditions on the anti-bacterial performance and stability of silver nanoparticles capped with different polymers. *Water Research*, 46:691–699.

Zhang P, Ma Y, Liu S, Wang G, Zhang J, He X, Zhang J, Rui Y, Zhang Z. 2017. Phytotoxicity, uptake and transformation of nano-CeO2 in sand cultured romaine lettuce. *Environmental Pollution*, 220: 1400-1408.

Zhang W, Yao Y, Li K, Huang Y and Chen Y. 2011. Influence of dissolved oxygen on aggregation kinetics of citrate-coated silver nanoparticles. *Environmental Pollution*, 159: 3757–3762.

Zhang X, Qin J, Xue Y, Yu P, Zhang B, Wang L, Liu R. 2014. Effect of aspect ratio and surface defects on the photocatalytic activity of ZnO nanorods. *Scientific Reports*, 4: 4596.

Zhang X. 2015. Gold nanoparticles: Recent advances in the biomedical applications. Cell *Biochemistry and Biophysics*, 72(3):771-775.

Zhao J, Castranova V. 2011. Toxicology of nanomaterials used in nanomedicine. *Journal of Toxicology and Environmental Health B*, 14: 593–632.

Zhao X, Wang S, Wu Y, You H, Lv L. 2013. Acute ZnO nanoparticles exposure induces developmental toxicity, oxidative stress and DNA damage in embryo-larval zebrafish. *Aquatic Toxicology*, 136– 137: 49– 59.

Zhou D, Ji Z, Jiang X, Dunphy DR, Brinker J and Keller A. 2013. Influence of material properties on TiO2 nanoparticle agglomeration. *PLoSONE,* 8(11): e81239.

Zhou D, Keller AA. 2010. Role of morphology in the aggregation kinetics of ZnO nanoparticles. *Water Research*, 44: 2948–2956.

Zhu H, Han J, Xiao J Q, Jin Y. 2008.Uptake, translocation, and accumulation of manufactured iron oxide nanoparticles by pumpkin plants. *Journal of Environmental Monitoring*, 10 (6):713 −717.

Zong J, Cobb SL, Cameron NR. 2017. Peptide-functionalized gold nanoparticles: versatile biomaterials for diagnostic and therapeutic applications. *Biomaterials Science,* 5: 872−886.

Zopes D, Stein B, Mathur S and Graf C. 2013. Improved stability of "naked" gold nanoparticles enabled by in situ coating with mono and multivalent thiol PEG ligands. *Langmuir,* 29: 11217−11226.

Zuverza-Mena N, Martínez-Fernandez D, Du W, Hernandez-Viezcas JA, Bonilla-Bird N, Lopez-Moreno ML, Komarek M, Peralta-Videa JR, Gardea-Torresdey JL. 2017. Exposure of engineered nanomaterials to plants: Insights into the physiological and biochemical responses-A review. Plant Physiology and Biochemistry, 110:236–264.

APPENDICES

APPENDIX A

Table A2.1: Review on the genotoxicity of metal-based ENPs to aquatic organisms

Organism group	Organism name	ENP	ENP Properties	Duration	Dosage	Exposure media	Endpoint	Assay	Results	Refs
Fish	*T. carolinus*	TiO_2	32 nm anatase, 65 nm rutile	24 -72h	150, 300 mg/L	Saline water,pH 8, 5.77 mg/L DO	DNA strand breaks	Comet	The tail lengths of all $nTiO_2$ injected groups were significantly longer than those of the control groups, time and dose dependent effect.	[1]
	T. carolinus	TiO_2	32nm anatase, 65nm rutile	24 -72h	150, 300 mg/L	saline water,pH 8, 5.77 mg/L DO	Nucleus damage	MN	$nTiO_2$ induced time dependent erythrocyte nuclear abnormalities.	[1]
	D. rerio	ZnO	50-100 nm, spherical, irregular and short-rods	144h	1-100 mg/L	ZCM, pH 7.2, DO > 6.3 mg/L	DNA strand breaks	Comet	DNA damage was enhanced with increasing nZnO concentrations.	[2]
	D. rerio	ZnO	50-100 nm, spherical, irregular and short-rods	144h	1-100 mg/L	ZCM, pH 7.2, DO > 6.3 mg/L	mRNA expression	qRT-PCR	Transcription of Bcl-2 in nZnO-treated groups was significantly down-regulated by 0.62-fold and 0.60-fold at 50 and 100 mg/L nZnO, respectively, but no significant differences observed in the mRNA expression following Zn^{2+} exposure.	[2]
	O. mykiss	CuO	51 nm, spherical, ζ: -21 mV, SA: 18 m2/g	15-38h	10 µg/mL	Saline solution	DNA strand breaks	Comet	Significant DNA damage with respect to controls was detected only when Cu was injected as $CuSO_4$.	[3]
	P. mesopotamicus	TiO_2	< 25 nm, ζ: −27.8 to -31.9 mV	96h	0- 100 mg/L	DTW, pH 7.5, DO 6.0 ± 0.6 mg/L.	DNA strand breaks	Comet	No statistically significant differences between the UV or visible light groups were observed with Comet assay.	[4]
	P. mesopotamicus	TiO_2	< 25 nm, ζ: −27.8 to -31.9 mV	96h	0- 100 mg/L	DTW, pH 7.5, DO 6.0 ± 0.6 mg/L.	Chromosome damage	MN	Nucleus alterations were significantly higher in the group exposed to 10 mg/L of $nTiO_2$ under UV light, compared to the group exposed to the same concentration under visible light.	[4]
	A. anguilla	Fe_3O_4	100 nm, silica coated, ζ:-10.45 mV, SA:20.2 m^2/g	2-72h	25 µg/L	HBSS	ENA	MN	Exposure to Fe_3O_4 alone displayed a significant increase in ENA at both early (2, 4, 8) and late (16, 24, 48, 72) h of exposure.	[5]

A. anguilla	Fe_3O_4-Hg complex		2-72h	50 µg/L	HBSS	8-OHdG	IBL International GmbH kit	Fe_3O_4-Hg co-exposure revealed an increase in 8-OHdG levels at all the exposure length (except 16 h), suggesting that both Fe_3O_4 and Hg independently oxidized DNA.	[5]
O. latipes	Ag	49.6 nm, cubo- and decahedral, ζ: -29.9 mV	96h	1, 25 µg/L	fresh water,pH 7-8	Gene expression	RT-PCR	Ag-NPs led to cellular and DNA damage as well as carcinogenic and oxidative stresses, the ionic Agled to a lower overall stress response when compared with the nAg.	[6]
D. rerio	Ag	5-20 nm, spherical	24h	30-120 mg/L	water based solution	Gene expression	RT-PCR	The metal-sensitive MT2 mRNA was induced in the liver tissues of nAg-treated fish, suggesting that Ag+ ions were released from nAg after treatment. The p53-related pro-apoptotic genes Bax, Noxa, and p21 were also up regulated.	[7]
O. latipes	CMC-nZVI	49.3nm, CMC coated, ζ:-26.52	96h, 14 d	1, 100 mg/L	ERM,pH 7.2, DO 2-3 mg/L	Gene expression	PCR	The mRNA expression of catalase was lower with CMC-nZVI or Fe(II) treatment (12.5–50 mg/L) than with control treatment, but was induced with n Fe_3O_4-containing treatment (12.5–50 mg/L)	[8]
O. latipes	Fe_3O_4	NR	96h, 14 d	1, 100 mg/L	ERM,pH 7.2, DO 2-3 mg/L	Gene expression	PCR	Long periods of aqueous exposure to Fe_3O_4 at a low concentration triggered defence mechanisms of antioxidant enzymes and caused minor mortality.	[8]
O. latipes	Ag	23.5 nm, ζ:-23.3 mV	28 d	1, 25 µg/L	Milli-Q water,pH 7	Gene expression	RT-PCR	The lower dosage of nAg induced higher transcription levels of stress-induced biomarker genes than the higher dosage.	[9]
D. rerio	Ag	1.7-3.10 nm, ζ:-55.55 mV	28 d	5-50 µg/L	NR	Gene expression	Agilent 4 × 44K zebrafish microarray.	Microarray analysis revealed a dose-dependent response pattern.	[10]
D. rerio	Au	14 nm, citrate coated, spherical, ζ:-50 mV	20 d	16, 55 mg/g	DTW and contaminated sediment, pH 8	Gene expression	RAPD-PCR	Expression of genes involved in oxidative stress, detoxification and DNA repair was observed.	[11]

								Gold accumulation demonstrated the lower bioavailability of nAu compared to ionic Au.	[11]
D. rerio	TiO_2	21 nm	28 d	1,10 µg/L	FFW	Gene expression	RAPD-PCR	Genomic instability in the form of point mutations, genomic and chromosome rearrangements, deletions, and insertions was detected.	[12]
P. promelas	Ag	20 nm, citrate coated	96h	56 µg/L	MHW, pH 8	Gene expression	DNA microarray	A common pathway in all treatments was cell cycle: G2/M DNA damage checkpoint regulation.	[13]
P. promelas	Ag	20 nm, PVP coated	96h	56 µg/L	MHW,pH 8	Gene expression	qPCR	There were 185, 423, and 615 differentially expressed genes unique to AgNO3, PVP-AgNP, and citrate-AgNP,respectively, relative to control.	[13]
D. labrax	TiO_2	2838 nm	7 d	1 mg/L	ASW,pH 8.3	Gene expression	qPCR	Ahrr, erβ2, abcc1 and abcg2 genes were down-regulated with respect to controls.	[14]
O. mykiss	Ag	20 nm in DIW, > 50 nm aggregates in drinking water, ζ:-5.5Mv	96h	0.06-6 µg/L	DW	Gene expression	qPCR	Ag^+ more toxic than Ag NPs	[15]
O. mykiss	Ag	20 nm in DIW, > 50 nm aggregates in drinking water, ζ:-5.5Mv	96h	0.06-6 µg/L	DIW	Gene expression	DNA microarray	The DNA break levels were lower with nAg and could not be explained by the presence of ionic Ag.	[15]
D. rerio	SiO_2	68.06 nm	7 d	2.5, 5 mg/L	NR	DNA fragmentation	DNA laddering	DNA from control tissues was intact, whereas the tissues treated with SiO_2 were all fragmented.	[16]
P. reticulata	SnO_2	27 nm	5 d	150 mg/L	NR	Aberrant cells	CA	The frequency of aberrant cells in the experimental fish did not differ significantly from that in the control group.	[17]
O. mykiss	Ag	1-10 nm, PS coated, ζ:-13 to -16	48h	3.1 - 31 µg/mL	DTW	DNA damage	DNA precipitation	At the highest concentration Ag^+ and nAg elevated ROS by 3- and 2-folds, respectively.	[18]

		in water; −47 to−77 in medium							
D. rerio	TiO_2	25-28 nm, ζ:-26.6 mV, SA:48.7 m^2/g	6 d	0.1 mg/L	FFW	DNA oxidation	8-OHdG	A significant upregulation of sod1 gene transcription was observed in 10 and 30 ug/L PCP exposure groups (1.5-fold and 1.8-fold,respectively).n-TiO2 treatment alone did not induce DNA damage, as well as generation of ROS.	[19]
C. batrachus	$Cu/CuSO_4$	<50 nm; 15-20 nm after 6 h sonication, spherical	21 d	100 µg/L	NR	Gene expression	RT-PCR	The expressionof 3β-hsd increased significantly to 2.8 and 2.6($p<0.01$) fold in CuSO4 and Cu-NPs treated groups,respectively when compared to control.	[20]
L. rohita	Ag	18 and 29 nm, ζ: -55, -31.4 mV, spherical	7 d	100-800 µg/L	TW, pH 7.5-8.4;5.8-7.3 mg/L DO	DNA strand breaks	Comet	DNA strand breaks were dose, time and size dependent with a higher DNA damage occurring in 800 mg /L of 29 nm than 18 nm at d 7.	[21]
						Gene expression	RT-PCR	Stress related genes were down-regulated, due to the production of free radicals and ROS.	[21]
D. rerio	ZnO	<100 nm; >200-<1800 in DTW, SA: 25 m2/g	96 h	0.2-6 mg/L	DTW, pH 7.1, 93% DO	Gene expression	qRT-PCR	A concentration-dependent increase in DNA strand breaks was detected.	[22]
	$ZnCl_2$		96 h	0.1-3 mg/L	ammonium: <20 mg/L	DNA strand breaks	Comet	DNA damage was higher in Zn(II)than nZnO-exposed larvae.	[22]
O. mykiss	Ag	20 nm; 11.6 nm after filtration, spherical, ζ: 0 mV	96 h	40 µg/L	10%MWW,pH 7.55-8.45, conductivity: 273-340 S/cm; DOC:3.44-8.4; TOC: 7.7-10.3 mg/L	DNA strand breaks	Alkaline precipitation	No significant variation in DNA strand breaks were observed with nAg and $AgNO_3$.	[23]
O. mykiss	$AgNO_3$		96 h	4 µg/L					[23]
D. rerio	CuO	51 nm, 336–364 nm in E3 medium, irregular, ζ:-33 mV	96 h	5-120 mg/L	E3 medium, pH 6.8–7.2	Apoptosis	Acridine orange staining	Both 40 and 60 mg/L treated embryos showed apoptotic signals than the control. The apoptotic signals were found in both the head and tail regions with intense staining.	[24]

	Zebrafish	Ag	10 nm citrate coated, spherical	12-36 h	0.2-1 mg/L	NR	Gene expression	qRT-PCR	Genes in haemoglobin complex were down-regulated in exposed embryos at 24 h.	[25]
	Zebrafish	Ag	40 nm citrate coated, spherical	12-36 h	0.2-1 mg/L	NR	DEGs	Microarray	nAg affected erythrogenesis mostly by their particles other than released ions.	[25]
	Zebrafish	Ag	26 nm ζ:-27.0, 14.53 m^2/g	48 h	1000 µg/L	MHW	Transcriptome responses	Microarray	At 24 h, 237 genes were significantly differentially expressed in at least one treatment; that number increased to 918 at 48 h.	[26]
	Zebrafish	Cu	26 nm, ζ:-0.69 mV, SA 30.77 m^2/g	48 h	100 µg/L	MHW	Transcriptome responses	Microarray		
	Zebrafish	TiO_2	25 nm, ζ:-25.1 mV, SA:45.41 m^2/g	48 h	1000 µg/L	MHW	Transcriptome responses	Microarray		
	P.mesopotamicus	TiO_2 anatase	<25 nm, 543.9 in DTW, ζ:27.8 mV	21 d	100 mg/L	Conductivity 1.3±0.2 mS/cm, hardness 50.0 mg/L	DNA strands break	Comet	Pure anatase caused more oxidative damage without co-exposure to UV.	[27]
		TiO_2 anatase:rutile (80%:20%)	25 nm, 871.8 in DTW, ζ:-27.6 mV	21 d	100 mg/L	DTW, pH 7, DO: 6.0±0.6 mg/L	Micronuclei abnormalities	MN	The mixture anatase:rutile caused more sub-lethal effects when exposed under UV.	[27]
	P. mesopotamicus	Ag	50 nm, 57 nm in DTW, ζ:-12 mV	24 h	2.5-25 µg/L	DTW, pH 7, total hardness 49 ± 0.1 mg/L	DNA strand breaks	Comet	Significant DNA damage was reported on fish exposed to 10 and 25 µg/L nAg	[28]
	D. labrax	TiO_2	24 nm, 972-1448 nm in ASW, spheroid irregular	7 d	1 mg/L	ASW, pH 8	DNA strands break	Comet	Exposure to $nTiO_2$ alone was responsible for chromosomal alteration but ineffective in DNA damage.	[29]
	D. labrax	$CdCl_2$			0.1 mg/L		Apoptotic cells	Diffusion assay	Genome template stability was reduced after $CdCl_2$ and $nTiO_2$ exposure.	[29]
	D. labrax	TiO_2+$CdCl_2$					Nuclear and micronuclei abnormalities	MN	Co-exposure prevented chromosomal damage and led to a partial recovery of the genome template stability.	[29]
							Genome stability	RADP PCR	Increased DNA damage compared to controls was observed in erythrocytes from fish exposed to $CdCl_2$ ($p < 0.05$), but not to $nTiO_2$.	[29]
Fish cell line	*O. mykiss*	TiO_2	anatase: 10-20 nm, ζ: -43, -15, SA:132.73 m^2/g; 2:8 anatase:rutile, 20-150 nm, ζ:-65, -12 mV, SA:20.75 m^2/g	4h	1.6 - 4.8 µg/mL	MEM, pH 6.3-7.8	DNA strand breaks	Comet	DNA damage was observed at 4.8 µg/mL $nTiO_2$.	[30]

	C. catla	Ag	40.3 to 55.2 nm, spherical	24h	2-64 µg/mL	Leibovitz's L-15,pH 7.85–7.93, 4.5 to 5.8 mg/L DO	DNA strand breaks	Comet	Concentration dependent increase in tail DNA (%) compared to the control cells.	[30]
	L. rohita	Ag	40.3 to 55.2 nm, spherical	24h	2-64 µg/mL	Leibovitz's L-15,pH 7.85–7.93, 4.5 to 5.8 mg/L DO	Nuclear fragmentation	Hoechst staining	Apoptotic cells, condensation and fragmentation of the nuclei were observed at 64 µg/mL after 24 h (dose dependent effect), while no nuclear changes were observed in control cells.	[31]
	GFSk-S1	TiO_2	5 nm, anatase	2; 24h	1, 10, 100 µg/mL	L-15	DNA strand breaks	Comet	UVA irradiation of nTiO_2-treated cells caused further increases in DNA damage, most likely due to hydroxyl radical formation.	[32]
	GFSk-S1	TiO_2	11-34.5 nm	4 - 48h	5, 50 µg/mL	MEM,DIW	DNA strand breaks	Comet	The presence of ENPs in the absence of UVA gave a reduction in strand breakage over the negative control.	[33]
	GFSk-S1	TiO_2	11-34.5 nm	4 - 48h	5, 50 µg/mL	MEM,DIW	Cytogenetic damage	MN	The DNA damage was linked to delayed cell proliferation and cell death.	[33]
	O. latipes	Ag	30 nm, spherical	24h	0.05–5 µg/cm2	Tissue culture	Chromosome damage	CA	Concentration-dependent genotoxic effect. The damage included chromatid lesions, isochromatid lesions, chromatid exchanges and centromere spreading	[34]
Midge	*C. riparius*	CeO_2	15, 30 nm	24h	1 mg/L	Culture medium	DNA strand breaks	Comet	The smaller-sized nCeO_2 caused more DNA strand breaks.	[35]
	C. riparius	SiO_2	7, 10 nm	24h	1 mg/L	Culture medium	DNA strand breaks	Comet	Neither exposure to SiO_2 nor TiO_2 had a genotoxic effect to *C. riparius.*	[35]
	C. riparius	TiO_2	7 , 20 nm	24h	1 mg/L	Culture medium	DNA strand breaks	Comet	Size and NP dependent effect.	
	C. riparius	Ag	40–70 nm	24h - 25 d	0.5 - 4 mg/L (acute)	DTW	Gene expression	DD-PCR	Up regulation of CrBR2.2 gene	[36]
	C. riparius	Ag	40–70 nm	24h - 25 d	0 - 1 mg/L (chronic)	DTW	DNA strand breaks	Comet	A dose dependent increase in DNA damage was observed	[36]

	C. tentans	alumina (alpha, gamma)	a=20–50 nm, g= 80–400 nm, spherical, ζ: g= -18.7, a=19.7 mV, SA: a=13, g=73 m^2/g	10 d	5 - 5000 mg/kg	MH EPA water, pH 7.3 and alkalinity (64 mg/L $CaCO_3$)	DNA fragmentation	DNA laddering	DNA cleavage occurred at 5000 mg/kg concentrations of precipitated silica, Fe_2O_3 and Sb_2O_5 NPs	[37]
	C. tentans	silica (Fume, Calcined, Precipitated)	F=100–400 nm, C= 50–300 nm, P= 20–100 nm, ζ: F= -21.1,C= -14.6,P= -1.76, SA: F=24, C=17, P=157 mV	10 d	5 - 5000 mg/kg	MH EPA water, pH 7.3 and alkalinity (64 mg/L $CaCO_3$)	DNA fragmentation	DNA laddering		
	C. tentans	Fe_2O_3	50–150 nm, spherical, ζ: -18.5 mV, SA:235 m^2/g	10 d	5 - 5000 mg/kg	MH EPA water, pH 7.3 and alkalinity (64 mg/Ll $CaCO_3$)	DNA fragmentation	DNA laddering	For g- and a-alumina treatments, the inter-nucleosome DNA ladder bands occurred at lower concentrations of 50 and 500 mg/kg, respectively.	[37]
	C. tentans	Sb_2O_5	5000–15000 nm, mixed shape (spheres, irregular), ζ:2.35 mV,SA:3 m2/g	10 d	5 - 5000 mg/kg	MH EPA water, pH 7.3 and alkalinity (64 mg/L $CaCO_3$)	DNA fragmentation	DNA laddering		
Crustacean	*D. magna*	Ag	40 nm, citrate coated	24h	100 µg/L	MHRW	Gene expression	q-RT-PCR	A total of 466 genes were differentially expressed by at least one of the treatments.	[38]
	D. magna	Ag	35 nm, PVP coated	24h	100 µg/L	MHRW	Gene expression	Microarray hybridization	DNA damage repair genes were induced by the PVP nAg, but not the other treatments.	[38]
	D. magna	CeO_2	15, 30, 45 nm	24h	1 mg/L	M4	DNA strand breaks	Comet	Size dependent DNA strand breaks, 15 nm CeO_2 caused more damage.	[39]
	D. magna	SiO_2	7,10,14 nm	24h	1 mg/L	M4	DNA strand breaks	Comet	Neither exposure to SiO_2 nor TiO_2 caused DNA strand breaks.	[39]
	D. magna	TiO_2	7, 20, 200 nm	24h	1 mg/L	M4	DNA strand breaks	Comet		
	D. magna	CeO_2	15, 30 nm	24h	1 mg/L	Culture medium	DNA strand breaks	Comet	The smaller-sized $nCeO_2$ caused more DNA strand breaks.	[35]
	D. magna	SiO_2	7, 10 nm	24h	1 mg/L	Culture medium	DNA strand breaks	Comet	Neither exposure to SiO_2 nor TiO_2 had a genotoxic effect.	[35]
	D. magna	TiO_2	7 , 20 nm	24h	1 mg/L	Culture medium	DNA strand breaks	Comet		

	D. magna	Ag	<50 nm	24h	0.5 - 1.5 µg/L	M4	DNA strand breaks	Comet	Both nAg and Ag ions increased DNA strand breaks	[40]
	D. magna	Au	3.8 nm, 8 nm in MHW, MPA coated, spherical, ζ: −18.5 mV	24h	1, 10, 50 µg/L	MHW	Gene expression	qRT-PCR	Positively charged nAu induced a greater ROS response than negatively charged nAu.	[41]
	D. magna	Au	4.9 nm, 12.8 nm in MHW, citrate coated, spherical, ζ:−15.3 mV	24h	1, 10, 50 µg/L	MHW	Gene expression	qRT-PCR	Mortality was only observed for the free ligand CTAB at 10 µg/L.	[41]
	D. magna	Au	5.7 nm, 17.9 nm in MHW, PAH coated, spherical, ζ: 17.9 mV	24h	1, 10, 50 µg/L	MHW	Gene expression	qRT-PCR	Both positively charged nAu and only one negatively nAu impacted expression of genes associated with cellular stress.	[41]
	D. magna	Au	50x14 nm, 20.7 nm in MHW, CTAB coated, rod, ζ:16.7 mV	24h	1, 10, 50 µg/L	MHW	Gene expression	qRT-PCR		[41]
Mussel	*M. galloprovincialis*	CuO	40-500 nm (DIW), sea water-above DLS detection limit, ζ: 26.3 in DIW, -7.72 mV in seawater	21 d	10 µg/L	Seawater, DIW, pH 7.6 - 7.8	Micronuclei frequency	MN	Micronuclei frequency increased significantly in mussels exposed to nCuO compared to bulk CuO.	[42]
	M. galloprovincialis	CuO	40-500 nm (DIW), sea water-above DLS detection limit, ζ: 26.3 in DIW, -7.72 mV in seawater	21 d	10µg/L	Seawater, DIW ,pH 7.6 - 7.9	Gene expression	RT-PCR	Transcription levels of cancer-related genes did not vary significantly.	[42]
	M.galloprovincialis	CuO	<50 nm, spherical, SA:29 m^2/g	15 d	10 µg/L	Natural seawater, pH 7.8	DNA strand breaks	Comet	Ionic forms presented higher DNA damage than nanoparticles	[43]
	M.galloprovincialis	Ag	<100 nm, spherical, SA: 5m^2/g	15 d	10 µg/L	Natural seawater, pH 7.9	DNA strand breaks	Comet	Ionic forms presented higher DNA damage than nanoparticles	[43]
	M.galloprovincialis	TiO_2	15–47 nm, oblong, SA: 54 m^2/g	96h	100 µg/L	ASW	DNA strand breaks	Comet	An increase in DNA damage was observed in isolated gill cells exposed in vitro to TCDD ($p < 0.05$), but not to $nTiO_2$ alone.	[44]

	M. edulis	Ag	13 nm, MPEG-SH coated, cubic	4h	0.01-10 mg/L	HBSS	DNA strand breaks	Comet	Significant increases in DNA strand breaks at 10 mg/L. No damage at low concentrations, this may be related to the short exposure period.	[45]
	M. galloprovincialis	TiO_2	24 nm primary size, 972 - 1448 in ASW, spheroid and irregular	96h	0.1 mg/L	ASW, pH 8	DNA strand breaks	Comet	$nTiO_2$ exposure did not affect DNA integrity, while $CdCl_2$ induced DNA strand breaks. In co-exposure experiments, the DNA damage was reduced to control level.	[46]
	M. galloprovincialis	TiO_2 + $CdCl_2$		96h	0.1 mg/L	ASW, pH 8	Gene expression	RT-PCR	*In vivo* exposure to $nTiO_2$ did not affect mt-20 gene transcription. A significant up-regulation of mt-20 with respect to controls was observed in the gills of mussels exposed to both $CdCl_2$ alone and combined with $nTiO_2$.	[46]
	U. tumidus	ZnO	35 nm	14 d	1.3 µM	DTW, pH 7.3, 8.67±0.51 mg/L DO	DNA fragmentation	DNA precipitation	DNA fragmentation was induced by exposure to organic toxins, nifedipine (Nfd 10 µM) alone and in combination with nZnO, but not by nZnO alone.	[47]
	M. galloprovincialis	TiO_2	10-65 nm, 130-304 nm in ASW, irregular and spherical	96h	100 µg/L	ASW	Gene expression	qRT-PCR	Transcriptomic analysis identified 48-, 49 and 62DEGs in response to $nTiO_2$, TCDD and n-TiO_2/TCDD, respectively.	[48]
	M. galloprovincialis	TCDD/ TiO_2+TCDD		96h	0.25 µg/L	ASW	Gene expression	qRT-PCR	No mortality was observed at both experimental conditions.	[48]
	L. fortunei	TiO_2	20 nm, 500 nm in Itapuã water, anatase	2- 4 h (Comet)	1-50 µg/mL	Itapuã water, Brazil, pH 7.6, DO: 1.90 mg/L	DNA strand breaks	Comet	$nTiO_2$ increased DNA damage levels at 5 µg/mL after 2 h. After 4 h, DNA strand breaks were observed at all tested concentrations.	[49]
	L. fortunei	TiO_2	ζ: 15.65-18.29 mV, SA: 46.26 m^2/g	24 h (MN)	1-50 µg/mL	Total hardness: 30 mg $CaCO_3$/L	Chromosome damage	MN	$nTiO_2$ did not increase the MN frequency	[49]
	M. edulis	TiO_2 benzo (a) pyrene	62-146 nm, uncoated	96h	0.2-2 mg/L	Seawater	Chromosomal damage	MN	Chromosomal damage was detected in mussels exposed to single compound, which was further increased after exposure to the combination of $nTiO_2$ or benzo (a) pyrene.	[50]

	M.trossulus	CuO	<50 nm, mean: 290 nm, 206 - 383 in SW, SA: 25-40 m^2/g		0.02 mg/L	Seawater	DNA strand breaks	Comet	nCuO exposure produced remarkable effects and increased DNA damage significantly. [51]
		$CuCl_2$			0.02 mg/L	Seawater	DNA strand breaks	Comet	Both forms of Cu accumulated to different extents in mussel tissues. [51]
Snail	*L. luteola*	ZnO	50 nm, polygonal, ζ: -15.3 mV, SA: >10.8 m^2/g	24, 96h	10 -32 µg/mL	TW	DNA strand breaks	Comet	nZnO induce DNA damage in digestive gland cells through oxidative stress [52]
	L. luteola	Ag	32 nm, spherical, ζ:−12.5 mV	96h	4, 12, 24 µg/L	TW	DNA strand breaks	Comet	Positive correlation was observed among ROS generation, apoptosis, and DNA damage [53]
	L. luteola	Ag	32.40 nm, spherical, ζ:−12.5 mV	96h	10-100 µg/L	DIW pH 7.03- 8.20	DNA strand breaks	Comet	nAg increased lipid peroxidation without uptake into the cells whereas Ag+ increased DNA damage. [54]
	L. luteola	TiO_2	34.1 nm, ζ:-13.9 mV	7 d	9, 28 µg/L	TW, pH 7.5-8.06, 6.2 to 8.05 mg/L DO, 267 to 282 mg/mL $CaCO_3$,total hardness 178 to183 mg/mL	DNA strand breaks	Comet	A dose and time dependent effect was observed [55]
	L. luteola	CuO	43.5 nm, ζ:-13.7 mV	5 d	7, 21 µg/L	TW, pH 7.24 -8.06, 6.54 to 7.9 mg/L DO, 259 to 284 mg/ml $CaCO_3$.	DNA strand breaks	Comet	A dose and duration dependent increase in DNA damage. [56]
	L. luteola	TiO_2	34.1 nm, ζ:-13.9 mV	96h	28-84 µg/mL	TW,pH 7.5 -8.06, 6.20 to 8.05 mg/l DOC	DNA strand breaks	Comet	High levels of DNA damage at the highest concentration. [57]
	L. luteola	TiO_2	34.1 nm, ζ:-13.9 mV	96h	28-84 µg/mL	TW,pH 7.5 -8.06, 6.20 to 8.05 mg/l DOC	Apoptosis	Annexin V-FITC and propidium iodide staining	Significant increase in Annexin V (+) cells (13.10 %) and late necrotic cells (17.59 %). [57]
	R. leuteola	MgO	35 nm, 154 in TW, ζ:-19 mV	24; 96 h	0-51 µg/mL	TW, pH 6.9 to 7.94, 6.8 to 8.20 mg/L DO; conductivity: 247-298.6 µM/cm; hardness: 159 -180 µg/mL	DNA strand breaks	Comet	DNA damage and enzyme increased more effectively at the higher concentration of MgO NPs at 96h. [58]

Clam	*M. balthica*	Ag	20 and 80 nm, PVP coated	35 d	150-120 µg/g	NR	DNA strand breaks	Comet	No DNA damage, a form dependent bioaccumulation was observed, ions > NPs > micro sized particles	[59]
		CuO	<100 nm	35 d	150-120 µg/g	NR	DNA strand breaks	Comet	No DNA damage, a form dependent bioaccumulation was observed, ions > NPs > micro-sized particles	[59]
	S. plana	CuO	197 nm (DIW), 810 nm (seawater), ζ:26.3 mV DIW, -8.3 in seawater	21 d	10 µg/L	Seawater	DNA strand breaks	Comet	DNA strand breaks were observed for both soluble Cu and nCuO treatments.	[60]
Polychaete	*A. marina*	TiO_2	32.4 nm, SA: 46.3 m^2/g	10 d	1 -3 g/kg	Marine sediment	DNA strand breaks	Comet	Significant DNA damage was observed with $nTiO_2$ compared to the controls and bulk TiO_2.	[61]
	H. diversicolor	CuO	197 nm in DIW, 810 nm in seawater, ζ:26.3 DIW, -8.3 in seawater	21 d	10 µg/L	Seawater	DNA strand breaks	Comet	DNA strand break was observed for both soluble Cu and nCuO treatments	[60]
	L. acuta	TiO_2	NR	48 h	1 mg/L	NR	DNA strand breaks	Comet	Co-exposure induced an increase in the ROS levels, and damage in lipid and DNA.	[62]
	L. acuta	Arsenic	NR	48 h	0.05 mg/L	NR	DNA strand breaks	Comet	DNA damage was higher in co-exposure than exposure to only arsenic or $nTiO_2$.	[62]
Ascidian	*C. intestinalis*	Ni	<100 nm, 128.8-151.4 nm in seawater	2 h	0.001-0.1 mg/mL	Seawater	Sperm DNA fragmentation	In Situ Cell Death Detection Kit	Ni NPs generated oxidative stress that in turn induced lipid peroxidation and DNA fragmentation, and altered sperm morphology.	[63]
		$NiCl_2$			0.001-0.1 mg/mL	Seawater	Sperm DNA fragmentation	In Situ Cell Death Detection Kit	No significant variation was observed in sperm DNA between $NiCl_2$ and the control groups.	[63]
Bacteria	*S.typhimurium, E. coli*	TiO_2	140 nm, SA: 38.5 m2/g	NR	100-5000 µg/ plate	Milli-Q water, pH 4.8	Mutagenicity	Ames	No mutagenicity observed	[64]

S.typhimurium, *E. coli*	TiO_2	<100 nm, uncoated, ζ: 5.04 mV	48h	0 - 2500 mg/L	Milli Q water, pH 4.09–5.36	Mutagenicity	Ames	A reduction in the number of revertent colonies was observed with TiO_2, but no mutagenicity.	[65]
S.typhimurium, *E. coli*	$TiSiO_4$	<50 nm, uncoated, ζ:-23.4 mV	48h	0 - 2500 mg/L	ASTM hard water, pH 7.04–7.71	Mutagenicity	Ames	No mutagenicity observed	[65]
S.typhimurium, *E. coli*	Au	10x35 nm, rod, CTAB coated, ζ:15.3 mV	48h	0 - 2500 mg/L		Mutagenicity	Ames	No mutagenicity observed	[65]
S.typhimurium, *E. coli*	CuO	30–50 nm	NR	10 - 500 mg/L	NR	Mutagenicity	Ames	No significant mutagenicity was observed at the tested concentrations.	[66]
	ZnO	NR	NR	10 - 500 mg/L	NR	Mutagenicity	Ames	No significant mutagenicity was observed at the tested concentrations.	[66]
	NiO	30 nm	NR	10 - 500 mg/L	NR	Mutagenicity	Ames	No significant mutagenicity was observed at the tested concentrations.	[66]
	TiO_2	<25 nm	NR	10 - 500 mg/L	NR	Mutagenicity	Ames	No significant mutagenicity was observed at the tested concentrations.	[66]
S.typhimurium, *E. coli*	Ag	8.6 nm, SMA coated, spherical, ζ: -40 mV	48h	0.05-1.6 µg/plate	Top agar (containing 0.5% NaCl)	Base-pair substitutions	Ames	SMA-nAg did not cause mutagenic effect	[67]
E. coli	TiO_2	20 nm	72h	0.01 µg/plate	LB	DNA fragmentation	DNA ladder	Presence of TiO_2 caused more plasmid DNA and chromosome DNA damage than UV radiation only.	[68]
E. coli	CuO	20-100nm, ζ: -16.5 mV	24h	100 µg/mL	E. coli media MMD	DNA fragmentation	DNA ladder	nCu and nCuO caused more damage than their micro sized counterparts at the same Cu concentration.	[69]
L. brevis	CuO	20-100 nm, ζ: -16.5 mV	24h	100 µg/mL	Lactobacilli MRS broth	DNA fragmentation	DNA ladder		
E. coli	CuO	30 nm, SA: 25.5 m^2/g	8h	0.635-6.35 mg/L	LB	DNA strand breaks	Bioluminescence	nCuO induced the formation of ROS and single-strand DNA breaks.	[70]
S.typhimurium, *E. coli*	ZnO	165 nm, ζ: -26 mV	48h	0.008 - 8 µg/plate	Top gar	Mutagenicity	Ames	nZnO showed a two fold increase in revertant colonies compared to the negative control in TA98, TA1537 and *E. coli*.	[71]
E. coli	TiO_2	124 nm, ζ: - 17.6 mV	48h	0.008 - 8 µg/plate	Top gar	Mutagenicity	Ames	$nTiO_2$ showed a statistical significant increase in the number of revertant colonies in TA98, TA1537 and *E. co*li (WP2 uvrA)	[71]

	P. aeruginosa	Al_2O_3	13 nm, 362-726 nm in lake water, irregular and spherical, ζ: 25.9 mV, SA: 85–115 m^2/g	24h	0.25, 0.5,1 mg/L	Lake water	DNA strand breaks	DNA alkaline unwinding	nAl_2O_3 caused more DNA damage than the bulk particles in both bacterial strains.	[72]
	B. altitudinis	bulk-Al_2O_3	986-1679 nm in lake water, ζ: 3.05 mV	24h	0.25, 0.5,1 mg/L	Lake water	DNA strand breaks	DNA alkaline unwinding	Both n Al_2O_3 and bulk Al_2O_3 caused more DNA damage to Gram-negative bacteria than to Gram-positive bacteria.	[72]
	N. europaea	TiO_2	41 nm, 85.8 in media, elliptical	6 h	1-50 mg/L	SCM, pH 7.45, 2 mg/L DO	Gene expression	qRT-PCR	amoA gene was up-regulated under the stress of either 50 mg/L $nCeO_2$ or their combination with $nTiO_2$.	[73]
	N. europaea	CeO_2	35nm, 113.6 nm in media, irregular	6 h	1-50 mg/L		Gene expression	qRT-PCR	The ZnO/CeO_2 mixture impacted AMO activity profile; the amoA gene expressions were gradually down-regulated with the increase of the co-existing $nCeO_2$.	[73]
	N. europaea	ZnO	95 nm, irregular	6 h	1-50 mg/L		Gene expression	qRT-PCR		
	P. putida	Al_2O_3	<50 nm, ζ: >40 mV	16 h	0.1-1000 mg/L	NR	DNA changes	RAPD-PCR	Treatment with n Al_2O_3 led to a decrease in the genetic stability of DNA (GTS, %) compared with the negative control.	[74]
	P. putida	bulk-Al_2O_3		16 h	0.1-1000 mg/L	NR	DNA changes	RAPD-PCR	nAl_2O_3 induced modifications of the genetic material to a greater extent than the same compounds in the macro form.	[74]
	E. coli	Ag	<20 nm	4 h	30, 60 μg/mL	PBS, pH 7.4	DNA changes	RAPD-PCR	The presence or absence of bands in the gel images suggested changes in the DNA sequence by NPs.	[75]
	E. coli	CuO	<20 nm	4 h			DNA changes	RAPD-PCR		
Algae										
	D. tertiolecta	ZnO	100 nm, 470-1040 nm in ASW, ζ: -10.51 mV	24; 72 h	5-100 mg/L	Filtered ASW, pH 8	DNA strand breaks	Comet	At 25 mg Zn/L, the highest effect was observed with the 55% of nuclei damaged.	[76]
	D. tertiolecta	SiO_2	10-20 nm, 1300-1800 nm in ASW, ζ: -12.15 mV	24; 72 h	125,200 mg/L	35‰ of salinity	DNA strand breaks	Comet	After 24 h, at 125 mg/L, more than 70% of intact nuclei were observed. After 72	[76]

						h, an increasing genotoxic effect was observed.	
D. tertiolecta	TiO_2	25 nm, 1300-1350 nm in ASW, ζ: -10.7 mV	24; 72 h	7.5,20 mg/L	Comet	After 24 h, nuclei were already damaged with >70% of the nuclei extremely damaged after 72 h.	[76]

References: [1] Vignardi*et al.* 2015, [2] Zhao*et al.* 2013, [3] Isani*et al.* 2013, [4] Clemente *et al.* 2013, [5] Mohmood*et al.* 2015, [6] Chae*et al*. 2009, [7] Choi *et al.* 2010, [8] Chen *et al.* 2011, [9] Pham *et al.* 2012, [10] Griffitt*et al*. 2013, [11] Dedeh*et al.* 2014, [12] Rocco *et al.* 2015, [13] Garcia-Reyero*et al*. 2015, [14] Vannuccini*et al.* 2015, [15] Gagne *et al.* 2012, [16] Ramesh *et al.* 2013, [17] Krysanov*et al.* 2009, [18] Massarsky*et al.* 2014, [19] Fang *et al*. 2015, [20] Murugananthkumar *et al*. 2016, [21] Sharma *et al.* 2016, [22] Boran and Ulutas 2016, [23] Bruneau *et al.* 2016, [24] Ganesan *et al.* 2016, [25] Cui *et al.* 2016,[26] Griffitt *et al.* 2009, [27] Clemente *et al*. 2015, [28] Bacchetta *et al.* 2017, [29] Nigro *et al.* 2015, [30] Sekar *et al.* 2014, [31] Taju *et al.* 2014, [32] Reeves *et al.* 2008, [33] Vevers and Jha 2008, [34] Wise *et al.* 2010, [35] Lee *et al.* 2009, [36] Prakash *et al.* 2011, [37] Oberholster *et al.* 2011, [38]Poynton *et al.* 2012, [39] Kim and Choi 2008 [40] Park and Choi 2010, [41] Dominguez *et al.* 2015, [42] Ruiz *et al.* 2015, [43] Gomes *et al.* 2013, [44] Canesi *et al*. 2014, [45] Munari *et al.* 2014, [46] Torre *et al.* 2015, [47] Falfushynska *et al.* 2015, [48] Banni et al. 2016,[49] Girardello et al. 2016,[50]Farkas *et al.* 2015, [51] Chelomin *et al.* 2017, [52] Ali *et al.* 2012, [53] Ali 2014, [54] Ali *et al*. 2014, [55] Ali, 2015, [56] Ali and Ali 2015,[57] Ali *et al.* 2015,[58]Ali *et al.* 2016, [59] Dai *et al.* 2013, [60] Buffet *et al.* 2013, [61] Galloway *et al.* 2010, [62] Nunes *et al*. 2017, [63] Gallo *et al.* 2016, [64] Warheit*et al*. 2007, [65] Lopes *et al*. 2012, [66]Ko and Kong 2014 [67] Chen *et al.* 2015,[68] Huang *et al.* 2008, [69] Kaweeteerawat *et al*. 2015, [70]Bondarenko *et al*. 2012, [71] Kumar *et al*. 2011, [72] Bhuvaneshwari *et al*. 2016, [73] Yu *et al.* 2016, [74] Załęska-Radziwiłł and Doskocz 2016, [75] Amjady *et al.* 2016, [76] Schiavo et al. 2016

Table A2.1 Abbreviations: SA-surface area, MN- micronucleus assay, CA - chromosome aberration, RT-PCR - real-time polymerase chain reaction, DD-PCR- Differential display PCR, RAPD-PCR- Random Amplified Polymorphism DNA-PCR, DIW –de-ionised water, HBSS-Hanks' balanced salt solution, LB- Luria–Bertani, ERM- embryo rearing medium, MEM- minimal essential media, ASW- artificial sea water, PS-polyacrylate sodium, DTW- dechlorinated tap water, FFW-Fresh filtered water, DW-drinking water, SCM- Steric cultivation medium, DO-dissolved oxygen, 8-hydroxy-2' -deoxyguanosine (8-OHdG), ENA- erythrocytes nuclear abnormalities, ZCM- zebrafish culture medium, DEGs-Differentially Expressed Genes, CTAB- cetyl-trimethyl ammonium bromide, PAH- polyallylamine hydrochloride, MPA- mercaptopropionic acid, 10% MWW-diluted (10%) municipal wastewater

Table A3.1: Composition of 10% BG-11algal medium

	Macronutrients	Volume (mL) per 1 L
A	$CaCl_2.2H_2O$	1
B	$NaNO_3$	10
C	K_2HPO_4	1
D	$MgSO_4 \cdot 7(H_2O)$	1
E	$NaHCO_3$	1
	Micronutrients	
	H_3BO_3	
	$MnCl_2 \cdot 4(H_2O)$	
	$ZnSO_4 \cdot 7H_2O$	1
F	$CuSO_4 \cdot 5H_2O$	
	$Co(NO_3)_2 . 6H_2O$	
	$NaMoO_4.2H_2O$	
	Citric acid	
G	Na_2-EDTA.$2H_2O$	1
H	$Fe(NH_3)$-citrate	1

Table A3.2: Composition of Hoagland's medium

Macronutrient	Per liter of nutrient solution
KNO_3	5 ml of 1 M
$Ca(NO_3)_2$ $4H_2O$	5 ml of 1 M
$MgSO_4 \cdot 7(H_2O)$	2 ml of 1 M
KH_2PO_4	2 ml of 1 M

Micronutrients	Per liter (g)
H_3BO_3	2.86
$MnCl_2 \cdot 4(H_2O)$	1.81
$ZnSO_4 \cdot 7H_2O$	0.22
$CuSO_4 \cdot 5H_2O$	0.08
MoO_3	0.02
Fe-EDTA	1-5 ml of 1000 mg/L

Minus nitrogen	
$Ca(NO_3)_2$ $4H_2O$	0.75 ml of 1 M
$Ca(H_2PO_4)_2 \cdot H_2O$	10 ml of 0.05 M
$CaSO_4 \cdot 2H2O$	200 ml of 0.01 M
K_2SO_4	5 ml of 0.5 M
$MgSO_4.7H_2O$	2 ml of 1 M

Table A3.3: Composition of unfiltered tap water

Physical and Aesthetic determinands	Unit of measure	Specification
Conductivity	mS/m	> 0.0 to < 170.0
pH at 25 ºC	N/A	> 5.0 to < 9.7
Free Chlorine	mg/L	> 0.01 to < 5.0
Residual Chlorine	mg/L	> 0.01 to < 5.0
Total Chlorine	mg/L	> 0.01 to < 5.0
Total Dissolved Solids	mg/L	> 0.0 to < 999.0
Turbidity Aesthetic	NTU	> 0.01 to < 5.0
Turbidity Operational	NTU	> 0.01 to < 1.0
Chemical determinands-organic determinands		
Bromoform	µg/L	> 0.0 to < 100.0
Chloroform	µg/L	> 0.0 to < 300.0
Dibromochloromethane	µg/L	> 0.0 to < 100.0
Dichlorobromomethane	µg/L	> 0.0 to < 60.0
Microcystin as LR	µg/L	> 0.0 to < 1.0
Phenols	µg/L	> 0.0 to < 10.0
Total Organic Carbon as C	mg/L	> 0.0 to < 9.99
Total trihalomethanes as THM	µg/L	> 0.0 to < 199.0
Chemical determinands - micro determinands		
Aluminium as Al	µg/L	> 0.0 to < 300.0
Antimony as Sb	µg/L	> 0.0 to < 20.0
Arsenic as As	µg/L	> 0.0 to < 10.0
Cadmium as Cd	µg/L	> 0.0 to < 5.0
Cobalt as Co	µg/L	> 0.0 to < 499.0
Copper as Cu	µg/L	> 0.0 to < 2000.0
Cyanide (recoverable) as CN	µg/L	> 0.0 to < 200.0
Iron as Fe	µg/L	> 0.0 to < 300.0
Lead as Pb	µg/L	> 0.0 to < 20.0
Manganese as Mn	µg/L	> 0.0 to < 100.0
Mercury as Hg	µg/L	> 0.0 to < 6.0
Nickel as Ni	µg/L	> 0.0 to < 70.0
Selenium as Se	µg/L	> 0.0 to < 20.0
Uranium as U	µg/L	> 0.0 to < 30.0
Vanadium as V	µg/L	> 0.0 to < 200.0
Chemical determinands - macro determinands		
Ammonia as N	mg/L	> 0.0 to < 1.5
Chloride as Cl	mg/L	> 0.0 to < 300.0
Fluoride as F	mg/L	> 0.0 to < 1.5

Nitrate as N	mg/L	> 0.0 to < 11.0
Nitrite as N	mg/L	> 0.0 to < 0.9
Sodium as Na	mg/L	> 0.0 to < 200.0
Sulphate as SO_4	mg/L	> 0.0 to < 250.0

Microbiological determinands		
Confirmed *E. Coli*	CFU/100mL	> 0.0 to < 0.0
Cryptosporidium species	mg/L	> 0.0 to < 0.0
Cytopathogenic Viruses	mg/L	> 0.0 to < 0.0
Faecal Coliforms	CFU/100mL	> 0.0 to < 1.0
Total Coliforms	CFU/100mL	> 0.0 to < 10.0

Other determinands		
Bromide	mg/L	> 0.0 to < 4.0
Calcium as Ca	mg/L	> 0.0 to < 150.0
Calcium Hardness as $CaCO_3$	mg/L	> 0.0 to < 370.0
Magnesium as Mg	mg/L	> 0.0 to < 70.0
Magnesium Hardness as $CaCO_3$	mg/L	> 0.0 to < 280.0
Orthophosphate as PO_4	mg/L	> 0.0 to < 1.0
Potassium as K	mg/L	> 0.0 to < 50.0
Silica as Si	mg/L	> 0.0 to < 25.0
Total Hardness as $CaCO_3$	mg/L	> 0.0 to < 660.0

(a)

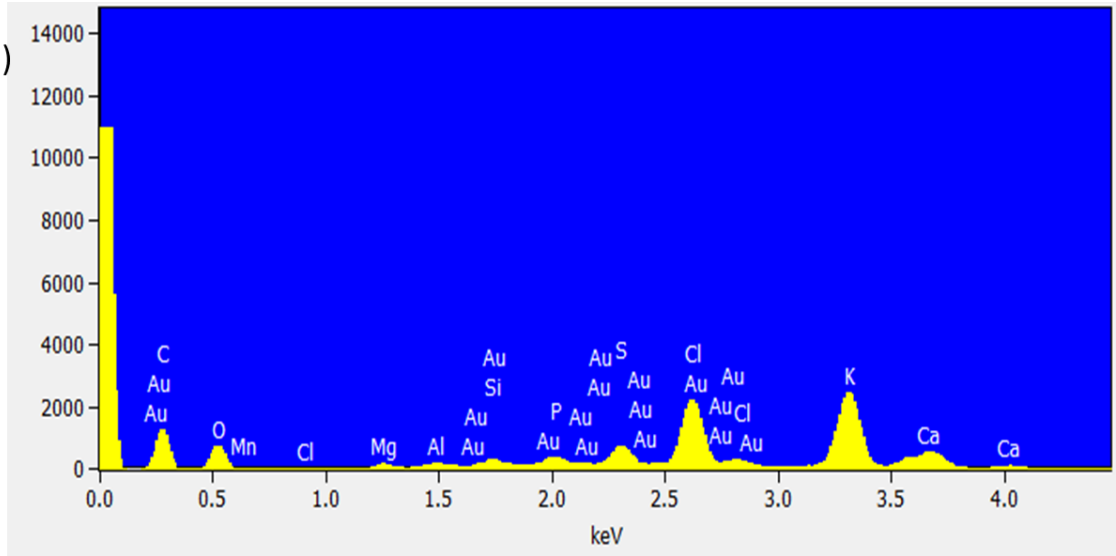
14000
12000
10000
8000
6000
4000
2000
0
C
Au
Au
O
Mn
Cl
Mg
Al
Au
Au
Si
Au
P
Au
Au
Au
Au
S
Au
Au
Au
Cl
Au
Au
Au
Cl
Au
Au
K
Ca
Ca
0.0
0.5
1.0
1.5
2.0
2.5
3.0
3.5
4.0
keV

(b)

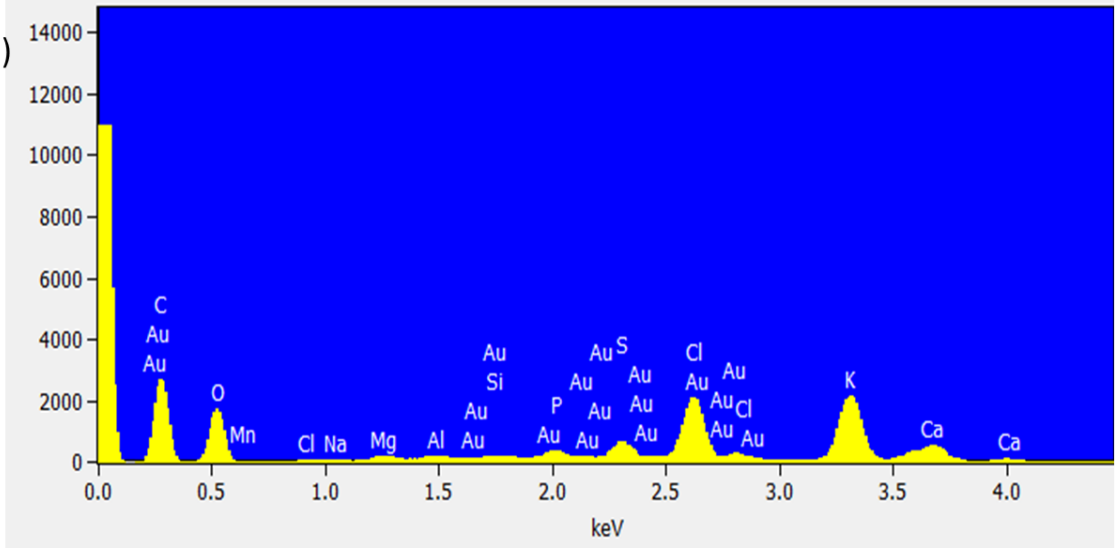
14000
12000
10000
8000
6000
4000
2000
0
C
Au
Au
O
Mn
Cl
Na
Mg
Al
Au
Au
Si
Au
P
Au
Au
Au
Au
S
Au
Au
Au
Cl
Au
Au
Au
Cl
Au
Au
K
Ca
Ca
0.0
0.5
1.0
1.5
2.0
2.5
3.0
3.5
4.0
keV

(c)

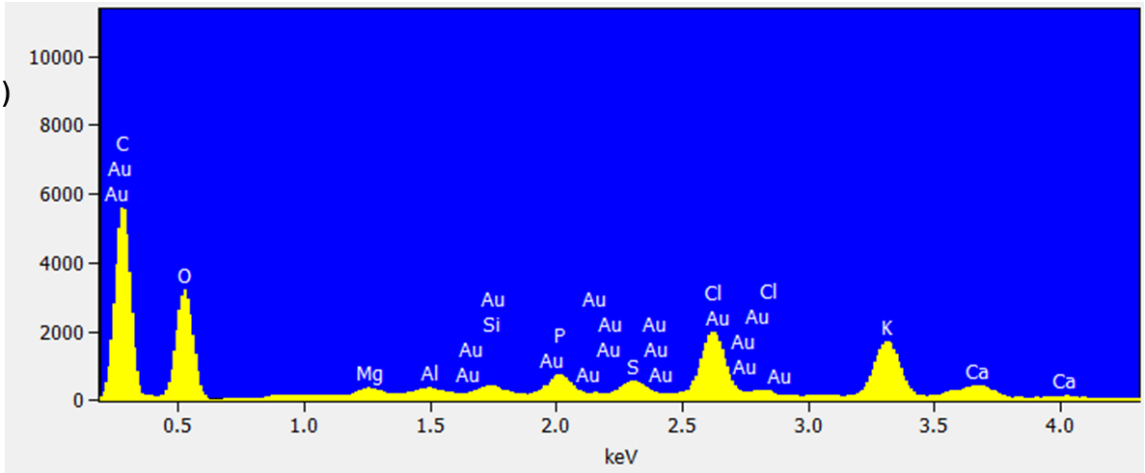
10000
8000
6000
4000
2000
0
C
Au
Au
O
Mg
Al
Au
Au
Si
Au
P
Au
Au
Au
Au
S
Au
Au
Cl
Au
Cl
Au
Au
Au
Au
K
Ca
Ca
0.5
1.0
1.5
2.0
2.5
3.0
3.5
4.0
keV

(d)

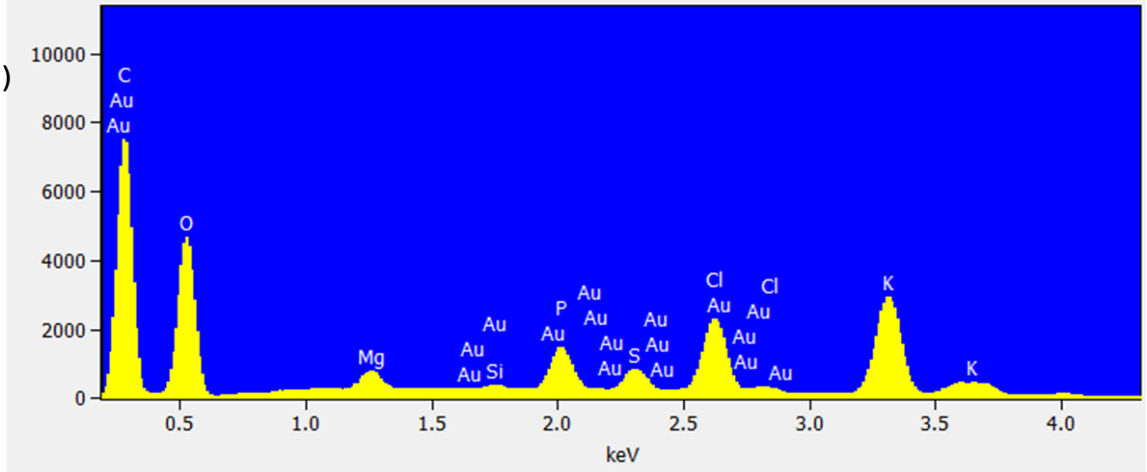
10000
8000
6000
4000
2000
0
C
Au
Au
O
Mg
Au
Au
Si
Au
P
Au
Au
Au
Au
S
Au
Au
Cl
Au
Cl
Au
Au
Au
Au
K
K
0.5
1.0
1.5
2.0
2.5
3.0
3.5
4.0
keV

(e)

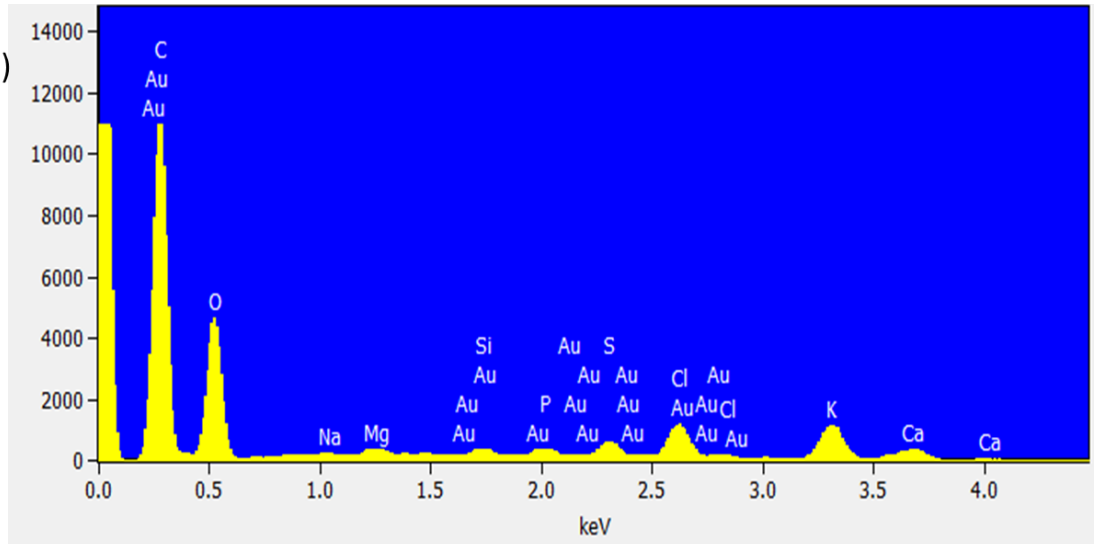
14000
12000
10000
8000
6000
4000
2000
0
C
Au
Au
O
Na
Mg
Si
Au
Au
Au
P
Au
Au
Au
S
Au
Au
Au
Cl
Au
Au
Au
Cl
Au
Au
K
Ca
Ca
0.0
0.5
1.0
1.5
2.0
2.5
3.0
3.5
4.0
keV

(f)

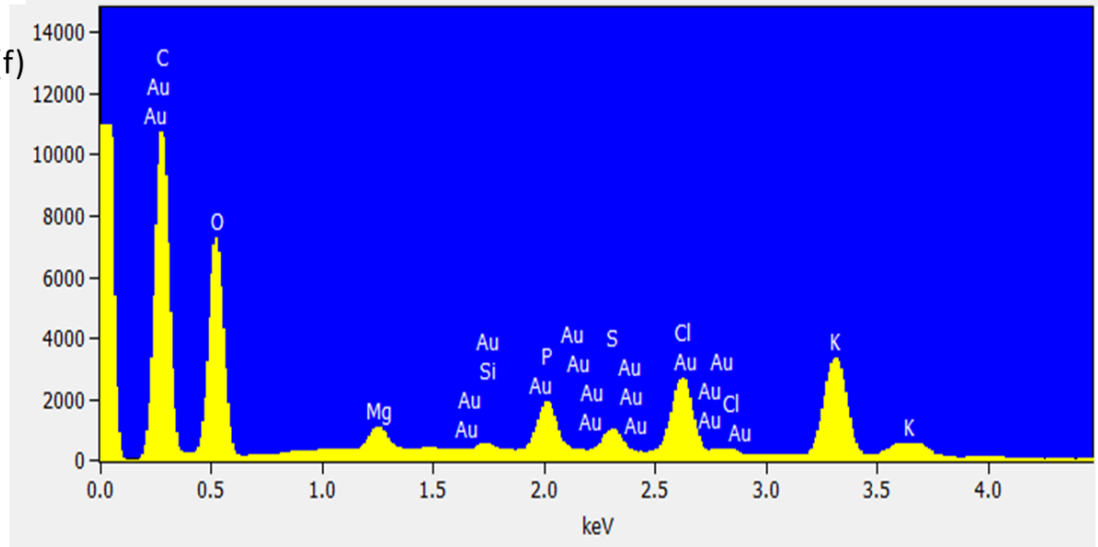
14000
12000
10000
8000
6000
4000
2000
0
C
Au
Au
O
Mg
Au
Si
Au
Au
P
Au
Au
Au
Au
S
Au
Au
Au
Cl
Au
Au
Au
Au
Cl
Au
K
K
0.0
0.5
1.0
1.5
2.0
2.5
3.0
3.5
4.0
keV

(g)

Element Line	Weight %	Weight % Error	Atom %	Atom % Error
C K	49.48	± 0.93	62.65	± 1.18
O K	30.65	± 1.03	29.14	± 0.98
Mg K	0.65	± 0.07	0.41	± 0.04
Si K	0.31	± 0.06	0.17	± 0.03
S K	1.34	± 0.20	0.64	± 0.09
Cl K	7.71	± 0.20	3.31	± 0.09
K K	7.86	± 0.36	3.06	± 0.14
Ca K	1.46	± 0.15	0.56	± 0.06
Ce L	0.54	± 0.30	0.08	± 0.04
Total	100.00		100.00	

(h)

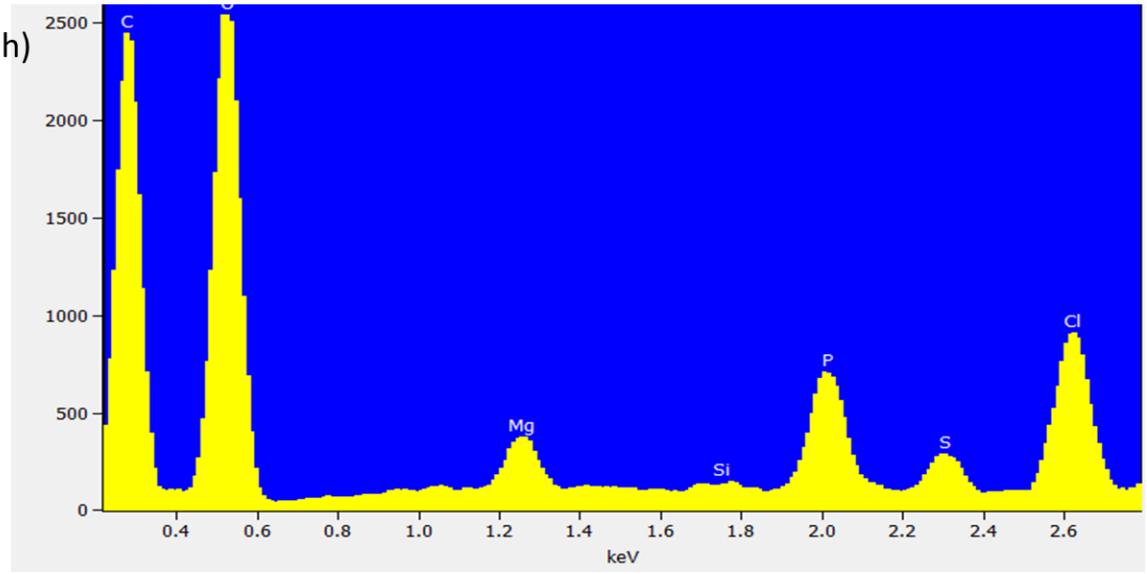

Figure A4.1: EDX spectra corresponding to SEM images confirming the presence and distribution of Au and CeO_2 NPs on plant roots surface and the absence of NPs on the control samples: (a) 5 nm cit, (b) 20 nm cit, (c) 40 nm cit, (d) 5 nm BPEI, (e) 20 nm BPEI, (f) 40 nm BPEI, (g) CeO_2 NPs and (h) control samples.

APPENDIX B

Optimization of PCR conditions for RADP assay

Random Amplified Polymorphic DNA (RAPD) was performed by two 10-base pair RAPD primers; OPB1 (5'-GTTTCGCTCC -3') and OPB14 (5'-TCCGCTCTGG-3') sourced form Inqaba Biotechnical Industries (Pty) Ltd (Pretoria, South Africa). Amplification was performed in 25 µL reaction volumes consisting of 0.5 µL primers, 10 µL DIW, 12.5 µL GoTaq® G2 Hot Start Green Master Mix (GoTaq® G2 Hot Start Polymerase, dNTPs, $MgCl_2$ and reaction buffers: Promega, USA), and 2 µL genomic DNA using a Polymerase Chain Reaction (PCR) thermocycler (T100™ Thermal Cycler). For the negative control, genomic DNA was not added and DIW was used to make up the 25 µL volume. RAPD PCR conditions used by Wu *et al.*

(2013) were followed. The PCR steps consisted of DNA denaturation for 5 min at 95 °C, followed by 30 cycles of 40 s at 95 °C, 40s at 56 °C, and 2 min at 72 °C, then final extension for 10 min at 72 °C. The amplified DNA was separated at 90 mV for 1 h and visualised using a UV transilluminator. Following these PCR steps, no bands were obtained in 1% and 1.5% ethidium bromide-stained agarose gel dissolved in 1 X TAE buffer (Tris-acetate-EDTA buffer, pH 7.5).

A gradient PCR was then used to find optimum annealing temperatures for each primer. A temperature range between 35 and 50° C was selected based on primer melting temperatures as provided by the supplier (39.5 °C for OPB1 and 43.6 °C for OPB14). The annealing temperatures tested for each primer were in the range of 35- 50 °C. The RAPD-PCR protocol consisted of the following steps: a 35 cycle warming step at 95 °C for 5 min, DNA denaturation at 95°C for 1 min, annealing (30 –50 °C) for 1 min, extension 74 °C for 1 min, and final extension at 74 °C for 10 min. The amplified product was gel electrophoresed at 80 mV for 2 h and visualised using a UV transilluminator. No DNA bands were observed at any of the tested temperatures. Following the same procedure, the study was repeated with bovine serum albumin (BSA) in an attempt to enhance binding between the DNA and primer at an annealing temperature range of 35–50 °C (50.0, 48.7, 46.8, 44.3, 40.8, 37.8, 35.9, 35.5 and 35.0 °C). A comparison of results generated with and without BSA, showed the former had clear bands, and hence BSA was used in this study as DNA-primer binding enhancer. The annealing temperatures (46.8 °C for OPB1 and 44.3 °C for OPB14) with more visible bands for each primer were selected for the experiments.

Table A5.1: DNA concentrations (ng/µL) and purity (OD_{260}/OD_{280}) after 72 and 168 h

NP type	NP concentration (mg/L)	DNA concentration (ng/µL)		OD_{260}/OD_{280}	
		72 h	168 h	72 h	168 h
5 nm cit-Au	0.0625	298.2	156.3	1.91	1.88
	0.25	127.1	100.6	1.88	1.79
	1	98.8	101.2	1.71	1.72
20 nm cit-Au	0.625	101.5	110.2	2.02	2.1
	0.25	231.4	123.3	2.03	1.92
	1	236.8	152.3	1.94	1.89
40 nm cit-Au	0.0625	100.5	105.3	1.96	1.79
	0.25	128.7	112.1	1.94	1.81
	1	110.5	99.8	1.84	1.78
5 nm BPEI Au	0.0625	214.8	110.2	2.01	1.99
	0.25	195.8	101.2	2.05	1.87
	1	99.5	96.9	2.09	1.78
20 nm BPEI Au	0.0625	170.4	180.6	2.01	1.78
	0.25	164.1	183.9	1.99	1.81
	1	114.9	181.9	1.99	1.85
40 nm BPEI Au	0.0625	240.5	170.2	2.04	1.76
	0.25	166.9	151.1	1.88	1.79
	1	199.7	145.3	1.86	1.79
CeO_2 NPs	0.0625	40.5	50.2	1.81	1.70
	0.25	56.9	48.6	1.77	1.72
	1	59.7	39.9	1.82	1.71